FINAL REPORT

TO

NATIONAL AERONAUTICS AND SPACE ADMINISTRATION

August 1966

EXPERIMENTAL MAPPING FROM RANGER PHOTOGRAPHY

NASA DEFENSE PURCHASE REQUEST NO. T-43327 (G)

Prepared by

DEPARTMENT OF THE ARMY, CORPS OF ENGINEERS

ARMY MAP SERVICE

WASHINGTON, D. C. 20315

ABSTRACT

With the advent of the space age has come the realization of close-up photography of the surfaces of other planets. The phenomenal success of three missions of the National Aeronautics Space Administration's (NASA) Ranger Program has provided close-range observations of the surface of the moon. These close-range observations, although yielding an abundance of topographic information, are devoid of the geometric standards required for normal stereophotogrammetric mapping procedures. The photogrammetric reduction of this photography, therefore, required a modification in the conventional photogrammetric mapping procedures and equipment. This report describes the studies, development, and production performed during the investigation of "Experimental Mapping from Ranger Photography," and concludes that: (a) it is possible to obtain hypsometric data by stereophotogrammetric methods from photography having an extremely small parallactic angle, and that the maximum precision for a single z-observation ranges from 0.01 mm (at the normal ratios of 0.62) to 0.09 (at the ratio of 0.03); (b) specially modified first-order analog and analytical stereoplotters afford the most efficient means for expedient map production from stereoscopic pairs having non-standard geometric qualities, such as: unconventional focal length, uncommon formats, large variances from a normalized orientation, large-scale differences between photographs, and small base-to-height relationship; (c) Analytical Topographic Compilation is technically feasible, and provides a method of utilizing photography

that cannot be accommodated on standard-type or modified analog instruments; (d) these approaches (Analytical Topographic Compilation, and the use of analytical and modified analog stereoplotters) are the solution to the prime objective which was to develop optimum methods for the reduction of Orbiter photography; and (e) the approaches used for the Ranger photography provide the most practical means for the production of lunar topographic maps from unconventional photography.

FOREWORD

This report describes the studies, development and production performed during the investigation of "Experimental Mapping from Ranger Photography," Production Order Number 95514-012, approved 29 April 1965. This project was conducted under an Army Map Service (AMS)-NASA agreement, NASA Defense Purchase Request No. T-43327(G).

Because of the scope, the complexity, and the priority, this project was basically divided into four phases: (a) Base-height Study, (b) Analog Stereoplotter Capability Extension, (c) Analytical Topographic Mapping, and (d) Experimental Mapping Proper. The Base-height Study was conducted by R. W. Harpe; the Analytical Topographic Compilation phase by D. L. Light; the Analog Stereoplotter Capability Extension, the Experimental Mapping Proper, other supporting phases, and the coordination and consolidation of all phases were conducted by L. D. Bowles. The entire project was conducted under the supervision of J. B. Theis, Chief, Investigations and Improvements Branch, under the general direction of V. P. Bauer, Chief, Department of Applied Cartography. It would be impossible to mention by name the numerous technicians who have contributed to this project. Therefore, particular acknowledgment is made only to those whose efforts exceeded an approximate one-half man-year. Acknowledgment is made to L. Hummon, L. Schenk, and J. Faish, and to the personnel under Mr. Faish's supervision for the instrumentation support.

Acknowledgment is also extended to H. Cook and J. Barrett for their support in the analytical reduction methods, and to R. Thomas and S. Lanham for their cartographic support.

For simplicity in presentation, this report is divided into the previously mentioned four basic phases with the chapters and sections arranged in the approximate order of the investigation sequence.

Any mention herein of a commercial product does not constitute endorsement by the United States Government.

EXPERIMENTAL MAPPING FROM RANGER PHOTOGRAPHY

TABLE OF CONTENTS

CHAPTER 1

GENERAL INTRODUCTION

1. PURPOSE. Studies and investigations were made to provide methods and equipment to permit maximum exploitation of stereographic measurements of lunar imagery from Ranger and the forthcoming Orbiter photography.

2. SCOPE. The development and exploitation of methods in support of mapping from Ranger and planned Orbiter photography encompassed: (a) a Base-height Study; (b) an extension of the physical ranges of a first-order analog stereoplotter; (c) Analytical Topographic Compilation which included the development and exploitation of programs for mathematical correction of the effect of lens distortion, an Analog Plotter/Mathematical Orientation Method, a Comparator/Analytical Method, and a Digital Contouring Method; and (d) experimental mapping from Ranger photography utilizing analog and analytical stereoplotters and the developed analytical methods.

PHASE ONE

CHAPTER 2

BASE HEIGHT STUDY

1. INTRODUCTION. One of the characteristics of Ranger photography is an unconventionally small base-height ratio. The base is the distance between exposure positions; the height is the altitude of exposure above the surface being photographed. In Ranger, the base-height ratio goes from almost zero, just before impact, up to 0.2. The Orbiter base-height ratio, for the low-resolution mapping camera, will be about 0.3. Nothing existed in the available literature on what precision and accuracy could be obtained with such geometry. This study, therefore, was a rigorous investigation to determine the precision of Z-coordinate observations; that is, the measurement of elevations, at the small base-height ratios of Ranger and Orbiter photography. The results of this study were published in Army Map Service Technical Report No. 55, "Experiments with Minimum to Optimum Base-Height Ratios," dated February 1966.

2. SUMMARY OF TECHNICAL REPORT NO. 55. This study involved a statistical analysis of repetitive observations of a variable number of points in a series of stereoscopic grid models to determine the expected precision of a single observation of the Z-coordinate at the small base-height ratios of Ranger and Orbiter photography. These models consisted of 12 different base-height ratios ranging from 0.03 to 0.62, and also three projection distances. The study was made with precision grid plates which provided optimum conditions. Therefore, the results cannot be projected directly

to indicate the precision of Z-coordinate measurements made under operational conditions where the resolution of the photography and the residual Y-parallaxes present in the stereoscopic model are factors which tend to adversely affect precision of photogrammetric measurements. However, past experience has shown that a correlation can be expected between stereoscopic grid model measurements and the measurements made from photography. In the experiments performed, the results indicated that the maximum obtainable precision of a single observation in the Z-coordinate ranges from 0.01 mm (at the normal base-height ratio of 0.62) to 0.09 mm (at the base-height ratio of 0.03). It was concluded from this study that at the weakest Ranger base-height ratio (0.07), which AMS had considered using in stereocompilation, the precision of observation based on the grid model experiments is of the order of 0.04 mm. At a model scale of 1:1,000,000, this would correspond to $\pm$ 40 meters of uncertainty on the lunar surface.

PHASE TWO

CHAPTER 3

ANALOG STEREOPLOTTER CAPABILITY EXTENSION

SECTION I. PURPOSE AND SCOPE

1. PURPOSE. The abnormal tilts, the large-scale differences between successive exposures, and the low base-height ratios of the Ranger photography exceeded, in some respect, at least one of the physical ranges of each of the AMS conventional stereoplotters. Such geometry is indicative of any probe-type photography in which the photographic system is heading into the photographed surface. To accommodate all three of these abnormalities, an extension of the physical ranges of a first-order analog instrument was undertaken. The Zeiss Stereoplanigraph C-8 was selected for this purpose.

2. SCOPE. Two approaches were taken in the capability extension of the Zeiss Stereoplanigraph C-8: (a) the incorporation of Balplex 525 projectors in the Stereoplanigraph C-8; and (b) the manufacture of special Stereoplanigraph-focal-length cameras and accessories to replace the commonly used 152.4-mm-focal-length Stereoplanigraph cameras.

SECTION II. CAPABILITY EXTENSION UTILIZING BALPLEX 525 PROJECTORS

3. INTRODUCTION. The use of the Balplex 525 projectors to extend the physical range of the Stereoplanigraph was initiated as an interim solution to accommodate the abnormal Y-tilt of the Ranger photography, until the special Stereoplanigraph-C-8-focal-length cameras were received from the manufacturer. This special-purpose instrument was termed the "Stereo-balplexigraph" (fig. 3-1).

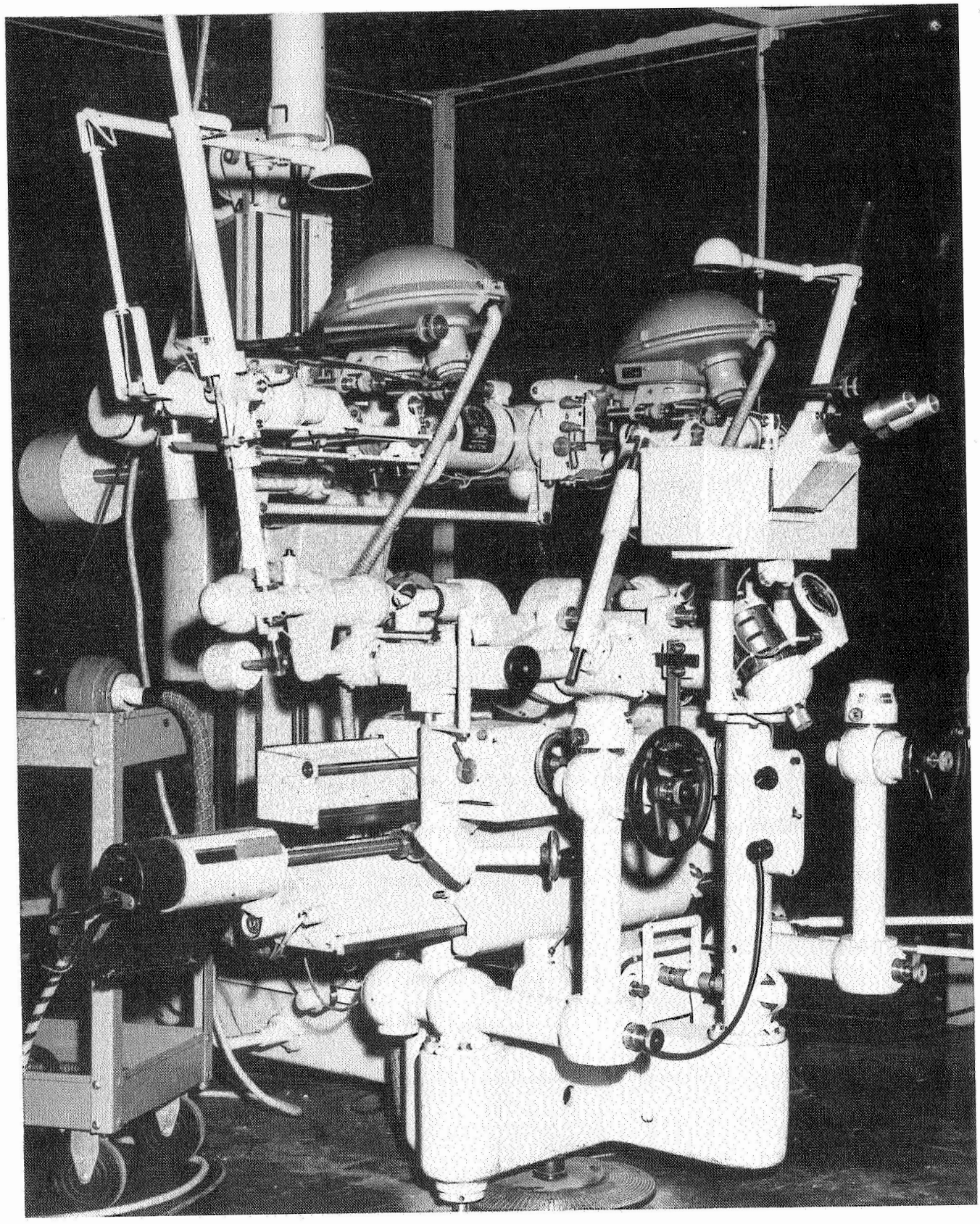

Figure 3-1. Stereobalplexigraph.

4. CAPABILITY EXTENSION. a. Equipment. (1) Zeiss Stereoplanigraph C-8. The Zeiss Stereoplanigraph C-8 is a first-order, universal instrument. It can accommodate vertical, convergent, or oblique photography with base-height ratios ranging from 0.0 to approximately 1.3, and can be used for both photogrammetric control extension and compilation. In addition, its viewing-and-plotting-scale flexibility exceeds that of most analog stereoplotters in that photographs may be viewed from 1.4 to 22.5 magnification, depending upon the projection and principal distances, and plotting can be accomplished directly at any of 30 different scales.

(2) Balplex 525 Projectors. The Balplex 525 projectors (wide-angle) were developed by the U.S. Geological Survey and manufactured by the Bausch and Lomb Optical Company. The projectors have a principal distance of 55 mm and use a 110- x 110-mm diapositive plate, 82.5-x 82.5-mm image size. At the optimum projection distance (opt. proj. dist.) 525 mm; the model scale is 9.5 times the plate scale.

b. Procedure. The modification of the Stereoplanigraph C-8, to extend its capability, consisted of replacing the standard (152.4-mm-fl.) Stereoplanigraph C-8 cameras with wide-angle (55-mm-fl.) Balplex projectors. The smaller format of the Balplex cameras eliminated the restraint in achieving the required common Y-tilt, imposed by the standard cameras coming in contact with the camera supporting frame.

c. Results. A summary of the accommodation ranges as a result of this modification are expressed in table 3-I.

5. RESOLUTION TEST. Resolution tests were conducted to indicate the resolving power of the Stereobalplexigraph.

Table 3-I. Stereobalplexigraph Accommodation Ranges

Elements	Range
Projection Distance (Z)	600 mm Maximum (Stereoplanigraph Limitation)
	525 mm Optimum
	390 mm Minimum
Model Scale	9.5 x Diapositive Scale (at opt. proj. dist.)
Viewing Scale	42.8 x Diapositive Scale (at opt. proj. dist.)
bX	0 to ± 300 mm
bY	± 60 mm
bZ	± 45 mm
φ (Tip)	+ 30° to - 30°
Φ (Common Tip)	30°
ω (Tilt)	± 9°
ξ (Common Tilt)	± 54°
$\mathcal{H}$ (Swing)	± 110° Approximate

a. Material. The resolution plate (110 x 110 mm) for this test was prepared from a 9- x 9-inch diapositive plate consisting of a series of standard U.S. Air Force, black-on-white, resolution targets printed along the diagonals. Target spacing corresponded to angular displacements of 0° and 45° from the optical axis.

b. Procedure. Resolution was determined by projecting the targets at various projection distances and viewing the resulting image at a 4.5x ocular magnification. The minimum resolution, in lines per millimeter, was determined at each angular position at projection distances ranging from 450 to 600 mm.

c. Results. The results of the resolution tests are given in table 3-II.

Table 3-II. Results of Stereobalplexigraph Resolution Test in Lines/mm

Projection Distance (mm)	Angle from Optical Axis	
	0°	45°
600	60	25
575	64	26
550	70	27
525	72	28
500	64	25
475	46	23
450	22	20

6. GRID FLATNESS TEST. The flatness of the mapping plane is of critical importance, since any deviation enters into the measuring process with its full amount. The use of grid plates and the measurement of vertical deformation of a grid model is usually considered the supreme performance test of a plotting instrument.

a. Materials. A pair of precision grid plates (9 x 9 x 0.25 inch) prepared by the Bausch and Lomb Reduction Printer were used to prepare a pair of positive grid plates (4.33 x 4.33 x 0.25 inch) on the Wild U-3, Model B, printer.

b. Procedure. The positive grid plates were used to form grid stereomodels at projection distances ranging from 391 to 600 mm and base-height ratios ranging from 0.10 to 0.59. Each of the grid models was leveled to the four corner grid intersections. Each of the 22 to 30 grid intersections (varied according to the base-height ratio) were read and recorded three times by one operator. The geometry for each of the grid models is shown in table 3-III.

Table 3-III. Stereobalplexigraph Grid Model Geometry

Model No.	Projection Distance (mm)	Base (mm)	Base-Height Ratio
1	391.00	229.74	0.59
2	525.00	292.23	0.56
3	600.00	294.57	0.49
4	568.48	103.09	0.18
5	498.00	51.53	0.10

c. Results. (1) Model Flatness. The grid flatness test results for each of the models are shown in tables 3-IV through 3-VIII. All tables were made directly from the computer tab runs, therefore, the number of figures shown are greater than the significant figure. The computer program was written to handle many and varied conditions. The figures are good to two decimal places since the least reading on the instrument used is 0.01 mm. Symbol clarification for tables 3-IV through 3-VIII is given in table 3-XVII. An average of the standard deviation of the five vertical model flatness test results may be considered to be the average flatness obtainable for many combinations of projection distances and base settings. The average standard deviation

$$(A_V \sigma_{S_Z}) = \Sigma Z \frac{\text{SIGMAL}}{n} = \frac{0.189}{5} 0.04 \text{ mm.}$$

(2) Indicated Vertical Accuracy. In an over-all appraisal of the Stereobalplexigraph it may be permissible to adhere to conventional concepts which recognize vertical accuracy as the criterion of performance. In these terms, the statement of vertical accuracy, based on the average standard deviation of the five model flatness tests and an average of the projection distances, indicates a vertical accuracy of one part in 12,900.

Table 3-IV. Stereobalplexigraph Grid Flatness Analysis Expressed in mm for Model 1

Point Number	SIGMA Z	RMSE Z
1	.3785939E-01	.3091206E-01
2	.5537749E-01	.4521553E-01
3	.5259911E-01	.4294700E-01
4	.2581989E-01	.2108185E-01
5	.5887840E-01	.4807402E-01
6	.5715476E-01	.4666667E-01
7	.3366502E-01	.2748737E-01
8	.3651484E-01	.2981424E-01
9	.2581989E-01	.2108185E-01
10	.2943920E-01	.2403701E-01
11	.2581989E-01	.2108185E-01
12	.4966555E-01	.4055175E-01
14	.5802298E-01	.4737557E-01
15	.3214550E-01	.2624669E-01
16	.2708013E-01	.2211083E-01
17	.7461010E-01	.6091889E-01
18	.8346656E-01	.6815016E-01
19	.5773503E-01	.4714045E-01
20	.5656854E-01	.4618802E-01
21	.6271629E-01	.5120764E-01
22	.1287116E 00	.1050926E 00
23	.1247664E 00	.1018714E 00

Determination of Flatness for Entire Model

Z SIGMAL	Z STEML	Z SIGMA 3.3L	Z SIGMA 3L
.034	.004	.113	.103
Z SIGMA 2L	**Z SIGMA 1.6449L**	**Z PEL**	**Z RMSEL**
.069	.056	.023	.034

Table 3-V. Stereobalplexigraph Grid Flatness Analysis
Expressed in mm for Model 2

Point Number	SIGMA Z	RMSE Z
1	.5597618E-01	.4570436E-01
2	.3265986E-01	.2666667E-01
3	.2708013E-01	.2211083E-01
4	.2449490E-01	.2000000E-01
5	.4830459E-01	.3944053E-01
6	.4654747E-01	.3800585E-01
7	.1527525E-01	.1247219E-01
8	.1527525E-01	.1247219E-01
9	.5627314E-01	.4594683E-01
10	.5972158E-01	.4876246E-01
11	.3265986E-01	.2666667E-01
12	.5131601E-01	.4189935E-01
13	.5291503E-01	.4320494E-01
14	.5773503E-01	.4714045E-01
15	.7958224E-01	.6497863E-01
16	.6429100E-01	.5249339E-01
17	.2380476E-01	.1943651E-01
18	.4654747E-01	.3800585E-01
19	.4932883E-01	.4027682E-01
20	.3316625E-01	.2708013E-01
21	.4795831E-01	.3915780E-01
22	.5131601E-01	.4189935E-01
23	.3958114E-01	.3231787E-01
24	.4654747E-01	.3800585E-01
25	.5416026E-01	.4422166E-01
26	.4690416E-01	.3829708E-01
27	.3000000E-01	.2449490E-01

Determination of Flatness for Entire Model

Z SIGMAL	Z STEML	Z SIGMA 3.3L	Z SIGMA 3L
.028	.003	.091	.083
Z SIGMA 2L	Z SIGMA 1.6449	Z PEL	Z RMSEL
.055	.045	.019	.027

Table 3-VI. Stereobalplexigraph Grid Flatness Analysis Expressed in mm for Model 3

Point Number	SIGMA Z	RMSE Z
1	.3651484E-01	.2981424E-01
2	.2828427E-01	.2309401E-01
3	.3366502E-01	.2748737E-01
4	.6191392E-01	.5055250E-01
5	.5916080E-01	.4830459E-01
6	.3055050E-01	.2494438E-01
9	.4618802E-01	.3771236E-01
10	.5322906E-01	.4346135E-01
11	.4725816E-01	.3858612E-01
12	.4725816E-01	.3858612E-01
14	.4320494E-01	.3527668E-01
15	.5627314E-01	.4594683E-01
16	.5715476E-01	.4666667E-01
17	.5163978E-01	.4216370E-01
20	.6976150E-01	.5696003E-01
21	.8286535E-01	.6765928E-01
22	.1045626E 00	.8537499E-01
23	.9219544E-01	.7527726E-01
25	.5686241E-01	.4642796E-01
26	.4546061E-01	.3711843E-01
27	.6027714E-01	.4921608E-01
28	.6000000E-01	.4898980E-01

Determination of Flatness for Entire Model

Z SIGMAL	Z STEML	Z SIGMA 3.3L	Z SIGMA 3L
.036	.004	.117	.107
Z SIGMA 2L	**Z SIGMA 1.6449**	**Z PEL**	**Z RMSEL**
.071	.058	.024	.035

Table 3-VII. Stereobalplexigraph Grid Flatness Analysis Expressed in mm for Model 4

Point Number	SIGMA Z	RMSE Z
1	.2516612E-01	.2054805E-01
2	.3651484E-01	.2981424E-01
3	.4434712E-01	.3620927E-01
4	.4546060E-01	.3711843E-01
5	.8286535E-01	.6765928E-01
6	.8225975E-01	.6716480E-01
7	.6298148E-01	.5142416E-01
8	.7527727E-01	.6146363E-01
9	.6608076E-01	.5395471E-01
10	.5802298E-01	.4737557E-01
11	.5715476E-01	.4666667E-01
12	.6831301E-01	.5577734E-01
13	.6683313E-01	.5456902E-01
14	.3915780E-01	.3197221E-01
15	.4281744E-01	.3496029E-01
16	.5507570E-01	.4496912E-01
17	.5228129E-01	.4268749E-01
18	.6683313E-01	.5456902E-01
19	.8981462E-01	.7333333E-01
20	.9966611E-01	.8137704E-01
21	.7164728E-01	.5849976E-01
22	.3415650E-01	.2788867E-01
23	.5033223E-01	.4109609E-01
24	.6506407E-01	.5312459E-01
25	.6271629E-01	.5120764E-01

Determination of Flatness for Entire Model

Z SIGMAL	Z STEML	Z SIGMA 3.3L	Z SIGMA 3L
.036	.004	.119	.109
Z SIGMA 2L	**Z SIGMA 1.6449**	**Z PEL**	**Z RMSEL**
.072	.060	.024	.036

Table 3-VIII. Stereobalplexigraph Grid Flatness Analysis
Expressed in mm for Model 5

Point Number	SIGMA Z	RMSE Z
1	.4041452E-01	.3299832E-01
2	.1036018E 00	.8459052E-01
3	.1514376E 00	.1236482E 00
4	.1224745E 00	.1000000E 00
5	.1331666E 00	.1087300E 00
6	.1460593E 00	.1192570E 00
7	.1006645E 00	.8219219E-01
8	.7325754E-01	.5981453E-01
9	.3415650E-01	.2788867E-01
10	.5887841E-01	.4807402E-01
11	.7257180E-01	.5925463E-01
12	.6952218E-01	.5676462E-01
13	.8621678E-01	.7039571E-01
14	.7527726E-01	.6146363E-01
15	.6806859E-01	.5557777E-01
16	.6557439E-01	.5354126E-01
17	.5416026E-01	.4422166E-01
18	.6531973E-01	.5333333E-01
19	.8812869E-01	.7195678E-01
20	.1037625E 00	.8472177E-01
21	.8524475E-01	.6960204E-01
22	.8981462E-01	.7333333E-01
23	.8205689E-01	.6699917E-01
24	.8850612E-01	.7226494E-01
25	.1748333E 00	.1427508E 00
26	.1617611E 00	.1320774E 00
27	.6904105E-01	.5637178E-01
28	.5715476E-01	.4666667E-01
29	.3829708E-01	.3126944E-01
30	.2081666E-01	.1699673E-01

Determination of Flatness for Entire Model

Z SIGMAL	Z STEML	Z SIGMA 3.3L	Z SIGMA 3L
.055	.006	.180	.164
Z SIGMA 2L	**Z SIGMA 1.6449**	**Z PEL**	**Z RMSEL**
.109	.090	.037	.054

7. DISCUSSION. a. Capability Extension. The modification of the Stereoplanigraph C-8 utilizing Balplex 525 projectors increased its common tip range from 18^{o} to 30^{o} . In addition, its bZ range was increased from $\pm$ 20 to $\pm$ 45 mm. The Stereobalplexigraph, however, will not accommodate the lower altitude Ranger photography since the change in altitude between exposures exceeds the absorption of scale difference capability of the instrument.

b. Resolution. Resolution tests showed that the Stereobalplexigraph will accommodate material with qualities superior to that used for mapping the earth. However, the Ranger material does not have sufficient inherent resolution to withstand the total magnification at the viewing scale of the instrument. The resulting resolution of the Ranger material at the viewing scale is approximately 2 lines/mm. As a result of the low resolution the instrument operator could not remove the Y-parallax in the model. Subsequent minor modifications to reduce the overall magnification of this instrument did not prove successful, as any attempt to reduce the viewing scale also reduced the size of the floating reference mark to a point where it could not be distinguished from the imagery. A major modification to the floating reference system could have eliminated the problem. However, the contract time frame did not allow this extensive modification and a complete recalibration of the viewing system of the Stereoplanigraph C-8.

c. Grid Flatness Test. The grid model flatness test results would have shown a superior indicated vertical accuracy for the instrument if the base-height ratio of each of the models had been held at the normal 0.56. The base-height ratios were not held constant, however, so that an

average model deformation could be determined that would give an average indicated vertical accuracy for the many combinations of projection distances and base settings inherent in the Ranger photography.

8. CONCLUSIONS. It was concluded that:

a. The Stereobalplexigraph is more versatile than most first-order analog instruments as it is capable of accommodating photography with 30^{o} of inherent common tip.

b. The resolving power of the Stereobalplexigraph, at optimum projection distance, is comparable to most first-order analog instruments. However, the resolution of the photography used must be capable of withstanding the total system magnification.

c. The indicated vertical accuracy of the instrument is comparable to first-order analog instruments.

SECTION III. CAPABILITY EXTENSION UTILIZING SPECIAL-FOCAL-LENGTH STEREOPLANIGRAPH C-8 CAMERAS

9. INTRODUCTION. To extend the physical ranges of the AMS Stereoplanigraph C-8, a complete line of plotting cameras, ranging from 100 to 600 mm in focal length, and accessories were ordered from the manufacturer, Carl Zeiss, Oberkochen, West Germany. Two pairs of these cameras (100- and 210-mm-fl) were ordered specifically to obtain maximum exploitation of Ranger and Orbiter imagery. These special plotting cameras and accessories increased the common tip Δbz range of the Stereoplanigraph. However, the contracting and delivery time frame allowed only limited experimentations. One pair of the special cameras (210-mm-fl) was selected for immediate use, as it would provide the maximum model scale that the inherent resolution of the Ranger VIII A camera photography could withstand (fig. 3-2).

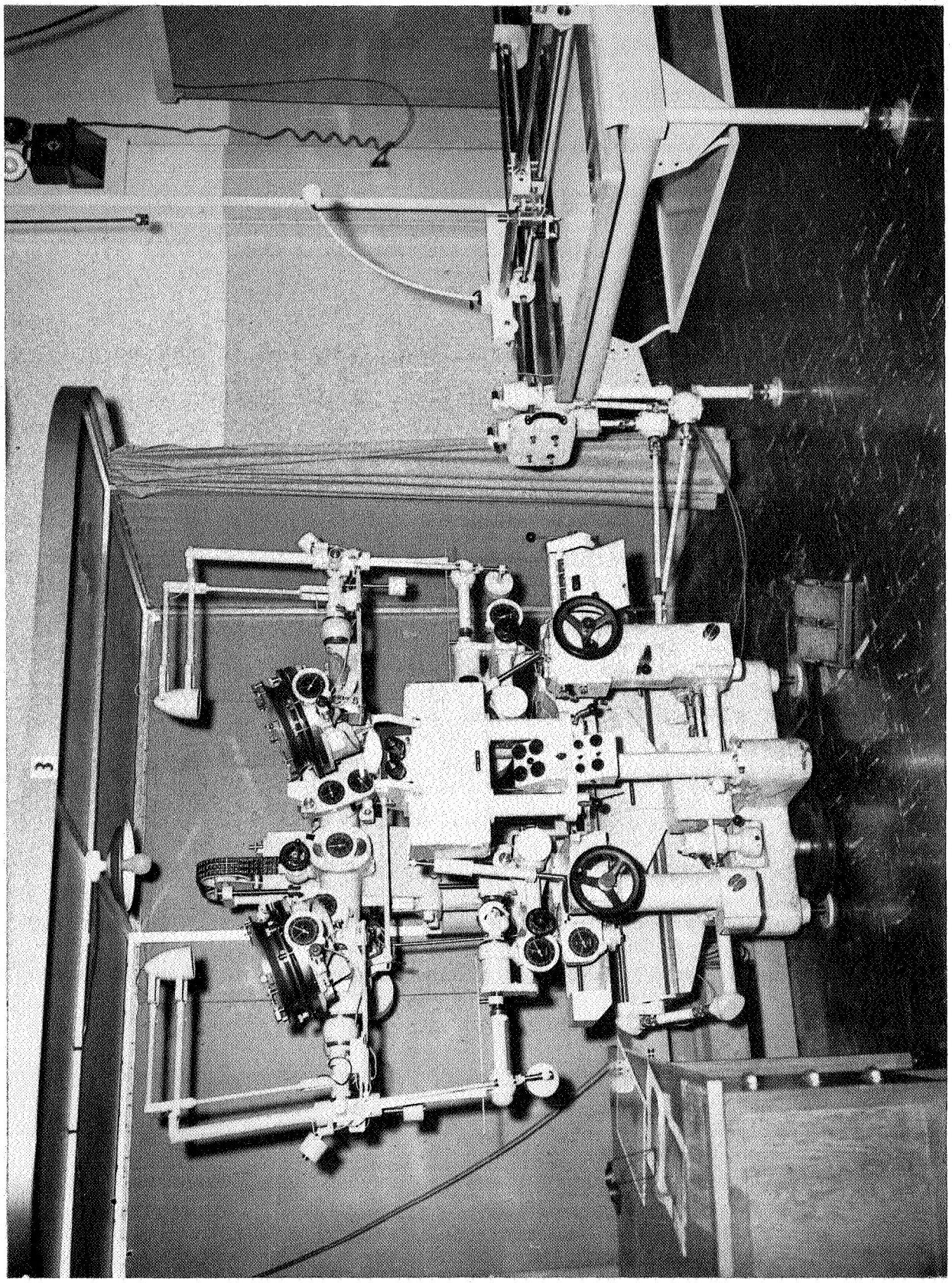

Figure 3-2. 210-mm-Focal-length Stereoplanigraph C-8.

10. CAPABILITY EXTENSION. a. Equipment. (1) Zeiss Stereoplanigraph C-8. Refer to chapter 3, section II, paragraph 4.a.(1).

(2) 210-mm-focal-length Stereoplanigraph C-8 Cameras. The 210-mm-focal-length Stereoplanigraph C-8 cameras were designed and manufactured by Carl Zeiss. The cameras are distortion-free and have a principal distance of 210 mm and use a positive or diapositive plate up to 230 x 230 mm.

b. Procedure. The extension of the common tip (Φ) range of the Stereoplanigraph encompassed the manufacturing and mounting of special forks, lighting sources and 210-mm-focal-length plotting cameras. The first step in the assembly and adjustment process was the replacement of the standard forks with the special, long forks. Then, after the mounting and precise rotation of the cameras about their Z-axes, with respect to the long forks, a considerably increased freedom in Φ was obtained. An additional increase in Φ was obtained by precision milling of the camera frames to allow them to pass inside the camera and light source support units. The installation and adjustment of these special components allowed the common tip range of the Stereoplanigraph to be extended from 18 to 25 degrees.

c. Results. The results of this modification are expressed in table 3-IX, as a summary of the physical ranges.

11. RESOLUTION TEST. Resolution tests were performed to indicate the combined resolving power of the 210-mm-focal-length cameras and the Stereoplanigraph optical train.

a. Material. The resolution plate for this test consisted of a series of Standard U.S. Air Force, black-on-white, resolution targets

Table 3-IX. 210-mm-focal-length Stereoplanigraph Physical Ranges

Elements	Range
Projection Distance (Z)	600 mm Maximum 200 mm Minimum
Model Scale	2.9x Diapositive Scale (at max. proj. dist.)
Viewing Scale	13x Diapositive Scale (at max. proj. dist.)
bX	0 to ± 300 mm
bY	± 30 mm
bZ	± 20 mm
φ (Tip)	+ 25° to - 30°
Φ (Common Tip)	25°
ω (Tilt)	9°
ξ (Common Tilt)	± 54°
(Swing)	360°

printed along a diagonal of a 9- x 9- x 0.25-inch glass diapositive plate. The targets had a resolution of 144 lines/mm. Target spacing corresponded to angular displacement of 0°, 20°, 30°, 40°, and 45° from the optical axis.

b. Procedure. Resolution was determined by projecting the targets at various projection distances and viewing the resulting image at an additional 4.5x magnification. The minimum resolution, in lines per millimeter, was determined at each angular position at projection distances ranging from 200 to 600 mm.

c. Results. The results of the resolution tests are given in table 3-X.

Table 3-X. Results of 210-mm-focal-length Stereoplanigraph Resolution Tests in Lines/mm

Projection Distance (mm)	Angle from Optical Axis					
	0°	10°	20°	30°	40°	45°
600	62	61	59	58	57	57
500	54	54	54	54	53	53
400	50	50	50	50	49	49
300	37	37	37	36	35	35
200	26	26	26	26	26	26

12. GRID FLATNESS TEST. Grid stereomodels were set to provide an indication of instrument accuracy.

a. Material. A set of precision 240- x 240- mm positive grid plates with a 22.5-mm grid spacing was used. The grid plates were prepared by the Stereoplanigraph C-8 manufacturer.

b. Procedure. The grids were used by one operator to form one grid stereomodel at five projection distances ranging from 200 to 600 mm at a base-height ratio of 0.43. Each of the grid models was leveled to the four corner grid intersections. Twenty-three grid intersections of each of the absolutely oriented models were read and recorded six times. The projection distances and base settings for each of the grid models are shown in table 3-XI.

Table 3-XI. 210-mm-focal-length Stereoplanigraph Grid Model Geometry

Model No.	Projection Distance (mm)	Base (mm)
1	200	85.44
2	300	128.63
3	400	171.17
4	500	214.01
5	600	256.72

c. Results. (1) Model Flatness. The grid flatness test for each of the models is shown in tables 3-XII through 3-XVI. All tables were made directly from computer tab runs. The figures are good to two decimal places since the least reading on the instrument is 0.01 mm. Symbol clarification for tables 3-XII through 3-XVI is given in table 3-XVII. Based on the five vertical model flatness test results, the average standard deviation

$$(A_V\ \sigma_{S_Z}) = \Sigma Z\ \frac{\text{SIGMAL}}{n} = \frac{0.081}{5} = 0.016 \text{ mm.}$$

Table 3-XII. 210-mm-focal-length Stereoplanigraph Grid Flatness Analysis Expressed in mm for Model 1

Point Number	SIGMA Z	RMSE Z
1	.1224745E-01	.1118034E-01
2	.1722401E-01	.1572330E-01
3	.1211060E-01	.1105542E-01
4	.1275266E-08	.1164153E-08
5	.1643168E-01	.1500000E-01
6	.1095445E-01	.1000000E-01
7	.2401388E-01	.2192158E-01
8	.2366432E-01	.2160247E-01
9	.1471960E-01	.1343710E-01
10	.1032796E-01	.9428090E-02
11	.1966384E-01	.1795055E-01
12	.2804758E-01	.2560382E-01
13	.2449490E-01	.2236068E-01
14	.2483277E-01	.2266912E-01
15	.1897367E-01	.1732051E-01
16	.1366260E-01	.1247219E-01
17	.2160247E-01	.1972027E-01
18	.1751190E-01	.1598611E-01
19	.1834848E-01	.1674979E-01
20	.1378405E-01	.1258306E-01
21	.1329160E-01	.1213352E-01
22	.1264911E-01	.1154701E-01
23	.7527727E-02	.6871843E-02

Determination of Flatness for Entire Model

Z SIGMAL	Z STEML	Z SIGMA 3.3L	Z SIGMA 3L
.016	.001	.053	.048
Z SIGMA 2L	**Z SIGMA 1.6649L**	**Z PEL**	**Z RMSEL**
.032	.026	.011	.016

Table 3-XIII. 210-mm-focal-length Stereoplanigraph Grid Flatness Analysis Expressed in mm for Model 2

Point Number	SIGMA Z	RMSE Z
1	.1760682E-01	.1607275E-01
2	.1643168E-01	.1500000E-01
3	.2250926E-01	.2054805E-01
4	.1549193E-01	.1414214E-01
5	.1861899E-01	.1699673E-01
6	.9831921E-02	.8975275E-02
7	.2136976E-01	.1950783E-01
8	.2000000E-01	.1825742E-01
9	.1632993E-01	.1490712E-01
10	.3881580E-01	.3543382E-01
11	.2639444E-01	.2409472E-01
12	.1722401E-01	.1572330E-01
13	.1211060E-01	.1105542E-01
14	.2658320E-01	.2426703E-01
15	.3224903E-01	.2943920E-01
16	.1505545E-01	.1374369E-01
17	.1722401E-01	.1572330E-01
18	.1169045E-01	.1067187E-01
19	.2190890E-01	.2000000E-01
20	.2401388E-01	.2192158E-01
21	.1329160E-01	.1213352E-01
22	.1602082E-01	.1462494E-01
23	.2073644E-01	.1892969E-01

Determination of Flatness for Entire Model

Z SIGMAL	Z STEML	Z SIGMA 3.3L	Z SIGMA 3L
.019	.002	.063	.057
Z SIGMA 2L	**Z SIGMA 1.6449L**	**Z PEL**	**Z RMSEL**
.038	.031	.013	.019

Table 3-XIV. 210-mm-focal-length Stereoplanigraph Grid Flatness Analysis Expressed in mm for Model 3

Point Number	SIGMA Z	RMSE Z
1	.2097618E-01	.1914854E-01
2	.2250926E-01	.2054805E-01
3	.5163978E-02	.4714045E-02
4	.2065591E-01	.1885618E-01
5	.1602082E-01	.1462494E-01
6	.1861899E-01	.1699673E-01
7	.2160247E-01	.1972027E-01
8	.1861899E-01	.1699673E-01
9	.1275266E-08	.1164153E-08
10	.1760682E-01	.1607275E-01
11	.1974842E-01	.1802776E-01
12	.2136976E-01	.1950783E-01
13	.2136976E-01	.1950783E-01
14	.1549193E-01	.1414214E-01
15	.1751190E-01	.1598611E-01
16	.2041241E-01	.1863390E-01
17	.2000000E-01	.1825742E-01
18	.9831921E-02	.8975275E-02
19	.1366260E-01	.1247219E-01
20	.1329160E-01	.1213352E-01
21	.1264911E-01	.1154701E-01
22	.5163978E-02	.4714045E-02
23	.1169045E-01	.1067187E-01

Determination of Flatness for Entire Model			
Z SIGMAL	Z STEML	Z SIGMA 3.3L	Z SIGMA 3L
.015	.001	.051	.046
Z SIGMA 2L	Z SIGMA 1.6449	Z PEL	Z RMSEL
.031	.025	.010	.015

Table 3-XV. 210-mm-focal-length Stereoplanigraph Grid Flatness Analysis Expressed in mm for Model 4

Point Number	SIGMA Z	RMSE Z
1	.1471960E-01	.1343710E-01
2	.7527727E-02	.6871843E-02
3	.5477226E-02	.5000000E-02
4	.1602082E-01	.1462494E-01
5	.4082483E-02	.3726780E-02
6	.2250926E-01	.2054805E-01
7	.8164966E-02	.7453560E-02
8	.1224745E-01	.1118034E-01
9	.2401388E-01	.2192158E-01
10	.1329160E-01	.1213352E-01
11	.2228602E-01	.2034426E-01
12	.1471960E-01	.1343710E-01
13	.2295479E-08	.2095476E-08
14	.1505545E-01	.1374369E-01
15	.1602082E-01	.1462494E-01
16	.1471960E-01	.1343710E-01
17	.1471960E-01	.1343710E-01
18	.2041241E-01	.1863390E-01
19	.8366600E-02	.7637626E-02
20	.1549193E-01	.1414214E-01
21	.2658320E-01	.2426703E-01
22	.1722401E-01	.1572330E-01
23	.1505545E-01	.1374369E-01

Determination of Flatness for Entire Model

Z SIGMAL	Z STEML	Z SIGMA 3.3L	Z SIGMA 3L
.014	.001	.047	.043
Z SIGMA 2L	**Z SIGMA 1.6449L**	**Z PEL**	**Z RMSEL**
.029	.024	.010	.014

Table 3-XVI. 210-mm-focal-length Stereoplanigraph Grid Flatness Analysis Expressed in mm for Model 5

Point Number	SIGMA Z	RMSE Z
1	.7527727E-02	.6871843E-02
2	.2136976E-01	.1950783E-01
3	.1169045E-01	.1067187E-01
4	.8164966E-02	.7453560E-02
5	.2401388E-01	.2192158E-01
6	.2658320E-01	.2426703E-01
7	.2160247E-01	.1972027E-01
8	.1861899E-01	.1699673E-01
9	.1760682E-01	.1607275E-01
10	.1632993E-01	.1490712E-01
11	.2401388E-01	.2192158E-01
12	.2065591E-01	.1885618E-01
13	.3209361E-01	.2929733E-01
14	.1378405E-01	.1258306E-01
15	.1751190E-01	.1598611E-01
16	.6324555E-02	.5773503E-02
17	.1471960E-01	.1343710E-01
18	.2588436E-01	.2362908E-01
19	.1169045E-01	.1067187E-01
20	.1378405E-01	.1258306E-01
21	.2073644E-01	.1892969E-01
22	.1211060E-01	.1105542E-01
23	.2000000E-01	.1825742E-01

Determination of Flatness for Entire Model

Z SIGMAL	Z STEML	Z SIGMA 3.3L	Z SIGMA 3L
.017	.001	.057	.052
Z SIGMA 2L	Z SIGMA 1.6449L	Z PEL	Z RMSEL
.034	.028	.012	.017

Table 3-XVII. Symbol Clarification for Tables 3-IV through 3-VIII and 3-XII through 3-XVI.

Terminology	Symbols in Tables	Equations
Arithmetic Mean	$\bar{Z}$	$\frac{\Sigma Z_p}{AN}$ where: Z_p = numerical value of specific point; AN = number of readings per point.
Residual	ΔZ	$Z_p - \bar{Z}$
Standard Deviation for Individual Point	SIGMA Z	$\left[\frac{\Sigma(\Delta Z)^2}{AN-1}\right]^{\frac{1}{2}}$
Root Mean Square Error for Individual Point	RMSE Z	$\left[\frac{\Sigma(\Delta Z)^2}{AN}\right]^{\frac{1}{2}}$
Standard Deviation for All Points	Z SIGMA L	$\left[\sum_{i=1}^{n} (\Delta Zi)^2\right]^{\frac{1}{2}}$ where: n = Number of Points Observed
Standard Error of the Mean of All Points	Z STEM L	$\frac{\text{Z SIGMAL}}{[n]^{\frac{1}{2}}}$
Maximum Error for All Points	Z SIGMA 3.3L	(3.3) (Z SIGMAL)
Three Sigma for All Points	Z SIGMA 3L	(3.0) (Z SIGMAL)
Two Sigma for All Points	Z SIGMA 2L	(2.0) (Z SIGMAL)
90% Error for All Points	Z SIGMA 1.6449L	(1.6449)(Z SIGMAL)
Root Mean Square Error for All Points	Z RMSEL	$\left[\frac{\sum_{i=1}^{n} (\quad Zi)^2}{n}\right]^{\frac{1}{2}}$
Probable Error for All Points	Z PEL	(0.6745) (Z SIGMAL)
10^{-1}; 10^{-2}; and etc.	E-01; E-02, etc.	

(2) Indicated Vertical Accuracy. The indicated vertical accuracy for the 210-mm-focal-length Stereoplanigraph is one part in 24,400. The indicated vertical accuracy was computed from the average standard deviation of the five vertical model flatness test results and an average of the projection distances.

13. DISCUSSION. a. Capability Extension. The modification of the Stereoplanigraph C-8 utilizing 210-mm-focal-length Stereoplanigraph plotting cameras allows the accommodation of photography with 25° of inherent common tip. The 210-mm-focal-length Stereoplanigraph C-8 will accommodate up to 13 percent of scale difference between exposures comprising a stereoscopic image. Although no test utilizing Ranger photography has been initiated, theoretically the absorption of scale difference can be increased to accommodate photographs, with a scale factor diffence up to six, by pairing the special focal-length cameras which range from 100 to 600 mm.

b. Resolution. Resolution tests showed that the 210-mm-focal-length Stereoplanigraph C-8 will resolve a minimum of 57 lines/mm at the maximum projection distance and 26 lines/mm at the minimum projection distance. In order to exploit the maximum resolving power of the 210-mm-focal-length Stereoplanigraph C-8, the Ranger material should have a minimum resolution of 176 lines/mm.

c. Grid Flatness Test. A comparison of the results of the 210-mm-focal-length Stereoplanigraph grid model flatness test with the results of previous grid model flatness tests of the 152.4-mm-focal-length Stereoplanigraph showed an increased indicated vertical accuracy approximately equal to one part in 8,400.

14. CONCLUSIONS. It was concluded that the 210-mm-focal-length Stereoplanigraph C-8 will:

a. Accommodate photography with 25° of inherent common tip.

b. Exploit the Ranger photography with inherent resolution up to 176 lines/mm at diapositive scale.

c. Provide stereoscopic models at projection distances ranging from 200 to 600 mm with an average standard deviation of 0.016 mm from a true plane.

SECTION IV. SELECTED BIBLIOGRAPHY

"Comparative Evaluation of Stereoplotting Equipment." Army Map Service Draft Report. Undated.

"Evaluation of Balplex Equipment." Army Map Service Technical Development Final Report. Washington: U. S. Army Map Service. 1 May 1959.

LYON, D. Basic Metrical Photogrammetry. St. Louis: John S. Swift Company. 1960.

PHASE THREE

CHAPTER 4

LENS DISTORTION CORRECTION

SECTION I. INTRODUCTION

1. GENERAL. One reason for utilizing analytical approaches to photogrammetric problems is the fact that known systematic errors, such as lens distortion, can be corrected in the mathematical reduction. Although a standard camera calibration certificate is not available for the Ranger cameras, the Jet Propulsion Laboratory (JPL) furnished a three-point graph representing the radial lens distortion at a calibrated focal length of 26.09 mm. This chapter defines the elements of interior orientation that were used in the Ranger analytical computation, and discusses a computer program that was written to compute the radial distortion equation from the Ranger camera calibration data. These equations were used to correct the effect of radial lens distortion in the analytical adjustments discussed in chapter 6.

2. PROBLEM DEFINITION. The main problem to be dealt with in this chapter is called "interior orientation." By interior orientation, it is understood that the bundle of rays that existed, between the object and the lens, at the instant of exposure is geometrically reconstructed.

3. GEOMETRICAL DEFINITION. In a geometrical sense, the interior orientation is determined as the data that fix the perspective center with respect to the image plane during photography. These elements are illustrated in figure 4-1 and are defined as follows:

a. The principal point (x_p, y_p) is the position of the image plane at the foot of the perpendicular from the perspective center to the image plane.

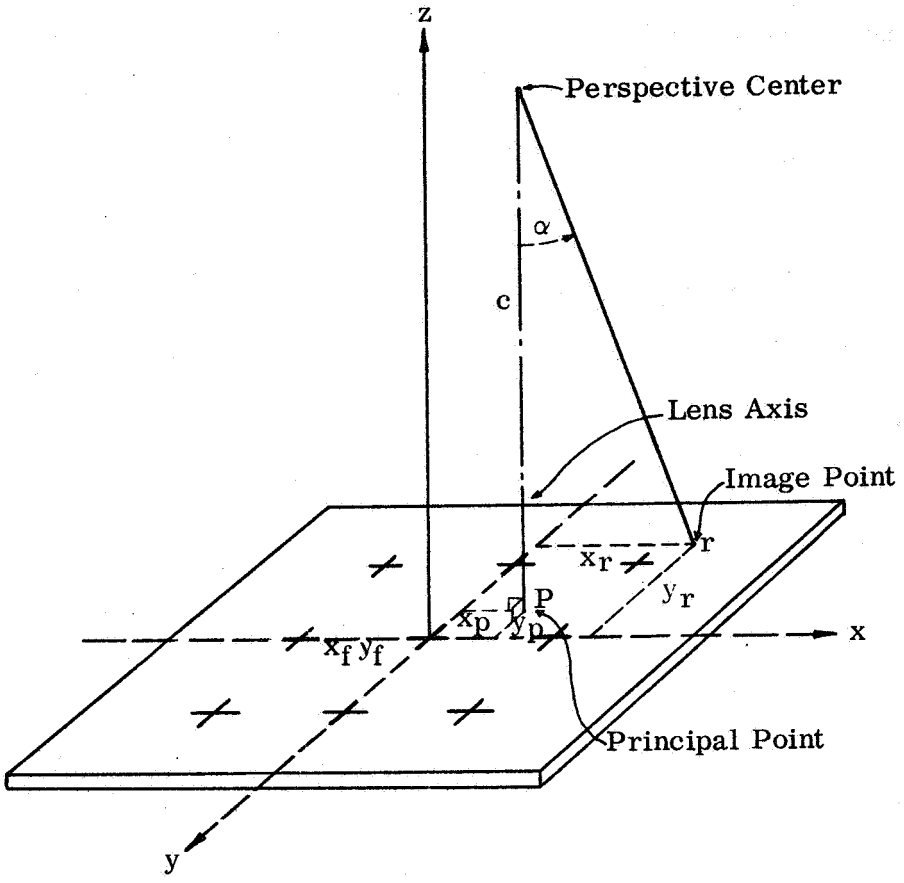

Figure 4-1. Interior Geometry.

b. The length of this perpendicular or the distance from the perspective center to the image plane is called the principal distance [focal length (c)].

c. Radial lens distortion is usually given in tabular or graphic values. It is the amount a point is displaced radially away from its true position, on the photography, due to radial lens distortion.

4. RANGER VIII A CAMERA DATA. Since a standard calibration certificate is not available for the Ranger A camera, some assumptions were made, and then associated with the information obtained from JPL. These assumptions for Ranger VIII A camera are as follows:

a. No clearly defined principal point (x_p, y_p) is given, hence it was assumed to be zero, coinciding with the intersection of the four reticle marks that surround the center reticle. Ideally, this value does coincide with the fiducial intersections, but is seldom exactly true.

b. The length of the perpendicular (c), the focal length, is 26.09 mm, as furnished by JPL to AMS. The given (c) is often published as 25.00 mm.

c. A three-point graph, copied from the JPL three-point radial distortion graph, is shown in figure 4-2. The radial distortion Δr is directed radially away from (positive) or toward (negative) the principal point, and it is a function of the radial distance r (called d, by Schmid[1]) from the principal point. All radial distortion (Δr) values, as given by the JPL graph, are negative. Lens distortion may be represented by:

(1) A graph of Δr plotted with respect to α as in figure 4-2.

(2) A polynomial of the form:

$$\Delta r = K_0 r + K_1 r^3 + K_2 r^5 + K_3 r^7 + \cdots .$$

[1] Superscripts refer to similarly numbered entries in the Literature Cited section of the chapter.

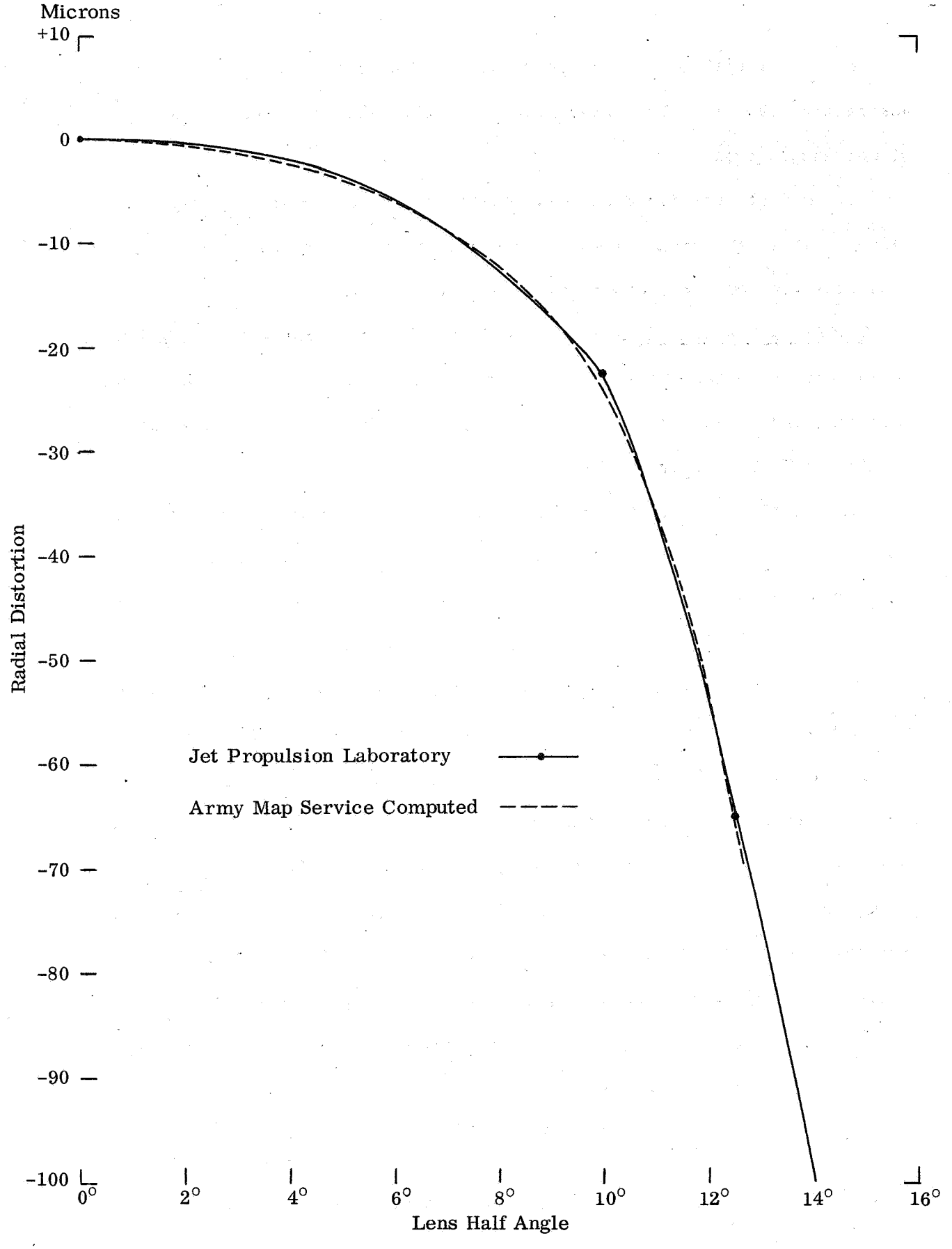

Figure 4-2. Ranger VIII A Camera Radial Distortion Curve.

SECTION II. MATHEMATICAL TREATMENT

5. GENERAL FORM OF RADIAL DISTORTION EQUATION. The general form for the radial distortion curve that is accepted by photogrammetrists such as, Schmid[1], Brown[2], Sewell[3], and Doyle[4] is a polynominal of the form

$$\Delta r = K_0 r + K_1 r^3 + K_2 r^5 + K_3 r^7 + \cdots$$

where Δr is the radial distortion at a point x, y

r is the radial distance from the principal point (x_p, y_p)

K's are the unknown lens distortion parameters.

Also, $r = c \tan \alpha$, where α is the angle given in figure 4-1.

6. LEAST SQUARES CURVE FIT. Given a set of Δrs and αs for a camera of given focal length, c, the normal equations can be formed provided that a minimum of four sets of Δr and α are given. More than four are required to benefit from least squares.

a. Observation Equations. Given N observations from the calibration certificate, where N is usually less than 11, the observations can be formed in matrix notation as follows:

$$\begin{bmatrix} \Delta r_1 \\ \Delta r_2 \\ \vdots \\ \vdots \\ \Delta r_n \end{bmatrix} = \begin{bmatrix} r_1 & r_1^3 & r_1^5 & r_1^7 \\ r_2 & r_2^3 & r_2^5 & r_2^7 \\ \vdots & \vdots & \vdots & \vdots \\ \vdots & \vdots & \vdots & \vdots \\ r_n & r_n^3 & r_n^5 & r_n^7 \end{bmatrix} \begin{bmatrix} K_0 \\ K_1 \\ K_2 \\ K^3 \end{bmatrix} \qquad (4\text{-}1)$$

or $$\Delta r = RK, \qquad (4\text{-}2)$$

b. Normal Equations. The normals can be formed by multiplying each side of equations (4-2) by the transpose of matrix R called "R^T".

Then $[R^T R]\ (K) = [R^T \Delta r]$ are the normal equations. (4-3)

In detail they are:

$$\begin{bmatrix} \Sigma r^2 & \Sigma r^4 & \Sigma r^6 & \Sigma r^8 \\ \Sigma r^4 & \Sigma r^6 & \Sigma r^8 & \Sigma r^{10} \\ \Sigma r^6 & \Sigma r^8 & \Sigma r^{10} & \Sigma r^{12} \\ \Sigma r^8 & \Sigma r^{10} & \Sigma r^{12} & \Sigma r^{14} \end{bmatrix} \begin{bmatrix} K_0 \\ K_1 \\ K_2 \\ K_3 \end{bmatrix} = \begin{bmatrix} \Sigma r \Delta r \\ \Sigma r^3 \Delta r \\ \Sigma r^5 \Delta r \\ \Sigma r^7 \Delta r \end{bmatrix} \quad (4\text{-}4)$$

where Σ_r considers all rs from 1 to N.

The solution to equations (4-3) by taking the inverse is

$$(K) = [R^T R]^{-1} [R^T \Delta r]$$

or the four unknown coefficients (K) may be obtained by considering equations (4-4) as a set of simultaneous linear equations in four unknowns. The resulting equation representing the lens distortion for the given data is $\Delta r_i = K\ r_i + K_1 r_i^3 + K_2 r_i^5 + K_3 r_i^7$; K_0, K_1, K_2 and K_3 and is the direct input to the Comparator/Analytical Photogrammmetric System described in chapter 6. For example, the corrected photo coordinates are then computed by the expressions

$$x_i' = x_i \left(1 - \frac{\Delta r_i}{r_i}\right)$$

$$y_i' = y_i \left(1 - \frac{\Delta r_i}{r_i}\right).$$

x_i', y_i' are photo coordinates corrected for the effect of radial distortion. x_i, y_i are photo coordinates reduced to the principal point, but not corrected for distortion.

SECTION III. RANGER VIII A CAMERA DISTORTION DATA

7. GIVEN RADIAL DISTORTION DATA FROM JPL. During a coordination trip by AMS personnel to JPL, a radial distortion graph was obtained. The graph is based on three points with Δr and the angle α given for the three points at a focal length of 26.09 mm.

8. GRAPH OF DISTORTION. Figure 4-2 is a copy of the original JPL data with additional values interpolated by AMS to provide data to define the polynomial to be fitted. Distortion at α = 12.5 degrees is -65 microns.

SECTION IV. COMPUTER PROGRAM FOR COMPUTING RADIAL DISTORTION CURVE

9. GENERAL. This program was written in order to develop a capability to utilize any radial distortion configuration such as Ranger, Orbiter, etc. The program is written in FORTRAN IV for the Honeywell-800 Computer. Since it is in FORTRAN, it can be easily adapted to most computers.

10. INPUT. The input to the program is by punch cards as follows:

Card No.	Columns	Input
1	1 - 48	User's option, such as name and no. of camera.
2	2	Set to 1 for Δr and azimuth, α . Set to 2 for Δr and radial distance, r.
	30 - 45	Focal length.
	66 - 67	No. of sets of Δr and azimuth or of Δr and radial distance.
	80	Last card indicator.
3,4..n		If Δr and azimuth.
	7 - 22	Δr.
	35 - 42	Azimuth or if radial distance instead of azimuth.
	30 - 45	Radial distance.

11. OUTPUT. The program fits the curve, computes residuals and RMSE of the fit. Each of these items can be seen in the output sheets. (See

figure 4-3.) Note that focal lengths of 26.09, 41.5975, 55.1806, etc., are shown. These represent the focal lengths of enlarged photographs (plates), so images of overlapping photographs would be nearly the same scale, and, therefore, measurements could be made by a stereocomparator.

SECTION V. APPLICATION TO LUNAR ORBITER MISSIONS

12. DATA UTILIZATION. Cameras for the Lunar Orbiter missions will be calibrated and calibration certificates will be furnished to all users. The program described in this chapter will be utilized to compute the radial distortion curves for these cameras. These data can be utilized in all photogrammetry applications that correct for radial distortion.

SECTION VI. LITERATURE CITED

1. SCHMID, H. H. "A General Analytical Solution to the Problem of Photogrammetry," Ballistic Research Laboratories Report No.1065. Aberdeen, Md.: Aberdeen Proving Ground. Jul 1959.

2. BROWN, D. "A Treatment of Analytical Photogrammetry with Emphasis on Ballistic Camera Applications," RCA Data Reduction Technical Report No. 39. New York: Radio Corporation of America. Aug 1957.

3. SEWELL E. D. "Aerial Cameras," in Manual of Photogrammetry, M. M. Thompson, ed. Falls Church, Va.: American Society of Photogrammetry. 1966: Vol I, Ch IV.

4. DOYLE, F. J. "Analytical Photogrammetry." Ibid. Ch X.

LINEAR VALUES ARE IN METERS EXCEPT VALUES WITH * ARE IN MICRONS.

ARIZONA TEST DATA, TYPE T-11 CAMERA, NO. 63-112

FOCAL LENGTH .1520120 SUM (RESIDUALS) -.0000001 RMSE .0000012

ANGLE (DEG.)	7.5	15.0	22.5	27.5	30.0	32.5	35.0	37.5	40.0	42.5	45.0
* DISTORTION DELTA R	1.0	1.0	-6.0	-9.0	-10.0	-9.0	-6.0	4.0	10.0	10.0	-2.0
* CALCULATED DELTA R	1.6	-.0	-5.7	-9.3	-9.7	-8.3	-4.6	1.7	8.9	12.1	-2.6
* RESIDUALS	-.6	1.0	-.3	.3	-.3	-.7	-1.4	2.3	1.1	-2.1	.6

K0 .11072891E-03 K1 -.80874316E-01 K2 .85212697E 01 K3 -.22766072E 03

RANGER VIII, CAMERA A

FCCAL LENGTH .0760900 SUM (RESIDUALS) .0000003 RMSE .0000005

ANGLE (DEG.)	.5	4.0	5.0	6.0	7.0	8.0	9.0	10.0	11.0	12.0	12.5
* DISTORTION DELTA R	.0	-2.0	-4.0	-6.5	-8.5	-12.5	-17.0	-23.5	-36.0	-54.0	-65.0
* CALCULATED DELTA R	-.2	-2.6	-4.0	-5.9	-8.5	-12.1	-17.1	-24.4	-35.7	-53.2	-65.5
* RESIDUALS	.2	.6	-.0	-.6	.0	-.4	.1	.9	-.3	-.8	.5

K0 -.73480024E-03 K1 -.21376057E 03 K2 .49506588E 07 K3 -.23981750E 12

RANGER VIII, CAMERA A, PLATE NO. 499

FOCAL LENGTH .0551806 SUM (RESIDUALS) .0000005 RMSE .0000010

ANGLE (DEG.)	.5	4.0	5.0	6.0	7.0	8.0	9.0	10.0	11.0	12.0	12.5
* DISTORTION DELTA R	.0	-4.2	-8.5	-13.7	-18.0	-26.4	-36.0	-49.7	-76.1	-114.2	-137.5
* CALCULATED DELTA R	-.4	-5.4	-8.4	-12.6	-18.1	-25.6	-36.1	-51.7	-75.5	-112.6	-138.5
* RESIDUALS	.4	1.2	-.0	-1.2	.1	-.9	.2	2.0	-.7	-1.6	1.1

K0 -.73479992E-03 K1 -.47786252E 02 K2 .24740815E 06 K3 -.26792093E 10

Figure 4-3. Output Sheet for Radial Lens Distortion Program.

LINEAR VALUES ARE IN METERS EXCEPT VALUES WITH * ARE IN MICRONS.

RANGER VIII, CAMERA A, PLATE NO. 515

FOCAL LENGTH .0415975 SUM (RESIDUALS) .0000004 RMSE .0000008

ANGLE (DEG.)	.5	4.0	5.0	6.0	7.0	8.0	9.0	10.0	11.0	12.0	12.5
* DISTORTION DELTA R	.0	-3.2	-6.4	-10.4	-13.6	-19.9	-27.1	-37.5	-57.4	-86.1	-103.6
* CALCULATED DELTA R	-.3	-4.1	-6.4	-9.5	-13.6	-19.3	-27.2	-39.0	-56.9	-84.9	-104.4
* RESIDUALS	.3	.9	-.0	-.9	.1	-.7	.1	1.5	-.5	-1.2	.8

K0 -.73479696E-03 K1 -.84089667E 02 K2 .76611667E 06 K3 -.14598994E 11

RANGER VIII, CAMERA A, PLATE NO. 563

FOCAL LENGTH .0530918 SUM (RESIDUALS) .0000005 RMSE .0000010

ANGLE (DEG.)	.5	4.0	5.0	6.0	7.0	8.0	9.0	10.0	11.0	12.0	12.5
* DISTORTION DELTA R	.0	-4.1	-8.1	-13.2	-17.3	-25.4	-34.6	-47.8	-73.3	-109.9	-132.3
* CALCULATED DELTA R	-.3	-5.2	-8.1	-12.1	-17.4	-24.6	-34.8	-49.8	-72.6	-108.4	-133.3
* RESIDUALS	.3	1.1	-.0	-1.2	.1	-.8	.2	1.9	-.6	-1.5	1.0

K0 -.73480044E-03 K1 -.51620327E 02 K2 .28870166E 06 K3 -.33772295E 10

RANGER VIII, CAMERA A, PLATE NO. 565

FOCAL LENGTH .0411782 SUM (RESIDUALS) .0000004 RMSE .0000008

ANGLE (DEG.)	.5	4.0	5.0	6.0	7.0	8.0	9.0	10.0	11.0	12.0	12.5
* DISTORTION DELTA R	.0	-3.2	-6.3	-10.3	-13.4	-19.7	-26.8	-37.1	-56.8	-85.2	-102.6
* CALCULATED DELTA R	-.3	-4.0	-6.3	-9.4	-13.5	-19.1	-27.0	-38.6	-56.3	-84.0	-103.4
* RESIDUALS	.3	.9	-.0	-.9	.1	-.7	.1	1.5	-.5	-1.2	.8

K0 -.73479970E-03 K1 -.85810433E 02 K2 .79778948E 06 K3 -.15513828E 11

Figure 4-3. Continued.

CHAPTER 5

ANALOG PLOTTER/MATHEMATICAL ORIENTATION SYSTEM

SECTION I. INTRODUCTION

1. PROBLEM DEFINITION. Relative orientation of Ranger VIII stereomodels can be achieved in the stereoplanigraph with Ranger VIII photography; but, due to physical limitations of the instrument, absolute orientation cannot be achieved largely because of the excessive tilts inherent in this photography. GETRAN (General Transformation, previously titled X, Y, Z Transformation Program [Absolute Orientation]) was developed out of a need to continue where the stereoplanigraph leaves off in order to achieve absolute orientation of the stereoplanigraph x, y, z-coordinates. GETRAN is a program for a rigorous least squares transformation of one orthogonal coordinate system to another. It also considers the curvature of the defined spheroid.

2. GENERAL DESCRIPTION. Section II below has been designed to provide the reader with not only a general description of the program and its options, but also a general description of the mathematics used throughout the program. In this section, the descriptions are in the exact order of the logical execution of the program. This provides the reader with the basic logic pattern used in the program and provides a quick reference as to what is happening at any point in the program. Specific formulae which were used in the transformations, the adjustment, and various miscellaneous mathematical special purpose formulae used in the program are given in section III.

3. SYSTEM CONFIGURATION. GETRAN is coded in FORTRAN IV programming language and is designed to be operational on the Honeywell-800 system. This system has a 16,000 word position memory. Each word has a 48-bit structure which eliminates the necessity of double precision.

SECTION II. GENERAL DESCRIPTION OF PROGRAM OPERATION.

4. USER OPTIONS. The program has been designed to be as flexible as possible within the limits of memory storage capacity of the Honeywell-800.

a. Digital Contouring Format Option. The user may elect to have the adjusted data written in a format that is acceptable to a digital contouring program (described in chapter 7).

b. Surface Control Input Options. Several types of input options are available for the surface control values. The user may enter surface control values in a right-handed rectangular Cartesian coordinate system (X, Y, and Z). The adjusted answers will be in the same X, Y, and Z system (curvature correction is not considered in this option). Or, the user may enter surface control values in the Planetodetic* (φ, λ, and h) Coordinate System. Values for φ and λ may be entered either as decimal degrees or degrees, minutes, and seconds. The value of the elevation, h, is entered in meters.

c. Variable Solution Option. There are three types of solutions

---

*The Analog Plotter/Mathematical Orientation System is a completely general system which can be applied to any ellipsoid of any planet. The use of such terms as geodetic and selenodetic would be incorrect because these terms refer to specific heavenly bodies. The need for a vocabulary of general terms that could be used to refer to any planet was established. The terms used in this chapter will be defined when they are first introduced.

> planetodetic [Greek planētēs to wander + daisia, stem of daiesthai, to divide.] Relating to the geometry of planetodetic lines of a planet (defined in the same way as the geometry of the geodetic lines for the planet Earth).

possible: non-conformal, modified conformal, and conformal.

(1) Non-conformal Solution. The user may elect to have the adjustment based on the non-conformal solution where scale X, scale Y, and scale Z are left at their computed values and are not necessarily equal.

(2) Modified Conformal Solution or Conformal Solution. The user may elect to have the adjustment based on a conformal solution. If this option is elected, the program will compute a common scale for X and Y and examine the difference between this common scale and the non-conformal scale Z. Should this difference be large, the program will compute a modified conformal solution where scale X and Y are forced to a common scale, and scale Z is held at its non-conformal value. Should this difference be small, the scale X, scale Y, and scale Z will be forced to the common scale. In either one of the two conditions, the program will make the necessary adjustments to the other orientation parameters.

d. More Than One Adjustment. The user may wish to run more than one adjustment. The program is designed to accommodate an infinite number of separate solutions. This eliminates the necessity of recompiling the program for every solution.

5. MAXIMUM AND MINIMUM NUMBER OF CONTROL POINTS. a. Maximun Number of Control Points. The program consumes a large porition of memory. Due to this fact, it was necessary to limit the number of surface control points that may be entered to 50 for any single solution.

b. Minimum Number of Control Points. Because three independent scales are determined for scale X scale Y, and scale Z, a unique solution is obtained with four surface control points. Therefore, a minimum solution is obtained with four points.

c. Error Check. In any attempt to use less than four or more than 50 surface control points as stated above, the program will generate an error, calculations will be terminated, and the program will go to the next solution.

6. PLANETODETIC CONVERSION. a. Planetodetic Coordinate System to Local Space Rectangular Coordinate System (LSRCS). The program will convert the Planetodetic Coordinate System to an LSRCS for the control net that was entered into the program. The planetodetic coordinates are projected onto the equatorial plane, which yields planetocentric* coordinates. A centroid value for both the planetodetic system and the planetocentric system is computed. The planetocentric system is then passed through a rotation matrix to obtain the LSRCS. At this point, a false value is added to the X, Y, and Z values to make them positive.

b. Translating the System and Program Edit for φ, λ, and h and the Computed LSRCS Values. These false values, mentioned in the previous paragraph, translate the system to a positive region. These values are removed after the adjustment problem is completed immediately before the LSRCS is returned to the Planetodetic Coordinate System. An edit of the original φ, λ, and h values that were entered and the corresponding LSRCS Y, Y and Z values are given.

7. FINAL ORIENTATION -- NON CONFORMAL SOLUTION. a. Centroid. A centroid is first calculated for the LSRCS. This is done in order to reduce the magnitude of the numbers. Also, a centroid is calculated for the instrument

---

*planetocentric [Greek planētēs to wander + -centric.] Relating to, measured from, or as if observed from a planet's center.

values corresponding to the known surface control in order to make the instrument system compatible with the surface control system.

b. Final Orientation Using Least Squares. The observation equations are formed for the control net (net refers to the known surface control and the corresponding instrument values to known surface control). The least squares iterative process is then carried out until no further change in the successive approximations of the unknowns, scale X, scale Y, and scale Z, ω, φ, κ, X_o, Y_o and Z_o are detected.

c. Program Monitor. The program will monitor the first three iterations to make sure that no negative scale factors are generated and that the angles ω, φ, and κ do not go larger than 2π. Should negative scale factors or angles greater than 2π be generated, the program takes the absolute values of all the scale factors and zeros the angles. After three iterations, the program releases control and no further intervention is obtained. Practice has shown that it is useless to monitor beyond three iterations, and that adequate approximations are obtained in this manner.

8. NON-CONFORMAL, CONFORMAL, OR MODIFIED CONFORMAL SOLUTION. The program computes a common scale using the non-conformal values of scale X and scale Y. The program then checks to see if a conformal solution is desired.

a. Non-conformal. A non-conformal solution utilizes the three different scale factors, scale X, scale Y and scale Z to transform the observed x, y, z-coordinates of the relatively oriented stereomodel.

b. Conformal. If the conformal solution has been called for through program option, the program will examine the difference between the common scale and the non-conformal scale Z. Should this difference be small, the

program will force the three non-conformal scales equal to the common scale and make adjustments to the other parameters ω, φ, κ, X_o, Y_o, and Z_o to conform to the conformal requirements.

c. Modified Conformal. Should the difference between the common scale and the non-conformal scale Z be large, a modified conformal solution will be computed forcing scale X and scale Y to be equal to the common scale, holding scale Z at its non-conformal value, and making adjustments to the other parameters.

d. Constrained Solution. This constraint is accomplished by employing a matrix bordering technique given by Dr. H. H. Schmid.[1]

e. Results. Practice is in agreement with theory and has shown that a modified conformal solution yields smaller residuals than the conformal solution, and that the non-conformal solution yields smaller residuals than either the modified conformal or conformal solutions.

f. Advantages and Disadvantages. Each solution (non-conformal, modified conformal, and conformal) has its advantages and disadvantages. The user must determine which solution will give the best results for the given circumstances.

g. Final Adjustment. The program then computes the final adjustment based on the type of solution called.

9. STATISTICAL ANALYSIS. At this point a statistical analysis is computed. Errors for all the computed parameters are computed and standard errors for the problem are determined.

10. INTERMEDIATE PROGRAM EDIT. A complete edit is given. This edit shows the level of the approximations for each iteration, program monitor

intervention, the solution to the non-conformal parameters, the conformal (or modified conformal) solution, and the statistical error analysis.

11. SOLUTION EDIT. A listing of the instrument values and the corresponding known surface control in the LSRCS is given. Also, the adjusted instrument values and the amount the adjusted instrument values deviated (Delta Values) from the known surface control are listed for evaluation purposes.

12. AUTOMATIC STATISTICAL POINT DELETION. Once the program has obtained the final adjusted values, the program will then compute a sigma for each point and compare the point sigma to the sigma of the problem. If a single point(s) is (are) larger than 3.3 sigma for the problem, the probability of a measuring blunder is quite high and this point is tagged as a deleted point. The program then branches back to the beginning of the computations and computes a new solution deleting the tagged point(s) as the computations are executed. The solution is based on the untagged point(s) and the edits are as described in the above paragraphs. This automatic deletion is done only once.

13. LOCAL SPACE RECTANGULAR COORDINATE SYSTEM TO PLANETODETIC COORDINATE SYSTEM. This procedure is the reverse of the procedure previously described in section II, paragraph 6. Briefly, the false values are removed from each point, passed through the rotation matrix to obtain the planetocentric coordinates, and the final planetodetic coordinates (φ , λ , and h) are obtained for each adjusted point.

14. MERCATOR PROJECTION. Once the planetodetic coordinates are obtained, they are carried into the spherical Mercator projection. The spherical form of the Mercator projection is used because the eccentricity of the moon has not yet been determined.

a. Mercator Edit. An edit showing the final computed planetodetic

coordinates for each adjusted control point is listed along with its corresponding Mercator projection value. If the Control Data Corporation (CDC) contouring program format option is called, a punch tape is written on magnetic tape and also a write tape is written in the proper CDC format.

b. Known Control Edit Completed. This completes the output of the known control points and the adjusted instrument values.

15. PASS POINTS. a. Definition. All instrument readings that do not have corresponding known surface control values are considered to be model image points (pass points).

b. Instrument Values to LSRCS. Each pass point read by the computer has the instrument centroid for the net subtracted from the x, y, and z for that point. A set of system equations are formed to determine the adjusted values. The known control centroid is then added to the adjusted values. Thus, the local space rectangular values are formed.

c. LSRCS to Planetodetic Coordinate System. Taking the local space rectangular values, the planetodetic coordinate values are obtained by first rotating to the planetocentric coordinate system and then calculating the planetodetic φ , λ ,and h for each point.

d. Planetodetic Coordinate System to Mercator Projection. Taking the planetodetic φ , λ , and h, the spherical Mercator projection values are computed. This is done for each pass point. The number of pass points that the program will handle is unlimited.

e. Pass Point Edit. An edit of the instrument values that were entered and their corresponding spherical Mercator projection values are given.

f. Last Card Indicator. A last card indicator is inserted or added after the last pass point. When the last pass point has been read, the

program will examine to see if the user has indicated that another solution is desired. If another solution is not desired, the program is terminated. If another solution is desired, the storage areas are initialized and the process is repeated for the next solution.

SECTION III. MATHEMATICAL ANALYSES AND DEFINITIONS

16. INTRODUCTION. In the pages that follow, the mathematics necessary to achieve absolute orientation and the Mercator map projection coordinates are given. The order in which the mathematics appear is in the same logical order that they are executed in GETRAN.

17. PLANETODETIC COORDINATE SYSTEM TO PLANETOCENTRIC COORDINATE SYSTEM AND THEN TO LSRCS[2]. a. Planetocentric Coordinate System. A useful coordinate system that is often used in analytical photogrammetry is the Planetocentric Coordinate System. This system is a right-handed orthogonal system (fig. 5-1), with an origin at the center of the spheroid; the Z' axis is positive, upward, passing through the North Polar Axis; the X' and Y' axes lie in the plane of the equator with the X' axis passing through the prime meridian.

b. Representation of a Standard Ellipsoid of Revolution. Any standard ellipsoid of revolution can be represented by

a = semi-major axis,

b = semi-minor axis,

and e = eccentricity,

where the eccentricity, e, is defined as

$$e=[(a^2 - b^2) / (a^2]^{\frac{1}{2}}. \qquad (5\text{-}1)$$

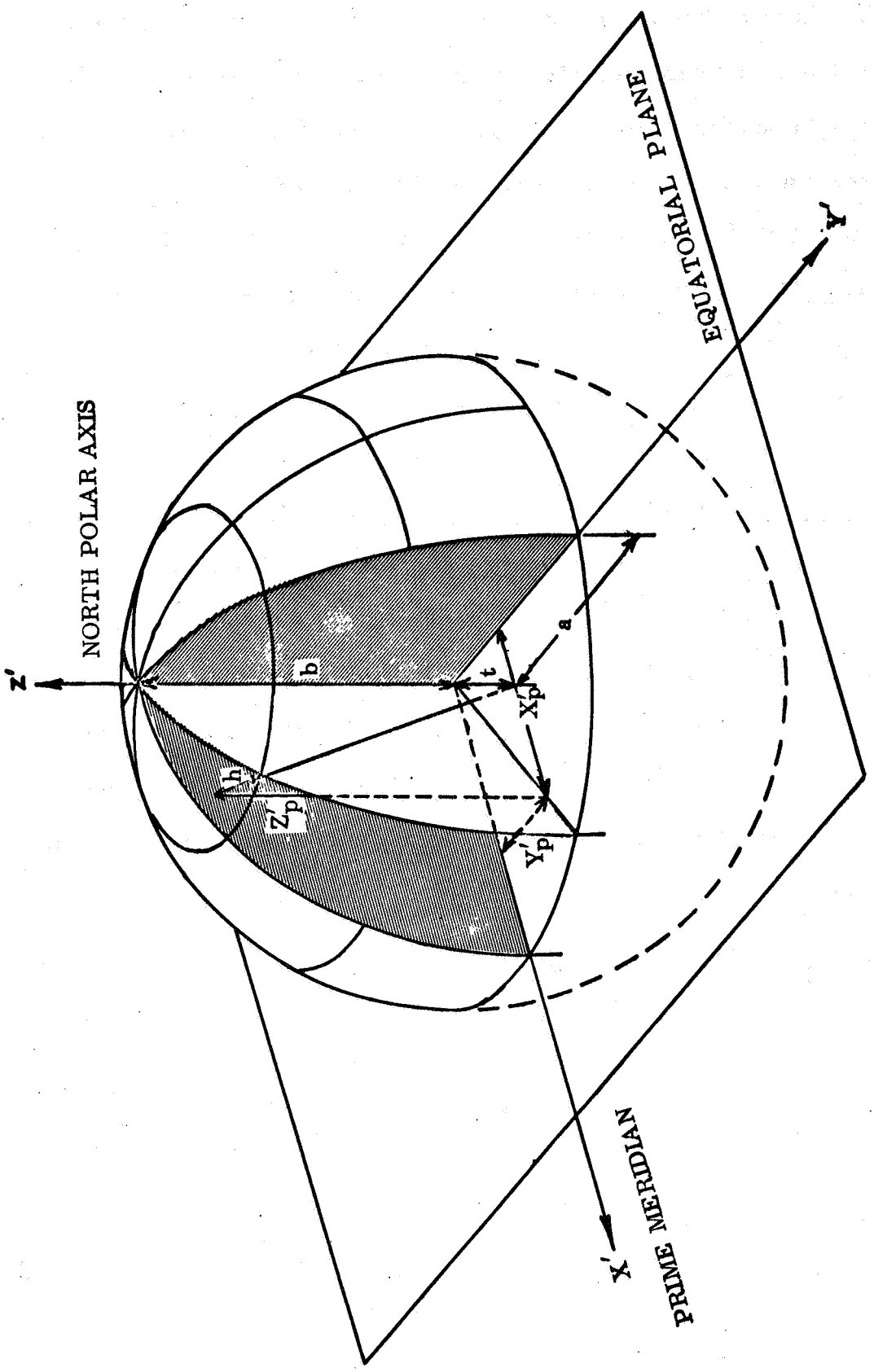

Figure 5-1. Planetocentric Coordinate System.

c. Planetodetic Coordinate System to Planetocentric Coordinate System. If a point is taken (fig. 5-1) which represents the camera station at an elevation, h, above the ellipsoid with planetodetic coordinates

φ = latitude,

λ = longitude,

the planetocentric coordinates can be found from the planetodetic coordinates by the formulae

$$N = (a)/(1 - e^2 \operatorname{Sin}^2 \varphi)^{\frac{1}{2}} \tag{5-2}$$

$$X' = (N + h) \operatorname{Cos} \varphi \operatorname{Cos} \lambda \tag{5-3}$$

$$Y' = (N + h) \operatorname{Cos} \varphi \operatorname{Sin} \lambda \tag{5-4}$$

$$Z' = (N (1 - e^2) + h) \operatorname{Sin} \varphi. \tag{5-5}$$

d. Point(s) Definition. Thus, a point can be defined in the Planetocentric Coordinate System as a point having coordinates X_p', Y_p', and Z_p'. (See figure 5-1.) Of course, any number of points can be carried from the Planetodetic System to the Planetocentric System.

e. Advantage of LSRCS. Once the desired points have been defined in the Planetocentric System, it is advantageous to redefine these points in the LSRCS. The advantages of doing this are: (1) the magnitude of the numbers are considerably reduced and therefore requires only single precision arithmetic for data processing purposes, and (2) the LSRCS is the more common system and is more readily understood.

f. Definitions. The LSRCS, illustrated in figure 5-2, has its origin normal to the ellipsoid with an origin O. The Y-axis is defined in such a way that it points positively to the polar North and negatively to the polar South. An elevation, h_o, is generally taken as negative so that the Z-coordinate values representing the surface terrain all remain positive.

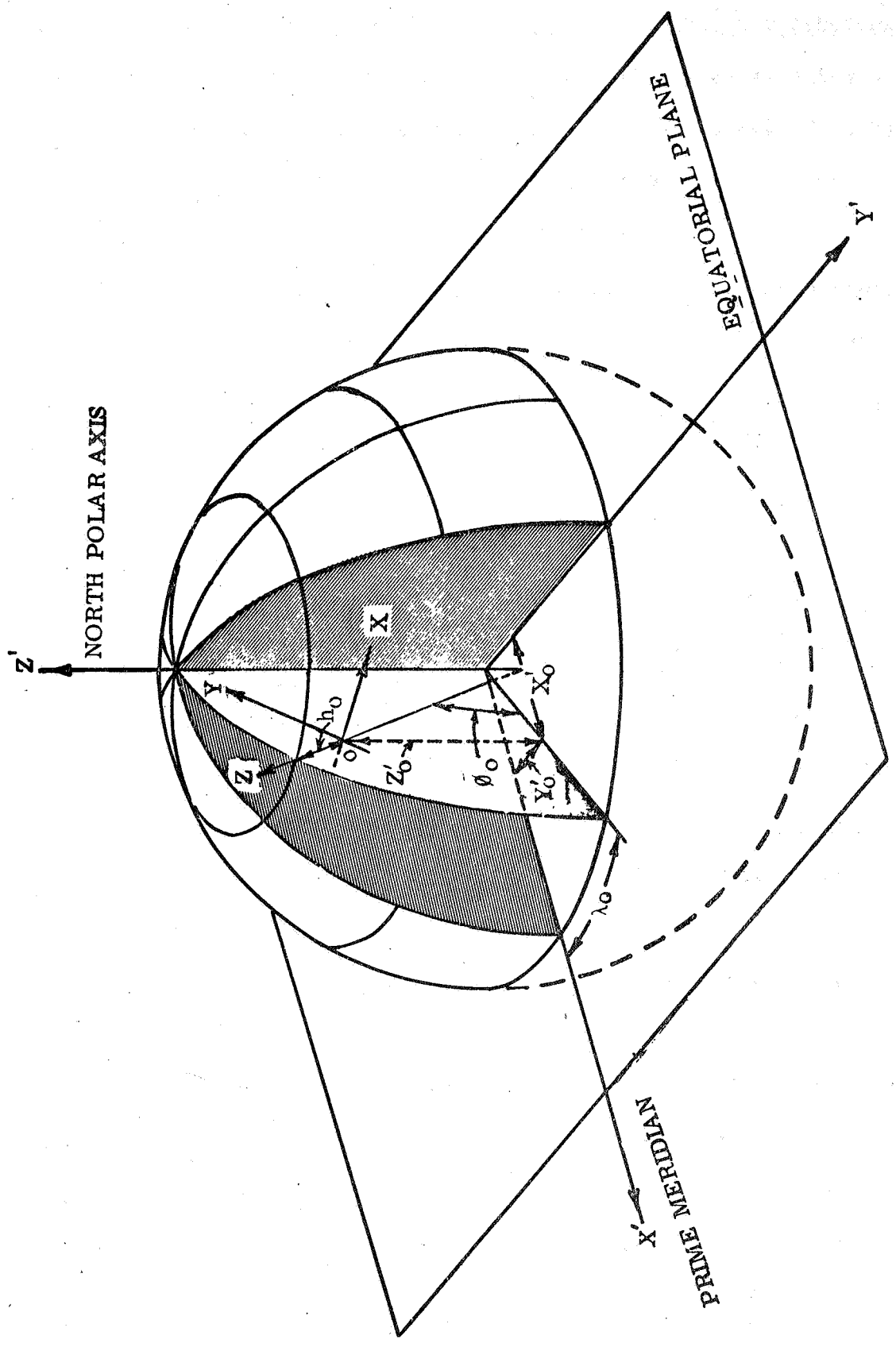

Figure 5-2. Local Space Rectangular Coordinates.

g. Translation and Rotation. In order to accomplish this, it is necessary to translate and rotate the planetocentric coordinates. This is done by first establishing a mean value or centroid value for X', Y', and Z', also φ , and λ values for the points that are being used. Let the centroid value be called X_o', Y_o', Z_o', φ_o, and λ_o as illustrated in figure 5-2. Once this has been established, a point transformation can be accomplished with the following matrix equation:

$$\begin{bmatrix} X_n \\ Y_n \\ Z_n \end{bmatrix} = \begin{bmatrix} -\sin\lambda_o & \cos\lambda_o & 0 \\ -\sin\varphi_o\cos\lambda_o & -\sin\varphi_o\sin\lambda_o & \cos\varphi_o \\ \cos\varphi_o\cos\lambda_o & \cos\varphi_o\sin\lambda_o & \sin\varphi_o \end{bmatrix} \begin{bmatrix} X_n' - X_o' \\ Y_n' - Y_o' \\ Z_n' - Z_o' \end{bmatrix} \cdot \quad (5\text{-}6)$$

h. Translation to Positive Region. Once the LSRCS values have been established for all the points of interest, false X, Y, and Z values are added to all the points which translate these values to a positive region so that analyses can be accomplished more readily. These false values for X, Y, and Z will, of course, be subtracted before these points are transformed back to the Planetodetic Coordinate System after the adjustment.

18. ADJUSTMENT (ABSOLUTE ORIENTATION). Once the control net is in the LSRCS, the corresponding instrument values to the control net can now be compatible. The instrument system is ready for absolute orientation. The two systems, instrument and control, are illustrated in figure 5-3.

a. Difference between the Instrument System and the Control System. It can be seen in figure 5-3 that the small stereoplanigraph measurement system differs from the ground control system in scale, translation, and

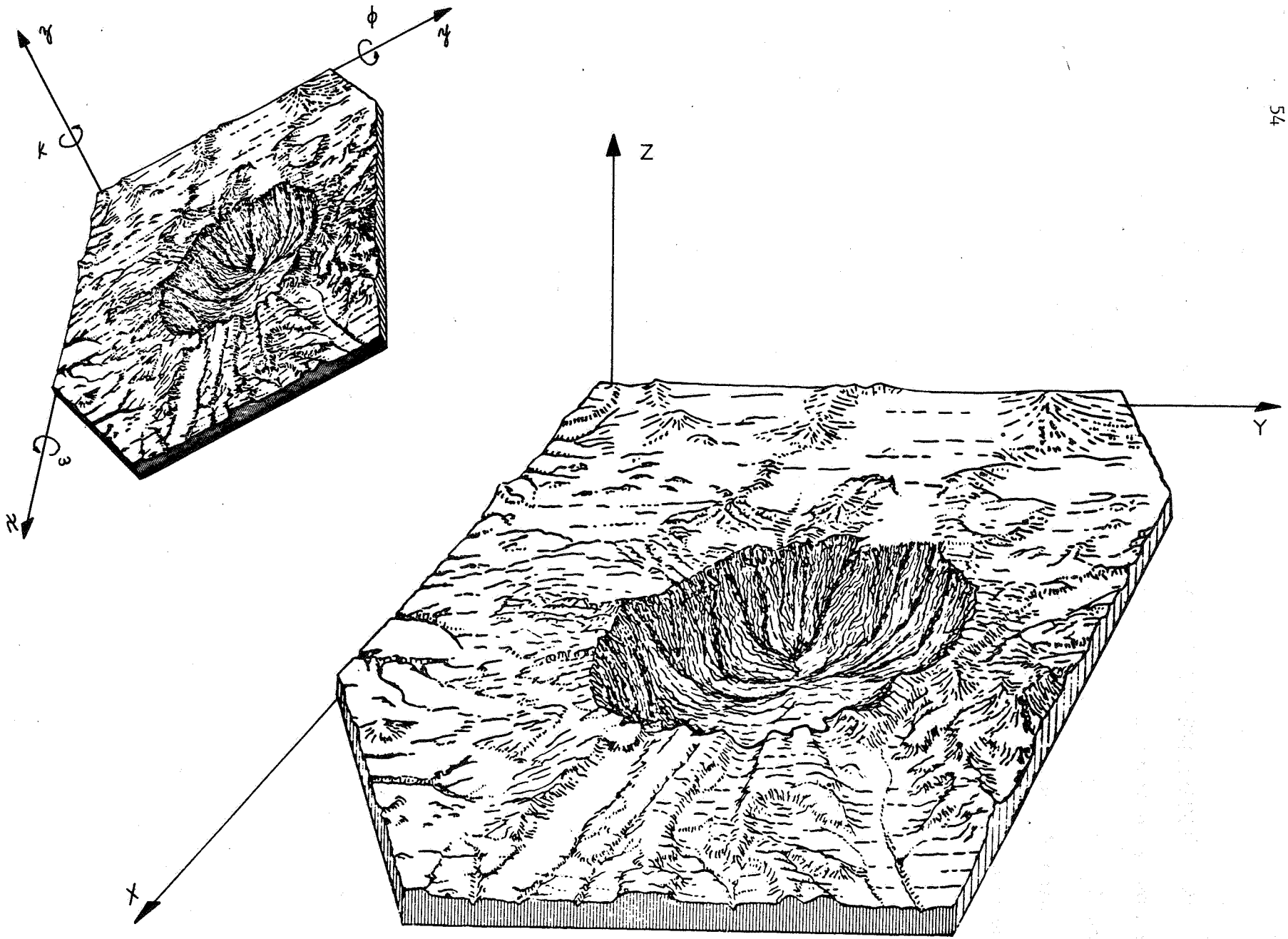

Figure 5-3. Instrument-Surface Control System.

alignment of the axis. All that remains is to define the mathematical equations that will link the instrument system to the ground control system.

b. Mathematical Conventions.[3] (1) Coordinate Convention. The mathematics used in the adjustment is defined on a right-handed Cartesian coordinate system.

(2) Angular Rotation Convention. There are three angles of rotation for the problem. They are ω, φ, and $\varkappa$, and are illustrated in figures 5-3, 5-6, 5-7, 5-8.

(a) Omega (ω). The angle ω is defined as the rotation of the instrument system zy-plane in a counterclockwise direction to the control system ZY-plane.

(b) Phi (φ). The angle φ is defined as the rotation of the instrument system xz-plane in a counterclockwise direction to the control system XZ-plane.

(c) Kappa ($\varkappa$). The angle $\varkappa$ is defined as the rotation of the instrument system xy-plane in a counterclockwise direction to the control system XY-plane.

c. Derivation of the Non-linear Observation Equations Using Taylor's Theorem for Linearization.[4 5] First, the instrument system can be related to the control system by establishing correspondence between the axis of the two systems. This correspondence is commonly referred to as the "orientation elements." There are nine orientation elements which establish an angular relationship between the various axes. These angular relationships are illustrated in figure 5-4.

∠	x	y	z
X	xX	yX	zX
Y	xY	yY	zY
Z	xZ	yZ	zZ

Figure 5-4. Angles between the Various Axes

These relationships lead directly to the direction cosines shown in figure 5-5.

Cos(∠)	x	y	z
X	Cos (xX)	Cos (yX)	Cos (zX)
Y	Cos (xY)	Cos (yY)	Cos (zY)
Z	Cos (xZ)	Cos (yZ)	Cos (zZ)

Figure 5-5. Direction Cosines.

Using the conventions previously established, the angles ω , φ , and κ can be defined as shown in figures 5-6, 5-7, and 5-8. However, these definitions must be brought into a homogeneous system in order to utilize them. Taking the definitions in figures 5-6, 5-7, and 5-8, three matrices can be defined as

$$A_\kappa = \begin{bmatrix} \text{Cos } \kappa & \text{Sin } \kappa & 0 \\ -\text{Sin } \kappa & \text{Cos } \kappa & 0 \\ 0 & 0 & 1 \end{bmatrix} , \qquad (5\text{-}7)$$

$$A\varphi = \begin{bmatrix} \text{Cos } \varphi & 0 & -\text{Sin } \varphi \\ 0 & 1 & 0 \\ \text{Sin } \varphi & 0 & \text{Cos } \varphi \end{bmatrix}, \qquad (5\text{-}8)$$

and

$$A\omega = \begin{bmatrix} 1 & 0 & 0 \\ 0 & \text{Cos } \omega & \text{Sin } \omega \\ 0 & -\text{Sin } \omega & \text{Cos } \omega \end{bmatrix}. \qquad (5\text{-}9)$$

By multiplying equations 5-7, 5-8, and 5-9 together, the following result is obtained:

$$A = A\kappa\, A\varphi\, A\omega \qquad (5\text{-}10)$$

where A = final matrix

and

$$A = \begin{bmatrix} a_{11} & a_{12} & a_{13} \\ a_{31} & a_{22} & a_{23} \\ a_{31} & a_{32} & a_{33} \end{bmatrix} \qquad (5\text{-}11)$$

where $a_{11} = \text{Cos } \varphi \text{ Cos } \kappa$

$a_{12} = \text{Cos } \omega \text{ Sin } \kappa + \text{Sin } \omega \text{ Sin } \varphi \text{ Cos } \kappa$

$a_{13} = \text{Sin } \omega \text{ Sin } \kappa - \text{Cos } \omega \text{ Sin } \varphi \text{ Cos } \kappa$

$a_{21} = -\text{Cos } \varphi \text{ Sin } \kappa$

$a_{22} = \text{Cos } \omega \text{ Cos } \kappa - \text{Sin } \omega \text{ Sin } \varphi \text{ Sin } \kappa$

$a_{23} = \text{Sin } \omega \text{ Cos } \kappa + \text{Cos } \omega \text{ Sin } \varphi \text{ Sin } \kappa$

$a_{31} = \text{Sin } \varphi$

$a_{32} = -\text{Sin } \omega \text{ Cos } \varphi$

$a_{33} = \text{Cos } \omega \text{ Cos } \varphi$.

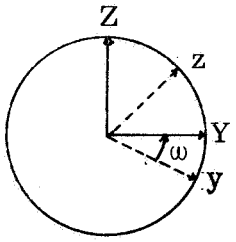

Cos(∠)	x	y	z
X	1	0	0
Y	0	Cos (ω)	Cos(270° + ω)
Z	0	Cos (90° + ω)	Cos (ω)

or

Cos(∠)	x	y	z
X	1	0	0
Y	0	Cos (ω)	Sin (ω)
Z	0	-Sin (ω)	Cos (ω)

Figure 5-6. Definition of Orientation Element ω .

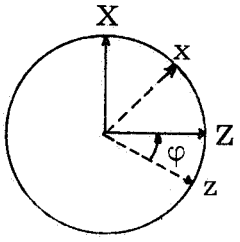

Cos(∠)	x	y	z
X	Cos (φ)	0	Cos (90° + φ)
Y	0	1	0
Z	Cos (270° + φ)	0	Cos (φ)

or

Cos(∠)	x	y	z
X	Cos (φ)	0	-Sin (φ)
Y	0	1	0
Z	Sin (φ)	0	Cos (φ)

Figure 5-7. Definition of Orientation Element φ .

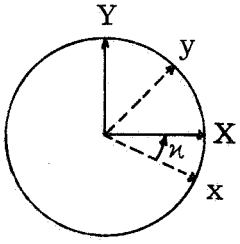

Cos(∠)	x	y	z
X	Cos (κ)	Cos (270° + κ)	0
Y	Cos (90° + κ)	Cos (κ)	0
Z	0	0	1

or

Cos(∠)	x	y	z
X	Cos (κ)	Sin (κ)	0
Y	-Sin (κ)	Cos (κ)	0
Z	0	0	1

Figure 5-8. Definition of Orientation Element κ .

Now, a scale factor (S) and translation elements (X_o, Y_o, and Z_o) are needed. For the reader who is familiar with photogrammetry these parameters are common. However, because of the unusual geometry of the Ranger VIII photography and the lack of adequate control, it was decided that the three scale factors (S_x, S_y, and S_z) should be allowed to vary. Thus, by introducing these three scale factors with the usual exterior orientation elements, nine unknown parameters were defined. They are S_x, S_y, S_z, ω, φ, κ, X_o, Y_o, and Z_o. Utilizing the A matrix given in equation 5-11, the transformation is defined as

$$\begin{bmatrix} f_x \\ f_y \\ f_z \end{bmatrix} = \begin{bmatrix} X \\ Y \\ Z \end{bmatrix} = \begin{bmatrix} S_x & 0 & 0 \\ 0 & S_y & 0 \\ 0 & 0 & S_z \end{bmatrix} \begin{bmatrix} \\ A \\ \\ \end{bmatrix} \begin{bmatrix} x \\ y \\ z \end{bmatrix} + \begin{bmatrix} X_o \\ Y_o \\ Z_o \end{bmatrix} \qquad (5\text{-}12)$$

or

$$f_x = S_x [\, x(\cos\varphi \cos\kappa) + y(\cos\omega \sin\kappa + \sin\omega \sin\varphi \cos\kappa) + z(\sin\omega \sin\kappa - \cos\omega \sin\varphi \cos\kappa)\,] + X_o - X = 0 \qquad (5\text{-}13)$$

$$f_y = S_y [\, x(-\cos\varphi \sin\kappa) + y(\cos\omega \cos\kappa - \sin\omega \sin\varphi \sin\kappa) + z(\sin\omega \cos\kappa + \cos\omega \sin\varphi \sin\kappa)\,] + Y_o - Y = 0 \qquad (5\text{-}14)$$

$$f_z = S_z [\, x(\sin\varphi) - y(\sin\omega \cos\varphi) + z(\cos\omega \cos\varphi)\,] + Z_o - Z = 0 \qquad (5\text{-}15)$$

where

x, y, and z = instrument values

X, Y, and Z = known surface control values

S_x, S_y, and S_z = independent scale factors for x, y, and z

X_o, Y_o, and Z_o = translation values

ω = rotation of the YZ-plane about the X axis

φ = rotation of the ZX-plane about the Y axis

and

κ = rotation of the XY-plane about the Z axis.

Also,

$$f_x = f(S_x^\circ + \Delta S_x, S_y^\circ + \Delta S_y, S_z^\circ + \Delta S_z, \omega^\circ + \Delta\omega, \varphi^\circ + \Delta\varphi, \kappa^\circ + \Delta\kappa, X_o^\circ + \Delta X_o) \quad (5\text{-}16)$$

$$f_y = f(S_x^\circ + \Delta S_x, S_y^\circ + \Delta S_y, S_z^\circ + \Delta S_z, \omega^\circ + \Delta\omega, \varphi^\circ + \Delta\varphi, \kappa^\circ + \Delta\kappa, Y_o^\circ + \Delta Y_o) \quad (5\text{-}17)$$

$$f_z = f(S_x^\circ + \Delta S_x, S_y^\circ + \Delta S_y, S_z^\circ + \Delta S_z, \omega^\circ + \Delta\omega, \varphi^\circ + \Delta\varphi, \kappa^\circ + \Delta\kappa, Z_o^\circ + \Delta Z_o) \quad (5\text{-}18)$$

where ΔS_x, ΔS_y, ΔS_z, $\Delta\omega$, $\Delta\varphi$, $\Delta\kappa$, ΔX_o, ΔY_o, and ΔZ_o are the first and successive corrections to the first approximation S_x°, S_y°, S_z°, ω°, φ°, κ°, X_o°, Y_o°, and Z_o°. Under normal conditions, good geometry in the stereo model is:

$$S_x \approx S_y \approx S_z; \quad (5\text{-}19)$$

however, under adverse conditions, these three scales will not generally be approximately equal.

d. Linearization of the Transformation Equations Using Taylor's Theorem.[6] Since equations 5-13, 5-14, and 5-15 are non-linear, the least squares criterion does not apply. Therefore, the equations must be linearized. By Taylor's Theorem, neglecting second and higher order terms, the equations become:

$$f_x(S_x, \omega, \varphi, \kappa, X_o, X)^\circ + \left(\frac{\partial f_x}{\partial S_x}\right)^\circ \Delta S_x + \left(\frac{\partial f_x}{\partial \omega}\right)^\circ \Delta\omega + \left(\frac{\partial f_x}{\partial \varphi}\right)^\circ \Delta\varphi + \left(\frac{\partial f_x}{\partial \kappa}\right)^\circ \Delta\kappa + \left(\frac{\partial f_x}{\partial X_o}\right)^\circ \Delta X_o = 0 \quad (5\text{-}20)$$

$$f_y(S_y, \omega, \varphi, \kappa, Y_o, Y)^\circ + \left(\frac{\partial f_y}{\partial S_y}\right)^\circ \Delta S_y + \left(\frac{\partial f_y}{\partial \omega}\right)^\circ \Delta\omega + \left(\frac{\partial f_y}{\partial \varphi}\right)^\circ \Delta\varphi + \left(\frac{\partial f_y}{\partial \kappa}\right)^\circ \Delta\kappa + \left(\frac{\partial f_y}{\partial Y_o}\right)^\circ \Delta Y_o = 0 \quad (5\text{-}21)$$

$$f_z(S_z, \omega, \varphi, \kappa, Z_o, Z)^\circ + \left(\frac{\partial f_z}{\partial S_z}\right)^\circ \Delta S_z + \left(\frac{\partial f_z}{\partial \omega}\right)^\circ \Delta\omega + \left(\frac{\partial f_z}{\partial \varphi}\right)^\circ \Delta\varphi + \left(\frac{\partial f_z}{\partial \kappa}\right)^\circ \Delta\kappa + \left(\frac{\partial f_z}{\partial Z_o}\right)^\circ \Delta Z_o = 0 \quad (5\text{-}22)$$

In the above equations, terms of the equations whose first partial derivatives are zero have been omitted.

e. Results of the Taylor's Theorem Expansion. Performing the indicated operations shown in equations 5-20, 5-21, and 5-22 on equations 5-13, 5-14, and 5-15, the following result is obtained:

$$b_{11} = \left(\frac{\partial f_x}{\partial S_x}\right) = x\,(\cos\varphi\,\cos\kappa) + y\,(\cos\omega\,\sin\kappa + \sin\omega\,\sin\varphi\,\cos\kappa) + z\,(\sin\omega\,\sin\kappa - \cos\omega\,\sin\varphi\,\cos\kappa) \quad (5\text{-}23)$$

$$b_{12} = \left(\frac{\partial f_x}{\partial S_y}\right) = 0 \quad (5\text{-}24)$$

$$b_{13} = \left(\frac{\partial f_x}{\partial S_z}\right) = 0 \quad (5\text{-}25)$$

$$b_{14} = \left(\frac{\partial f_x}{\partial \omega}\right) = -\,y\,S_x\,(\sin\omega\,\sin\kappa - \cos\omega\,\sin\varphi\,\cos\kappa) + z\,S_x\,(\cos\omega\,\sin\kappa + \sin\omega\,\sin\varphi\,\cos\kappa) \quad (5\text{-}26)$$

$$b_{15} = \left(\frac{\partial f_x}{\partial \varphi}\right) = -\,x\,S_x\,(\sin\varphi\,\cos\kappa) + y\,S_x\,(\sin\omega\,\cos\varphi\,\cos\kappa) - z\,S_x\,(\cos\omega\,\cos\varphi\,\cos\kappa) \quad (5\text{-}27)$$

$$b_{16} = \left(\frac{\partial f_x}{\partial \kappa}\right) = -\,x\,S_x\,(\cos\varphi\,\sin\kappa) + y\,S_x\,(\cos\omega\,\cos\kappa - \sin\omega\,\sin\varphi\,\sin\kappa) + z\,S_x\,(\sin\omega\,\cos\kappa + \cos\omega\,\sin\varphi\,\sin\kappa) \quad (5\text{-}28)$$

$$b_{17} = \left(\frac{\partial f_x}{\partial X_o}\right) = 1 \quad (5\text{-}29)$$

$$b_{18} = \left(\frac{\partial f_x}{\partial Y_o}\right) = 0 \quad (5\text{-}30)$$

$$b_{19} = \left(\frac{\partial f_x}{\partial Z_o}\right) = 0 \quad (5\text{-}31)$$

$$b_{21} = \left(\frac{\partial f_y}{\partial S_x}\right) = 0 \quad (5\text{-}32)$$

$$b_{22} = \left(\frac{\partial f_y}{\partial S_y}\right) = -\,x\,(\cos\varphi\,\sin\kappa) + y\,(\cos\omega\,\cos\kappa - \sin\omega\,\sin\varphi\,\sin\kappa) + z\,(\sin\omega\,\cos\kappa + \cos\omega\,\sin\varphi\,\sin\kappa) \quad (5\text{-}33)$$

$$b_{23} = \left(\frac{\partial f_y}{\partial S_x}\right) = 0 \tag{5-34}$$

$$b_{24} = \left(\frac{\partial f_y}{\partial \omega}\right) = -\,y\,S_y\,(\,\mathrm{Sin}\,\omega\,\mathrm{Cos}\,\varkappa + \mathrm{Cos}\,\omega\,\mathrm{Sin}\,\varphi\,\mathrm{Sin}\,\varkappa\,) + z\,S_y\,(\,\mathrm{Cos}\,\omega\,\mathrm{Cos}\,\varkappa - \mathrm{Sin}\,\omega\,\mathrm{Sin}\,\varphi\,\mathrm{Sin}\,\varkappa\,) \tag{5-35}$$

$$b_{25} = \left(\frac{\partial f_y}{\partial \varphi}\right) = x\,S_y\,(\,\mathrm{Sin}\,\varphi\,\mathrm{Sin}\,\varkappa\,) - y\,S_y\,(\,\mathrm{Sin}\,\omega\,\mathrm{Cos}\,\varphi\,\mathrm{Sin}\,\varkappa\,) + z\,S_y\,(\,\mathrm{Cos}\,\omega\,\mathrm{Cos}\,\varphi\,\mathrm{Sin}\,\varkappa\,) \tag{5-36}$$

$$b_{26} = \left(\frac{\partial f_y}{\partial \varkappa}\right) = -\,x\,S_y\,(\,\mathrm{Cos}\,\varphi\,\mathrm{Cos}\,\varkappa\,) - y\,S_y\,(\,\mathrm{Cos}\,\omega\,\mathrm{Sin}\,\varkappa + \mathrm{Sin}\,\omega\,\mathrm{Sin}\,\varphi\,\mathrm{Cos}\,\varkappa\,) - z\,S_y\,(\,\mathrm{Sin}\,\omega\,\mathrm{Sin}\,\varkappa - \mathrm{Cos}\,\omega\,\mathrm{Sin}\,\varphi\,\mathrm{Cos}\,\varkappa\,) \tag{5-37}$$

$$b_{27} = \left(\frac{\partial f_y}{\partial X_o}\right) = 0 \tag{5-38}$$

$$b_{28} = \left(\frac{\partial f_y}{\partial Y_o}\right) = 1 \tag{5-39}$$

$$b_{29} = \left(\frac{\partial f_y}{\partial Z_o}\right) = 0 \tag{5-40}$$

$$b_{31} = \left(\frac{\partial f_z}{\partial S_x}\right) = 0 \tag{5-41}$$

$$b_{32} = \left(\frac{\partial f_z}{\partial S_y}\right) = 0 \tag{5-42}$$

$$b_{33} = \left(\frac{\partial f_z}{\partial S_z}\right) = x\,\mathrm{Sin}\,\varphi - y\,\mathrm{Sin}\,\omega\,\mathrm{Cos}\,\varphi + z\,\mathrm{Cos}\,\omega\,\mathrm{Cos}\,\varphi \tag{5-43}$$

$$b_{34} = \left(\frac{\partial f_z}{\partial \omega}\right) = -\,y\,S_z\,\mathrm{Cos}\,\omega\,\mathrm{Cos}\,\varphi - z\,S_z\,\mathrm{Sin}\,\omega\,\mathrm{Cos}\,\varphi \tag{5-44}$$

$$b_{35} = \left(\frac{\partial f_z}{\partial \varphi}\right) = x\,S_z\,\mathrm{Cos}\,\varphi + y\,S_z\,\mathrm{Sin}\,\omega\,\mathrm{Sin}\,\varphi - z\,S_z\,\mathrm{Cos}\,\omega\,\mathrm{Sin}\,\varphi \tag{5-45}$$

$$b_{36} = \left(\frac{\partial f_Z}{\partial \kappa}\right) = 0 \tag{5-46}$$

$$b_{37} = \left(\frac{\partial f_Z}{\partial X_o}\right) = 0 \tag{5-47}$$

$$b_{38} = \left(\frac{\partial f_Z}{\partial Y_o}\right) = 0 \tag{5-48}$$

$$b_{39} = \left(\frac{\partial f_Z}{\partial Z_o}\right) = 1 \cdot \tag{5-49}$$

f. Completing the Mathematical Derivation. Another set of equations must also be obtained in order to make the mathematics complete so that the least squares solution will be possible. They are:

$$\begin{aligned} l_1 = f_X - X = S_X [\, & x(\cos\varphi \cos\kappa) + \\ & y(\cos\omega \sin\kappa + \sin\omega \sin\varphi \cos\kappa) + \\ & z(\sin\omega \sin\kappa - \cos\omega \sin\varphi \cos\kappa)\,] + \\ & X_o - X \end{aligned} \tag{5-50}$$

$$\begin{aligned} l_2 = f_Y - Y = S_Y [\, & x(-\cos\varphi \sin\kappa) + \\ & y(\cos\omega \cos\kappa - \sin\omega \sin\varphi \sin\kappa) + \\ & z(\sin\omega \cos\kappa + \cos\omega \sin\varphi \sin\kappa)\,] + \\ & Y_o - Y \end{aligned} \tag{5-51}$$

$$\begin{aligned} l_3 = f_Z - Z = S_Z [\, & x(\sin\varphi) - \\ & y(\sin\omega \cos\varphi) + \\ & z(\cos\omega \cos\varphi)\,] + Z_o - Z \end{aligned} \tag{5-52}$$

where X, Y, and Z = known surface control values.

g. Introduction of Matrix Notation. Introducing matrix notation, let

$$B = \begin{bmatrix} b_{11} & b_{12} & b_{13} & b_{14} & b_{15} & b_{16} & b_{17} & b_{18} & b_{19} \\ b_{21} & b_{22} & b_{23} & b_{24} & b_{25} & b_{26} & b_{27} & b_{28} & b_{29} \\ b_{31} & b_{32} & b_{33} & b_{34} & b_{35} & b_{36} & b_{37} & b_{38} & b_{39} \end{bmatrix} \tag{5-53}$$

and

$$\Delta = \begin{bmatrix} \Delta S_x \\ \Delta S_y \\ \Delta S_z \\ \Delta\omega \\ \Delta\varphi \\ \Delta\kappa \\ \Delta X_o \\ \Delta Y_o \\ \Delta Z_o \end{bmatrix} \tag{5-54}$$

and

$$L = \begin{bmatrix} l_1 \\ l_2 \\ l_3 \end{bmatrix} \quad . \tag{5-55}$$

Now

$$B\Delta = L \quad . \tag{5-56}$$

The unknown corrections are the Δ matrix. Forming the normal equations, B^TB, we obtain

$$B^TB\Delta = B^TL \quad . \tag{5-57}$$

By multiplying both sides of equation 5-57 by the inverse of B^TB, or $(B^TB)^{-1}$, we obtain

$$(B^TB)^{-1} (B^TB) \Delta = (B^TB)^{-1} B^TL \tag{5-58}$$

which, of course, yields the desired result

$$\Delta = (B^TB)^{-1} B^TL \quad . \tag{5-59}$$

The matrix algebra, indicated in equation 5-59, is then iterated until the successive approximations become so small that no significant change occurs. Convergence is achieved when the corrections to the first and successive approximations become of the order of 1.0×10^{-8}. The iterative process is halted when the system has converged. This is accomplished by computing a value, T_i, after each iteration. The equation used is

$$T_i = \sqrt{\frac{(\Delta S_{x_i}^2 + \Delta S_{y_i}^2 + \Delta S_{z_i}^2 + \Delta \omega_i^2 + \Delta \varphi_i^2 + \Delta \kappa_i^2 + \Delta X_{o_i}^2 + \Delta Y_{o_i}^2 + \Delta Z_{o_i}^2)}{3N - 7.0}} , \qquad (5\text{-}60)$$

where T_i = tolerance for the i iteration

N = number of observations

7.0 = number of unknowns, assuming one scale factor (S)

and the remaining values have been previously defined.

If

$$\left| (T_i - T_{i+1}) \right| \leq 1.0 \times 10^{-8} \qquad (5\text{-}61)$$

the iterative process is halted and the "non-conformal" solution is obtained. Non-conformal means that all scales, S_x, S_y, and S_z, are permitted to remain at their computed values.

h. Conformalization of the Non-conformal Solution (If It Is Desired).

(1) Constraining the Scale Factors. Having three independent scales, S_x, S_y, and S_z, it may be desired to obtain a common scale for a final solution

which results in a conformal solution. This can be accomplished by imposing the condition that

$$S_x = S_y \quad . \tag{5-62}$$

This condition can exist in a rectangular coordinate system when the angle, α, (fig. 5-9) is 45 degrees. It can be seen that the resultant, r, is

$$r = (S_x^2 + S_y^2)^{\frac{1}{2}} \quad . \tag{5-63}$$

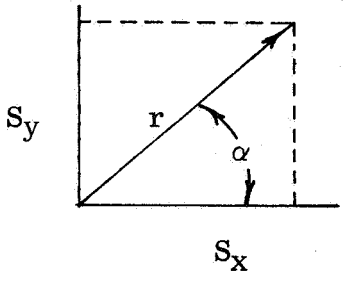

Figure 5-9. Resultant Scale .

Then, the common scale, S, is simply

$$S = r \cos \alpha = \left[\frac{(X^2 + Y^2)}{2} \right]^{\frac{1}{2}} \quad . \tag{5-64}$$

For a common scale for all three coordinates a further restriction is imposed, that is,

$$S = S_x = S_y = S_z \tag{5-65}$$

which appears to fit the conventional model.

(2) Adjustment of Non-conformal Parameters to Conform to the Constraints Imposed. Therefore, a common scale, S, is found such that the non-conformal scales, S_x, S_y, and S_z, are now said to have a common scale and are said to be conformal. Although S_x, S_y, and S_z can be forced to a common scale, the other unknowns (ω, φ, κ, X_o, Y_o, and Z_o) have values based on the non-conformal S_x, S_y, and S_z. Since S_x, S_y, and S_z have been forced to be equal, ω, φ, κ, X_o, Y_o, and Z_o must take on a corresponding change to attain a conformal solution utilizing one scalar. This conformalizing technique is derived from a paper by Dr. H. Schmid.[6]

(a) Matrix Bordering Technique.[1] This conformalization may be accomplished by bordering the normal equations with a constraint matrix, C, as follows:

According to equation 5-59, we have

$$\Delta = (B^T B)^{-1} B^T L \quad . \tag{5-66}$$

Let

$$N^{-1} = (B^T B)^{-1} \tag{5-67}$$

and

$$E = B^T L \tag{5-68}$$

yield

$$\Delta = N^{-1} E \quad . \tag{5-69}$$

Then, by bordering the system equations with the constraint matrices, C, C^T, and W, as shown in figure 5-10,

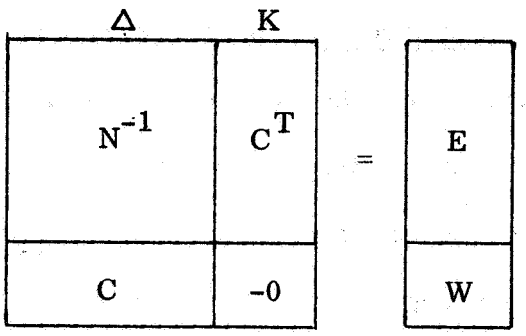

Figure 5-10. Bordering matrices.

Dr. Schmid has derived the following:

$$K = (CN^{-1}C^T)^{-1} (W - CN^{-1}E) \qquad (5\text{-}70)$$

where K = unknown multiplier,

and

$$\Delta' = N^{-1} (E + C^T K) \qquad (5\text{-}71)$$

where Δ' = the corrections that must be applied to all unknown parameters for a conformal solution,

and

$$\Delta_c = \Delta + \Delta' \qquad (5\text{-}72)$$

where Δ_c = conformal solution.

Now, all that remains is to derive the constraint matrices which have been called C and W. In equation 5-65 the condition was imposed that

$$S = S_x = S_y = S_z \qquad (5\text{-}73)$$

or

$$S_x + \Delta S_x' = S \tag{5-74}$$

$$S_y + \Delta S_y' = S \tag{5-75}$$

$$S_z + \Delta S_z' = S \tag{5-76}$$

where $\Delta S_x', \Delta S_y', \Delta S_z'$ = the incremental corrections needed to conformalize the system equations.

By subtracting S_x, S_y, and S_z from each side of equations 5-74, 5-75, and 5-76, respectively, the following result is obtained:

$$\Delta S_x' = S - S_x \tag{5-77}$$

$$\Delta S_y' = S - S_y \tag{5-78}$$

$$\Delta S_z' = S - S_z \ . \tag{5-79}$$

By forming the constraint matrix, C, the following result is obtained:

$$C = \begin{bmatrix} 1 & 0 & 0 & 0 & 0 & 0 & 0 & 0 & 0 \\ 0 & 1 & 0 & 0 & 0 & 0 & 0 & 0 & 0 \\ 0 & 0 & 1 & 0 & 0 & 0 & 0 & 0 & 0 \end{bmatrix} \tag{5-80}$$

and the vector, W, is

$$W = \begin{bmatrix} \Delta S_x' \\ \Delta S_y' \\ \Delta S_z' \end{bmatrix} \ . \tag{5-81}$$

Now, performing the indicated matrix algebra in equations 5-70, 5-71, and 5-72, the conformal solution is obtained.

(b) Variation of the Bordering Technique to Achieve a Modified Conformal Solution. Some other interesting things can be done using the bordering technique. When a modified conformal solution

is desired where

$$S = S_x = S_y \neq S_z \quad , \tag{5-82}$$

where S_z is held at its non-conformal value, and where S_x and S_y are set equal to the scale computed from equation 5-64, the solution can be accomplished simply by making the following change to the vector, W:

$$W = \begin{bmatrix} \Delta S_x' \\ \Delta S_y' \\ 0 \end{bmatrix} \quad . \tag{5-83}$$

This modified conformal solution is in the program, GETRAN. If a conformal solution is called for by the programmer, and the non-conformal S_z deviates by some predetermined amount from the computed S, the program will automatically select the modified conformal restrictions on matrix W. Otherwise, the conformal solution will be given with matrix W formed as indicated in equation 5-81.

i. Adjustment of the Instrument Values. Once a solution to the problem has been obtained, the instrument readings are passed through the transformation equations, equations 5-13, 5-14, and 5-15, along with the computed unknowns to obtain an adjusted value in the LSRCS.

19. LSRCS BACK TO THE PLANETOCENTRIC COORDINATE SYSTEM AND THEN BACK TO THE PLANETODETIC COORDINATE SYSTEM.[2] In order to be able to easily convert to one of the many projection systems, it is highly desirable to return to the Planetodetic Coordinate (φ , λ , and h) System.

a. LSRCS Back to the Planetocentric Coordinate System. Remembering that a false value was added to the X, Y, and Z's in order that only positive numbers would be obtained, these false values are subtracted from the X, Y, and Z's before they can be carried back to the Planetocentric Coordinate System. Subtracting the false values, the coordinates may then be transformed by the following matrices to obtain the corresponding planetocentric coordinate values for the adjusted points (this is the inverse of equation 5-6):

$$\begin{bmatrix} X_n' \\ Y_n' \\ Z_n' \end{bmatrix} = \begin{bmatrix} -\sin\lambda_o & -\sin\varphi_o\cos\lambda_o & \cos\varphi_o\cos\lambda_o \\ \cos\lambda_o & -\sin\varphi_o\sin\lambda_o & \cos\varphi_o\sin\lambda_o \\ 0 & \cos\varphi_o & \sin\varphi_o \end{bmatrix} \begin{bmatrix} X_n \\ Y_n \\ Z_n \end{bmatrix} + \begin{bmatrix} X_o' \\ Y_o' \\ Z_o' \end{bmatrix} \qquad (5\text{-}84)$$

where X_n', Y_n', and Z_n' = planetocentric coordinate values for n number of points

φ_o and λ_o = centroid values originally calculated for equation 5-6

X_n, Y_n, and Z_n = adjusted local space values

X_o', Y_o', and Z_o' - centroid values originally calculated for equation 5-6.

b. Planetocentric Coordinate System Back to the Planetodetic Coordinate System. Once the planetocentric values have been calculated, all that remains is to generate the proper φ, λ, and h for the points in question. This is accomplished by employing the following formulae:

$$\lambda = \arccos\left(X_n' / R_n \right) \qquad (5\text{-}85)$$

or

$$\lambda = \arcsin\left(Y_n' / R_n \right) \qquad (5\text{-}86)$$

where $R_n = [\ (X_n')^2 + (Y_n')^2]^{\frac{1}{2}}$.

A criteria for determining whether to use equation 5-85 or 5-86 is simply to determine the value of (X_n'/R_n) and the value of (Y_n'/R_n) and use the argument and corresponding equation that is numerically smaller. Unfortunately, the values for φ and h are not as easy to determine as λ . The values of φ and h must be obtained by using an iterative process. First, an initial value for t (fig. 5-1) is computed from

$$t_1 = e^2 Z_n' \qquad (5\text{-}87)$$

where t_1 = the distance that the normal line misses the origin for iteration number 1

e = the eccentricity which was previously calculated from equation 5-1

Z_n' = distance above the equatorial plane for n number of points.

Once t_1 is known, an initial value of φ can be found by the equation

$$\varphi_1 = \arcsin \{ (Z_n' + t_1) / [R_n^2 + (Z_n' + t_1)^2]^{\frac{1}{2}} \} \ . \qquad (5\text{-}88)$$

The values are refined by using the equation

$$t_2 = (a\, e^2 \operatorname{Sin} \varphi_1) / (1 - e^2 \operatorname{Sin}^2 \varphi_1)^{\frac{1}{2}} = N_1\, e^2 \operatorname{Sin} \varphi_1 \qquad (5\text{-}89)$$

where a = semi-major axis.

The values of φ and t are iterated by using equations 5-88 and 5-89 until the successive approximations to φ and t are negligible. Once a final value for φ and t is obtained, the elevation, h, may be calculated by using

$$h = [\ X_n'^2 + Y_n'^2 + (Z_n' + t_n)^2]^{\frac{1}{2}} - [a / (1 - e^2 \operatorname{Sin}^2 \varphi_n)^{\frac{1}{2}}]$$
$$= [\ R_n^2 + (Z_n' + t_n)^2]^{\frac{1}{2}} - N \ . \qquad (5\text{-}90)$$

The determination of φ, λ, and h is then complete. It must be remembered that the arcsin and arccos functions must have a range of

$$-360^{o} \leq \text{angle} \leq +360^{o} \quad .$$

20. STATISTICAL ANALYSIS OF THE SOLUTION TO THE ADJUSTMENT PROBLEM.

a. Analysis of Each Point. First, an analysis is made on each point. The known control value is subtracted from the adjusted value, or

$$\Delta X = X_A - X \quad , \tag{5-91}$$

where ΔX = the difference between the known value and the computed value

X_A = the computed value

X = the value entered as known control, or which was carried from the Planetodetic Coordinate System to the LSRCS.

Similar values are computed for Y and Z.

b. Computed Sigma Value for X_A, Y_A, and Z_A. A sigma value is computed for X_A, Y_A, and Z_A using the formula

$$\text{SIGMAX} = \{ [\sum_{i}^{n} (\Delta X)^2] / (n - 1) \}^{\frac{1}{2}} \tag{5-92}$$

where n = the number of observations, or the number of control points for that solution.

c. Computed Sigma Value for the Problem. Then, a sigma for the problem is computed using

$$\text{SIGMA} = \{ [\sum_{i}^{n} (\Delta X_n)^2 + \sum_{i}^{n} (\Delta Y_n)^2 + \sum_{i}^{n} (\Delta Z_n)^2] / (3n - 7) \}^{\frac{1}{2}} . \tag{5-93}$$

d. Error Analysis of All Parameters. An error analysis for each of the computed parameters is determined by taking the inverse of the normal equations matrix defined in equation 5-67 and letting

$$Q = N^{-1} = \begin{bmatrix} n_{11} & n_{12} & n_{13} & n_{14} & n_{15} & n_{16} & n_{17} & n_{18} & n_{19} \\ n_{21} & n_{22} & n_{23} & n_{24} & n_{25} & n_{26} & n_{27} & n_{28} & n_{29} \\ n_{31} & n_{32} & n_{33} & n_{34} & n_{35} & n_{36} & n_{37} & n_{38} & n_{39} \\ n_{41} & n_{42} & n_{43} & n_{44} & n_{45} & n_{46} & n_{47} & n_{48} & n_{49} \\ n_{51} & n_{52} & n_{53} & n_{54} & n_{55} & n_{56} & n_{57} & n_{58} & n_{59} \\ n_{61} & n_{62} & n_{63} & n_{64} & n_{65} & n_{66} & n_{67} & n_{68} & n_{69} \\ n_{71} & n_{72} & n_{73} & n_{74} & n_{75} & n_{76} & n_{77} & n_{78} & n_{79} \\ n_{81} & n_{82} & n_{83} & n_{84} & n_{85} & n_{86} & n_{87} & n_{88} & n_{89} \\ n_{91} & n_{92} & n_{93} & n_{94} & n_{95} & n_{96} & n_{97} & n_{98} & n_{99} \end{bmatrix} \qquad (5\text{-}94)$$

and, using only the diagonal elements in the following formula, the errors are obtained

$$\text{STD. } E_i = \text{SIGMA } (Q_{ii})^{\frac{1}{2}} \qquad (5\text{-}95)$$

where STD. E = standard error

SIGMA = defined in equation 5-93

n_{ii} = a term of the matrix, Q (as defined above)

i = indicates the diagonal element used.

For example, where i is equal to 4,

$$\text{STD. } E_4 = \text{SIGMA } (Q_{44})^{\frac{1}{2}} .$$

The correlation between the diagonal elements and the standard errors are listed in table 5-I.

Table 5-I. Element-parameter Table

ii	STD. E_i
11	Scale X
22	Scale Y
33	Scale Z
44	ω
55	φ
66	κ
77	X_o
88	Y_o
99	Z_o

21. AUTOMATIC STATISTICAL POINT DELETION. GETRAN has been designed so that once a solution has been obtained and a corresponding sigma for a problem has been calculated, a standard can be developed so that elimination of points based on probability is obtained.

a. Method. Taking each observation used in the solution of the adjustment problem and computing an individual sigma for each observation using the formula

$$R_i = [(X_{A_i} - X_i)^2 + (Y_{A_i} - Y_i)^2 + (Z_{A_i} - Z_i)^2]^{\frac{1}{2}} \qquad (5\text{-}96)$$

where R_i = the computed sigma for the i th observation

X_{A_i}, Y_{A_i}, Z_{A_i} = the adjusted values of X, Y, and Z based on the values obtained from the adjustment problem

X_i, Y_i, Z_i = the values entered for surface control.

b. Range. If for any observation(s)

$$R_i \geq 3.3 \text{ SIGMA} \quad , \tag{5-97}$$

where SIGMA = the sigma for the problem,

that observation(s) is (are) deleted and a new solution is calculated based on the remaining points after deletion. The program will not delete beyond a minimum solution, which is four points. If no point(s) is (are) deleted, the original solution is used for the final calculations because no single observation was computed to be beyond the 3.3 SIGMA range.

22. SPHERICAL MERCATOR PROJECTION.[7] a. Assumption. The moon is assumed to be a sphere with a radius of 1738 kilometers. Until such time as better approximations to the moon's semi-major and semi-minor axes can be determined, the spherical Mercator projection is used. The semi-major axis is presently said to equal the semi-minor axis; and, therefore, the eccentricity is zero.

b. Defining Equations. Assuming a cylinder tangent to the equator and λ equal to zero (0) and coincident with the prime meridian, the Mercator projection is defined by the following equations:

$$X = \lambda a \tag{5-98}$$

where X = the Mercator projected X, or Easting,

λ = longitude

a = semi-major axis, or the radius in this case;

and

$$Y = [\ \ln (\cos P / \sin P)\ ]\ a \tag{5-99}$$

where Y = the Mercator projected Y, or Northing,

P = (co-latitude) / 2 = (90^{o} - φ) / 2 .

Of course, once a better determination of the semi-major axis, a, and the semi-minor axis, b, is obtained, a far more complex set of equations would be used.

SECTION IV. - CONCLUSIONS

23. GETRAN. It was concluded that the program, GETRAN, can be used to:

a. Provide a dense network of photogrammetric control (supplementary control) from known surface coordinates.

b. Provide a mathematical adjustment (absolute orientation) of a relatively oriented digitized stereomodel, including preparation for entry into a digital contouring program.

SECTION V. RECOMMENDATIONS

24. SYSTEM APPLICATION. Because of the amount of time required to read a dense network of points that adequately defines the entire surface of the stereomodel on a stereophotogrammetric instrument (input data which is entered into GETRAN), it is recommended that this system be used only:

a. To provide a network of supplementary control from known surface coordinates.

b. When the geometry of the photographs exceeds the physical limitations of the stereophotogrammetric instruments.

SECTION VI. LITERATURE CITED

1. SCHMID, H. H. and SCHMID, E. "A Generalized Least Squares Solution for Hybrid Measuring Systems." The Canadian Surveyor. Mar 1965: Vol XIX, p 30.

2. DOYLE, F. J. "Analytical Photogrammetry," in Manual of Photogrammetry. M. M. Thompson, ed. Falls Church, Va.: American Society of Photogrammetry. 1966: Vol I, pp 466-467.

3. TEWINKEL, G. C. "Basic Mathematics of Photogrammetry." Ibid. p 47.

4. _____. Ibid. pp 53-65.

5. LIGHT, D. L. "The Orientation Matrix." Photogrammetric Engineering. May 1966: Vol XXXII, No. 3, p 434.

6. SCHMID, H. H. and SCHMID, E. "A Generalized Least Squares Solution for Hybrid Measuring Systems." The Canadian Surveyor. Mar 1965: Vol XIX, pp 27-31.

SECTION VII. SELECTED BIBLIOGRAPHY

CHURCHILL, R. V. Complex Variables and Applications. New York: McGraw-Hill Book Company. 1960.

GRANVILLE, W. A., SMITH, P.F., and LONGLEY, W. R. Elements of Calculus. New York: Ginn and Company. 1956.

Automath 1800 Reference Manual. Wellesley Hills, Mass.: Honeywell Inc., Electronic Data Processing Division. 1965.

An Introduction to Engineering Analysis for Computers. White Plains, N. Y.: IBM Technical Publications Department. 1961.

LOVE, C. E. and RAINVILLE, E.D. Analytic Geometry. New York: The MacMillan Company. 1959.

SOKOLNIKOFF, I. S. and SOKOLNIKOFF E. S. Higher Mathematics for Engineers and Physicists. New York: McGraw-Hill Book Company, Inc. 1941.

TAYLOR, A. E. Calculus with Analytic Geometry. Englewood Cliffs, N. J.: Prentice-Hall, Inc. 1959.

CHAPTER 6

COMPARATOR/ANALYTICAL SYSTEM (SCHMID METHOD)

SECTION I. INTRODUCTION

1. GENERAL. Analytical photogrammetry was an ideal technique to employ in reducing Ranger photography. The physical limitations encountered in photogrammetric plotting instruments do not exist in the analytical approach except that the plate-size is limited to 9 x 9 inches on the measuring instrument. Once the data were measured, analytical methods were entirely computational. The speed of the computers, coupled with the inherent rigor of projective geometry, justified the use of the "Schmid Method" on the Ranger project. The Schmid Method has been thoroughly documented in several reports[1 2 3 4] published by the Ballistics Research Laboratories (BRL), Aberdeen Proving Ground, Maryland. These reports are readily available from BRL. Portions of the BRL work were sponsored by the U.S. Army Corps of Engineers, Geodesy, Intelligence, Mapping, Research and Development Agency (GIMRADA) for AMS.

2. SCOPE. This chapter documents, in general terms, the AMS version of the Schmid Method, and explains and illustrates (with computer printouts) the step-by-step approach used on the Ranger project. It should be noted that the output from this method was the input into the Digital Contouring Program described in chapter 7.

3. PROBLEM DEFINITION. A mathematical model was constructed to represent relations between points in the object space (ground), the perspective center in the lens, and the photo images. In the Schmid Method, the condition of colinearity is imposed so that the perspective center (O), the

photo image (r), and the object point (R) on the ground are on a straight line. Figure 6-1 illustrates this condition. The application of numerical analysis results in determining X, Y, Z-coordinates from linear x, y measurements on the photography.

SECTION II. MENSURATION

4. INSTRUMENTATION. There were two principal approaches to the problem of obtaining the coordinates of the photograph images. One was by monocular comparators; the other by stereocomparators. With a monocular comparator, corresponding images had to be marked on the photographs prior to mensuration. The stereocomparator technique permitted the simultaneous identification and measurement of points on two photographs. Due to the lack of clearly defined objects on the lunar surface, the stereocomparator approach was selected. Furthermore, stereoscopic viewing was essential since the computed coordinates were to be used as input into the Digital Contouring Program, as well as the data for the orientation of the photographs to the selenodetic control.

5. STEREOCOMPARATOR. Utilizing the Schmid Method, the Zeiss stereocomparator PSK was used to make the measurements on the Ranger project. The PSK has a least count of one micron (one millionth of a meter). It had been calibrated at AMS, and the precision had been validated to be in the one-micron class. The format is 9.5 x 9.5 inches with 8x- and 16x- ocular magnification. One unique quality of the PSK is its glass-against-glass measuring system. With this system, the effect of environmental changes

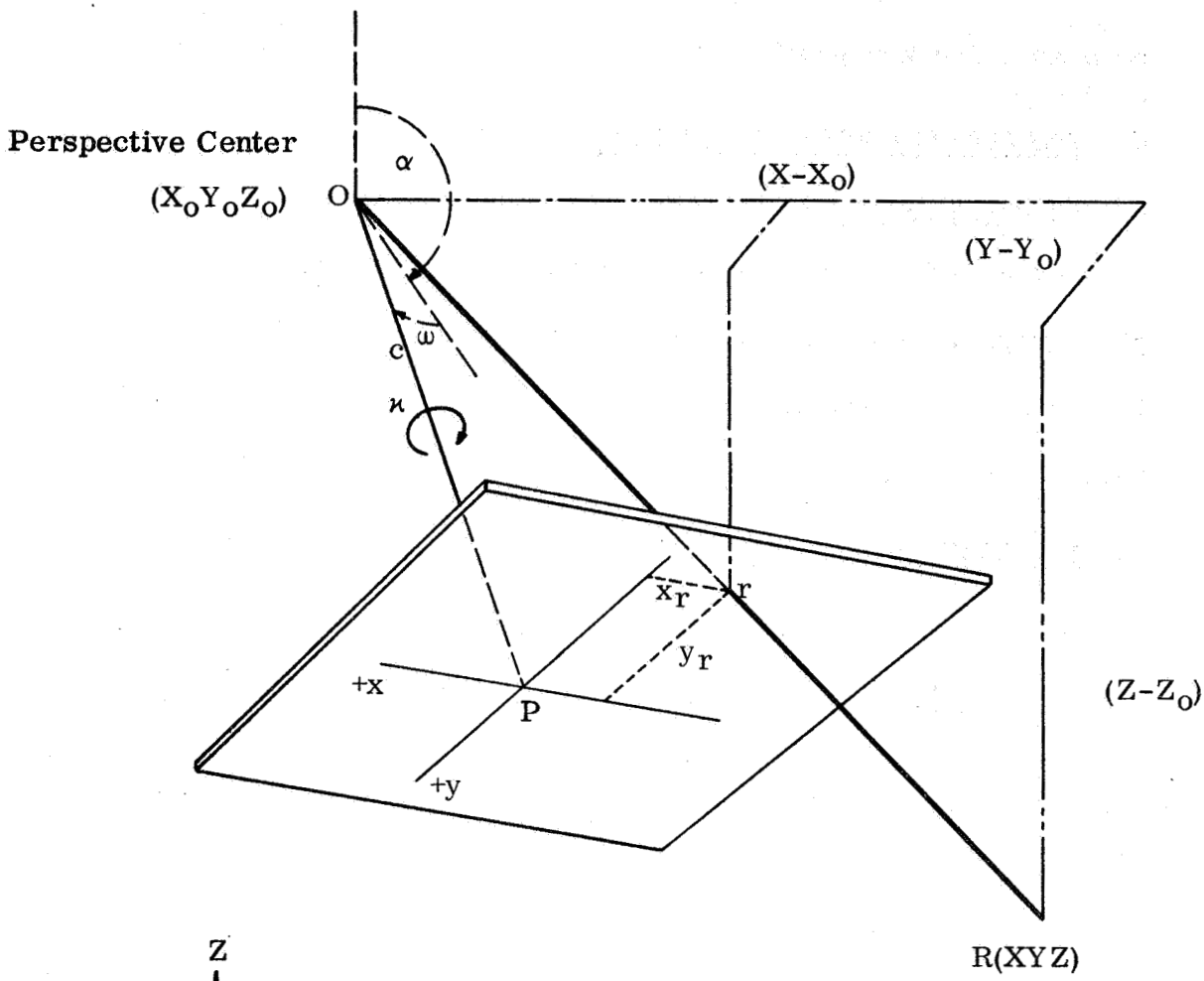

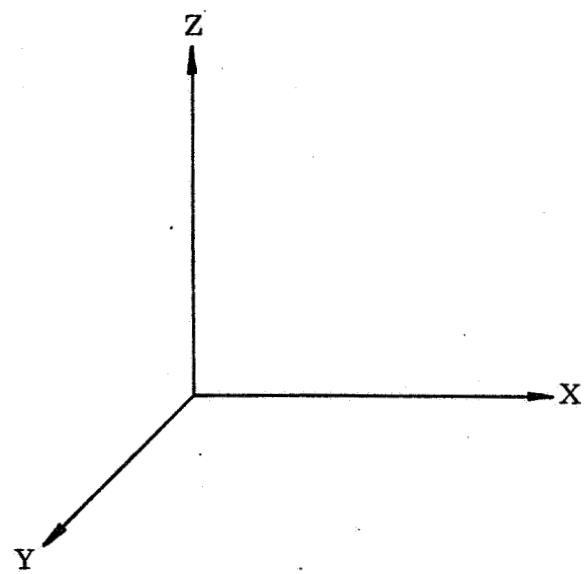

α,ω,κ are the angular orientations of the photograph.

x,y is the image coordinate system.

X,Y,Z are object space coordinates.

P is the principal point.

C corresponds to the focal length.

X_o, Y_o, Z_o are exposure station coordinates.

Figure 6-1. Geometry of the Schmid Method.[3]

on the measurements are minimized. The PSK is shown in figure 6-2. It has a hard-copy output on the typewriter and a punched-card capability on a modified key punch.

6. PHOTOGRAPH COORDINATE SYSTEM. Every photograph from the Ranger series had a set of four reticles around the center reticle which could be used as substitutes for the fiducial marks normally found on conventional photography. A diagram of the photo coordinates of these reticles is given in figure 4-1. Any image point "r" on the photograph may be located in this system by its coordinates (x_r, y_r).

7. STEREOCOMPARATOR PSK OUTPUT. The hard copy and card output were as follows:

Point Identification	Point Type	x_1	y_1	x_2	y_2
7D	5D	6D	6D	6D	6D

where D = number of digits,

x_1, y_1 = the photo coordinates for photo 1

x_2, y_2 are the coordinates of the same image in the overlapping photo.

Point type tells the computer point control, partial control, or an image point to be computed.

SECTION III. SCHMID METHOD OF ANALYTICAL PHOTOGRAMMETRY

8. PRELIMINARY COMPUTATIONS. Due to the high altitudes of the Ranger photography (in comparison to the altitudes of conventional cartographic photography), an object space coordinate system that considers the curvature of the lunar figure had to be defined. Various systems could be employed for this purpose, depending upon the magnitude of the area covered,

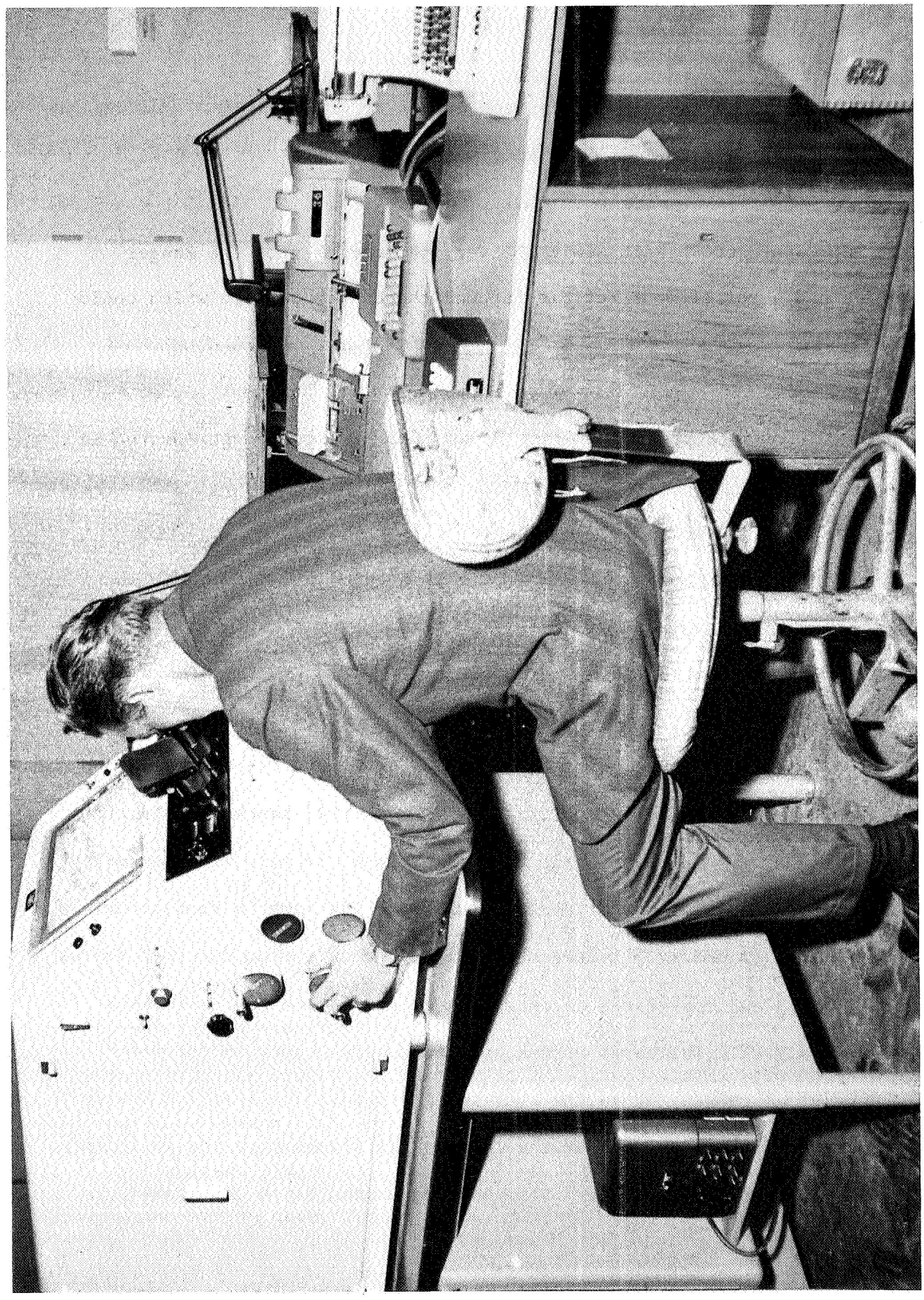

Figure 6-2. Zeiss Stereocomparator PSK.

and the accuracy required. The problem was to convert selenodetic spherical coordinates (latitude (ϕ), longitude (λ), and elevation (H), as referred to the selenodetic datum) into a system of arbitrarily oriented Cartesian coordinates and vice versa. The solution to this problem as applied by AMS is given by Schmid[1]

a. Selenodetic Control Point Transformation. The JPL furnished latitude (ϕ), longitude (λ), and height (H) above the lunar surface for each exposure station. Also, ϕ, λ surface positions beneath each reticle on the photograph were given. One NASA-DOD (AMS-65) selenodetic control point is located in the Ranger VIII area.[5] It is the crater "Schmidt." These horizontal data were associated with vertical data derived from AMS and Aeronautical Chart and Information Center (ACIC) source maps to control the mapping for the Ranger project. The basic selenodetic control, then, as described, is given in the ϕ, λ, H system.

(1) Problem Definition. The ϕ, λ, H system is transformed to a selenocentric system called X', Y', Z'. The X', Y' plane contains the lunar equator, with the X' axis passing through the zero meridian. The Z' axis passes through the lunar north pole. The moon is represented by a sphere of radius 1738 kilometers. Next, the selenocentric coordinates are rotated and translated to establish a local Cartesian coordinate system (X,Y,Z). The local system has its Z-axis normal to the lunar sphere at an origin "O" in the area being mapped. The positive X-axis was chosen in the direction of the Ranger VIII flight with the positive Y-axis being 90 degrees away, and pointing south, since the Schmid

Method is defined in a left-handed coordinate system. These coordinate systems are illustrated by figure 6-3.

(2) Mathematical Parameters of the Transformation. Schmid[1] fully documents the transformations; therefore, it is adequate here merely to define the parameters used in transforming the control used in the Ranger project and to summarize the steps involved. A local left-handed coordinate system was defined with its origin at

$$\phi_o = 1^\circ 04' 39.0''$$

$$\lambda_o = 340^\circ 19' 22.8''$$

$$H_o = 5000 \text{ meters}$$

This origin appears in the stereomodel (Photos 499-515) of Ranger VIII. The system is oriented in such a way that the positive X-axis has an azimuth (β) from the south of 253 degrees, making it approximately parallel to the direction of the Ranger VIII flight. The Z-axis is normal at the point of origin, and positive upwards. Additional parameters are alpha (α) which is rotation about the Y-axis and defined as $90-\phi_o$, and gamma (usually zero). Gamma is a small rotation that will cause the local system to be secant through the lunar sphere. It is not necessary unless very large areas are triangulated. It was set to zero for this project. In summary, the ϕ, λ, and H system is transformed to the X', Y', and Z' system; and, then the X', Y', and Z' system is transformed to the X, Y, and Z system.

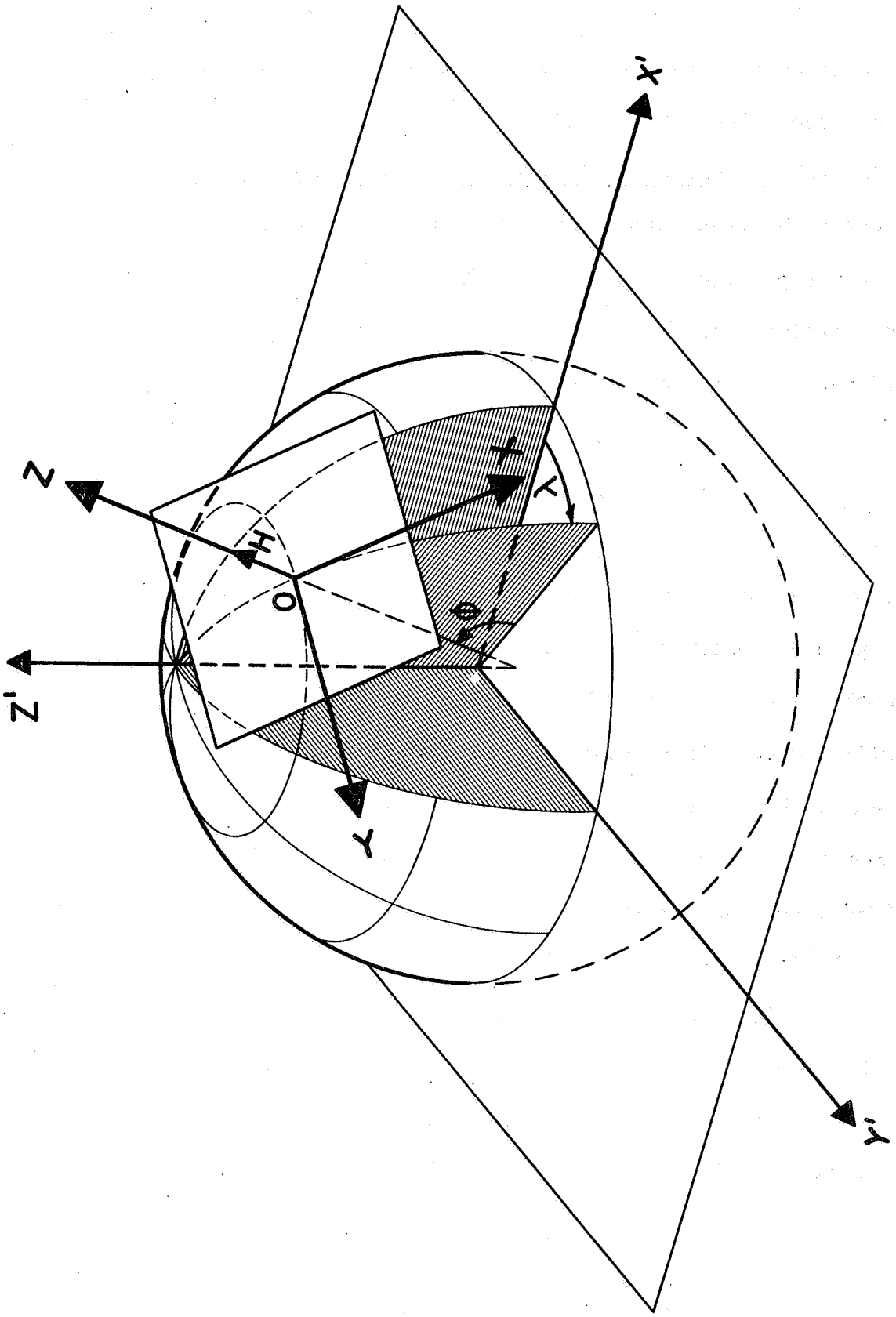

Figure 6-3. Coordinate Transformation.

b. The Inverse Transformation Problem. All photogrammetric computations are performed in the local Cartesian system (X,Y,Z); then, the problem is the inverse of that described in paragraph (2). The inverse is obtained by the transformation of the X, Y, and Z system to the X', Y', and Z' system and, then the X', Y', and Z' system is transformed to the ϕ, λ, and H system. The same parameters are used for the inverse, with the addition of X_o, Y_o, Z_o, which are the selenocentric coordinates of the origin point, ϕ_o, λ_o, H_o. An additional transformation is then performed to produce data for digital contouring. It is the transformation of the ϕ, λ, and H system to the N, E, and H Mercator system. N, E, and H are Mercator grid coordinates, Northing (N), Easting (E), and elevation (H). The Mercator projection was selected because the area to be mapped is very near the equator. The formulae for this conversion are

$$N = R \log \tan (45^{o} + \tfrac{1}{2} \phi),$$

$$E = R\lambda,$$

and H = Elevation

where R = a lunar radius of 1738 kilometers with the point of tangency at the equator.

λ is in radians.

c. Program Example. An example of the transformation output is included at the end of this chapter. (See figure 6-5.)

9. COMPARATOR REDUCTION. The Comparator Reduction Program is fully documented by Wooten[2]. The purpose of the Comparator Reduction Program is to correct the raw measured coordinates for comparator errors, radial distortion of the camera lens and, in general, to "refine"

the raw x, y values to be entered as input to the analytical photogrammetry computations. These various refinements will be discussed here in general terms. An example of the Comparator Reduction Program output is given at the end of this chapter. (See figure 6-6.)

a. Computation of the Arithmetic Means of the Comparator Readings.

$$(x') = \frac{\Sigma x'}{n} \; ; \; (y') = \frac{\Sigma y'}{n}$$

where n = the number of readings per point.

b. Correction for Lack of Perpendicularity of Comparator Ways.

$$\bar{x} = (x') + (y') \sin \alpha$$

and

$$\bar{y} = (y').$$

α is the angle of non-perpendicularity determined during the comparator calibration. For the PSK α is zero for all practical purposes.

c. Adjustment for Linear Scale Factors S_x and S_y.

$$x^{*'} = \bar{x} \cdot S_x \; ; \; y^{*'} = \bar{y} \cdot S_y$$

S_x and S_y are equal to one for the PSK on the Ranger project.

d. Computation of the Center of the Fiducial Mark System and the Swing Angle. The intersection of fiducials is computed to establish the center of the plate. Also, the swing angle (r) is determined so that fiducial marks in the line of flight become the x-axis.

e. Reduction of Point Readings to the Center of the Fiducial Mark System. The reduction of point readings to the center of the fiducial mark system is expressed by the following equations:

$$\boxed{x'} = (x^{*'}) - x'_f$$

and

$$\boxed{y'} = (y^{*'}) - y'_f$$

where $x^{*'}, y^{*'}$ = coordinates of point with respect to instrument coordinate system

x'_f, y'_f = fiducial center coordinate computed from the intersection of the four reticles surrounding the center reticle of the Ranger photography

$\boxed{x'}, \boxed{y'}$ = coordinates of point with respect to fiducial center.

f. Rotation of Coordinate Axes. The fiducials in the line of flight become the x-axis after rotation through the swing angle (r).

$$\boxed{x_r} = \boxed{x'} \cos r + \boxed{y'} \sin r$$

$$\boxed{y_r} = \boxed{y'} \cos r - \boxed{x'} \sin r$$

g. Reduction to Principal Point. Refer point coordinates to the principal point (x_p, y_p). The coordinates of the principal point for Ranger VIII were assumed to be zero.

$$\triangle x' = \boxed{x_r} - x'_p$$

$$\triangle y' = \boxed{y_r} - y'_p$$

h. Correction for Distortion. Radial distortion was corrected as a function of radial distance. The $\triangle x'$, $\triangle y'$ coordinates were corrected according to the polynomials developed in chapter 4. The refined comparator coordinates are denoted by l_x and l_y. These l_x, l_y are ready for the stereomodel computations.

i. Computation of Standard Errors.

$$m_x = \left(\frac{\Sigma vv}{n-1}\right)^{\frac{1}{2}} \qquad m_y = \left(\frac{\Sigma vv}{n-1}\right)^{\frac{1}{2}}$$

where v = arithmetic mean minus each reading of a specific setting.

j. Computation of Weights as a Function of Standard Error.

$$w_x = \frac{K_w}{m_x^2} \; ; \qquad w_y = \frac{K_w}{m_y^2}$$

where K_w represents the scaling factor. It is conveninent to let the plate coordinate weights w_x and w_y be one. Then, we let the plate residual m_x and m_y be 10 microns, so that

$$K_w = 1 \times 10^{-10} \text{ meters.}$$

k. Ground Weights (W_g). Let ground (M_g) error be 100 meters. Then,

$$W_g = \frac{K_w}{(M_g)^2}$$

$$= \frac{1 \times 10^{-10}}{(1 \times 10^2)^2}$$

$$= \frac{1 \times 10^{-10}}{1 \times 10^4}$$

$$= 1 \times 10^{-14} .$$

Actually, the standard error of the ground control for Ranger is unknown; however, 500 meters is probably more realistic than the 100 meters that is used. Several different solutions were run with various weight configurations. A relative weight number of 1×10^{-14} was finally selected for the Ranger computations.

10. STEREOMODEL COMPUTATIONS. a. The General Problem of Analytical Photogrammetry. The general problem of analytical photogrammetry is defined by Schmid [3] as the simultaneous orientation of any number of photo-

graphs, and the reconstruction of the object space by triangulating corresponding rays. Figure 6-4 illustrates these rays on a stereomodel formed from Ranger VIII photography. Various aspects of the Schmid Method will be discussed in the following paragraphs.

b. Orientation System. Figure 6-1 defines the three orientation angles (k, ω, α). The orientation matrices are

$$M_k \qquad M_\omega \qquad M_\alpha$$

$$\begin{bmatrix} -\cos k & -\sin k & 0 \\ -\sin k & \cos k & 0 \\ 0 & 0 & 1 \end{bmatrix} \quad \begin{bmatrix} 1 & 0 & 0 \\ 0 & \cos\omega & -\sin\omega \\ 0 & \sin\omega & \cos\omega \end{bmatrix} \quad \begin{bmatrix} \cos\alpha & 0 & -\sin\alpha \\ 0 & 1 & 0 \\ \sin\alpha & 0 & \cos\alpha \end{bmatrix}$$

$$M = M_k M_\omega M_\alpha .$$

After multiplication, M is stated compactly as

$$M = \begin{bmatrix} A_1 & B_1 & C_1 \\ A_2 & B_2 & C_2 \\ D & E & F \end{bmatrix} . \qquad (6\text{-}1)$$

c. Condition Equations. The colinearity condition equations for each point are

$$\begin{aligned} \ell_x - x_p &= c \left[\frac{(X - X_o)A_1 + (Y - Y_o)B_1 + (Z - Z_o)C_1}{(X - X_o)D + (Y - Y_o)E + (Z - Z_o)F} \right] \\ \ell_y - y_p &= c \left[\frac{(X - X_o)A_2 + (Y - Y_o)B_2 + (Z - Z_o)C_2}{(X - X_o)D + (Y - Y_o)E + (Z - Z_o)F} \right] . \end{aligned} \qquad (6\text{-}2)$$

These equations simply express the fact that the object point "R", the image point "r" and the exposure station (X_o, Y_o, Z_o) all lie on the same straight line. Each measured image point leads to two condition

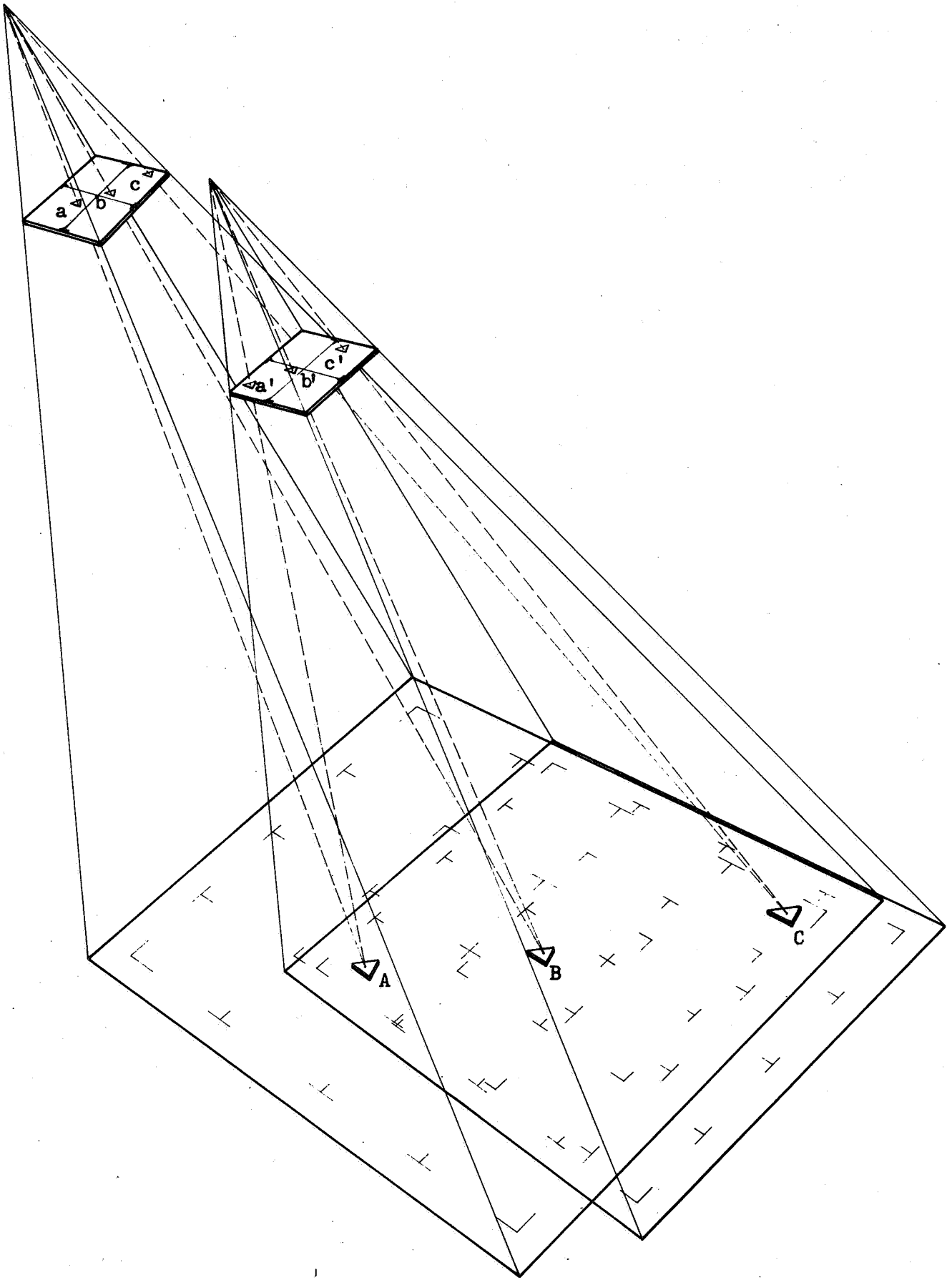

Figure 6-4. Ranger Stereomodel.

equations: (1) for the ℓ_x coordinate, and (2) for the ℓ_y. Equations 6-2 may be written

$$\begin{aligned}(\ell_x - x_p) - c\frac{m}{q} &= 0 = E_1 \\ (\ell_y - y_p) - c\frac{n}{q} &= 0 = E_2 \ .\end{aligned} \tag{6-3}$$

d. Linearized Observation Equations. Equations (6-3) can be written as functions of the form

$$\begin{aligned} & f(\ell) = F[(\alpha, \omega, k, x_p, y_p, c, X_o, Y_o, Z_o)_i \ \ (X, Y, Z)j] \\ \text{or} \quad & f(\ell) = F[0, X] \\ & \ell + \upsilon = F\ (0^\circ + \Delta 0,\ X^\circ + \Delta X). \end{aligned} \tag{6-4}$$

Where (ℓ) represents the observed (x, y) image coordinates; 0, the orientation parameters; X, the object space coordinates. 0° and X° are approximations. $\Delta 0$ and ΔX are successive corrections, then $0 = 0^\circ + \Delta 0$, and $X = X^\circ + \Delta X$. (x_p, y_p) and c (focal length) are considered constant for the problem.

By Taylor's Expansion[6], neglecting second and higher order terms, we have

$$f(\ell)^\circ + \frac{\partial f}{\partial \ell}\upsilon_\ell = F(0,X)^\circ + \frac{\partial F}{\partial 0}\Delta 0 + \frac{\partial F}{\partial X}\Delta X.$$

Then the matrix general forms of the observation equations are

$$\underset{(2,2)(2,1)}{A\upsilon} - \underset{(2,6)(6,1)}{B_o\ \Delta 0} - \underset{(2,3)(3,1)}{B_X\ \Delta X} = \underset{(2,1)}{\Delta \ell}\ , \ \Delta\ell = F(0,X)^\circ - \ell\ . \tag{6-5}$$

Equation 6-5 represents a completely linear set of observation equations (one each for ℓx and ℓy) that are used in an iterative process to determine successive approximations to the unknown orientation elements.

Let $$[A] = \begin{bmatrix} \frac{\partial F_1}{\partial \ell_x} & \frac{\partial F_1}{\partial \ell_y} \\ \frac{\partial F_2}{\partial \ell_x} & \frac{\partial F_2}{\partial \ell_y} \end{bmatrix} = \begin{bmatrix} 1 & 0 \\ 0 & 1 \end{bmatrix} ,$$

$$[B_o] = \begin{bmatrix} \frac{\partial F_1}{\partial \alpha} & \frac{\partial F_1}{\partial \omega} & \frac{\partial F_1}{\partial \kappa} & \frac{\partial F_1}{\partial x_p} & \frac{\partial F_1}{\partial y_p} & \frac{\partial F_1}{\partial c} & \frac{\partial F_1}{\partial X_o} & \frac{\partial F_1}{\partial Y_o} & \frac{\partial F_1}{\partial Z_o} \\ \frac{\partial F_2}{\partial \alpha} & \frac{\partial F_2}{\partial \omega} & \frac{\partial F_2}{\partial \kappa} & \frac{\partial F_2}{\partial x_p} & \frac{\partial F_2}{\partial y_p} & \frac{\partial F_2}{\partial c} & \frac{\partial F_2}{\partial X_o} & \frac{\partial F_2}{\partial Y_o} & \frac{\partial F_2}{\partial Z_o} \end{bmatrix} ,$$

and $$[B_X] = \begin{bmatrix} \frac{\partial F_1}{\partial X} & \frac{\partial F_1}{\partial Y} & \frac{\partial F_1}{\partial Z} \\ \frac{\partial F_2}{\partial X} & \frac{\partial F_2}{\partial Y} & \frac{\partial F_2}{\partial Z} \end{bmatrix} ,$$

where v is the vector of corrections to the observations (residuals)

$\Delta 0$ is the vector of corrections to the orientation elements

ΔX is the vector of corrections to the ground coordinates

$\Delta \ell$ is the constant term evaluated with the approximations.

For simplicity, B_o and B_X may be combined and equations (6-5) can be written as

$$Av + B\Delta - L = 0 . \qquad (6\text{-}6)$$

e. Least Squares Adjustment. Assuming the observations to be independent and normally distributed, the most probable values are obtained by minimizing $v^T P v$, where P denotes the weight matrix of the observations. It is convenient to consider P as a unit matrix which is done in the Schmid Method. A direct solution to the problem is obtained by minimizing the following function:

$$v^T P v - 2k^T(Av + B\Delta - L) = 0 . \qquad (6\text{-}7)$$

k denotes a vector of unknown Lagrange multipliers. A direct solution of the final normal equations derived from equation 6-7 is given by

$$\left[B^T (A P^{-1} A^T)^{-1} B\right]\Delta = \left[B^T (A P^{-1} A^T)^{-1} \ell\right] . \qquad (6\text{-}8)$$

Since "A" can be reduced to a unit matrix; equations 6-3 reduce to

$$[B^T P B]\Delta = [B^T P \ell] . \quad (6\text{-}9)$$

By introducing $[B^T P B] = [N]$

and $[B^T P \ell] = [C]$

we obtain $\Delta = [N]^{-1}[C]$. (6-10)

Δ is the correction vector for the unknowns and must be iterated to obtain the final orientation elements for each photograph, and the computed values for each observation.

f. Mean Error of Unit Weight. The mean error of an observation of unit weight is

$$m = \left(\frac{v^T P v}{r-u}\right)^{\frac{1}{2}}$$

where r = number of observations

u = number of unknown parameters.

g. Statistical Analysis of Parameters. The covariance matrix of the parameters is given by equation 6-10 as N^{-1}, which is the inverse of the normal equations. The precision of the orientation parameters (σ_p) is determined by

$$\sigma_p = m \sqrt{Q_{ii}}$$

where Q_{ii} = diagonal terms of N^{-1}.

This technique is also utilized to determine the precision of computing the X, Y, Z-coordinates. It is interesting to note from figure 6-4 that the angle of intersection between rays is much smaller at point "C" than at point "A". As a result, the geometrical precision for determining the Z-coordinate is significantly diluted in the forward positions of the model.

h. Example Computer Print-outs. Output of data for Ranger Model 499-515 is furnished at the end of this chapter as an example of the Schmid Two-camera Orientation Routine. (See figure 6-7.)

SECTION IV. SUMMARY

11. SUMMARY. The discussion of the mathematics of the Schmid Method and the problem examples were presented in this chapter to provide, in general terms, a summary of the analytical approach for obtaining X, Y, Z-coordinates for the Digital Contouring Program. The local cartesian coordinates computed with the Schmid Two-camera Orientation Routine were transformed by the inverse parameters of the coordinate transformation program to the Mercator projection (N,E,H). These coordinates were direct input for digital contouring. The application of the method described herein, and an analysis of the results, are explained in chapter 8.

SECTION V. LITERATURE CITED

1. SCHMID, H. H. "Some Remarks on the Problem of Transforming Geodetic Ellipsoidal Coordinates into Cartesian Coordinates with the Help of Reduced Latitude," Ordnance Computer Research Report. Aberdeen, Md.: Ballistic Research Laboratories, Aberdeen Proving Ground. 15 Apr 1959: Vol VI, No. 2.

2. WOOTEN, A. R. "Mono and Stereo Comparator Reduction Program for the ORDVAC," Ballistic Research Laboratories Memorandum Report No. 1406. Ibid. May 1962.

3. SCHMID, H. H. "A General Analytical Solution to the Problem of Photogrammetry," Ballistic Research Laboratories Report No. 1065. Ibid. Jul 1959.

4. BUTLER, L. M. "Computer Program for the 'Single Model Orientation' Case of the General Problem of Photogrammetry," Ballistic Research Laboratories Report No. 1704. Ibid. Oct 1965.

5. HARDY, M. and BOWLES, L. D. "Selenodetic Control for NASA Project Apollo," Preliminary Report. Washington: U. S. Army Map Service. Mar 1966. (NASA-T-21657(G).)

6. SCARBOROUGH, J. Numerical Mathematical Analysis. Baltimore: The Johns Hopkins Press. 1958: p 478.

```
TRANSFORMATION OF GEODETIC ELLIPSOIDAL COORDINATES INTO CARTESIAN COORDINATES                    PAGE   1

A   .173800000E 07  B   .173800000E 07  LAT    1  4    .0000  LONG  340 19    .0000  H   .500000000E 04  IDEN          1

ALPHA   88 55  21.0000   BETA  253  0    .0000   GAMMA    0  0    .0000   LAMBDA  340 19  22.8000

IDEN          1          XZERO   .174269179E 07          YZERO   .760785097E-04          ZZERO   .327767912E 05

PT NO 4990099          PHI(I)  -.22500000E 00   .00000000E-80   .00000000E-80
TYPE  1                LAMDA(I)  -.14956000E 02   .00000000E-80   .00000000E-80          H(I)   .33681400E 06

            X   -.17705246E 06              Y   -.49513444E 04              Z    .32423996E 06

TPHI   INVERSE
      .290275048E-01      -.950545878E-01       .225844270E-02
     -.947029348E-01      -.291144875E-01      -.818073537E-02
     -.853341340E-01      -.238640402E-02       .996349532E 00


PT NO 5150099          PHI(I)   .31300000E 00   .00000000E-80   .00000000E-80
TYPE  1                LAMDA(I)  -.16827000E 02   .00000000E-80   .00000000E-80          H(I)   .26179602E 06

            X   -.10287408E 06              Y   -.35986578E 04              Z    .25414499E 06

TPHI   INVERSE
      .301801755E-01      -.986190837E-01       .137689633E-02
     -.984873409E-01      -.302114486E-01      -.512757750E-02
     -.514422889E-01      -.179951242E-02       .998674348E 00


PT NO 4990002          PHI(I)   .76000000E 00   .00000000E-80   .00000000E-80
TYPE  1                LAMDA(I)  -.18645000E 02   .00000000E-80   .00000000E-80          H(I)   .70000000E 04

            X   -.32878550E 05              Y    .54009003E 02              Z    .16902298E 04

TPHI   INVERSE
      .345857809E-01      -.113028408E 00       .655265250E-03
     -.113018306E 00      -.345950309E-01      -.212875015E-02
     -.188415760E-01       .309507112E-04       .999822481E 00
```

97

Figure 6-5. Output for the Transformation of Geodetic Ellipsoidal Coordinates into Cartesian Coordinates Program.

TRANSFORMATION OF GEODETIC ELLIPSOIDAL COORDINATES INTO CARTESIAN COORDINATES PAGE 2

```
PT NO 4990004          PHI(I)   .18910000E 01   .00000000E-80   .00000000E-80
TYPE  1                LAMDA(I) -.18710000E 02   .00000000E-80   .00000000E-80          H(I)   .74000000E 04

            X   -.20907289E 05              Y   -.32309962E 05              Z    .19756765E 04

TPHI  INVERSE
      .346108387E-01     -.112981856E 00     -.167728453E-02
     -.113047002E 00     -.345011765E-01     -.199513901E-02
     -.119785086E-01     -.185114944E-01      .999756890E 00


PT NO 4990005          PHI(I)   .19270000E 01   .00000000E-80   .00000000E-80
TYPE  1                LAMDA(I) -.19978000E 02   .00000000E-80   .00000000E-80          H(I)   .70000000E 04

            X    .16325895E 05              Y   -.22062677E 05              Z    .17841424E 04

TPHI  INVERSE
      .345355411E-01     -.113032084E 00     -.175243110E-02
     -.113104221E 00     -.345672128E-01      .621212848E-03
      .935581350E-02     -.126433680E-01      .999876299E 00


PT NO 4990006          PHI(I)   .75000000E 00   .00000000E-80   .00000000E-80
TYPE  1                LAMDA(I) -.19894000E 02   .00000000E-80   .00000000E-80          H(I)   .70000000E 04

            X    .34034850E 04              Y    .11470330E 05              Z    .19589817E 04

TPHI  INVERSE
      .345531398E-01     -.113038271E 00      .675652115E-03
     -.113049740E 00     -.345539701E-01      .447637197E-03
      .195042118E-02      .657325528E-02      .999976494E 00


PT NO 4990007          PHI(I)  -.39800000E 00   .00000000E-80   .00000000E-80
TYPE  1                LAMDA(I) -.19824000E 02   .00000000E-80   .00000000E-80          H(I)   .70500000E 04

            X   -.88560191E 04              Y    .44279592E 05              Z    .14656463E 04

TPHI  INVERSE
      .345488740E-01     -.112997070E 00      .304358511E-02
     -.113039188E 00     -.345535845E-01      .303211134E-03
     -.507493723E-02      .253743973E-01      .999665136E 00
```

Figure 6-5. Continued.

```
PT NO 4990008          PHI(I)  -.34500000E 00   .00000000E-80   .00000000E-80
TYPE  1                LAMDA(I) -.18591000E 02   .00000000E-80   .00000000E-80          H(I)   .70500000E 04

            X   -.44292369E 05              Y    .31752131E 05              Z    .11988106E 04

TPHI  INVERSE
      .345347686E-01     -.113004276E 00      .293415711E-02
     -.113004593E 00     -.345930245E-01     -.223990459E-02
     -.253817194E-01      .181955424E-01      .999512226E 00


PT NO 5150002          PHI(I)   .11730000E 01   .00000000E-80   .00000000E-80
TYPE  1                LAMDA(I) -.20017000E 02   .00000000E-80   .00000000E-80          H(I)   .53000000E 04

            X    .10740511E 05              Y    .24462049E 03              Z    .26689626E 03

TPHI  INVERSE
      .345792159E-01     -.113152679E 00     -.197169454E-03
     -.113174220E 00     -.345870220E-01      .702135530E-03
      .616102269E-02      .140320353E-03      .999981011E 00


PT NO 5150003          PHI(I)   .20380000E 01   .00000000E-80   .00000000E-80
TYPE  1                LAMDA(I) -.19146000E 02   .00000000E-80   .00000000E-80          H(I)   .52500000E 04

            X   -.68958061E 04              Y   -.32667226E 05              Z   -.69748166E 02

TPHI  INVERSE
      .346264318E-01     -.113124577E 00     -.198326292E-02
     -.113212603E 00     -.346341428E-01     -.109705683E-02
     -.395571846E-02     -.187392663E-01      .999816579E 00


PT NO 5150004          PHI(I)   .20640000E 01   .00000000E-80   .00000000E-80
TYPE  1                LAMDA(I) -.20071000E 02   .00000000E-80   .00000000E-80          H(I)   .70000000E 04

            X    .20251852E 05              Y   -.25225287E 05              Z    .17001311E 04

TPHI  INVERSE
      .345261898E-01     -.113030207E 00     -.203498506E-02
     -.113113586E 00     -.345662999E-01      .813214131E-03
      .116056460E-01     -.144557518E-01      .999828155E 00
```

Figure 6-5. Continued

```
TRANSFORMATION OF GEODETIC ELLIPSOIDAL COORDINATES INTO CARTESIAN COORDINATES                PAGE    4

PT NO 5150008          PHI(I)    .30500000E 00    .00000000E-80    .00000000E-80
TYPE  1                LAMDA(I)  -.19970000E 02   .00000000E-80    .00000000E-80          H(I)    .70000000E 04

            X    .16551591E 04              Y    .25107097E 05              Z    .18185849E 04

TPHI  INVERSE
      .34553090IE-01     -.113029071E 00      .159365622E-02
     -.113041851E 00     -.345484757E-01      .604368951E-03
      .948515224E-03      .143880212E-01      .999896037E 00


PT NO 5150009          PHI(I)    .34400000E 00    .00000000E-80    .00000000E-80
TYPE  1                LAMDA(I)  -.19071000E 02   .00000000E-80    .00000000E-80          H(I)    .70000000E 04

            X   -.24179947E 05              Y    .15965093E 05              Z    .17594235E 04

TPHI  INVERSE
      .345636541E-01     -.113026946E 00      .151323618E-02
     -.113027245E 00     -.345904807E-01     -.124997874E-02
     -.138567031E-01      .914905070E-02      .999862134E 00


PT NO 5150010          PHI(I)    .11800000E 01    .00000000E-80    .00000000E-80
TYPE  1                LAMDA(I)  -.19106000E 02   .00000000E-80    .00000000E-80          H(I)    .70000000E 04

            X   -.15713511E 05              Y   -.80701815E 04              Z    .19105873E 04

TPHI  INVERSE
      .345824509E-01     -.113031129E 00     -.211340347E-03
     -.113050289E 00     -.345061104E-01     -.117801630E-02
     -.900487720E-02     -.462474584E-02      .999948761E 00

0000000
```

Figure 6-5. Continued.

COMPARATOR REDUCTION PROGRAM

NEGATIVE SOLUTION

LEFT PLATE 499

CORNER NO	X	Y	CORNER NO	X	Y	SHIFT
1	-.30390967	.29337467	5	-.30389833	.29337333	.00001141
2	-.29870233	.28841567	6	-.29869967	.28840800	.00000812
3	-.29359900	.29364767	7	-.29359900	.29364233	.00000533
4	-.29883900	.29860600	8	-.29882967	.29859667	.00001320

FINAL AVERAGED CORNER VALUES

CORNER NO	X	Y
1	-.30390400	.29337400
2	-.29870100	.28841183
3	-.29359900	.29364500
4	-.29883433	.29860133

GIVEN FOCAL LENGTH	COMPUTED FOCAL LENGTH	PLATE CENTER COORDINATES X	Y
.05510720	.05506674	-.29876770	.29350907

POINT NO.	TYPE	X	Y	STD. ERROR X	STD. ERROR Y	COMPUTED WT. X	COMPUTED WT. Y
4990002	1	-.00003445	.00001784	.00000228	.00000234	1.9256	1.8270
4990004	1	.00005369	-.00509967	.00000268	.00000451	1.3921	.4927
4990005	1	.00525755	-.00512412	.00001779	.00001009	.0316	.0982
4990006	1	.00517286	-.00000310	.00000679	.00000443	.2170	.5105
4990007	1	.00512762	.00514379	.00000836	.00000981	.1432	.1039
4990008	1	-.00006779	.00510513	.00000297	.00000424	1.1367	.5554
5150002	1	.00552022	-.00179220	.00000508	.00000456	.3876	.4803
5150003	1	.00184087	-.00563026	.00000515	.00001593	.3771	.0394
5150004	1	.00557115	-.00557156	.00000569	.00000519	.3087	.3710
5150008	1	.00552766	.00204824	.00001016	.00001078	.0968	.0860
5150009	1	.00184221	.00196883	.00000817	.00000764	.1497	.1715
5150010	1	.00184938	-.00183153	.00000700	.00001042	.2040	.0921
110	9	.00203722	.00628525	1.00000000	1.00000000	1.0000	1.0000
210	9	.00205102	.00573790	1.00000000	1.00000000	1.0000	1.0000
310	9	.00206195	.00530636	1.00000000	1.00000000	1.0000	1.0000
410	9	.00207446	.00481390	1.00000000	1.00000000	1.0000	1.0000
510	9	.00208694	.00432471	1.00000000	1.00000000	1.0000	1.0000
610	9	.00210062	.00378970	1.00000000	1.00000000	1.0000	1.0000
710	9	.00211269	.00331901	1.00000000	1.00000000	1.0000	1.0000
810	9	.00212692	.00276643	1.00000000	1.00000000	1.0000	1.0000
910	9	.00213940	.00228310	1.00000000	1.00000000	1.0000	1.0000
1010	9	.00215257	.00177489	1.00000000	1.00000000	1.0000	1.0000
1110	9	.00216482	.00130380	1.00000000	1.00000000	1.0000	1.0000
1210	9	.00217845	.00078179	1.00000000	1.00000000	1.0000	1.0000
1310	9	.00219108	.00029983	1.00000000	1.00000000	1.0000	1.0000

Figure 6-6. Output for Comparator Reduction Program.

Left Plate

1410	9	.00220517	-.00023610	1.00000000	1.00000000	1.0000	1.0000
1510	9	.00221779	-.00071406	1.00000000	1.00000000	1.0000	1.0000
1610	9	.00223083	-.00120607	1.00000000	1.00000000	1.0000	1.0000
1710	9	.00224445	-.00171817	1.00000000	1.00000000	1.0000	1.0000
1810	9	.00225778	-.00221738	1.00000000	1.00000000	1.0000	1.0000
1910	9	.00227101	-.00271172	1.00000000	1.00000000	1.0000	1.0000
2010	9	.00228430	-.00320624	1.00000000	1.00000000	1.0000	1.0000
2110	9	.00229668	-.00366589	1.00000000	1.00000000	1.0000	1.0000
2210	9	.00231187	-.00424794	1.00000000	1.00000000	1.0000	1.0000
2310	9	.00232436	-.00468904	1.00000000	1.00000000	1.0000	1.0000
2410	9	.00233923	-.00523565	1.00000000	1.00000000	1.0000	1.0000
2510	9	.00235127	-.00567723	1.00000000	1.00000000	1.0000	1.0000
2610	9	.00236533	-.00619044	1.00000000	1.00000000	1.0000	1.0000
2710	9	.00237755	-.00663472	1.00000000	1.00000000	1.0000	1.0000
2810	9	.00239344	-.00720930	1.00000000	1.00000000	1.0000	1.0000
2910	9	.00240800	-.00773131	1.00000000	1.00000000	1.0000	1.0000
3010	9	.00242245	-.00824415	1.00000000	1.00000000	1.0000	1.0000
3110	9	.00243553	-.00870344	1.00000000	1.00000000	1.0000	1.0000

APRIORI WT. X	APRIORI WT. Y	APRIORI WT. XY	ANGULAR WT.
1.00000000	1.00000000	.00000000	.00000000

Figure 6-6. Continued.

RIGHT PLATE 515

CORNER NO	X	Y	CORNER NO	X	Y	SHIFT
1	-.30211200	.28623500	5	-.30210800	.28623567	.00000406
2	-.29831900	.28234667	6	-.29831633	.28235067	.00000481
3	-.29434633	.28614300	7	-.29435033	.28614400	.00000412
4	-.29819933	.28997233	8	-.29819200	.28996800	.00000852

FINAL AVERAGED CORNER VALUES

CORNER NO	X	Y
1	-.30211000	.28623533
2	-.29831767	.28234867
3	-.29434833	.28614350
4	-.29819567	.28997017

GIVEN FOCAL LENGTH	COMPUTED FOCAL LENGTH	PLATE CENTER COORDINATES X	Y
.04155610	.04152559	-.29825618	.28618974

POINT NO.	TYPE	X	Y	STD. ERROR X	STD. ERROR Y	COMPUTED WT. X	COMPUTED WT. Y
4990002	1	-.00580446	.00190975	.00000509	.00002452	.3867	.0166
4990004	1	-.00570288	-.00323712	.00000546	.00001920	.3357	.0271
4990005	1	-.00031436	-.00332064	.00002240	.00001992	.0199	.0252
4990006	1	-.00040047	.00178876	.00001412	.00000504	.0501	.3934
4990007	1	-.00045555	.00702886	.00001578	.00002291	.0401	.0191
4990008	1	-.00598765	.00724725	.00000848	.00002152	.1391	.0216
5150002	1	.00001308	-.00000875	.00000594	.00000583	.2834	.2937
5150003	1	-.00384707	-.00380806	.00001071	.00000262	.0872	1.4523
5150004	1	.00001377	-.00378783	.00001433	.00000432	.0487	.5353
5150008	1	-.00001605	.00384652	.00000305	.00000822	1.0763	.1482
5150009	1	-.00388821	.00385750	.00000350	.00000197	.8180	2.5862
5150010	1	-.00386212	.00000038	.00000115	.00000361	7.5765	.7662
110	9	-.00375996	.00836780	1.00000000	1.00000000	1.0000	1.0000
210	9	-.00372059	.00778547	1.00000000	1.00000000	1.0000	1.0000
310	9	-.00369244	.00735193	1.00000000	1.00000000	1.0000	1.0000
410	9	-.00367071	.00683885	1.00000000	1.00000000	1.0000	1.0000
510	9	-.00364898	.00633995	1.00000000	1.00000000	1.0000	1.0000
610	9	-.00362849	.00577844	1.00000000	1.00000000	1.0000	1.0000
710	9	-.00360815	.00528436	1.00000000	1.00000000	1.0000	1.0000
810	9	-.00356893	.00470148	1.00000000	1.00000000	1.0000	1.0000
910	9	-.00356338	.00421463	1.00000000	1.00000000	1.0000	1.0000
1010	9	-.00353853	.00367084	1.00000000	1.00000000	1.0000	1.0000
1110	9	-.00352823	.00319801	1.00000000	1.00000000	1.0000	1.0000
1210	9	-.00352664	.00267350	1.00000000	1.00000000	1.0000	1.0000
1310	9	-.00349363	.00219298	1.00000000	1.00000000	1.0000	1.0000
1410	9	-.00349263	.00163998	1.00000000	1.00000000	1.0000	1.0000
1510	9	-.00346497	.00115294	1.00000000	1.00000000	1.0000	1.0000
1610	9	-.00345863	.00065328	1.00000000	1.00000000	1.0000	1.0000

Figure 6-6. Continued.

Right Plate

1710	9	-.00342661	.00013137	1.00000000	1.00000000	1.0000	1.0000
1810	9	-.00342286	-.00039519	1.00000000	1.00000000	1.0000	1.0000
1910	9	-.00342386	-.00088971	1.00000000	1.00000000	1.0000	1.0000
2010	9	-.00335870	-.00137605	1.00000000	1.00000000	1.0000	1.0000
2110	9	-.00335641	-.00182976	1.00000000	1.00000000	1.0000	1.0000
2210	9	-.00333659	-.00239505	1.00000000	1.00000000	1.0000	1.0000
2310	9	-.00332540	-.00284325	1.00000000	1.00000000	1.0000	1.0000
2410	9	-.00330844	-.00337803	1.00000000	1.00000000	1.0000	1.0000
2510	9	-.00328955	-.00383494	1.00000000	1.00000000	1.0000	1.0000
2610	9	-.00330481	-.00435622	1.00000000	1.00000000	1.0000	1.0000
2710	9	-.00329600	-.00479586	1.00000000	1.00000000	1.0000	1.0000
2810	9	-.00327231	-.00537031	1.00000000	1.00000000	1.0000	1.0000
2910	9	-.00325103	-.00588241	1.00000000	1.00000000	1.0000	1.0000
3010	9	-.00323849	-.00641013	1.00000000	1.00000000	1.0000	1.0000
3110	9	-.00324473	-.00688390	1.00000000	1.00000000	1.0000	1.0000

APRIORI WT. X	APRIORI WT. Y	APRIORI WT. XY	ANGULAR WT.
1.00000000	1.00000000	.00000000	.00000000

--END OUTPUT FOR THIS PROGRAM--

Figure 6-6. Continued.

STATION IDENTIFICATION RANGER NETWORK
INDICATORS OF VARIATION

CARTESIAN COORDINATES
NO REFRACTION
NO PRERUN
CXI EQUALS CYI
CXJ EQUALS CYJ
P ZEROI NOT GIVEN
P ZEROJ NOT GIVEN
COMPUTE MX
ITERATIONS NOT SET
SKIP MINIMUM SOLUTION
PPHI OR PX CONSTANT
OMIT DISTORTION CURVE
CONSTANT PLX
I AND J INTERSECTION
BOTH CAMERAS
DISTORTION NOT COMBINED

TOLERANCE 0.100000000E-08 DISTORTION CROSSOVER ONE 0.000000000E-79 DISTORTION MAXIMUM 0.000000000E-79
DISTORTION CROSSOVER TWO 0.000000000E-79

CAMERA ONE 499
CAMERA TWO 515

STATION 1 DATE 5-11-66

ORIGINAL ORIENTATION PARAMETERS AND INDICATORS

ALPHA	OMEGA	KAPPA	X ZERO	Y ZERO	Z ZERO
0.174151870E 03	0.872782200E 00	-0.198964520E 02	-0.177052460E 06	-0.495134440E 04	0.336498980E 06
1	1	1	0	0	1
K1	K2	K3	XP	YP	CX
0.000000000E-79	0.000000000E-79	0.000000000E-79	0.000000000E-79	0.000000000E-79	0.551072000E-01
0	0	0	0	0	0
CY					
0.551072000E-01					
0					

STATION 2 DATE 5-11-66

ORIGINAL ORIENTATION PARAMETERS AND INDICATORS

ALPHA	OMEGA	KAPPA	X ZERO	Y ZERO	Z ZERO
0.174152340E 03	0.841557470E 00	-0.204138870E 02	-0.102874080E 06	-0.359865780E 04	0.265954190E 06

Figure 6-7. Output for the Schmid Two - camera Orientation Routine

1	1	1	0	0	1
K1	K2	K3	XP	YP	CX
0.000000000E-79	0.000000000E-79	0.000000000E-79	0.000000000E-79	0.000000000E-79	0.415561000E-01
0	0	0	0	0	0

CY
0.415561000E-01
0

LEVEL OF RESIDUALS

SD1	0.374199086E-04	NO. OF POINTS	86
SD1	0.371745404E-04	NO. OF POINTS	86
SD1	0.371663039E-04	NO. OF POINTS	86
SD1	0.371662187E-04	NO. OF POINTS	86

DETERMINANTS

DMIN -0.000000000E-79 DMAX 0.000000000E-79

FINAL ORIENTATION PARAMETERS LEFT CAMERA

ALPHA	0.174059559E 03	OMEGA	0.879149157E 00	KAPPA	-0.197860281E 02	XZERO	-0.177052460E 06
YZERO	-0.495134440E 04	ZZERO	0.335383541E 06	K1	0.000000000E-79	K2	0.000000000E-79
K3	0.000000000E-79	XP	0.000000000E-79	YP	0.000000000E-79	CX	0.551072000E-01
CY	0.551072000E-01						

MEAN ERRORS OF UNKNOWNS

1	0.852381498E 00	2	0.158125267E 00	3	0.149042783E 01	4	0.000000000E-79
5	0.000000000E-79	6	0.110040394E 05	7	0.000000000E-79	8	0.000000000E-79
9	0.000000000E-79	10	0.000000000E-79	11	0.000000000E-79	12	0.000000000E-79
13	0.000000000E-79						

FINAL ORIENTATION PARAMETERS RIGHT CAMERA

ALPHA	0.174176341E 03	OMEGA	0.849284326E 00	KAPPA	-0.204777368E 02	XZERO	-0.102874080E 06
YZERO	-0.359865780E 04	ZZERO	0.266199695E 05	K1	0.000000000E-79	K2	0.000000000E-79
K3	0.000000000E-79	XP	0.000000000E-79	YP	0.000000000E-79	CX	0.415561000E-01
CY	0.415561000E-01						

Figure 6-7. Continued.

MEAN ERRORS OF UNKNOWNS

14	0.551810415E 00	15	0.180353126E 00	16	0.143528461E 01	17	0.000000000E-79
18	0.000000000E-79	19	0.699393941E 04	20	0.000000000E-79	21	0.000000000E-79
22	0.000000000E-79	23	0.000000000E-79	24	0.000000000E-79	25	0.000000000E-79
26	0.000000000E-79						

INVERSE OF NORMAL EQUATIONS COEFFICIENTS

(1, 1)	0.170385081E 05	(1, 2)	-0.569627930E 03	(1, 3)	-0.244498658E 04	(1, 4)	0.000000000E-79
(1, 5)	0.000000000E-79	(1, 6)	0.138656057E 11	(1, 7)	0.000000000E-79	(1, 8)	0.000000000E-79
(1, 9)	0.000000000E-79	(1,10)	0.000000000E-79	(1,11)	0.000000000E-79	(1,12)	0.000000000E-79
(1,13)	0.000000000E-79	(1,14)	0.980239893E 04	(1,15)	-0.430032152E 03	(1,16)	0.107052593E 02
(1,17)	0.000000000E-79	(1,18)	0.000000000E-79	(1,19)	0.791772090E 10	(1,20)	0.000000000E-79
(1,21)	0.000000000E-79	(1,22)	0.000000000E-79	(1,23)	0.000000000E-79	(1,24)	0.000000000E-79
(1,25)	0.000000000E-79	(1,26)	0.000000000E-79	(2, 2)	0.586362353E 03	(2, 3)	0.310545144E 04
(2, 4)	0.000000000E-79	(2, 5)	0.000000000E-79	(2, 6)	-0.494609023E 09	(2, 7)	0.000000000E-79
(2, 8)	0.000000000E-79	(2, 9)	0.000000000E-79	(2,10)	0.000000000E-79	(2,11)	0.000000000E-79
(2,12)	0.000000000E-79	(2,13)	0.000000000E-79	(2,14)	-0.353812101E 03	(2,15)	0.260881454E 03
(2,16)	0.283977232E 04	(2,17)	0.000000000E-79	(2,18)	0.000000000E-79	(2,19)	-0.301630792E 09
(2,20)	0.000000000E-79	(2,21)	0.000000000E-79	(2,22)	0.000000000E-79	(2,23)	0.000000000E-79
(2,24)	0.000000000E-79	(2,25)	0.000000000E-79	(2,26)	0.000000000E-79	(3, 3)	0.520937279E 05
(3, 4)	0.000000000E-79	(3, 5)	0.000000000E-79	(3, 6)	-0.204136371E 10	(3, 7)	0.000000000E-79
(3, 8)	0.000000000E-79	(3, 9)	0.000000000E-79	(3,10)	0.000000000E-79	(3,11)	0.000000000E-79
(3,12)	0.000000000E-79	(3,13)	0.000000000E-79	(3,14)	-0.116627484E 04	(3,15)	-0.266260022E 04
(3,16)	0.447629648E 05	(3,17)	0.000000000E-79	(3,18)	0.000000000E-79	(3,19)	-0.103918306E 10
(3,20)	0.000000000E-79	(3,21)	0.000000000E-79	(3,22)	0.000000000E-79	(3,23)	0.000000000E-79
(3,24)	0.000000000E-79	(3,25)	0.000000000E-79	(3,26)	0.000000000E-79	(4, 4)	0.100000000E-19
(4, 5)	0.000000000E-79	(4, 6)	0.000000000E-79	(4, 7)	0.000000000E-79	(4, 8)	0.000000000E-79
(4, 9)	0.000000000E-79	(4,10)	0.000000000E-79	(4,11)	0.000000000E-79	(4,12)	0.000000000E-79
(4,13)	0.000000000E-79	(4,14)	0.000000000E-79	(4,15)	0.000000000E-79	(4,16)	0.000000000E-79
(4,17)	0.000000000E-79	(4,18)	0.000000000E-79	(4,19)	0.000000000E-79	(4,20)	0.000000000E-79
(4,21)	0.000000000E-79	(4,22)	0.000000000E-79	(4,23)	0.000000000E-79	(4,24)	0.000000000E-79
(4,25)	0.000000000E-79	(4,26)	0.000000000E-79	(5, 5)	0.100000000E-19	(5, 6)	0.000000000E-79
(5, 7)	0.000000000E-79	(5, 8)	0.000000000E-79	(5, 9)	0.000000000E-79	(5,10)	0.000000000E-79
(5,11)	0.000000000E-79	(5,12)	0.000000000E-79	(5,13)	0.000000000E-79	(5,14)	0.000000000E-79
(5,15)	0.000000000E-79	(5,16)	0.000000000E-79	(5,17)	0.000000000E-79	(5,18)	0.000000000E-79
(5,19)	0.000000000E-79	(5,20)	0.000000000E-79	(5,21)	0.000000000E-79	(5,22)	0.000000000E-79
(5,23)	0.000000000E-79	(5,24)	0.000000000E-79	(5,25)	0.000000000E-79	(5,26)	0.000000000E-79
(6, 6)	0.115087473E 17	(6, 7)	0.000000000E-79	(6, 8)	0.000000000E-79	(6, 9)	0.000000000E-79
(6,10)	0.000000000E-79	(6,11)	0.000000000E-79	(6,12)	0.000000000E-79	(6,13)	0.000000000E-79
(6,14)	0.783985935E 10	(6,15)	-0.360088255E 09	(6,16)	-0.344443829E 08	(6,17)	0.000000000E-79
(6,18)	0.000000000E-79	(6,19)	0.659638531E 16	(6,20)	0.000000000E-79	(6,21)	0.000000000E-79
(6,22)	0.000000000E-79	(6,23)	0.000000000E-79	(6,24)	0.000000000E-79	(6,25)	0.000000000E-79
(6,26)	0.000000000E-79	(7, 7)	0.100000000E-19	(7, 8)	0.000000000E-79	(7, 9)	0.000000000E-79
(7,10)	0.000000000E-79	(7,11)	0.000000000E-79	(7,12)	0.000000000E-79	(7,13)	0.000000000E-79
(7,14)	0.000000000E-79	(7,15)	0.000000000E-79	(7,16)	0.000000000E-79	(7,17)	0.000000000E-79
(7,18)	0.000000000E-79	(7,19)	0.000000000E-79	(7,20)	0.000000000E-79	(7,21)	0.000000000E-79
(7,22)	0.000000000E-79	(7,23)	0.000000000E-79	(7,24)	0.000000000E-79	(7,25)	0.000000000E-79
(7,26)	0.000000000E-79	(8, 8)	0.100000000E-19	(8, 9)	0.000000000E-79	(8,10)	0.000000000E-79
(8,11)	0.000000000E-79	(8,12)	0.000000000E-79	(8,13)	0.000000000E-79	(8,14)	0.000000000E-79

Figure 6-7. Continued.

(8,15)	0.000000000E-79	(8,16)	0.000000000E-79	(8,17)	0.000000000E-79	(8,18)	0.000000000E-79
(8,19)	0.000000000E-79	(8,20)	0.000000000E-79	(8,21)	0.000000000E-79	(8,22)	0.000000000E-79
(8,23)	0.000000000E-79	(8,24)	0.000000000E-79	(8,25)	0.000000000E-79	(8,26)	0.000000000E-79
(9, 9)	0.100000000E-19	(9,10)	0.000000000E-79	(9,11)	0.000000000E-79	(9,12)	0.000000000E-79
(9,13)	0.000000000E-79	(9,14)	0.000000000E-79	(9,15)	0.000000000E-79	(9,16)	0.000000000E-79
(9,17)	0.000000000E-79	(9,18)	0.000000000E-79	(9,19)	0.000000000E-79	(9,20)	0.000000000E-79
(9,21)	0.000000000E-79	(9,22)	0.000000000E-79	(9,23)	0.000000000E-79	(9,24)	0.000000000E-79
(9,25)	0.000000000E-79	(9,26)	0.000000000E-79	(10,10)	0.100000000E-19	(10,11)	0.000000000E-79
(10,12)	0.000000000E-79	(10,13)	0.000000000E-79	(10,14)	0.000000000E-79	(10,15)	0.000000000E-79
(10,16)	0.000000000E-79	(10,17)	0.000000000E-79	(10,18)	0.000000000E-79	(10,19)	0.000000000E-79
(10,20)	0.000000000E-79	(10,21)	0.000000000E-79	(10,22)	0.000000000E-79	(10,23)	0.000000000E-79
(10,24)	0.000000000E-79	(10,25)	0.000000000E-79	(10,26)	0.000000000E-79	(11,11)	0.100000000E-19
(11,12)	0.000000000E-79	(11,13)	0.000000000E-79	(11,14)	0.000000000E-79	(11,15)	0.000000000E-79
(11,16)	0.000000000E-79	(11,17)	0.000000000E-79	(11,18)	0.000000000E-79	(11,19)	0.000000000E-79
(11,20)	0.000000000E-79	(11,21)	0.000000000E-79	(11,22)	0.000000000E-79	(11,23)	0.000000000E-79
(11,24)	0.000000000E-79	(11,25)	0.000000000E-79	(11,26)	0.000000000E-79	(12,12)	0.100000000E-19
(12,13)	0.000000000E-79	(12,14)	0.000000000E-79	(12,15)	0.000000000E-79	(12,16)	0.000000000E-79
(12,17)	0.000000000E-79	(12,18)	0.000000000E-79	(12,19)	0.000000000E-79	(12,20)	0.000000000E-79
(12,21)	0.000000000E-79	(12,22)	0.000000000E-79	(12,23)	0.000000000E-79	(12,24)	0.000000000E-79
(12,25)	0.000000000E-79	(12,26)	0.000000000E-79	(13,13)	0.100000000E-19	(13,14)	0.000000000E-79
(13,15)	0.000000000E-79	(13,16)	0.000000000E-79	(13,17)	0.000000000E-79	(13,18)	0.000000000E-79
(13,19)	0.000000000E-79	(13,20)	0.000000000E-79	(13,21)	0.000000000E-79	(13,22)	0.000000000E-79
(13,23)	0.000000000E-79	(13,24)	0.000000000E-79	(13,25)	0.000000000E-79	(13,26)	0.000000000E-79
(14,14)	0.714074168E 04	(14,15)	-0.276780106E 03	(14,16)	-0.372326378E 03	(14,17)	0.000000000E-79
(14,18)	0.000000000E-79	(14,19)	0.552594665E 10	(14,20)	0.000000000E-79	(14,21)	0.000000000E-79
(14,22)	0.000000000E-79	(14,23)	0.000000000E-79	(14,24)	0.000000000E-79	(14,25)	0.000000000E-79
(14,26)	0.000000000E-79	(15,15)	0.762800351E 03	(15,16)	-0.294733088E 04	(15,17)	0.000000000E-79
(15,18)	0.000000000E-79	(15,19)	-0.227736454E 09	(15,20)	0.000000000E-79	(15,21)	0.000000000E-79
(15,22)	0.000000000E-79	(15,23)	0.000000000E-79	(15,24)	0.000000000E-79	(15,25)	0.000000000E-79
(15,26)	0.000000000E-79	(16,16)	0.483102844E 05	(16,17)	0.000000000E-79	(16,18)	0.000000000E-79
(16,19)	-0.372599035E 09	(16,20)	0.000000000E-79	(16,21)	0.000000000E-79	(16,22)	0.000000000E-79
(16,23)	0.000000000E-79	(16,24)	0.000000000E-79	(16,25)	0.000000000E-79	(16,26)	0.000000000E-79
(17,17)	0.100000000E-19	(17,18)	0.000000000E-79	(17,19)	0.000000000E-79	(17,20)	0.000000000E-79
(17,21)	0.000000000E-79	(17,22)	0.000000000E-79	(17,23)	0.000000000E-79	(17,24)	0.000000000E-79
(17,25)	0.000000000E-79	(17,26)	0.000000000E-79	(18,18)	0.100000000E-19	(18,19)	0.000000000E-79
(18,20)	0.000000000E-79	(18,21)	0.000000000E-79	(18,22)	0.000000000E-79	(18,23)	0.000000000E-79
(18,24)	0.000000000E-79	(18,25)	0.000000000E-79	(18,26)	0.000000000E-79	(19,19)	0.464908529E 16
(19,20)	0.000000000E-79	(19,21)	0.000000000E-79	(19,22)	0.000000000E-79	(19,23)	0.000000000E-79
(19,24)	0.000000000E-79	(19,25)	0.000000000E-79	(19,26)	0.000000000E-79	(20,20)	0.100000000E-19
(20,21)	0.000000000E-79	(20,22)	0.000000000E-79	(20,23)	0.000000000E-79	(20,24)	0.000000000E-79
(20,25)	0.000000000E-79	(20,26)	0.000000000E-79	(21,21)	0.100000000E-19	(21,22)	0.000000000E-79
(21,23)	0.000000000E-79	(21,24)	0.000000000E-79	(21,25)	0.000000000E-79	(21,26)	0.000000000E-79
(22,22)	0.100000000E-19	(22,23)	0.000000000E-79	(22,24)	0.000000000E-79	(22,25)	0.000000000E-79
(22,26)	0.000000000E-79	(23,23)	0.100000000E-19	(23,24)	0.000000000E-79	(23,25)	0.000000000E-79
(23,26)	0.000000000E-79	(24,24)	0.100000000E-19	(24,25)	0.000000000E-79	(24,26)	0.000000000E-79
(25,25)	0.100000000E-19	(25,26)	0.000000000E-79	(26,26)	0.100000000E-19	(,)	

MEAN ERRORS OF UNKNOWNS BEING CORRECTED

Figure 6-7. Continued.

NC	T	N	X VX	Y VY	Z VZ	MX VLX	MY VLY	MZ
4990002	1	3	-0.327484191E 05 0.130130868E 03	-0.154433217E 03 -0.208442220E 03	0.129078333E 04 -0.399446467E 03	0.000000000E-79 0.370950979E-04 -0.282226957E-04	0.000000000E-79 -0.551197262E-04 0.406468188E-04	0.000000000E-79
4990004	1	3	-0.210219582E 05 -0.114669169E 03	-0.322366706E 05 0.732914213E 02	0.160416703E 04 -0.371509466E 03	0.000000000E-79 0.298133020E-04 0.493556058E-07	0.000000000E-79 -0.199309213E-04 -0.251570021E-04	0.000000000E-79
4990005	1	3	0.164043057E 05 0.784106577E 02	-0.223267230E 05 -0.264045975E 03	0.197105522E 04 0.186912819E 03	0.000000000E-79 -0.161738712E-04 0.765269859E-05	0.000000000E-79 0.117081140E-04 0.466717577E-04	0.000000000E-79
4990006	1	3	0.355015320E 04 0.146668201E 03	0.110296409E 05 -0.440689108E 03	0.206425251E 04 0.105270807E 03	0.000000000E-79 -0.886797079E-05 0.444842870E-05	0.000000000E-79 -0.629803965E-05 0.757633354E-04	0.000000000E-79
4990007	1	3	-0.870831370E 04 0.147705499E 03	0.442473888E 05 -0.322031847E 02	0.163156508E 04 0.165918785E 03	0.000000000E-79 -0.118956957E-04 -0.172496092E-04	0.000000000E-79 0.327808327E-04 0.924189919E-05	0.000000000E-79
4990008	1	3	-0.446804768E 05 -0.388107783E 03	0.319248444E 05 0.172713351E 03	0.136509071E 04 0.166280115E 03	0.000000000E-79 -0.172576523E-04 0.607204153E-04	0.000000000E-79 0.588298631E-04 -0.578921673E-04	0.000000000E-79
5150002	1	3	0.112904917E 05 0.549980749E 03	0.232055888E 03 -0.125646017E 02	0.519303691E 03 0.252407431E 03	0.000000000E-79 -0.201601904E-05 -0.878146182E-04	0.000000000E-79 0.556060518E-05 0.314102635E-04	0.000000000E-79
5150003	1	3	-0.663109894E 04 0.264707159E 03	-0.325781894E 05 0.890366006E 02	0.128205579E 03 0.197953745E 03	0.000000000E-79 -0.115426756E-04 -0.410258542E-04	0.000000000E-79 -0.220776922E-04 0.570278217E-05	0.000000000E-79

Figure 6-7. Continued.

5150004 1 3	0.200770282E 05	-0.248562619E 05	0.172374957E 04	0.000000000E-79	0.000000000E-79	0.000000000E-79
	-0.174823813E 03	0.369025129E 03	0.236184713E 02	-0.170747486E-04	-0.111833249E-04	
				0.213183040E-04	-0.604485719E-04	
5150008 1 3	0.152915834E 04	0.251481218E 05	0.178357795E 04	0.000000000E-79	0.000000000E-79	0.000000000E-79
	-0.126000761E 03	0.410248072E 02	-0.350069477E 02	-0.161823834E-05	-0.637407858E-05	
				0.191792075E-04	-0.124063664E-04	
5150009 1 3	-0.245066039E 05	0.161051925E 05	0.161108151E 04	0.000000000E-79	0.000000000E-79	0.000000000E-79
	-0.326656923E 03	0.140098508E 03	-0.148341987E 03	0.427720358E-05	-0.414942806E-04	
				0.444396962E-04	-0.362681018E-04	
5150010 1 3	-0.159366265E 05	-0.802911957E 04	0.176653001E 04	0.000000000E-79	0.000000000E-79	0.000000000E-79
	-0.223115468E 03	0.410619333E 02	-0.144057290E 03	0.580148285E-05	-0.451441124E-04	
				0.321451002E-04	-0.152420000E-04	
110 9 3	-0.340732259E 05	0.435525328E 05	0.428903165E 04	0.295429684E 04	0.216252676E 04	0.761806418E 04
	0.000000000E-79	0.000000000E-79	0.000000000E-79	0.208033387E-05	0.317851351E-04	
				-0.798450361E-05	-0.138826484E-04	
210 9 3	-0.323197568E 05	0.403301493E 05	0.324780917E 04	0.303383655E 04	0.211080196E 04	0.772127386E 04
	0.000000000E-79	0.000000000E-79	0.000000000E-79	0.165949884E-05	0.264244619E-04	
				-0.648723861E-05	-0.116971184E-04	
310 9 3	-0.310646005E 05	0.378582758E 05	0.265986996E 04	0.308575328E 04	0.206649983E 04	0.778007658E 04
	0.000000000E-79	0.000000000E-79	0.000000000E-79	0.250278122E-05	0.410628989E-04	
				-0.994976725E-05	-0.183505036E-04	
410 9 3	-0.297435193E 05	0.348416674E 05	0.234279742E 04	0.314380192E 04	0.201417414E 04	0.783726323E 04
	0.000000000E-79	0.000000000E-79	0.000000000E-79	0.212853778E-05	0.363472263E-04	
				-0.861525207E-05	-0.164420923E-04	
510 9 3	-0.284590378E 05	0.318823361E 05	0.206736431E 04	0.319831672E 04	0.196245854E 04	0.788730644E 04
	0.000000000E-79	0.000000000E-79	0.000000000E-79	0.226225549E-05	0.401887139E-04	

Figure 6-7. Continued.

				-0.933454786E-05	-0.183892076E-04	
610 9 3	-0.270519027E 05	0.285252656E 05	0.183749286E 04	0.326192305E 04	0.190777506E 04	0.794550506E 04
	0.000000000E-79	0.000000000E-79	0.000000000E-79	0.154102006E-05	0.287404867E-04	
				-0.648645300E-05	-0.133249484E-04	
710 9 3	-0.257637607E 05	0.255726172E 05	0.153372968E 04	0.332101864E 04	0.186234246E 04	0.800232578E 04
	0.000000000E-79	0.000000000E-79	0.000000000E-79	0.975917128E-06	0.190324920E-04	
				-0.418182112E-05	-0.892351824E-05	
810 9 3	-0.239278757E 05	0.221695942E 05	0.470110430E 03	0.340926945E 04	0.181730142E 04	0.810983107E 04
	0.000000000E-79	0.000000000E-79	0.000000000E-79	0.533575925E-06	0.109860288E-04	
				-0.233579973E-05	-0.521368162E-05	
910 9 3	-0.229669869E 05	0.191108666E 05	0.934012996E 03	0.344686136E 04	0.176845783E 04	0.811587156E 04
	0.000000000E-79	0.000000000E-79	0.000000000E-79	0.497765100E-06	0.107572024E-04	
				-0.222673183E-05	-0.516197821E-05	
1010 9 3	-0.214601229E 05	0.158278772E 05	0.436841189E 03	0.352059112E 04	0.172939768E 04	0.819155094E 04
	0.000000000E-79	0.000000000E-79	0.000000000E-79	-0.423019909E-06	-0.968981989E-05	
				0.192880358E-05	0.470342906E-05	
1110 9 3	-0.204270366E 05	0.128713062E 05	0.677151768E 03	0.356250241E 04	0.169022131E 04	0.820767894E 04
	0.000000000E-79	0.000000000E-79	0.000000000E-79	-0.288331243E-06	-0.695636195E-05	
				0.134533791E-05	0.341030041E-05	
1210 9 3	-0.194871561E 05	0.954629260E 04	0.139784076E 04	0.359727955E 04	0.164848472E 04	0.819880289E 04
	0.000000000E-79	0.000000000E-79	0.000000000E-79	-0.312990853E-06	-0.803361796E-05	
				0.149942332E-05	0.398280878E-05	
1310 9 3	-0.179577289E 05	0.662246235E 04	0.608128173E 03	0.366712463E 04	0.162404074E 04	0.827322709E 04
	0.000000000E-79	0.000000000E-79	0.000000000E-79	0.185032750E-06	0.503033321E-05	
				-0.911460429E-06	-0.251477986E-05	

Figure 6-7. Continued.

```
1410 9 3  -0.169615458E 05   0.312154559E 04   0.134201728E 04   0.370721624E 04   0.159320603E 04   0.826896132E 04
           0.000000000E-79   0.000000000E-79   0.000000000E-79  -0.313847853E-06  -0.920140602E-05
                                                                  0.158866769E-05   0.465194855E-05

1510 9 3  -0.155053045E 05   0.110246904E 03   0.760704130E 03   0.377548090E 04   0.157861512E 04   0.833516973E 04
           0.000000000E-79   0.000000000E-79   0.000000000E-79  -0.268437358E-06  -0.843150653E-05
                                                                  0.139813856E-05   0.429770136E-05

1610 9 3  -0.144986095E 05  -0.304875148E 04   0.121279832E 04   0.381609973E 04   0.156315696E 04   0.833941205E 04
           0.000000000E-79   0.000000000E-79   0.000000000E-79  -0.384146755E-06  -0.130414521E-04
                                                                  0.206374323E-05   0.670787109E-05

1710 9 3  -0.128671398E 05  -0.630950196E 04   0.472584675E 03   0.389411033E 04   0.156094381E 04   0.841719483E 04
           0.000000000E-79   0.000000000E-79   0.000000000E-79  -0.353136322E-06  -0.130737627E-04
                                                                  0.196636573E-05   0.677757478E-05

1810 9 3  -0.118495821E 05  -0.964352238E 04   0.102841981E 04   0.393765071E 04   0.155940452E 04   0.842109010E 04
           0.000000000E-79   0.000000000E-79   0.000000000E-79  -0.889909522E-06  -0.363622078E-04
                                                                  0.510997267E-05   0.190176241E-04

1910 9 3  -0.110345925E 05  -0.127845982E 05   0.186618104E 04   0.396452020E 04   0.156158488E 04   0.839603535E 04
           0.000000000E-79   0.000000000E-79   0.000000000E-79  -0.800995910E-06  -0.362149161E-04
                                                                  0.480595505E-05   0.190907071E-04

2010 9 3  -0.867206760E 04  -0.158899664E 05  -0.475427264E 03   0.408742703E 04   0.158881990E 04   0.856550663E 04
           0.000000000E-79   0.000000000E-79   0.000000000E-79  -0.312105737E-06  -0.157040249E-04
                                                                  0.198334335E-05   0.831556521E-05

2110 9 3  -0.784942578E 04  -0.187936257E 05   0.161721461E 03   0.411574895E 04   0.160394977E 04   0.854797847E 04
           0.000000000E-79   0.000000000E-79   0.000000000E-79  -0.179012407E-06  -0.101130216E-04
                                                                  0.120533101E-05   0.538897809E-05

2210 9 3  -0.640055610E 04  -0.224256540E 05   0.949260385E 02   0.417968123E 04   0.163635347E 04   0.858254080E 04
           0.000000000E-79   0.000000000E-79   0.000000000E-79  -0.149716243E-06  -0.998085045E-05
```

Figure 6-7. Continued.

```
                                                                0.109316578E-05   0.535369638E-05

2310 9 3  -0.537365381E 04  -0.253120926E 05   0.305855107E 03   0.422005745E 04   0.166641688E 04   0.858854631E 04
           0.000000000E-79   0.000000000E-79   0.000000000E-79   0.405681106E-07   0.315804073E-05
                                                                -0.324460199E-06  -0.170243067E-05

2410 9 3  -0.405053949E 04  -0.287699635E 05   0.366068703E 03   0.427518593E 04   0.171065349E 04   0.860842788E 04
           0.000000000E-79   0.000000000E-79   0.000000000E-79   0.162450760E-06   0.158239449E-04
                                                                -0.149075005E-05  -0.857539921E-05

2510 9 3  -0.278545875E 04  -0.317380581E 05   0.139487714E 03   0.433467633E 04   0.175612615E 04   0.864900196E 04
           0.000000000E-79   0.000000000E-79   0.000000000E-79   0.298538048E-07   0.369749267E-05
                                                                -0.313757180E-06  -0.201113302E-05

2610 9 3  -0.229139374E 04  -0.349947366E 05   0.172515240E 04   0.433864402E 04   0.179934692E 04   0.857264241E 04
           0.000000000E-79   0.000000000E-79   0.000000000E-79  -0.246355221E-07  -0.443338240E-05
                                                                 0.330210362E-06   0.242369754E-05

2710 9 3  -0.133105021E 04  -0.378204822E 05   0.202062435E 04   0.437583706E 04   0.184822134E 04   0.857226489E 04
           0.000000000E-79   0.000000000E-79   0.000000000E-79   0.289603008E-08   0.845489183E-06
                                                                -0.562833122E-07  -0.463615038E-06

2810 9 3   0.244744009E 03  -0.415768317E 05   0.179959013E 04   0.444597081E 04   0.192308398E 04   0.861151413E 04
           0.000000000E-79   0.000000000E-79   0.000000000E-79   0.158512847E-08   0.246485388E-05
                                                                -0.137003980E-06  -0.135520054E-05

2910 9 3   0.165589409E 04  -0.449465030E 05   0.161161795E 04   0.450797990E 04   0.199567901E 04   0.864380057E 04
           0.000000000E-79   0.000000000E-79   0.000000000E-79  -0.227644037E-07   0.122292967E-04
                                                                -0.566503498E-06  -0.673592439E-05

3010 9 3   0.287070641E 04  -0.483627394E 05   0.185540699E 04   0.455757411E 04   0.206987308E 04   0.865120032E 04
           0.000000000E-79   0.000000000E-79   0.000000000E-79   0.371173670E-08  -0.843635121E-06
                                                                 0.292303426E-07   0.465214669E-06
```

Figure 6-7. Continued.

3110 9 3	0.348604811E 04	-0.513048541E 05	0.295043907E 04	0.456966596E 04	0.212997431E 04	0.859881652E 04
	0.000000000E-79	0.000000000E-79	0.000000000E-79	0.856586411E-07	-0.128377458E-04	
				0.308324875E-06	0.708667585E-05	

SUM CF SGUARED PLATE RESIDUALS - LEFT CAMERA	0.603455972E-08
SUM CF SGUARED PLATE RESIDUALS - RIGHT CAMERA	0.414256133E-07
RMS CN SUM OF BCTH PLATE RESIDUALS	0.102518812E-03
SUM CF SGUARED SPATIAL RESIDUALS	0.186274607E-08
SUM CF SGUARED PLATE AND SPATIAL RESIDUALS	0.172552027E-05
RMS CN SUM OF PLATE AND SPATIAL RESIDUALS	0.102574193E-03

Figure 6-7. Continued.

```
T2CAMM                                                                                              00000000

100-08000000000000000000000000 499 515 RANGER NETWORK                                               CARD   1
111001000000011100100000001001100101113130                                                          CARD   2
+17415187+03+87278220+00-19896652+02              5-23-661                                          CARD   3
-17705246+06-49513444+04+33649898+06              5-11-661                                          CARD   4
+00000000+00+00000000+00+55107200-01+55107200-01  5-11-661                                          CARD   5
+17415234+03+84155747+00-20413887+02              5-23-662                                          CARD   6
-10287408+06-35986578+04+26595419+06              5-11-662                                          CARD   7
+00000000+00+00000000+00+41556100-01+41556100-01  5-11-662                                          CARD   8
+100000-14+000000+00+000000+00+100000-14+000000+00+100000-141                                       CARD   9
-32878550+05+54009003+02+16902298+04                               14990002    1                    CARD  10
-20907289+05-32309962+05+19756765+04                               14990004    1                    CARD  11
+16325895+05-22062677+05+17841424+04                               14990005    1                    CARD  12
+34034850+04+11470330+05+19589817+04                               14990006    1                    CARD  13
-88560192+04+44279592+05+14656463+04                               14990007    1                    CARD  14
-44292369+05+31752131+05+11988106+04                               14990008    1                    CARD  15
+10740511+05+24462049+03+26689626+03                               15150002    1                    CARD  16
-68958061+04-32667226+05-69748166+02                               15150003    1                    CARD  17
+20251852+05-25225287+05+17001311+04                               15150004    1                    CARD  18
+16551591+04+25107097+05+18185849+04                               15150008    1                    CARD  19
-24179947+05+15965094+05+17594235+04                               15150009    1                    CARD  20
-15713511+05-80701815+04+19105873+04                               15150010    1                    CARD  21
00000000000000000000000000000000000000000000000000000000000000000000000000                          CARD  22
+10000000+01+10000001+00+00000C00+00+10000000+01+10000000+01+00000000+00                            CARD  23
E N D   O F   I N P U T   D A T A
```

Figure 6-7. Continued.

CHAPTER 7

DIGITAL CONTOURING

SECTION I. INTRODUCTION

1. GENERAL. The requirement to study and develop techniques for obtaining cartographic information and maps from Ranger photography led AMS cartographers to consider two different general approaches to the problem. One approach was to modify conventional instruments, and the second approach was to utilize completely computational methods. The Ranger stereomodels were geometrically unusual: high tilts, extreme base-height ratios, and short focal lengths (1-inch in taking camera). These models, therefore, could not be absolutely oriented (leveled) in available, conventional analog photogrammetric plotters. This situation was the primary reason for resorting to computational methods. Moreover, at the beginning of the project, it was not certain that appropriate projectors could be obtained to modify existing universal plotters in the prescribed time frame. Therefore, it was decided that a mathematical adjustment and digital contouring approach should be developed that would provide a completely computational approach to the problem. This chapter describes a computerized contouring method that utilizes adjusted photogrammetric measurements (X, Y, Z-coordinates). This method, called "Analytical Topographic Compilation" (ATC), is illustrated in figure 7-1.

SECTION II. PHOTOGRAMMETRIC MENSURATION AND ADJUSTMENT APPROACHES

2. METHODS. Two different approaches for measuring and adjusting these data have been presented in chapters 5 and 6. A brief recap of the two approaches, Comparator/Analytical and Analog Plotter/Mathematical

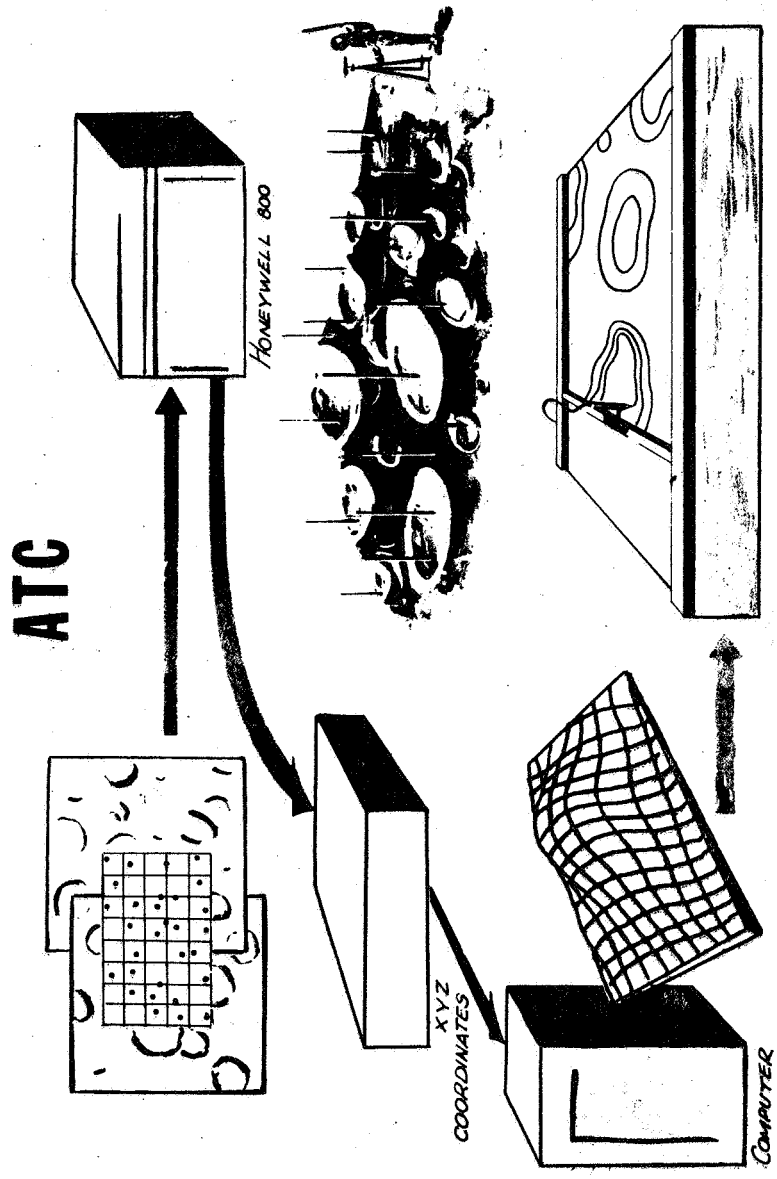

Figure 7-1. Analytical Topographic Compilation.

Orientation, is made below to re-emphasize that the output from both approaches is the input into the Digital Contouring Program. (See figure 7-2.)

a. Comparator/Analytical System. In all of these experiments, the Zeiss stereocomparator PSK and the Schmid Method[1] of analytical photogrammetry were employed. Utilizing this precision 1-2 micron comparator, a dense network of x, y-stereocomparator coordinates was measured in addition to the control point images and fiducial marks. In most cases, the network amounted to a gridded pattern of 0.5-mm squares over the stereomodel. The number of measurements ranged from about 1,000 to 5,000 per model, depending on the area covered and the type of surface terrain encountered. The final adjusted coordinates were transformed into the Mercator projection considering a lunar sphere of radius 1738 km. These Mercator coordinates are called Northing (N) and Easting (E) coordinates with their corresponding elevation (H). These N, E, and H values were the input into the Digital Contouring Program.

b. Analog Plotter/Mathematical Orientation System. The Zeiss stereoplanigraph C-8 was utilized in all of these experiments. As previously stated, the photography could not be leveled in the AMS stereoplanigraphs. However, by enlarging the photographs to the six-inch principal distance, a relative orientation of one photo to another was obtained and the relative base distance of the model could be set. With this arrangement, overlapping pairs of Ranger photographs were selected, such as 507-515, so that the difference in height of exposure stations (bZ) could be accommodated. The bZ was usually about $\pm$ 20 mm and the

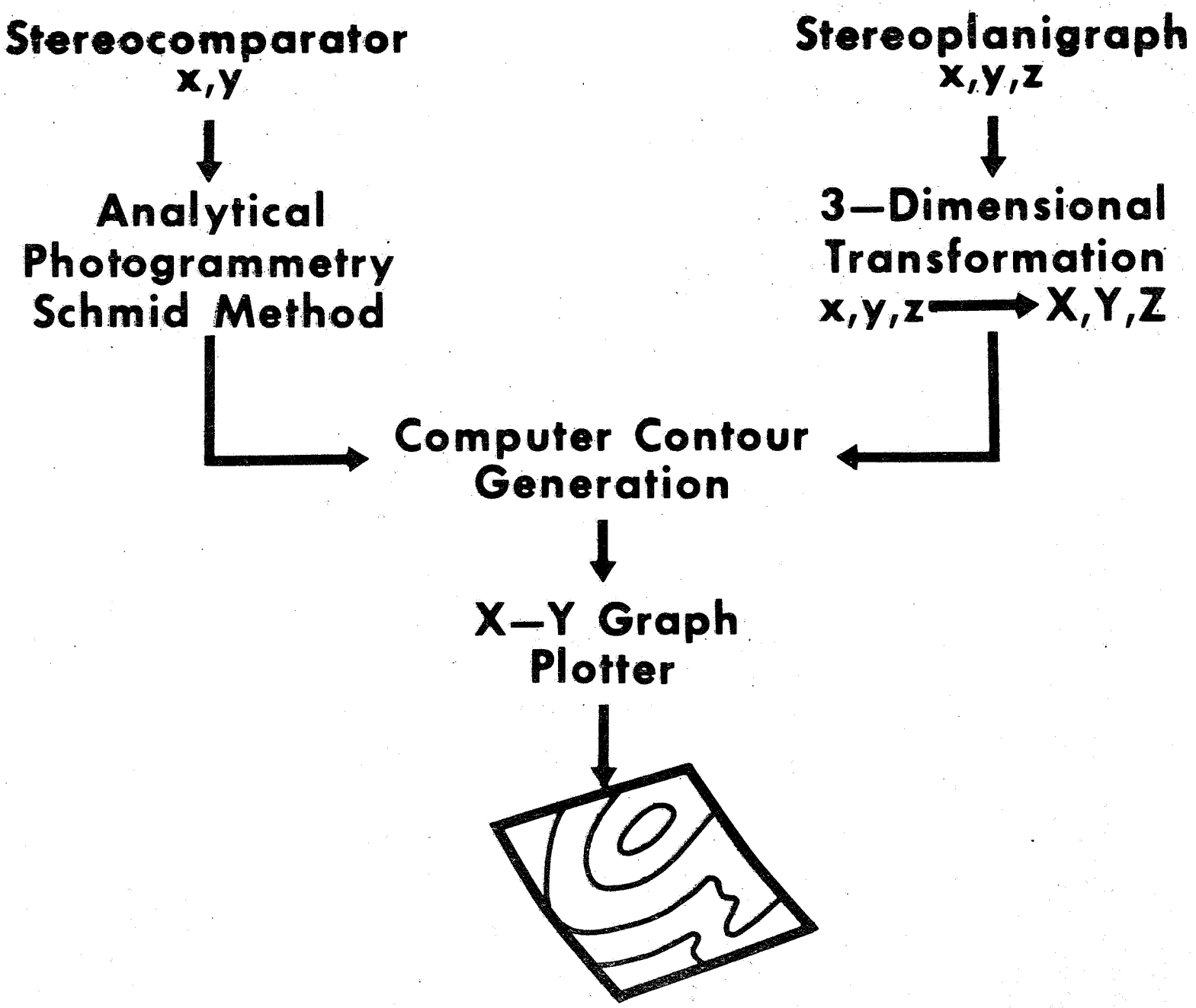

Figure 7-2. Analytical Topographic Compilation.

base setting (bX) was about 30 mm. With this configuration, instrument x, y, z-coordinates were observed and recorded. In most cases the network amounted to a gridded pattern of 1-mm squares over the entire stereomodel. These x, y, z-coordinates were then transformed by a three-dimensional linear transformation[2 3], that considers lunar curvature, to selenodetic coordinates and then to Mercator coordinates N, E, and corresponding H values (as mentioned previously in paragraph 2a). These N, E, and H values were the input into the Digital Contouring Program.

SECTION III. NUMERICAL SURFACE TECHNIQUES

3. BACKGROUND. To determine contours by computational methods from a stereomodel, the usual procedure is to represent the surface by a network of measured points, then by an equation. In addition, an efficient contouring method should make use of the many techniques which are consciously or subconsciously employed in manual contouring. It is possible to obtain a statistically valid surface of a data configuration that is completely unrealistic when it is compared to what the cartographer might expect, due to his knowledge of topography. With these considerations in mind, various ideas were explored with the idea of designing an AMS contouring program. First, however, literature on digital contouring had to be obtained and inquiry had to be made among various organizations to determine whether any digital contouring programs were available. It was determined that IBM[4], the Marquardt Corporation[5], CDC[6], and the X, Y-Plotter manufacturers have these programs. The Numerical Surface Techniques, described herein, are a consolidation of citations 4, 5, and 6, associated with additional concepts, to formulate a procedure for digital

contouring of topographic data.

4. DIGITAL CONTOURING PROCEDURE. a. Contour Program Input Data. Input into the contouring program consists of three coordinate values (X, Y, Z) for each data point. The X, Y, and Z's correspond to Easting and Northing grid coordinates and the elevation of the point of interest. These coordinates are the transformed photogrammetric measurements. Normally, they are randomly distributed as shown at the top of figure 7-3.

b. Mathematical Grid Construction. A uniform mathematical grid must be established over the model area. According to IBM, the grid interval should not exceed one-third of the average distance between the network of data points for accurate interpretation of the surface.

c. Mesh-point Values. Once the grid system has been established, the Z mesh-point values of the grid must be determined. This is accomplished by a continuous process of fitting planes to groups of observed data points. The size of these planes is defined by the grid (mesh) interval, which has been determined from the average interval between the measurements. Thus, the completeness of the contours becomes a function of the density of the measurements. The general form of the equation representing the plane is

$$Z = K + HX + DY \quad . \qquad (7\text{-}1)$$

To fit these planes, four to eight observed points should be selected so that the least squares solution will apply. Observed points closest to the area of interest are chosen for the plane fit. The number chosen can be controlled by defining a circle of a given radius. (See figure 7-4.) Equation 7-1 is then fitted to these points by the method of least squares.

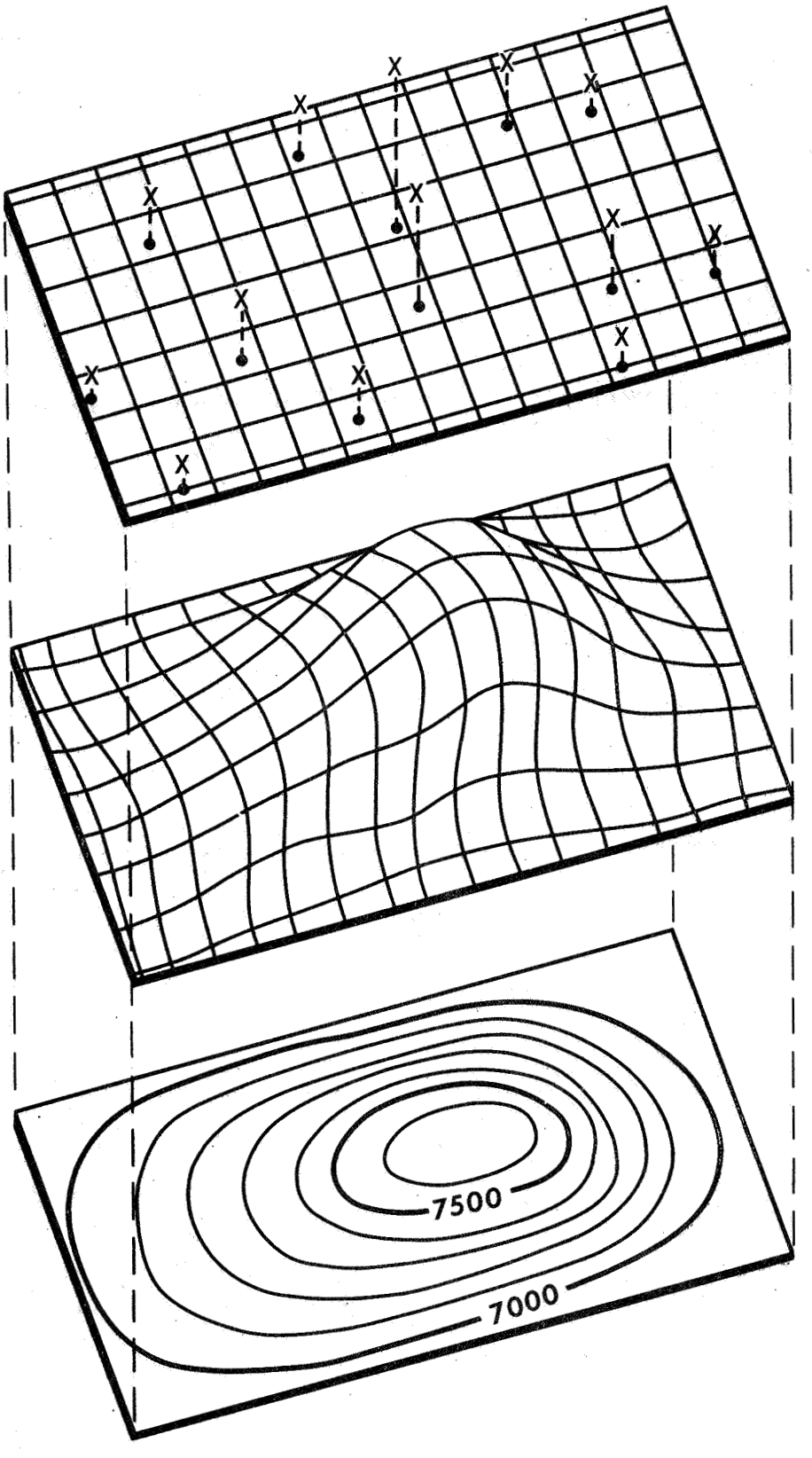

Figure 7-3. Numerical Surface Representation.

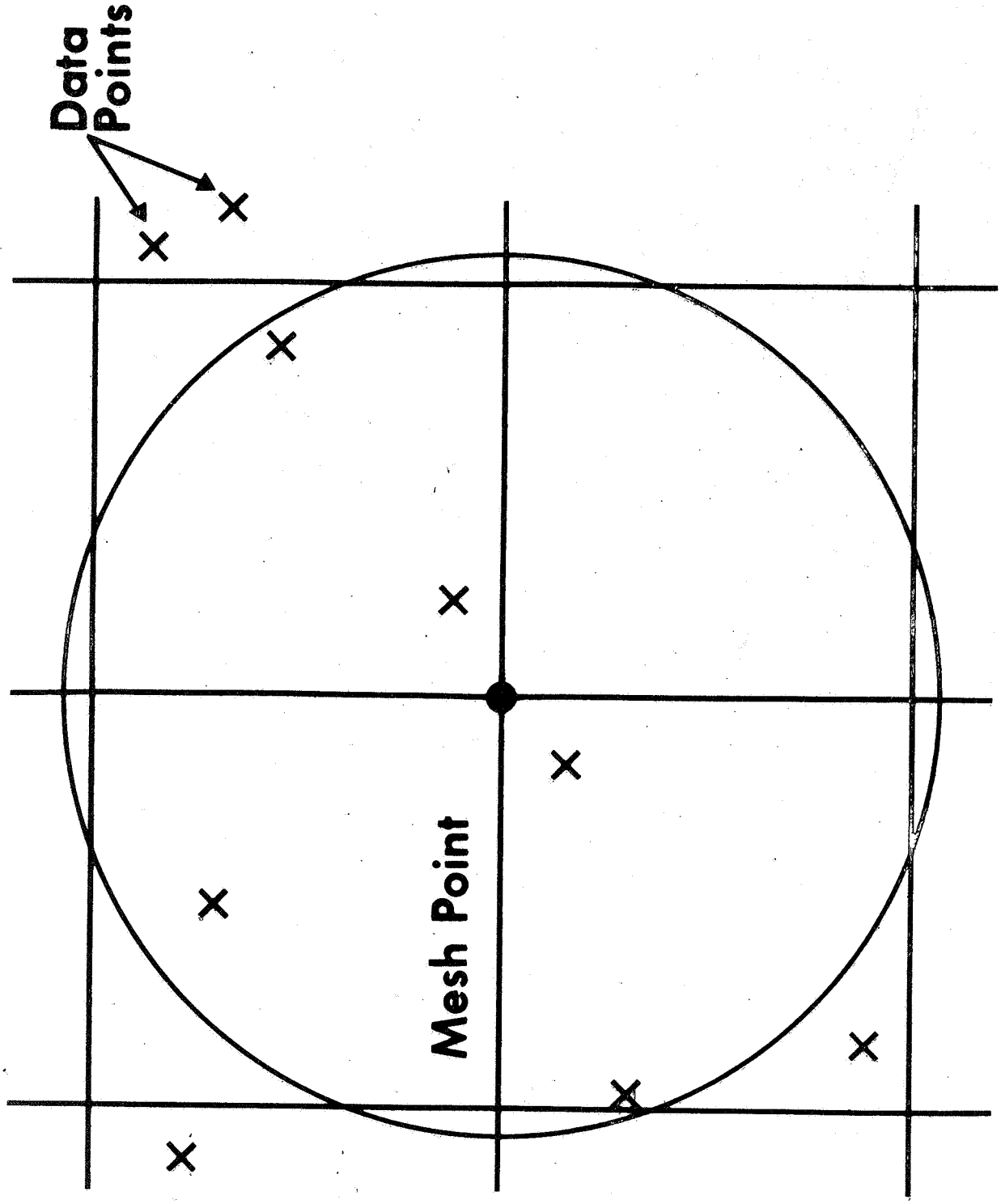

Figure 7-4. Circle with Five Random Data Points.

Figure 7-5 illustrates the fitted plane to five data points. To fit these planes, first the centroid of the selected data points is computed. Next, the plane passing through this centroid is established by a weighted, least squares fit. The weights are so determined that data points closer to the centroid are given greater weight than those further away. The values of the plane, at the corners of a particular grid square, are the mesh-points involved. (See figures 7-5 and 7-6.) Note from figure 7-5 that the least squares criteria provide the best fit. Three of the points are above the plane and two are under it. The observation equations for the plane $Z = K + HX + DY$ are

$$\begin{bmatrix} 1 & X_1 & Y_1 \\ 1 & X_2 & Y_2 \\ 1 & X_3 & Y_3 \\ \cdot & \cdot & \cdot \\ \cdot & \cdot & \cdot \\ \cdot & \cdot & \cdot \\ 1 & X_i & Y_i \end{bmatrix} \begin{bmatrix} K \\ H \\ D \end{bmatrix} = \begin{bmatrix} Z_1 \\ Z_2 \\ Z_3 \\ \cdot \\ \cdot \\ \cdot \\ Z_i \end{bmatrix} \qquad (7\text{-}2)$$

where the number of points is restricted to

$$4 \leq i \leq 8 \quad .$$

Now, let

$$M = \begin{bmatrix} 1 & X_1 & Y_1 \\ 1 & X_2 & Y_2 \\ 1 & X_3 & Y_3 \\ \cdot & \cdot & \cdot \\ \cdot & \cdot & \cdot \\ \cdot & \cdot & \cdot \\ 1 & X_i & Y_i \end{bmatrix} , \qquad (7\text{-}3)$$

$$A = \begin{bmatrix} K \\ H \\ D \end{bmatrix} , \qquad (7\text{-}4)$$

and $$C = \begin{bmatrix} Z_1 \\ Z_2 \\ Z_3 \\ \cdot \\ \cdot \\ \cdot \\ Z_i \end{bmatrix} . \qquad (7\text{-}5)$$

The weights can now be defined as $w = \frac{1}{D^2}$ (7-6)

where D = radial distance of a point (P) from the centroid.

Then, the weight matrix becomes

$$W = \begin{bmatrix} w_1 & & & & & \\ & w_2 & & & & \\ & & w_3 & & & \\ & & & \cdot & & \\ & & & & \cdot & \\ & & & & & w_i \end{bmatrix} , \qquad (7\text{-}7)$$

The normal equations are then defined as

$$[M^T W M] (A) = [M^T W C] . \qquad (7\text{-}8)$$

The solution is $$(A) = [M^T W M]^{-1} [M^T W C] . \qquad (7\text{-}9)$$

After all mesh-points, which surround the original data, have been determined by successive fitting of planes, these mesh-points are used to fill in the void areas where data do not exist. The final mesh-point values are obtained for each grid point in the model. This is illustrated by figure 7-6 where all mesh-points are dotted.

d. Smoothing. For topographic contouring, smoothing between mesh-point values should be performed with caution. The contours must portray the detail, and they must agree with the observed data. A suggested smoothing technique is to successively fit a second-degree equation to sets of three mesh-points in a row, in both the X and Y directions.

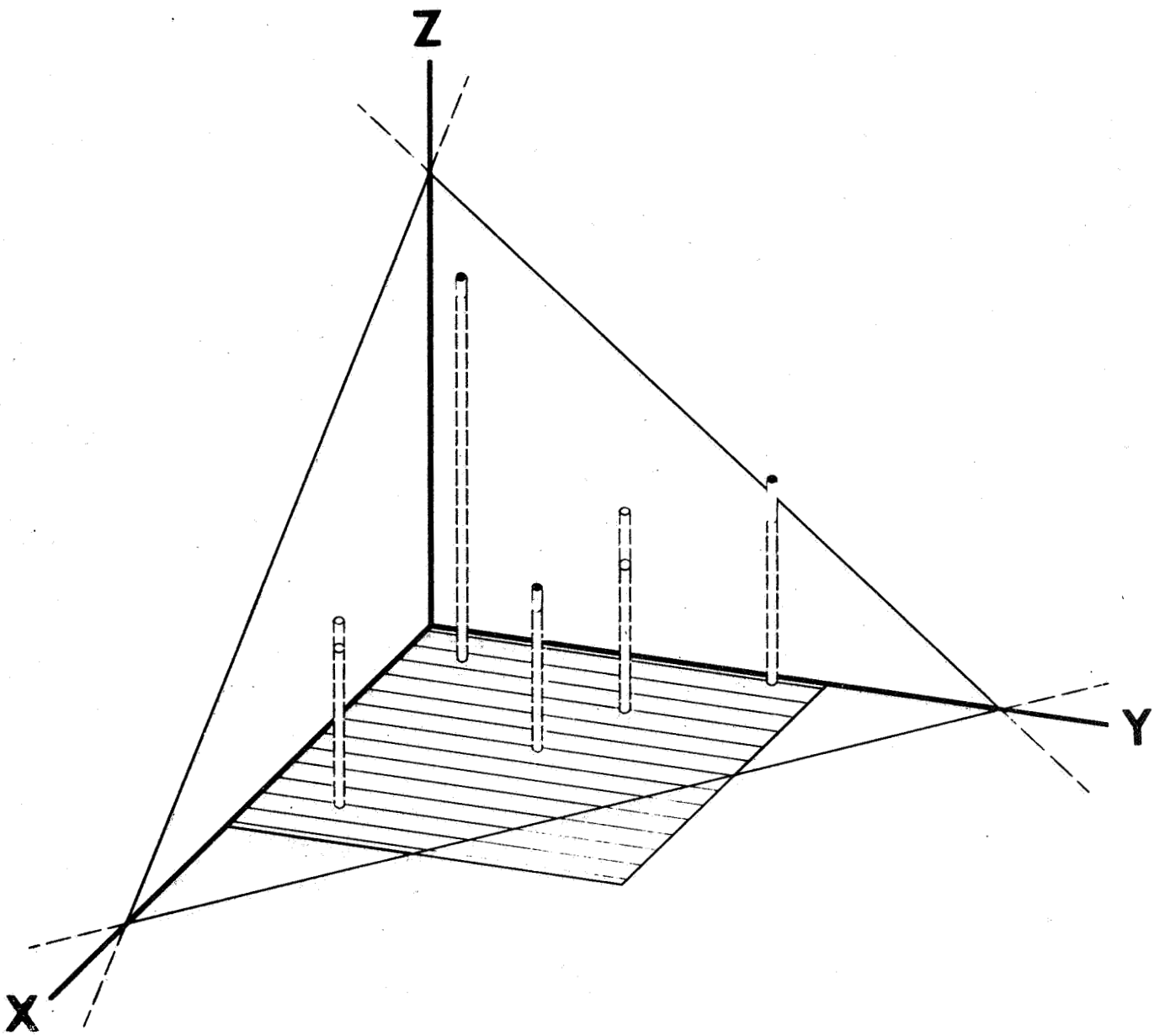

Figure 7-5. Plane Surface Fitting.

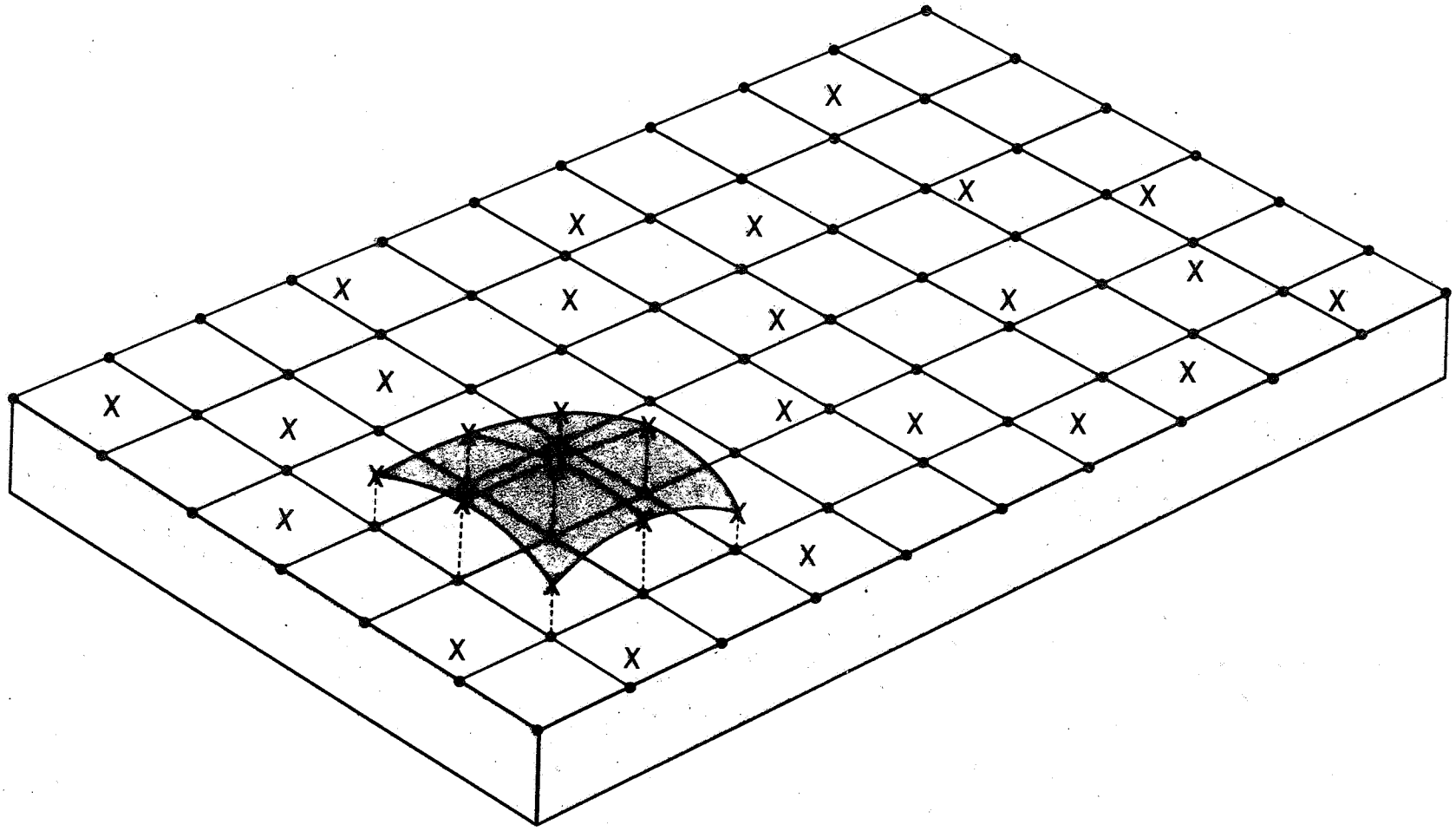

Figure 7-6. Configuration for Smoothing.

(See figure 7-6.) The Z-values corresponding to the required contours can be substituted into these equations, and the appropriate X, Y-coordinates, corresponding to the contour value of Z along the grid, can be determined. The general form of the equations for X and Y, respectively, are

$$Z = AX^2 + BX + C \quad , \tag{7-10}$$

$$Z' = A'Y^2 + B'Y + C' \quad . \tag{7-11}$$

Once the curve is formed, the X, Y-coordinates for a given contour elevation (Z) are

$$X = \frac{-B \pm \sqrt{B^2 - 4AC}}{2A} \quad , \tag{7-12}$$

and similarly for Y.

Topographic detail can then be retained by fitting a straight line across the diagonals of each grid square. This helps eliminate sharp turns in the contours, and should make smoother contours.

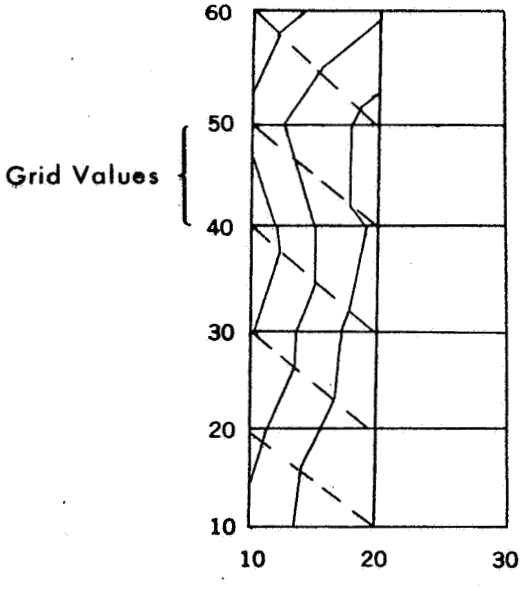

Figure 7-7. Plotting by Segments.

e. Plotting Contours. By this time, a huge volume of data has been generated. The remaining item is to present the X, Y-coordinates along the contours to be drawn by the graph plotter. To minimize the computer memory storage problem, plotting by segments (one grid interval at a time) is suggested. In this procedure, it is easier for the plotter to join successive points that fall on the given contour. This is illustrated by figure 7-7. Operational tests have shown that the procedure provides a logical and reliable representation of the given information.

SECTION IV. ANALYTICAL TOPOGRAPHIC COMPILATION EXAMPLE

5. EXAMPLE. Figure 7-8 is an exact reproduction of contours that were drawn by the ATC procedure. Figure 7-9 is the same data that has been refined by the cartographer. The data for figures 7-8 and 7-9 were scaled from a 1:1,000,000 lunar chart. The chart was chosen for the test run because of the crater topography. Two-thousand points were selected from a portion of the chart to be used as input into the contouring program. The resulting contours are comparable to the contours from which the data were taken. Basically, this method of digital contouring is similar to the work performed by a plane-table topographer. However, by using computers to process this mass of data, the contouring can be accomplished in approximately two hours per stereomodel. For the first lunar model, 4552 observed points over an area of 72 x 93 km were obtained. The altitude is about 300 km giving a photography scale of 1:12,000,000. The scale of the stereoplanigraph model was 1:1,000,000. Plotting scale (X, Y-Plotter) is 1:150,000 with 100-meter contour intervals. Although this plotting scale is unrealistic, when compared with the 1:12,000,000 photo scale, it is desirable to have a large manuscript to analyze the

contours more thoroughly. The manuscript is about 21 x 27 inches. Figures 7-10 and 7-11 are a small portion of this sheet. This compilation required the following equipment and time increments:

Operation		Time (min.)
Adjustment		43
Interpolate Contours	CDC-3600 Computer	36
Plot Contours	X,Y-Plotter	150

SECTION V. SUMMARY AND CONCLUSION

6. SUMMARY. ATC provides an objectively contoured manuscript which can be subjectively enhanced by suppressing at one place and slightly exaggerating at another, according to the cartographer's judgment and photo-interpretation skill. This combination of man and machine produces a graphic expression of the imagery that is agreeable with the data from which the contours are made. Work on the Ranger project indicated that ATC is technically feasible. ATC could take on increased emphasis if the mensuration of the required density of points could be significantly speeded up. These applications are discussed and illustrated in detail in chapter 8.

7. CONCLUSION. The ATC System provides a method of utilizing unusual photography that cannot be accommodated on standard-type or modified analog instruments. This method of contouring could be especially applicable to the Lunar Orbiter photography, if the reassembly of the framelets renders the photography unusable in analog plotters.

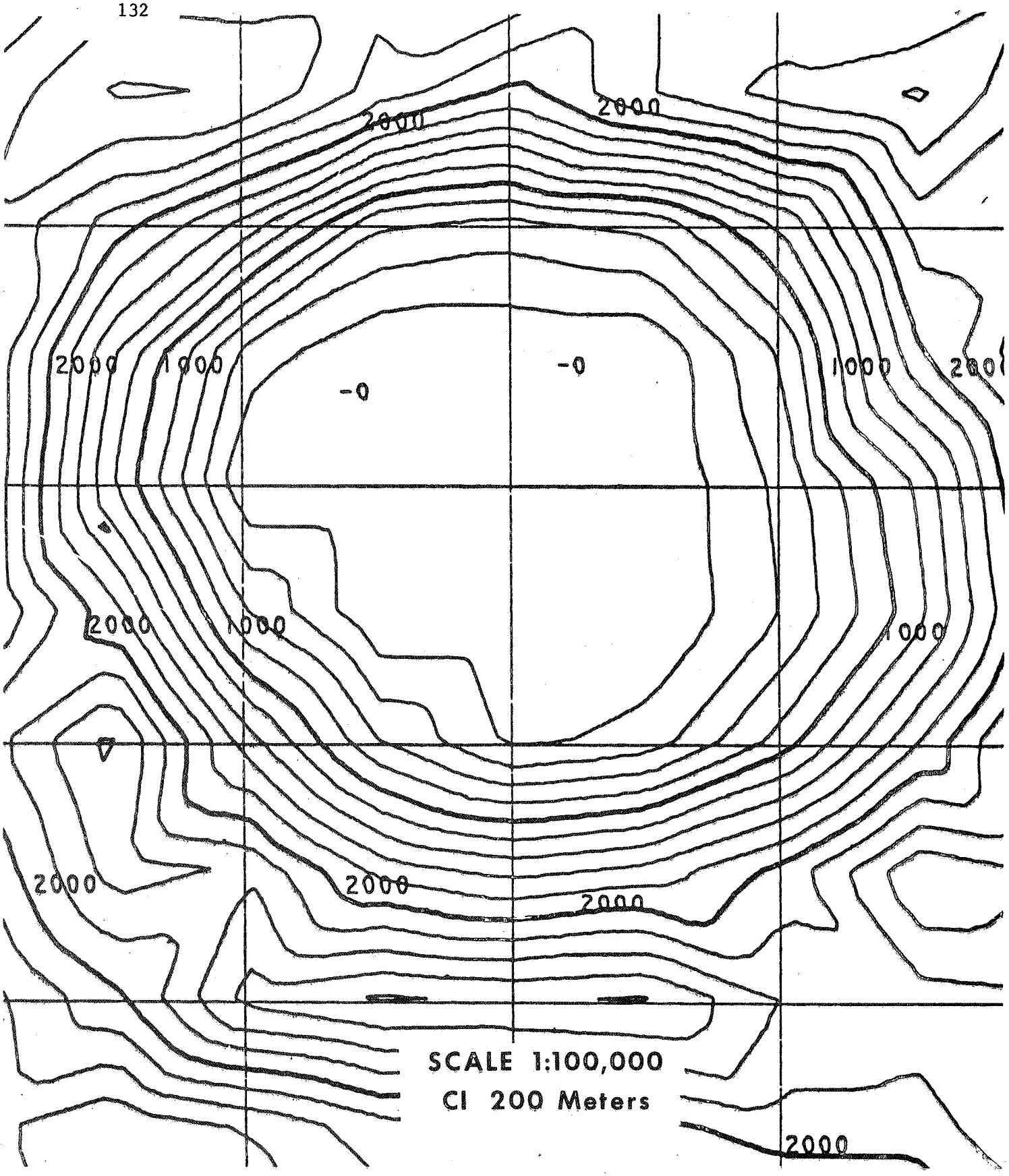

Figure 7-8. Analytical Topographic Compilation Raw Data.

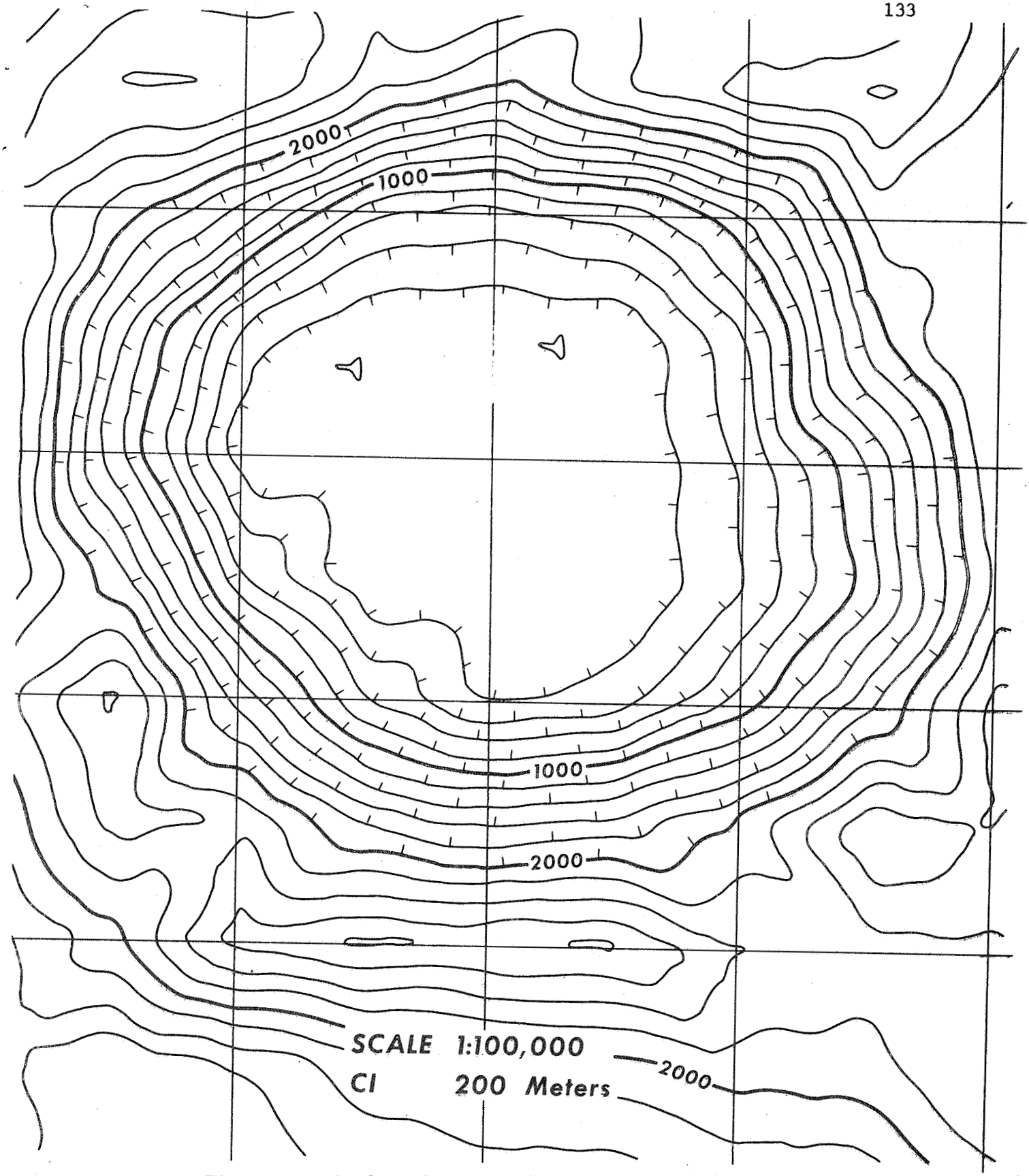

Figure 7-9: Analytical Topographic Compilation Refined.

Stereoplanigraph Scale	1:1,000,000
X,Y-Plotter Scale	1:150,000
Contour Interval	100 meters
Mesh Network	(900 x 900) meters

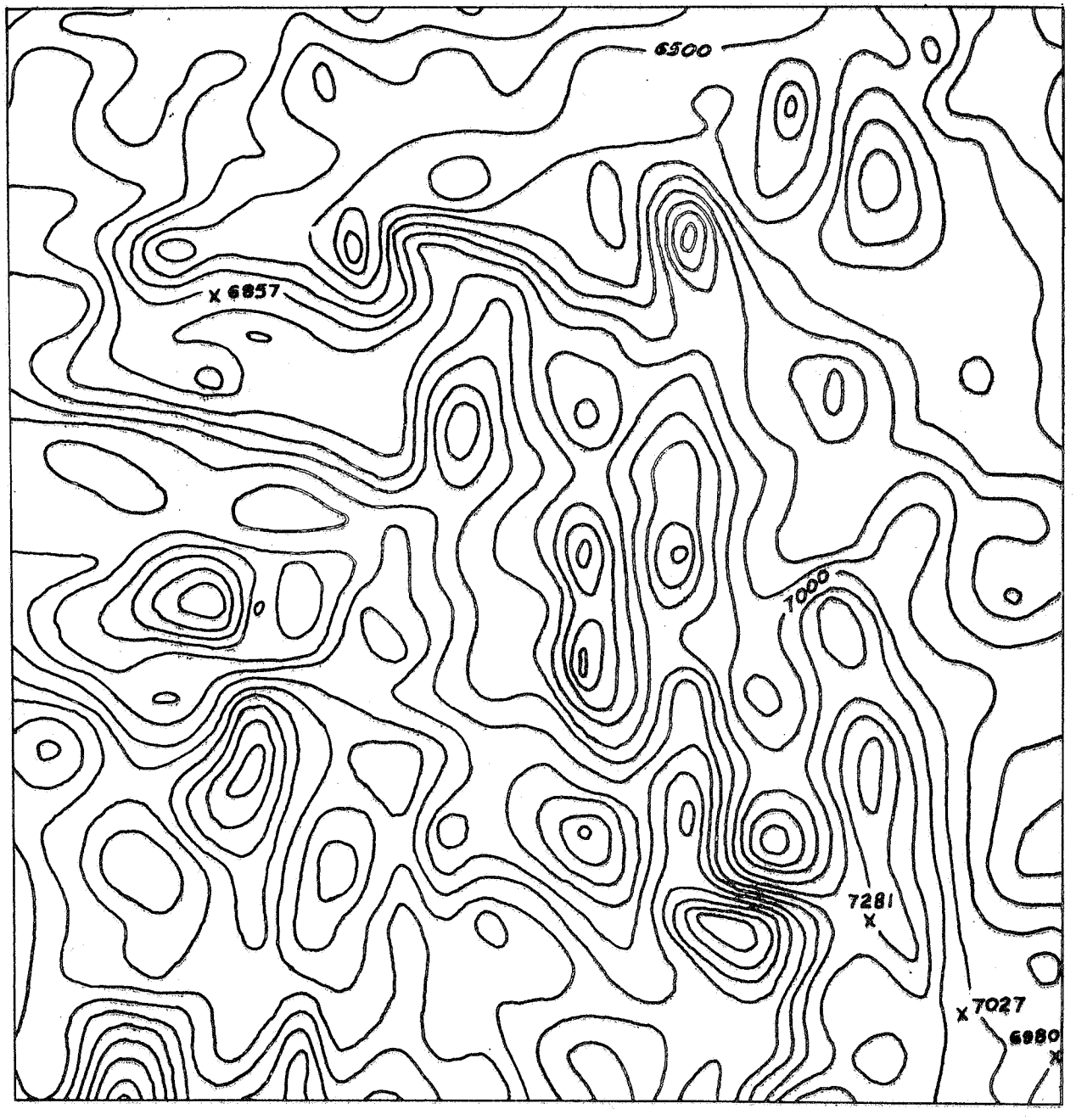

Figure 7-10. Ranger Raw Compilation.

Note: This compilation was run for the purpose of testing the programs in the total ATC system. Compilation is not on a Selenodetic Datum.

Stereoplanigraph Scale	1:1,000,000
X,Y-Plotter Scale	1:150,000
Contour Interval	100 meters
Mesh Network	(900 x 900) meters

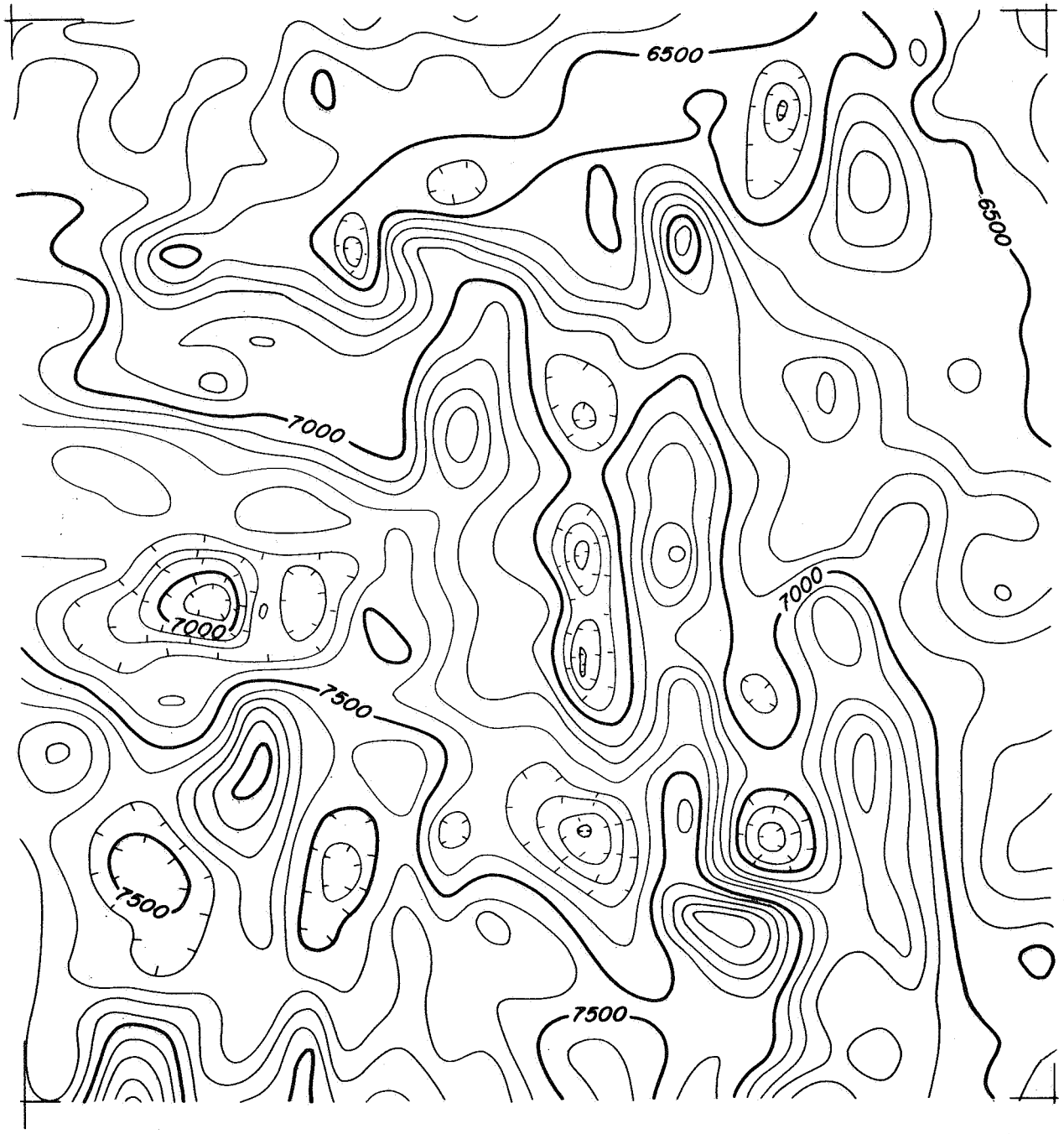

Figure 7-11. Ranger Refined Compilation.

Note: This compilation was run for the purpose of testing the programs in the total ATC system. Compilation is not on a Selenodetic Datum.

SECTION VI. LITERATURE CITED

1. SCHMID, H. "A General Analytical Solution to the Problem of Photogrammetry." Ballistic Research Laboratories Report No. 1065. Aberdeen, Md.: Aberdeen Proving Ground. Jul 1959.

2. LIGHT, D. L. "The Orientation Matrix." Photogrammetric Engineering. May 1966: Vol XXXII, No. 3, p 434.

3. TEWINKEL, G. C. "Analytic Absolute Orientation in Photogrammetry," Technical Bulletin No. 19. Washington: U. S. Coast and Geodetic Survey. Mar 1962.

4. "Numerical Surface Techniques and Contour Map Plotting, E 20-0117-0." White Plains, N. Y.: IBM, Data Processing Division.

5. PRAVER, G. A. "Real Terrain Through Computer Synthesis, P-789." Pomona, Calif.: The Marquardt Corporation. Nov 1965.

6. "Contouring Programs." Rockville, Md.: Control Data Corporation, Data Center, and Washington: IBM Service Bureau Corporation.

SECTION VII. SELECTED BIBLIOGRAPHY

BIRD, T. H. "Large Scale Lunar Photogrammetry - Problems and Progress." Presented to the ASP Annual Meeting, Washington, D. C. 28 Mar - 2 Apr 1965.

BOWLES, L. D. "Cartographic Experimentation with Ranger Photography." Presented to the ASP Semi-Annual Convention, Dayton, Ohio. 22-24 Sep 1965.

GAJDA, R. T. "Automation in Cartography." The Cartographer. May 1965: Vol II, No. 1, p 22.

GREYSUKH, V. L. and KOSMIN, V. V. "Analytical Representation of Local Relief on an Electronic Computer." Geodesy and Aerophotography. 1964: No. 6, p 341.

McCUE, G. A. and GREEN, J. "Pisgah Crater Terrain Analysis." Photogrammetric Engineering. Sep 1965: Vol XXXI, No. 5, p 810.

THEIS, J. B. "Automation and Photogrammetry." Photogrammetric Engineering. Mar 1965: Vol XXXI, No. 2, p 281.

PHASE FOUR

CHAPTER 8

EXPERIMENTAL MAPPING PROPER

SECTION I. PURPOSE AND SCOPE

1. PURPOSE. This phase was initiated to determine the practical application of the analytical compilation techniques and specially adapted first-order analog and analytical stereoplotters in support of mapping from Ranger and Lunar Orbiter photography.

2. SCOPE. Tests included proof of the developed methods, utilization of both conventional analog and analytical plotters, and a comparative analysis of the Z-coordinates derived from Ranger VIII imagery by the various approaches.

SECTION II. MATERIAL (GENERAL)

3. PHOTOGRAPHY. a. Description of Photographic System. The Ranger cameras were generally pointed along the velocity vector of the spacecraft. The camera system consisted essentially of six lenses which used high resolution vidicon tubes as image-recording sensors. Three of the cameras had approximate 25-mm-focal-length optics and three had approximate 76-mm-focal-length optics. Two cameras (one of each focal length) utilized a 1150-line full-scan vidicon, while the other four used a 300-line partial-scan vidicon. The imagery transmitted to earth was recorded on magnetic tape and on 35-mm film. The recorded imagery had a format of approximately 16 mm per side.

b. Selection of Photography. Lunar imagery obtained from the Ranger VIII mission was selected for experimental mapping because all camera axes trailed the velocity vector; hence, there was less nesting

of the images as compared with Ranger missions VII and IX. As a result, a more favorable base-height ratio existed.

4. SUPPORTING DATA. a. Ranger VIII Negatives. Duplicate Ranger VIII negatives labeled "SODUB" were furnished by JPL. The duplicate negatives were generated from the original negatives, termed "POD" (Prime Original Data), by a continuous-contact printer. The duplicate negative film stock was Eastman Kodak Type-5235 35-mm film which had a resolution equal to approximately 25 lines/mm.

b. Post-flight Data. Post-flight Ranger VIII data books containing trajectory data, camera data and other information regarding each exposure were furnished by JPL. From these data books information for each exposure was extracted.

c. Camera Calibration Data. It is necessary to have accurate and meaningful calibration data of an imaging system before photogrammetric data can be most effective. Although electronic distortions can be estimated prior to a system's use, actual image distortion must be established in the data obtained during the mission operation.

(1) Reseau System. Ranger utilized a matrix of reseau points superimposed on the vidicon tube from which the actual distortion characteristics of the transmitted data were determined. However, inquiry revealed that although the matrix of reseau points was used to determine the distortion characteristics, the dimension of the vidicon matrix of reseau points was based on the dimension of the master target; and that no precise measurements had been undertaken to determine the shape of the reseau system after it was superimposed on the vidicon tube.

Therefore, the dimension of the master matrix of reseau points, as shown in figure 8-1, was used as a basis to control all photographic plate processing of imagery acquired by the Ranger VIII A camera.

(2) Lens Distortion. Radial distortion of the Ranger lenses was not measured prior to flight. The approximate values, furnished to JPL by the manufacturer (Bausch and Lomb), were used to correct for the effect of radial distortion. The manufacturer's data were very sketchy in that the radial distortion was defined by a three-point curve. For the Ranger VIII A camera the magnitude of radial distortion at the side of the field is -0.065 mm. The radial distortion pattern for this camera is shown in figure 4-2.

(3) Transmission and Reassembly Distortions. The effect of transmission and reassembly distortions on the Ranger VIII imagery is not known. It is conceivable that the magnitude of these distortions could be greater than the lens distortion. In any event, the Ranger topographic compilations are influenced by the distortion characteristics.

(4) Lens Optical Data. A listing of the focal lengths of the pre-flight lens for each Ranger VIII camera was furnished by JPL. These focal lengths, shown in table 8-I, were determined by the camera manufacturer.

Table 8-I. Ranger VIII Lens Optical Data Expressed in mm

Camera No.	Front Focal Length	Flange Focal Length	Vertex to 2nd. Model Plane	Focal Length
42/42 P1	29.35	47.37		74.60
22/22 P2	29.55	47.34		74.86
40/37 P3				25.75
48/48 P4			14.11	25.80
38/32 A			14.16	26.09
47/47 B	29.45	47.36		74.60

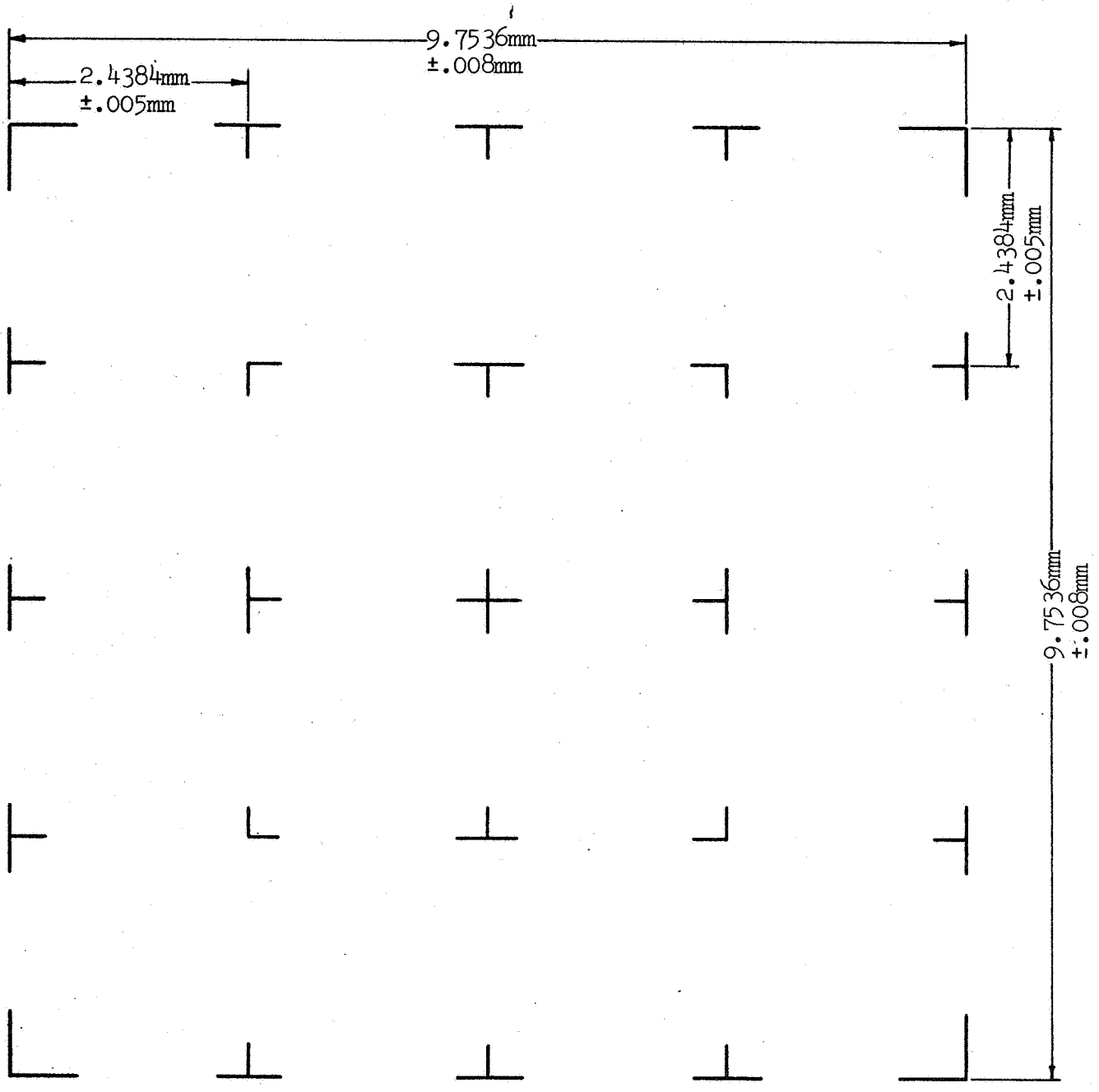

Figure 8-1. Master Matrix of Reseau Points.

5. PHOTOGRAPHIC PLATE PROCESSING. To preserve the maximum resolution of photography, it is desirable to compile with contact-scale diapositives. However, this was not possible with the Ranger photography as a result of the nonstandard format and focal lengths. In order to use the Ranger photography, two methods were employed in the photographic plate processing: (a) the use of a special printer (Wild U-3) to achieve a particular camera-projector combination; and (b) the use of an enlarging-reducing camera. The method employed depended upon the ratio necessary to make the focal length and/or format of the Ranger photography compatible with a specific mapping instrument.

6. PROJECTION. A Mercator projection was used as the framework for the Ranger VIII maps. The point of tangency at the lunar equator defined by a selenographic sphere, the radius of which is 1738 km. The point of origin is defined as the intersection of zero longitude and the lunar equator given by JPL. This framework is of the conformal type; i.e., small areas of the surface of the moon will retain true shapes on the projection; measured angles closely approximate true values; lines of constant azimuth appear as a straight line; and the scale factor is the same in all directions from a point.

7. CONTROL. Approximately 500 points, bounded by the selenocentric parallels of -2.4 and +2.9 degrees and the selenocentric meridians of +17.2 and +21.7 degrees, were measured on Ranger VIII photography with Mann Comparators. AMS Preliminary Report, "Selenodetic Control from Ranger Photography," dated March 1966[1], outlines the progress and future work regarding the determination of the selenodetic position of these

points. Due to the absence of the planned selenodetic control for vertical and horizontal positioning of the topographic data, it was necessary to use the following: (a) selenocentric coordinates of observed surface points (those covered by the reticles on the photographs) furnished by JPL; (b) previously established selenodetic control (one point) published in AMS Technical Report No. 29, (Part Two: AMS Selenodetic Control System 1964)[2], and (c) existing lunar map sources.

SECTION III. EXPERIMENTAL MAPPING

8. INTRODUCTION. Mapping procedures to use the Ranger photography ranged from conventional analog stereophotogrammetric methods to newly developed analytical methods in order to determine the local variations in the lunar topography. Conventional cartographic-quality photography was used to verify the validity of the analytical reduction methods that were developed.

9. ANALYTICAL REDUCTION VALIDITY TESTS. Arizona Test photography was used as a basis for the analyses of these tests. The photography was taken by a cartographic 6-inch-focal-length camera, flown at an altitude of 27,000 feet.

a. Comparative Analysis of Z-coordinates Derived by the Analog Plotter/Mathematical Orientation Method and the Conventional Analog Stereophotogrammetric Method. (1) Equipment. The Zeiss 6-inch-focal-length Stereoplanigraph C-8 was used both for measurement of the stereographic coordinates of the relatively oriented Arizona Test model, and for a conventional analog stereophotogrammetric absolute orientation and compilation of the same model.

(2) Procedure. (a) Analog Plotter/Mathematical Orientation Method. The Arizona Test model was relatively oriented to simulate the Ranger conditions (extreme tilts) at a scale approximately equal to 1:27,000. An instrument network of 4200 image points was measured at increments equal to 1 mm. In addition, relative stereographic coordinates for control points and prominent features, such as peaks, saddles, and depressions, were measured. A minimum of three observations were made and recorded by one operator for each point. The relative stereographic coordinates were then absolutely oriented by the Analog Plotter/Mathematical Orientation Method and put in contour form by the Digital Contouring Method. These methods were previously described in chapters 5 and 7. The data derived through these methods were portrayed with a 10-meter contour interval.

(b) Conventional Analog Stereophotogrammetric Method. The Arizona Test model was cleared of Y-parallax, leveled, and scaled at 1:27,000 to ground control. Topographic data were then derived by the conventional contouring method at 10-meter increments. Relative heights were also recorded for all prominent features and control points.

(3) Results. (a) Control. Each method used the same system of known control points for absolute orientation of the Arizona Test model. As shown in table 8-II,the standard error (σ_Z) for the Z-coordinates (when employing the Conventional Analog Stereophotogrammetric Method) yielded a σ_Z of 3.63 feet as compared to a σ_Z of 3.86 feet for the Analog Plotter/Mathematical Orientation Method.

Table 8-II. Arizona Test Model Z-coordinate Orientation (Feet)

Point ID	Control	Analog Plotter/ Mathematical Method	Comparator/ Analytical Method	Conventional Method
	Z	ΔZ	ΔZ	ΔZ
R9	1208.799	-0.56	+2.43	-0.52
T9	1180.699	-2.62	-2.39	-0.52
U9	1180.298	-1.84	-2.40	-0.52
S8	1164.501	-0.33	+0.13	-0.52
T8	1166.896	+1.08	+0.85	-0.52
R7	1138.599	+0.72	-2.26	-0.52
S7	1148.199	+3.64	+0.56	+6.03
U7	1172.300	-1.51	+0.20	-0.53
S6	1146.299	+4.33	+2.49	-0.56
T6	1161.401	+4.27	+5.05	+6.03
U6	1175.600	-0.92	-0.66	-0.56
R5	1134.101	-0.36	-0.56	-0.56
R4	1168.799	+9.55	-4.17	-8.40
S4B	1207.201	+3.12	+1.97	-0.52
T4	1325.600	+5.58	+0.36	+6.03
U4	1206.801	-5.05	-1.51	-3.84
Standard Error (σ_z)	=	3.86	2.30	3.63

$$\sigma_z = \sqrt{\frac{\Sigma \Delta z^2}{n-1}}$$

n = number of points

(b) Relative Heights. Ten prominent features were selected to determine if any differences existed in relative heights determined by the Conventional Stereophotogrammetric Method and those determined by the Analog Plotter/Mathematical Orientation Method. The selected features had an extreme vertical rise in comparison with their base (vertical rise = approximately 6 x the base). These features were selected because they would be indicative of many features on the moon. As shown in table 8-III, the average relative height loss in the 10 prominent features was 3.25 feet. This loss was due to the Analog Plotter/Mathematical Orientation Method.

Table 8-III. Arizona Test Model Relative Height Analysis Expressed in Feet

Point ID	Elevation Determined by Conventional Method	Elevation Loss Due to Analog Plotter/ Mathematical Orientation Method	Elevation Loss Due to Digital Contouring
1	1495	2	6
2	1323	3	4
3	1391	3	23
4	1385	1	29
5	1361	5	21
6	1364	6	23
7	1348	5	8
8	1312	0	17
9	1268	1	2
10	1325	0	0
Average Loss =		3.25 ft.	11.77 ft.

(c) Digital Contouring Program. An average density of model measurements was used as input into the Digital Contouring Program. An analysis of the digital contour plot revealed a major difference (elevation loss) in the input relative height and the output relative

height for the 10 selected prominent features. The elevation loss of 11.77 feet was attributed to the plane fitting process of the contouring program (See table 8-III.) It was determined that this loss was directly related to the density of the model measurements of features, which had an extreme vertical rise as compared to their base, and could be reduced by increasing the density of model measurements. In addition, since all special features were photo-identified at the time of their measurement, their relative height (as computed by the Analog Plotter/Mathematical Orientation Method) could be recovered and used in the cartographic shaping phase. Figure 8-2 shows an Arizona Test area compilation produced by the Conventional Analog Stereophotogrammetric Method. Figure 8-3 shows the raw data of the same area compiled by the Analog Plotter/Mathematical Orientation Method, and the subsequent digital contouring and X, Y graphical plotting technique. Figure 8-4 shows the raw data after cartographic shaping, and the recovery of the relative height of prominent features as computed by the Analog Plotter/Mathematical Orientation Method. Notice that no significant change occurs as a result of this shaping.

(d) Profile Comparison. Two sets of profiles were drawn from each contour compilation (figs. 8-2 and 8-4); the profiles covered the same topographic detail. A graphical comparison of profiles AB and CD (fig. 8-5) shows the agreement between the two compilations. Elevation differences taken at 18 evenly spaced points along each profile were manually interpolated. As shown in table 8-IV, after removing the effect of datum difference, the σ_Z of the differences for both profile lines is 3.65 feet.

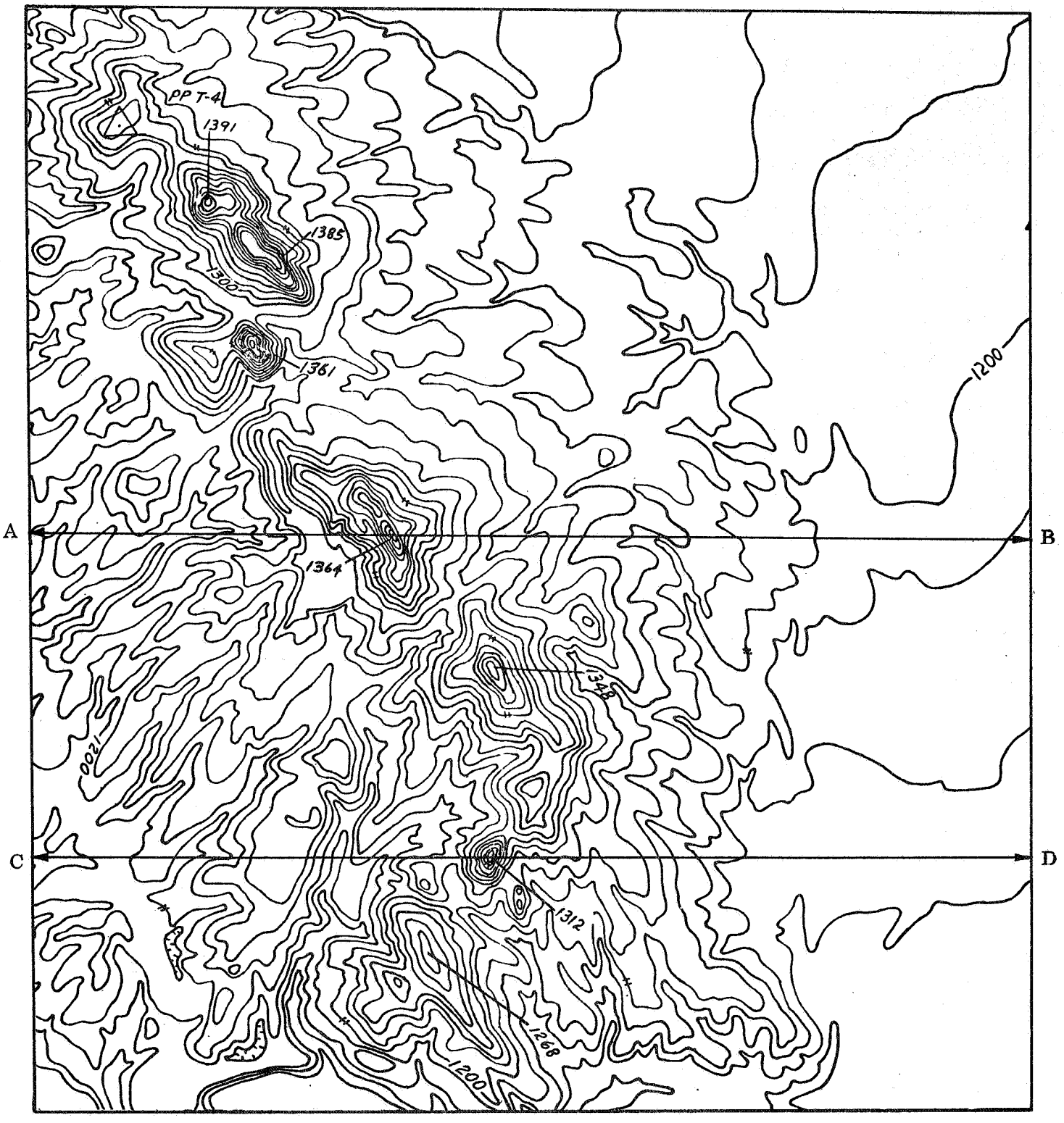

Figure 8-2. Arizona Test Area Compilation by the Conventional Analog Stereophotogrammetric Method.

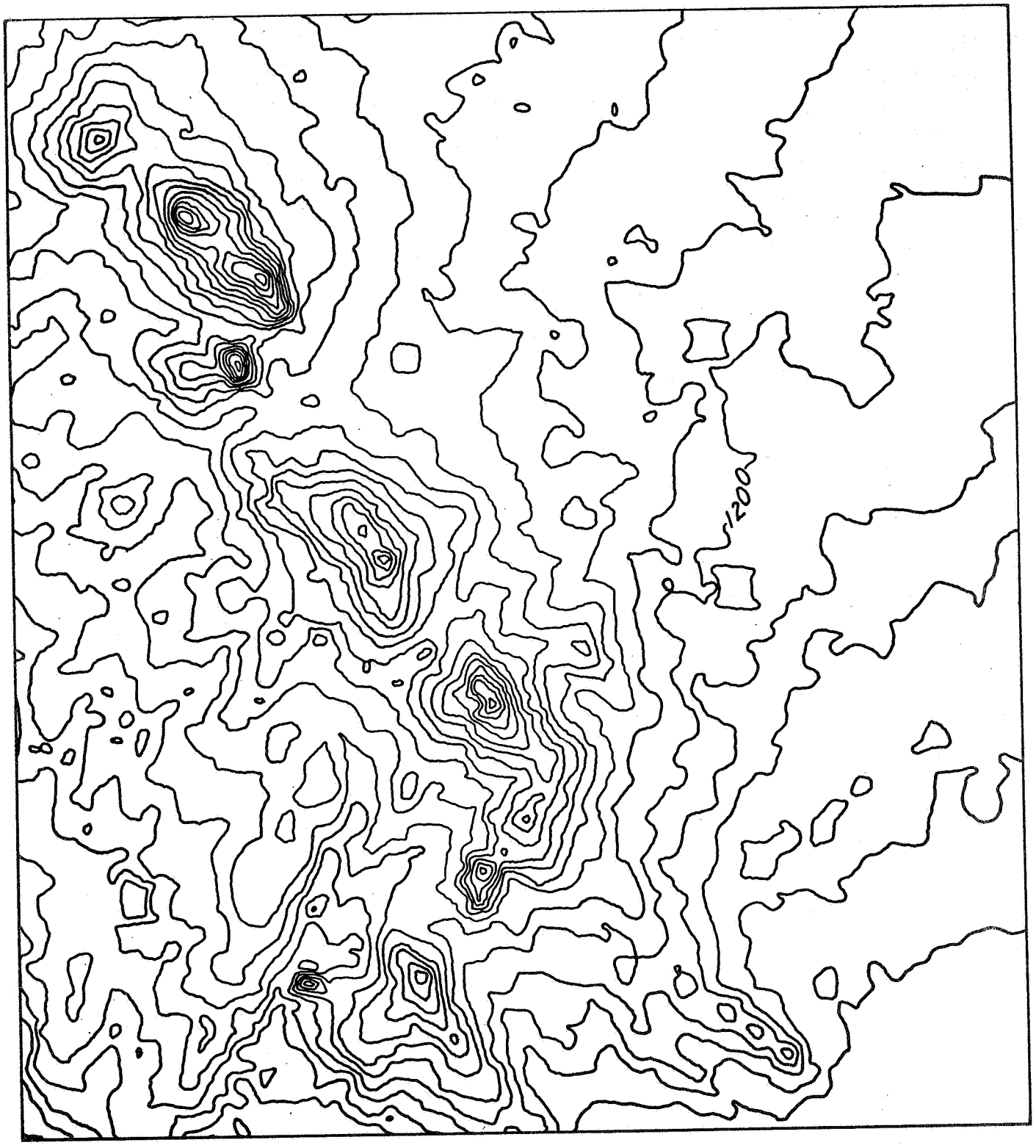

Figure 8-3. Arizona Test Area Compilation by the Analog Plotter/Mathematical Orientation Method, and the Digital Contouring and X, Y Graphical Plotting Technique.

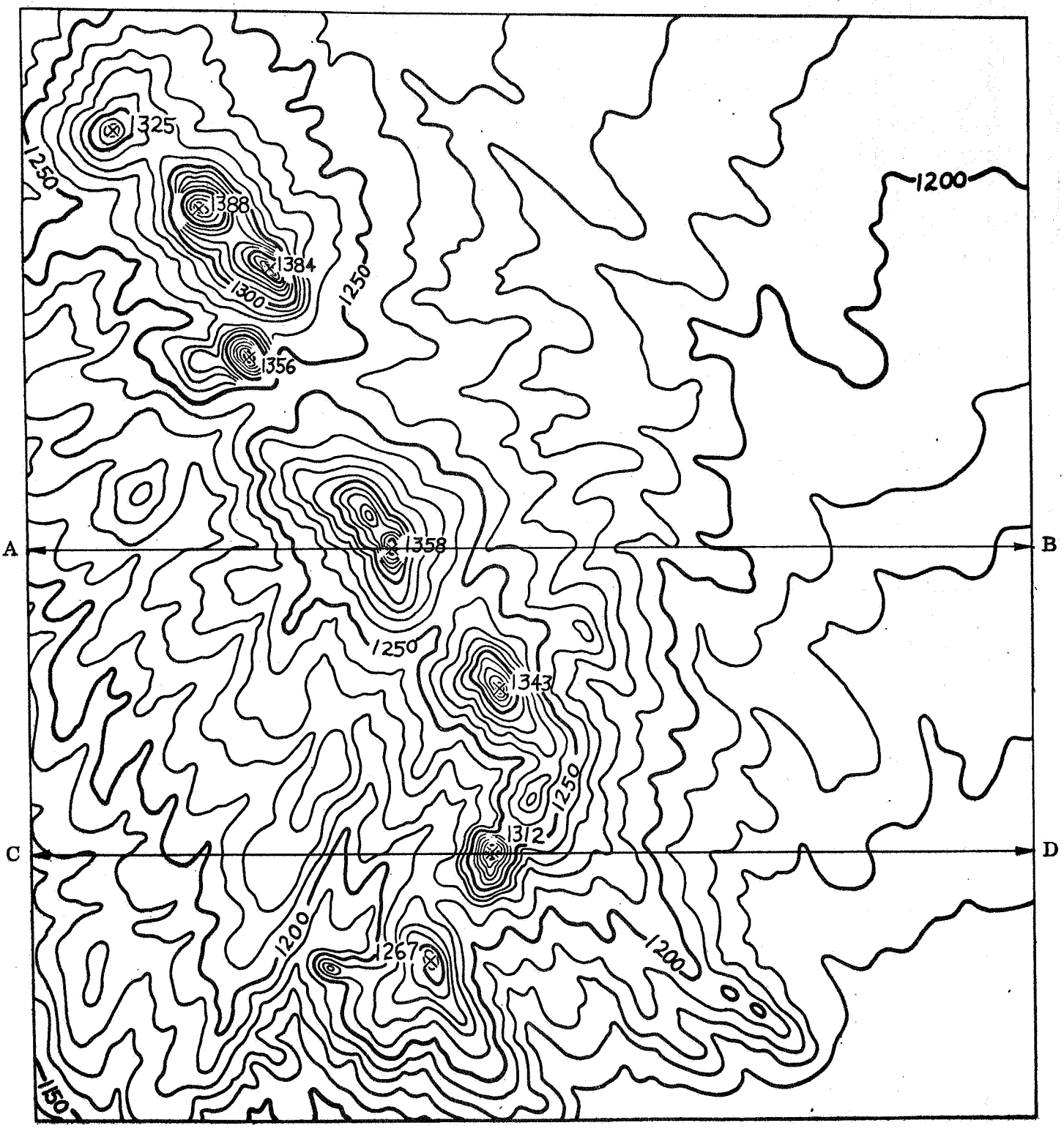

Figure 8-4. Arizona Test Area Compilation after Cartographic Enhancement of the X, Y Graph Plotter Output.

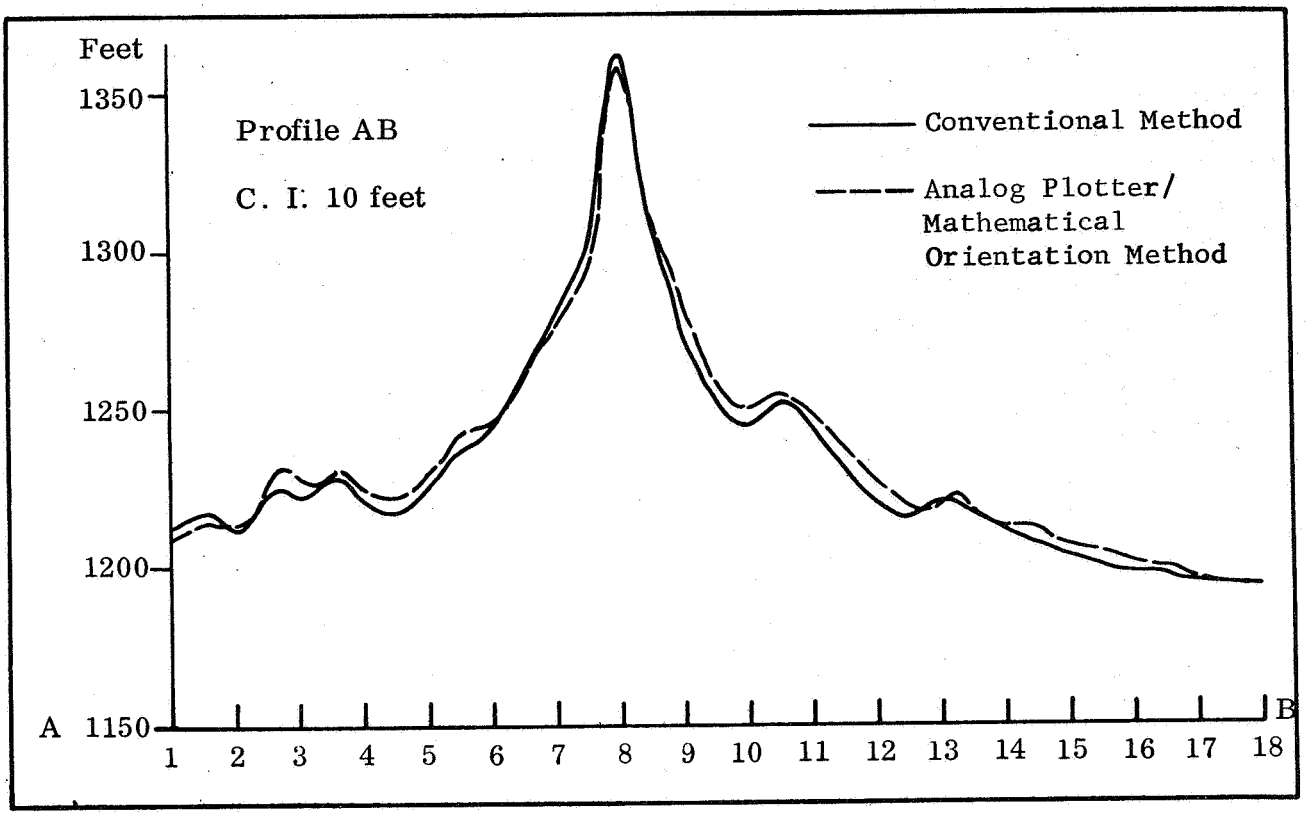

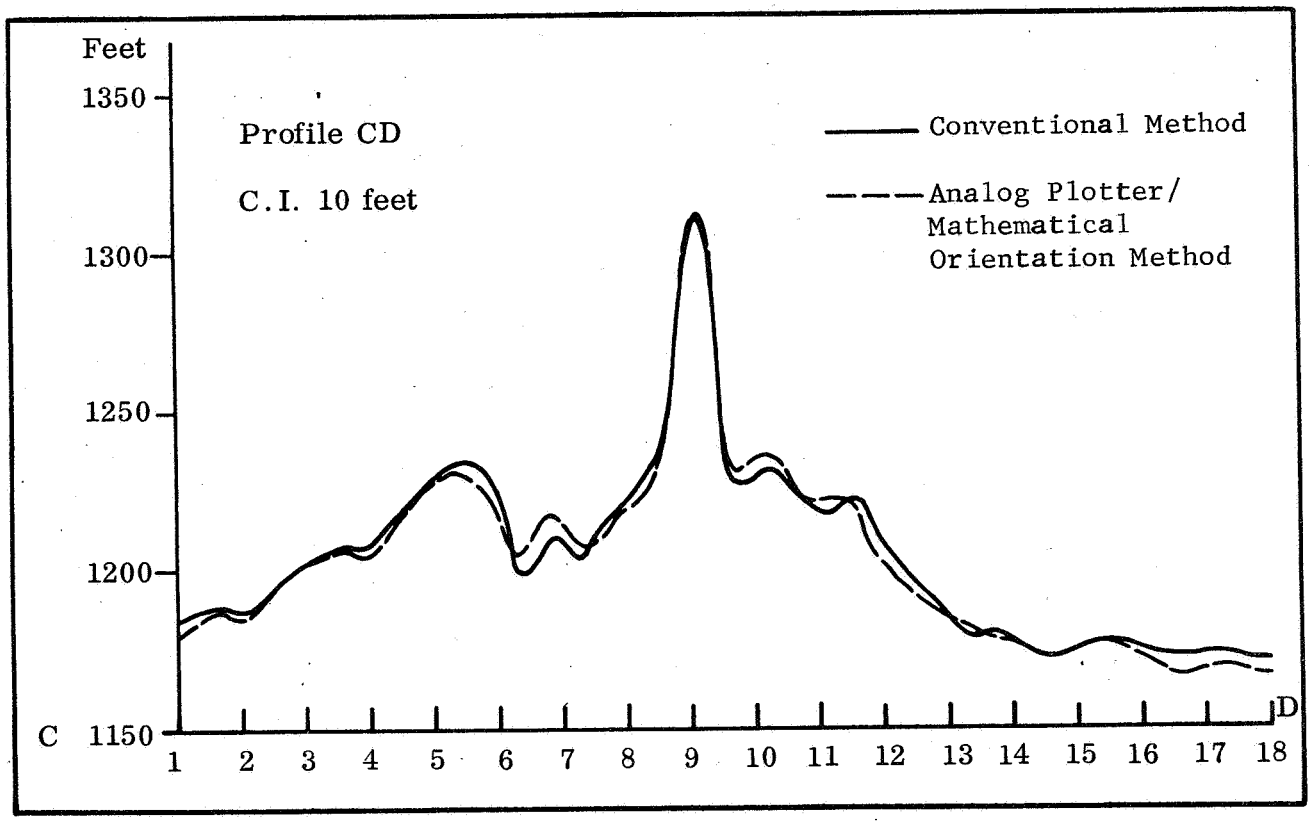

Figure 8-5. Arizona Profile Comparison.

Table 8-IV. Analysis of the Difference between Profiles of Arizona Test Compilations Produced by Conventional and Analog Plotter/Mathematical Orientation Methods (Feet)

Point	Profile A-B			Profile C-D		
	Z_i	$(Z_i-\bar{Z})$	$(Z_i-\bar{Z})^2$	Z_i	$(Z_i-\bar{Z})$	$(Z_i-\bar{Z})^2$
1	-4	-5.8	33.64	-5	-4.1	16.81
2	+2	+0.2	.04	-1	-0.1	.01
3	+6	+4.2	17.64	0	+0.9	.81
4	+4	+2.2	4.84	-2	-1.1	1.21
5	+6	+4.2	17.64	0	+0.9	.81
6	+3	+1.2	1.44	-5	-4.1	16.81
7	-3	-4.8	23.04	+7	+7.9	62.41
8	-5	-6.8	46.24	-2	-1.1	1.21
9	+4	+2.2	4.84	+2	+2.9	8.41
10	+5	+3.2	10.24	+7	+7.9	62.41
11	+3	+1.2	1.44	+4	+4.9	24.01
12	+5	+3.2	10.24	-5	-4.1	16.81
13	-2	-3.8	14.44	-2	-1.1	1.21
14	0	-1.8	3.24	0	+0.9	.81
15	+4	+2.2	4.84	0	+0.9	.81
16	+4	+2.2	4.84	-4	-3.1	9.61
17	+1	-0.8	.64	-5	-4.1	16.81
18	0	-1.8	3.24	-5	-4.1	16.81
Σ	+33		202.52	-16		257.78

Z_i = Elevation Differences in Feet

$\bar{Z} = \Sigma Z_{i/n} = +1.8$ $\qquad$ $\bar{Z} = \Sigma Z_{i/n} = -0.9$

$\sigma_z = \sqrt{\frac{\Sigma(Z_i-\bar{Z})^2}{n-1}} = 3.45$ feet $\qquad$ $\sigma_z = \sqrt{\frac{\Sigma(Z_i-\bar{Z})^2}{n-1}} = 3.89$ feet

Average $\sigma_z = 3.65$ feet

b. Comparative Analysis of Z-coordinates Derived by the Conventional Analog Stereophotogrammetric Method and the Comparator/Analytical Method.

(1) General. The Z-coordinate orientation results (table 8-II) of the Conventional Analog Stereophotogrammetric Method and the relative height determined for point 6 (table 8-III) by this method were used as the basis for this analysis. In support of the Comparator/Analytical Method a Zeiss stereocomparator PSK (fig. 6-2) was used to measure the x, y-coordinates of the same control points and the same prominent feature on the Arizona Test photographic plates. Only one prominent feature was selected to determine whether any difference existed in the relative height determined by the Conventional Analog Stereophotogrammetric and the Comparator/Analytical Methods. The justification for the selection of only one feature was based on the previous analysis. In that analysis it was found that the largest difference in the relative height, determined by each of the methods, would occur when a feature had an extreme vertical rise in comparison with its base.

(2) Digital Contouring Program. The Digital Contouring Program was not used for this test. Data derived from the Comparator/Analytical Method would have been in the same form (X, Y, Z-coordinates for each data point), and processed through the same Digital Contouring Program as those data derived from the Analog Plotter/Mathematical Orientation Method, previously discussed in paragraph 9a(3)(b). Therefore, if an equal density of test model data points had been furnished from each of the methods, the resulting difference from the input values would have been of the same magnitude as shown in table 8-III. As previously discussed, this difference could be reduced by increasing the density of model

measurements of a feature which had an extreme vertical rise.

(3) Procedure. (a) Comparator/Analytical Method. The mensuration phase of the Comparator/Analytical Method was similar to that of the Analog Plotter/Mathematical Orientation Method. In essence, the difference was that no z-coordinates were measured; only x, y-coordinates were determined for each photographic plate of the stereomodel. The x, y-coordinates were then adjusted to surface control (X, Y, Z) by the Comparator/Analytical Method previously described in chapter 6.

(b) Conventional Analog Stereophotogrammetric Method. The Arizona Test model and this method, previously described, were used.

(4) Results. (a) Control. As shown in table 8-II, the absolute orientation of the model by the Comparator/Analytical Method was superior to the Conventional Analog Stereophotogrammetric Method, yielding a σ_z of 2.30 and 3.63 feet, respectively.

(b) Relative Height. The difference in the relative height of the feature, derived by the two methods, was four feet.

10. RANGER VIII TOPOGRAPHIC COMPILATION BY THE CONVENTIONAL ANALOG STEREOPHOTOGRAMMETRIC METHOD. a. Equipment. The Zeiss Stereoplanigraph C-8 with special focal length plotting cameras (210 mm) was used for a direct compilation of Ranger VIII imagery. (This instrument was previously discussed in chapter 3, section III.)

b. Material. (1) Photography. The stereopair consisted of Ranger VIII A camera exposures 507 and 515 (figs. 8-6 and 8-7). The altitude of exposure for photos 507 and 515 is 321 and 283 km, respectively. The approximate base-height ratio of the stereopair, based on an average of the exposure altitudes, is 0.10.

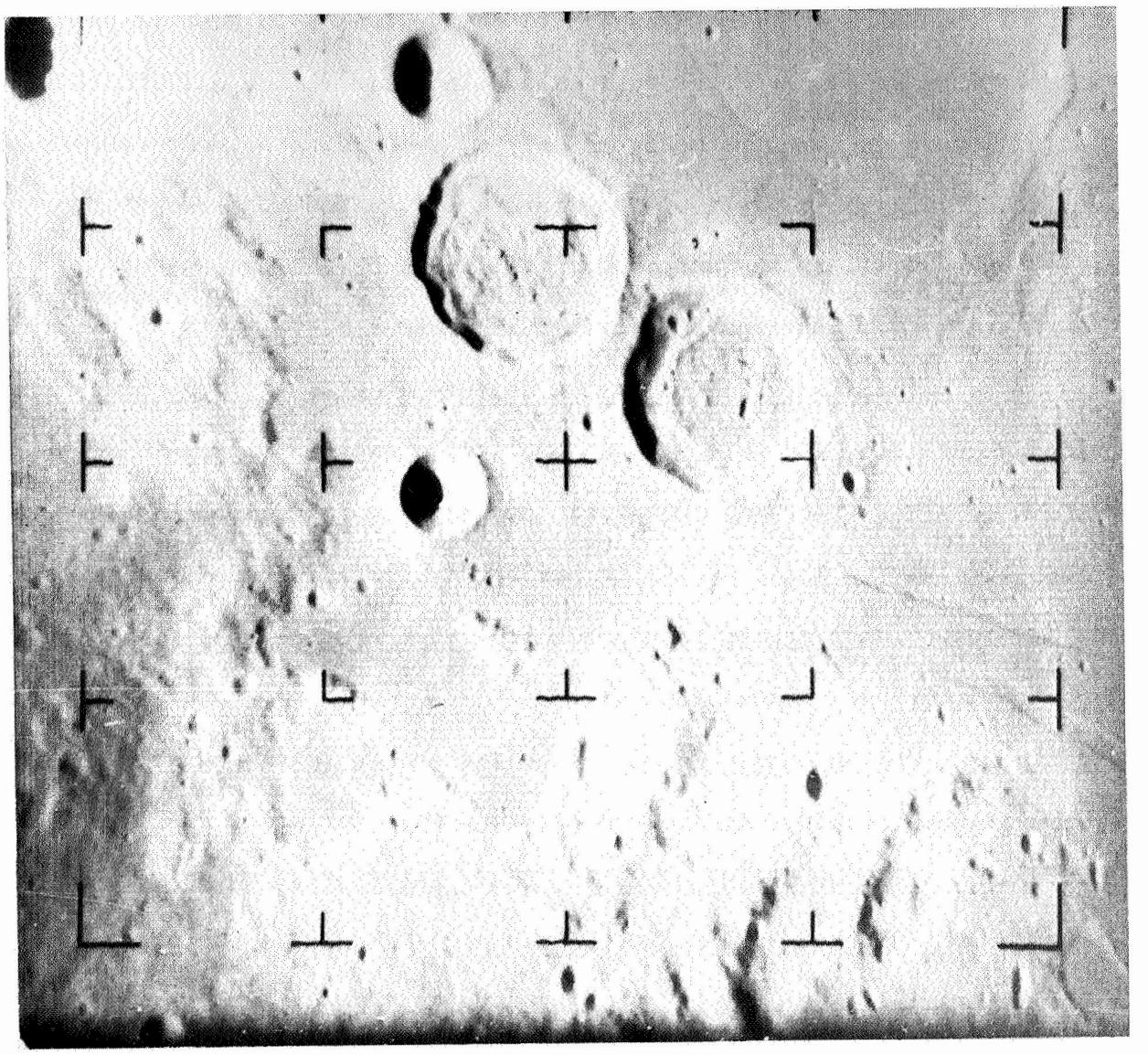

Figure 8-6. Ranger VIII Exposure 507.

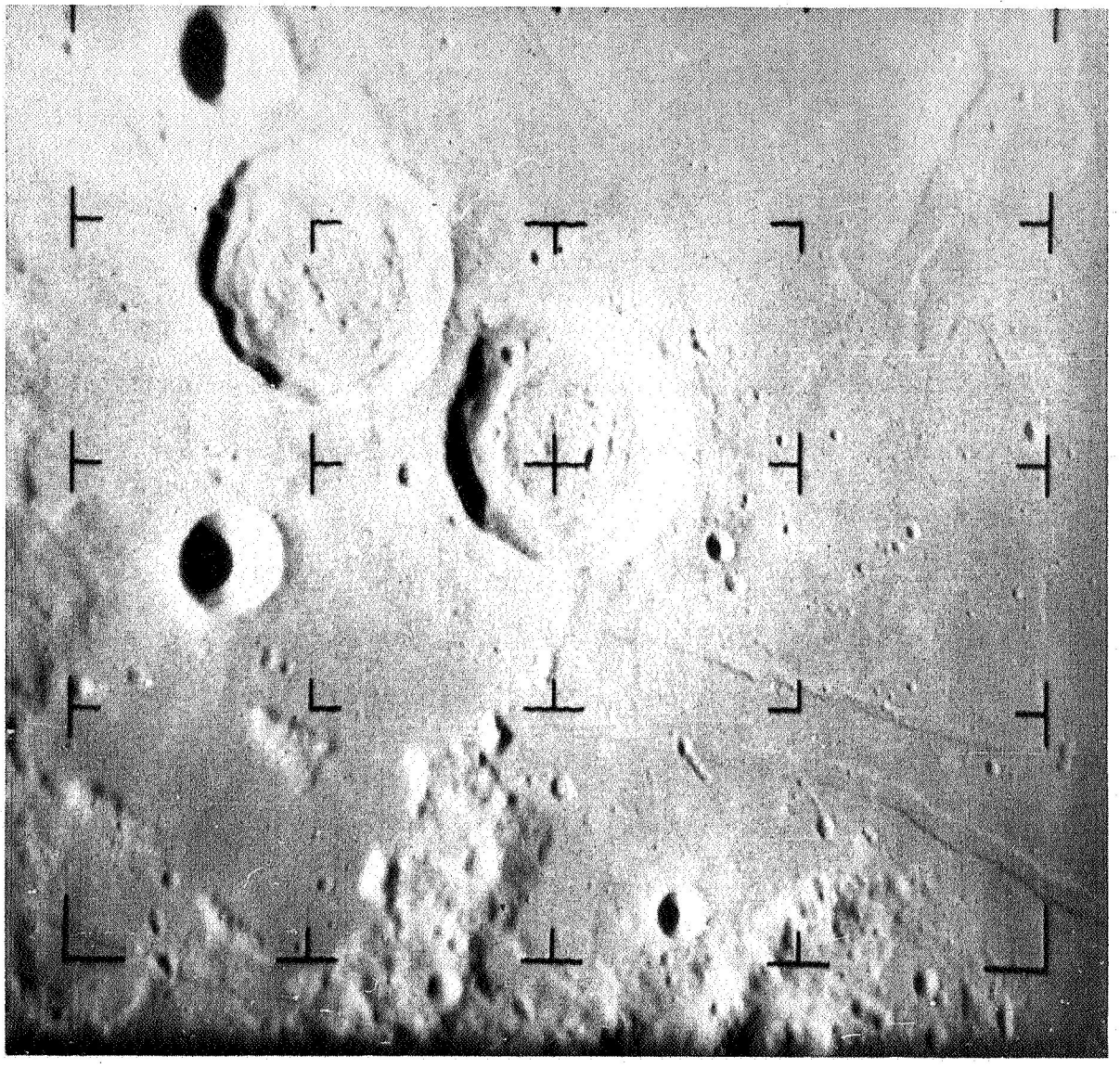

Figure 8-7. Ranger VIII Exposure 515.

(2) Diapositives. An enlarging-reducing camera was used to reproduce the 16-mm-format negatives on super flat 9- x 9- x .025-inch glass plates at an enlargement ratio to yield an equivalent focal length of 210 mm. The diapositive scales for exposures 507 and 515 were 1:1,528,571 and 1:1,347,619, respectively.

c. Procedure. (1) Orientation. (a) Relative. The diapositives were positioned in the projectors and oriented to each other to produce an observed parallax-free model. The model was then approximately horizontalized and scaled by employing a rough calculation of the inherent tilts in the photography and the position of observed surface points furnished by the JPL.

(b) Absolute. 1 Vertical. Absolute orientation was accomplished by horizontalizing the model to its observed mean plane. Special emphasis was made to arrive at a horizontalization solution that would yield crater rims of an approximate absolute elevation as those published in the previously mentioned AMS Technical Report, No. 29, (Part Two) and those shown on existing lunar map sources.

2 Horizontal. The position of observed surface points furnished by JPL and the selenodetic position of one point published in AMS Technical Report, No. 29 (Part Two) were used as horizontal control.

(2) Scale. (a) Model. After absolute orientation, the resulting model scale was 1:800,000.

(b) Viewing. Ocular magnification of 4.5x yielded a 1:177,778 viewing scale.

(c) Plotting. The topographic data were portrayed on a Mercator projection at a 1:250,000 scale.

(3) Curvature Correction. (a) Employing Standard Curvature Correction Formula. When photographs cover large surface distances, the effect of curvature is considerable. This effect causes the datum of any photograph to arch upward in a vertical bow. The effect of curvature on a stereomodel is removed by applying a correction to instrument elevations. A description of the adjustment and application process, as related to the Ranger topographic compilation, shown in figure 8-8, is as follows:

1 Mathematical Development. Lunar curvature is derived from the relationship

$$L_c = \frac{D^2}{2R} \tag{8-1}$$

L_c = lunar curvature in kilometers (km)

$2R$ = 3,476 km

D = distance measured from a point tangent to the surface of the moon, in kilometers

R = radius of moon.

Since all values on the model are recorded in millimeters, they must be converted to kilometers and substituted into relationship (8-1). This is accomplished by using:

$$1 \text{ millimeter (mm)} = \frac{1}{1000 \text{ meter}}, \quad \text{and } 1 \text{ meter (m)} = \frac{1}{1000 \text{ kilometer}}$$

Therefore,

$$L_c = \ell_c \left(\frac{1}{1000}\right) \left(\frac{1}{1000}\right) \left(\frac{1}{1/S}\right) = \frac{\ell_c \, S}{(1000)\quad(1000)} \tag{8-2}$$

ℓ_c = lunar curvature in millimeters at model scale

$1/S$ = model scale, where S is the denominator of the representative fraction.

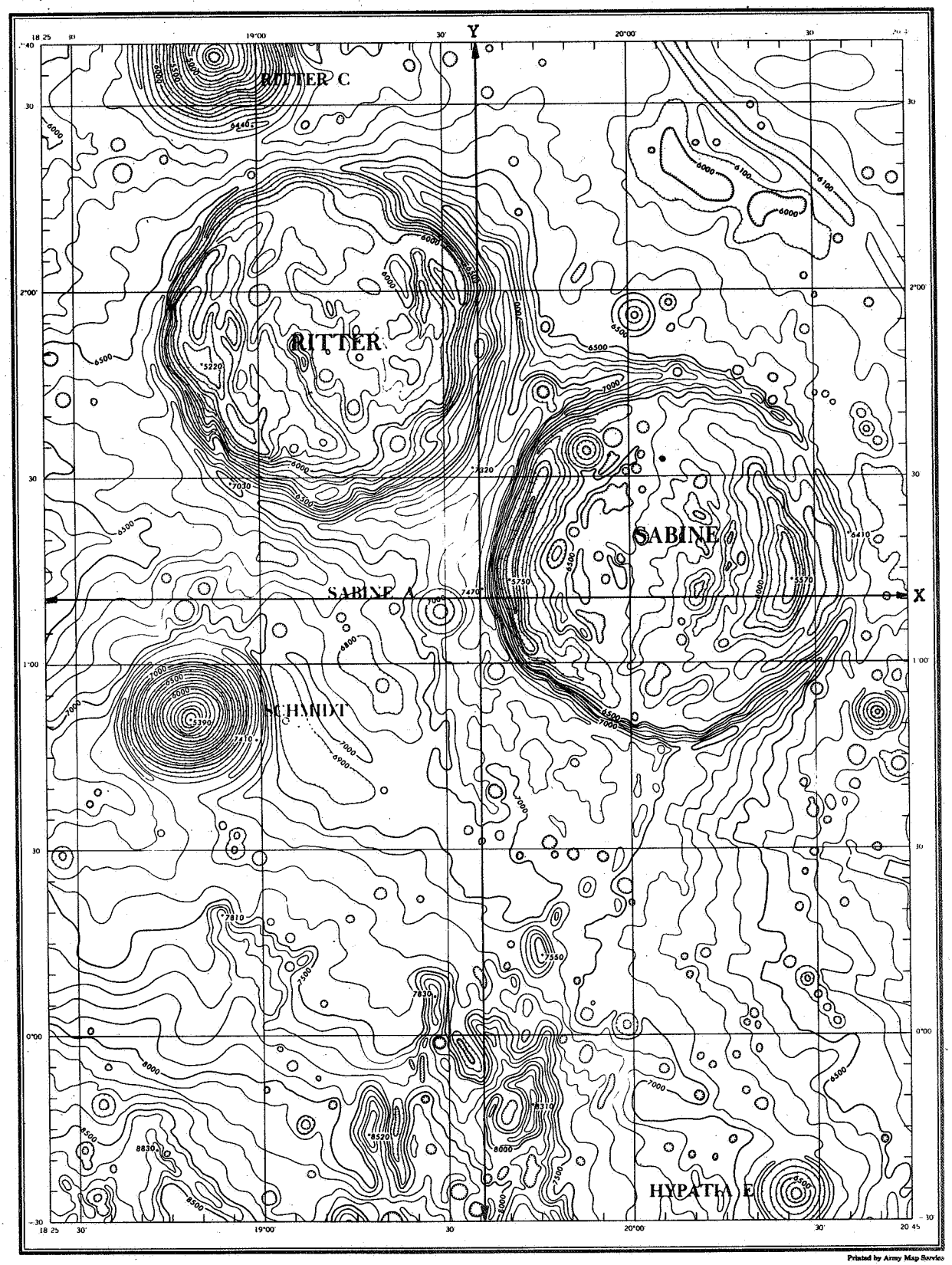

Prepared by the Army Map Service (AM), Corps of Engineers, U. S. Army, Washington, D. C. for the National Aeronautics and Space Administration. Compiled in 1966 on a 210 mm Focal Length Stereoplanigraph C-8 from Ranger VIII photography furnished by the Jet Propulsion Laboratory (JPL) dated 1965. Horizontal and vertical positioning of the topographic data was accomplished by utilizing the position of observed surface points furnished by JPL, selenodetic control published in AMS Technical Report No. 29, (Part Two), "Horizontal and Vertical Control for Lunar Mapping," and existing lunar map sources. The topographic data is portrayed with a one-sigma confidence interval. Named features were derived from and referred to "Named Lunar Formations" (1935) by M. Blagg and K. Müller.

Figure 8-8. Topographic Compilation Compiled from Ranger VIII Photography Using a 210-mm-focal-length Stereoplanigraph C-8.

Also,

$$D = \left(\sqrt{(x - \bar{x})^2 + (y - \bar{y})^2}\right)\left(\frac{1}{1000}\right)\left(\frac{1}{1000}\right)\left(\frac{1}{1/S}\right)$$

$$= \frac{\sqrt{(x - \bar{x})^2 + (y - \bar{y})^2}\ S}{(1000)\quad(1000)} \qquad (8\text{-}3)$$

where

x, y = instrument value of image points in the model

$\bar{x}$, $\bar{y}$ = mean value of all control points in the model

$\sqrt{(x - \bar{x})^2 + (y - \bar{y})^2}$ = distance from center of model (point of tangency) to control or features.

By substituting values from (8-2) and (8-3) into (8-1) one obtains

$$\frac{\ell_c\, S}{(1000)(1000)} = \frac{\left(\frac{\sqrt{(x - \bar{x})^2 + (y - \bar{y})^2}\ S}{(1000)\quad(1000)}\right)^2}{3476},$$

which simplifies to

$$\ell_c = \frac{(x - \bar{x})^2 + (y - \bar{y})^2 S}{3476 \times 10^6}, \qquad (8\text{-}4)$$

which represents lunar curvature in millimeters at a distance from $\bar{x}$, $\bar{y}$ at the scale of the model.

2 Application. ℓ_c is applied to the instrument z value of all points on the model by using a graph of centric circles (fig. 8-9). The radii of each represents lunar curvature in millimeters at a distance from $\bar{x}$, $\bar{y}$ at the scale of the model.

(b) Flattening of Model Employing Vertical Correction Based on Observed Drop-off from Center of Model. After applying corrections for all known factors attributing to model deformation, it was observed

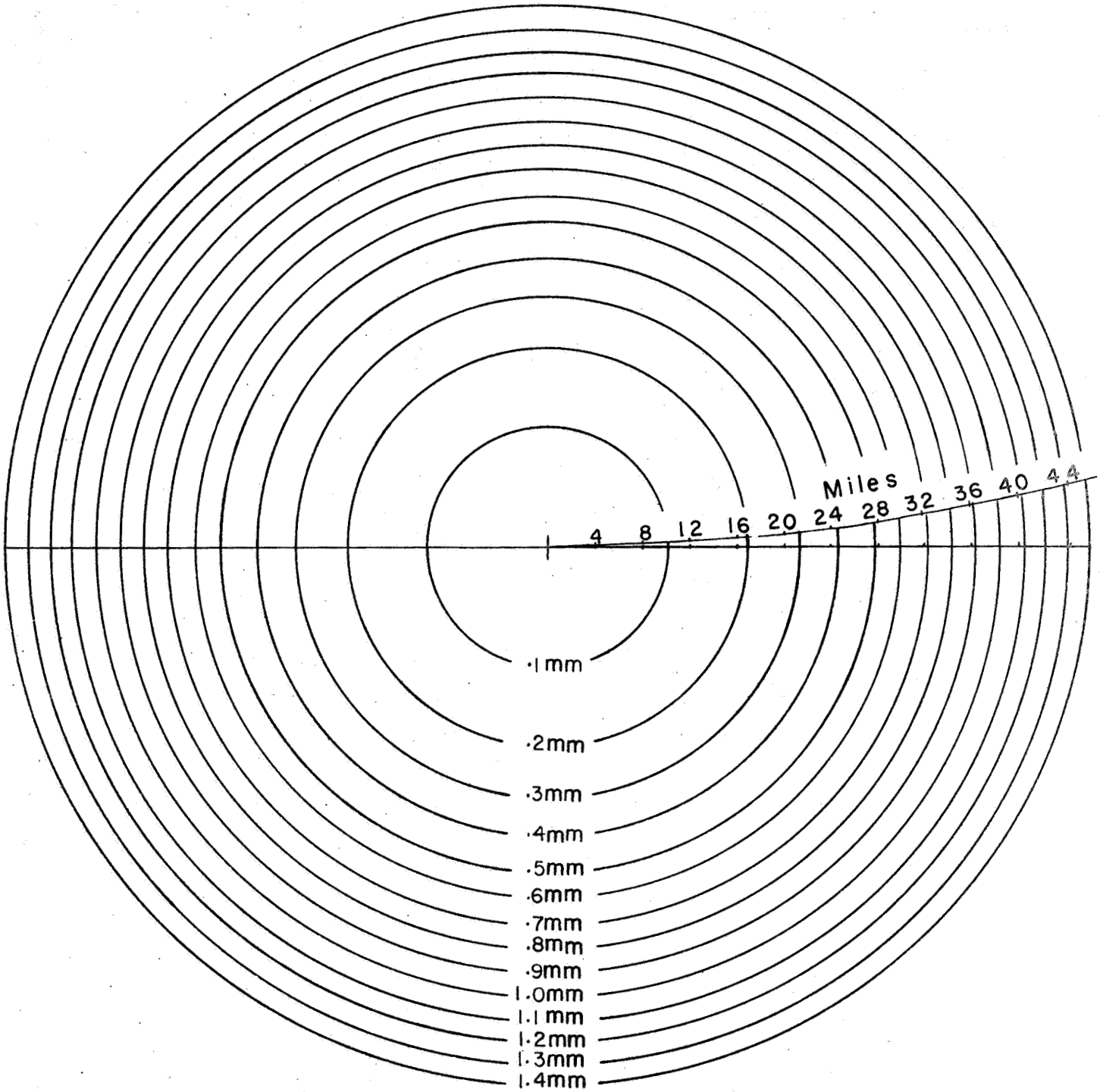

Figure 8-9. Lunar Curvature Correction Graph Based on the Standard Curvature Correction Formula.

that a drop-off existed in the east and west direction from the center of the compilation (fig. 8-8). The foremost question was whether this drop-off was due to the local Lunar topographic formation or to the transmission and reassembly distortions for which no information could be obtained. Of course, there was no conclusion. As an addition to this phase, but not intended for map reproduction, figure 8-10 shows the resulting compilation from photographs 507 and 515 when assuming that the datum plane is flat. The datum-plane correction graph (fig. 8-11) was constructed to represent the vertical correction required to reduce all the elevations to a common datum. Features, such as craters, flat areas, and large rills, were observed in the stereomodel to determine the degree of vertical correction necessary to reduce all features to a common plane. Differences (±) between instrument values and a theoretical plane were recorded for the construction of the graph. As the contours were being drawn, the instrument values were adjusted to correspond to the values of the correction graph line that was crossed.

(4) z-coordinate Observation Precision. The precision with which z-coordinates could be observed in the stereomodel was determined by one operator who took observations three times each on 25 selected points. From these observations a 1-sigma-heighting precision (σ_z) was calculated. For this model the 1-sigma-heighting capability is 110 meters (table 8-V).

(5) Contouring. Horizontal and vertical measurements within the model were made by means of a floating mark. Vertical elevations were determined by placing the floating mark on the imagery surface and reading

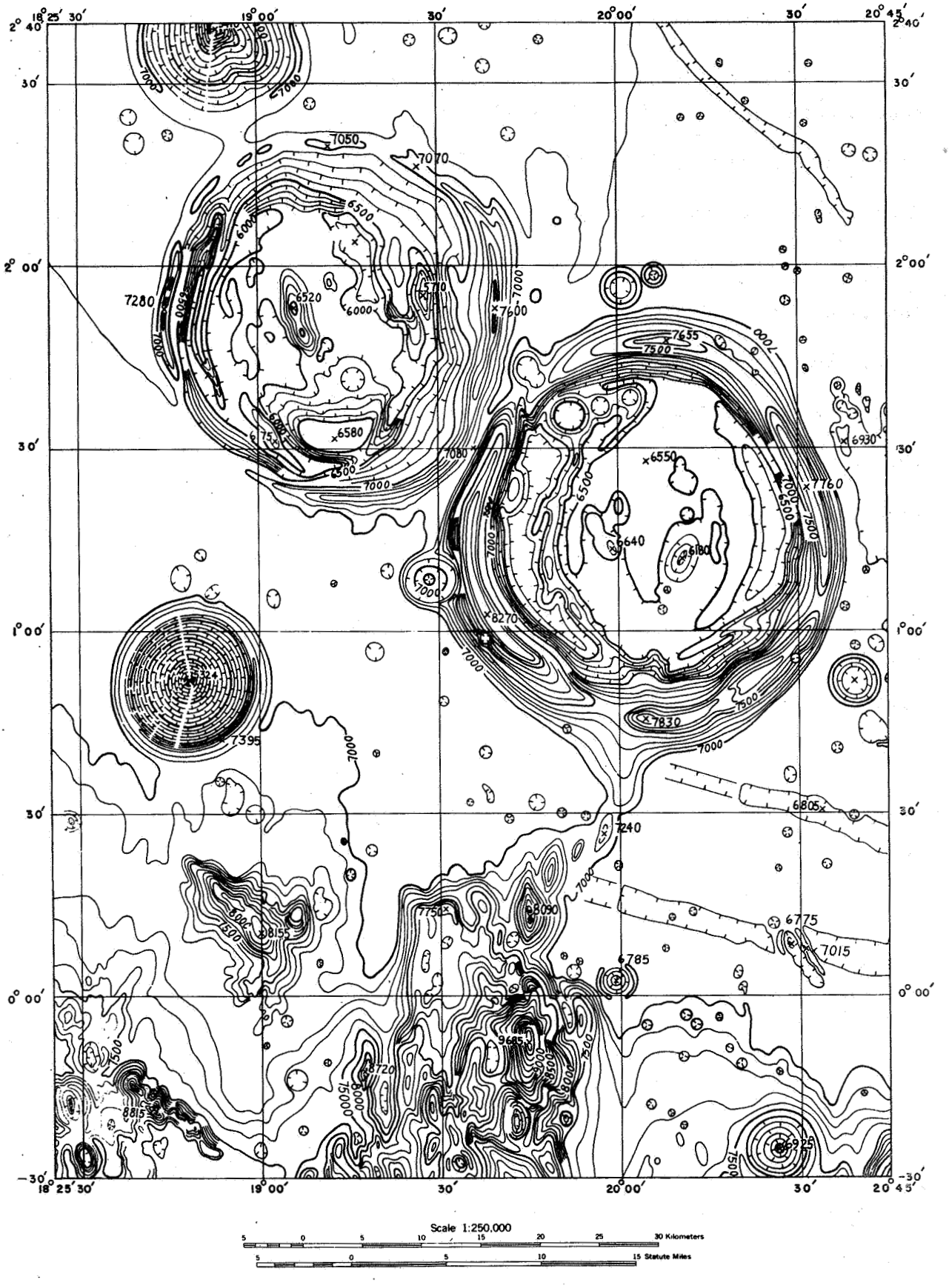

Figure 8-10. Ranger VIII Compilation by Conventional Analog Stereophotogrammetric Methods Using a 210-mm-focal-length Stereoplanigraph C-8 and Employing a Datum-plane Correction Graph.

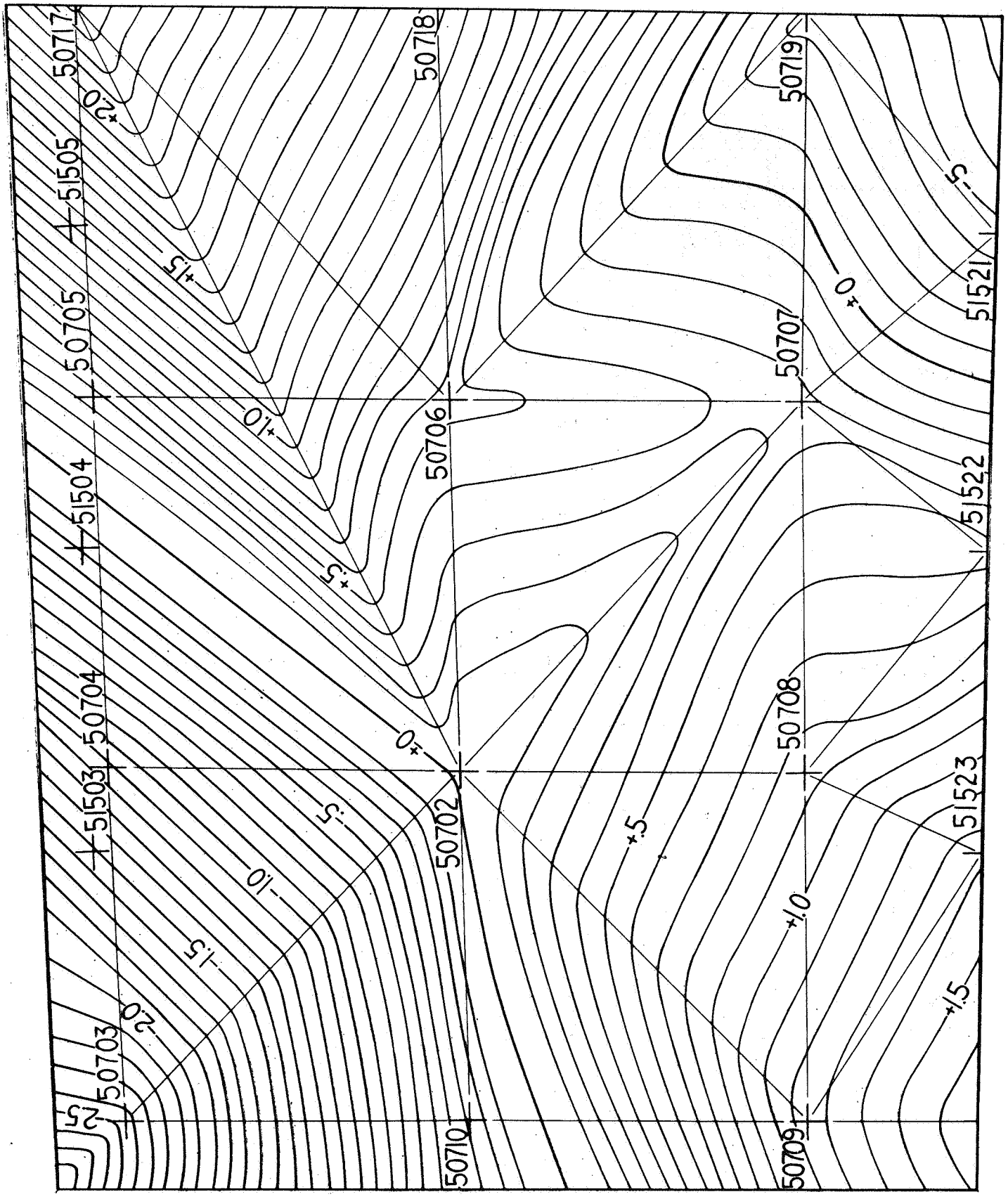

Figure 8-11. Datum-plane Correction Graph.

Table 8-V. Z-coordinate Observation Precision Expressed in mm (210-mm-focal-length Stereoplanigraph)

Pt. No.	Observations			$\bar{Z}$	Deviation from Mean			$\Sigma(Z_i-\bar{Z})^2$
	Z_1	Z_2	Z_3		$Z_1-\bar{Z}$	$Z_2-\bar{Z}$	$Z_3-\bar{Z}$	
1	306.59	306.57	306.76	306.64	-0.05	-0.07	+0.12	0.0218
2	306.18	306.02	305.87	306.02	+0.16	0.00	-0.15	0.0481
3	305.92	305.97	306.18	306.02	-0.10	-0.05	+0.16	0.0381
4	306.93	306.99	307.34	307.09	-0.16	-0.10	+0.25	0.0981
5	307.29	307.13	307.07	307.16	+0.13	-0.03	-0.09	0.0259
6	306.29	306.36	306.51	306.39	-0.10	-0.03	+0.12	0.0253
7	305.76	305.72	306.05	305.84	-0.08	-0.12	+0.21	0.0649
8	305.14	304.98	305.15	305.09	+0.05	-0.11	+0.06	0.0182
9	305.27	305.24	305.49	305.33	-0.06	-0.09	+0.16	0.0373
10	305.39	305.76	305.81	305.65	-0.26	+0.11	+0.16	0.1053
11	304.48	304.60	304.40	304.49	-0.01	+0.11	-0.09	0.0203
12	303.50	303.62	303.86	303.66	-0.16	-0.04	+0.20	0.0672
13	306.86	306.71	306.37	306.65	+0.21	+0.06	-0.28	0.1261
14	305.80	305.72	305.77	305.76	+0.04	-0.04	+0.01	0.0033
15	304.96	304.60	304.79	304.77	+0.15	-0.17	+0.02	0.0518
16	304.52	304.90	304.83	304.75	-0.23	+0.15	+0.08	0.0818
17	304.46	304.24	304.36	304.35	+0.11	-0.11	+0.01	0.0242
18	307.74	307.58	307.38	307.57	+0.17	+0.01	-0.19	0.0651
19	306.68	306.59	306.74	306.67	+0.01	-0.08	+0.07	0.0114
20	305.54	305.75	305.80	305.70	-0.16	+0.05	+0.10	0.0381
21	304.72	304.41	304.24	304.46	+0.26	-0.05	-0.22	0.1185
22	305.05	305.48	305.29	305.27	-0.22	+0.21	+0.02	0.0929
23	305.20	304.93	304.73	304.95	+0.25	-0.02	-0.22	0.1113
24	304.81	305.09	305.10	305.00	-0.19	+0.09	+0.10	0.0542
25	305.12	304.96	304.83	304.97	+0.15	-0.01	-0.14	0.0422

Z_1, Z_2, Z_3 = Observation per point (Z_i)

n = Number of observations

$\bar{Z} = \frac{\Sigma Z_i}{n}$ = Arithmetic mean of observations per point

$Z_i - \bar{Z}$ = Deviation of each observation from the arithmetic mean

$\Sigma(Z_i-\bar{Z})^2$ = Sum of the squares of the deviation of each observation from the arithmetic mean

$\sigma_Z = \sqrt{\frac{\Sigma(Z_i-\bar{Z})^2}{n-1}}$ = Standard deviation or precision of a single observation

$\sigma_Z = \sqrt{\frac{1.3915}{74}}$

$\sigma_Z = 0.1371$ mm

At the model scale of 1:800,000 the standard deviation is approximately 110 meters.

the metric height-indicating scale. Desired elevations were then portrayed in the form of contours with the use of a Coordinatograph connected to the Stereoplanigraph.

d. Results. (1) Employing Standard Curvature Correction Formula. The resulting compilation, compiled by the Conventional Analog Stereophotogrammetric Method and using the standard curvature correction formula, is shown in figure 8-8. A comparison of this compilation with the others produced by the methods yet to be discussed is analyzed in paragraph 14, "Comparative Analysis of Ranger Profiles."

(2) Employing Datum-plane Correction Graph. When this type of curvature correction was applied to the model, a compilation such as figure 8-10 resulted. No statistical analysis was made of this compilation; it was produced solely for visual comparison with figure 8-8. As can be seen, the relative height of local individual features on both figures are comparable; whereas, a significant difference occurs in the over-all contours of the topography.

11. RANGER VIII TOPOGRAPHIC COMPILATION USING THE ANALOG PLOTTER/MATHEMATICAL ORIENTATION METHOD. a. Equipment. The Zeiss Stereoplanigraph C-8 with 6-inch-focal-length plotting cameras was used to obtain instrument x, y, z-coordinates throughout the stereomodel. The 6-inch-focal-length cameras are the standard plotting cameras used to extend horizontal and vertical control and are used for special-type stereophotogrammetric compilations of the earth. Periodic grid flatness tests have shown that the combined effect of these cameras and the mechanical and optical train of the Stereoplanigraph yield an indicated vertical accuracy of one part in 15,800 at the optimum (300 mm) projection distance.

b. Material. (1) Photography. The stereopair consisted of A camera exposures 507 and 515, referred to in paragraph 10b(1).

(2) Diapositives. An enlarging-reducing camera was used to reproduce the 16-mm-format negatives on super flat 9- x 9- x 0.25-inch glass plates at an enlargement ratio to yield an equivalent focal length of 6 inches. The diapositive scale of exposures 507 and 515 was 1:2,106,299 and 1:1,856,955, respectively.

c. Procedure. (1) Relative Orientation. The diapositives were positioned in the cameras and oriented to one another to produce an observed parallax-free model. Horizontalization of the model to a mean plane could not be accomplished due to the physical limitation of the 6-inch-focal-length Stereoplanigraph. Therefore, the maximum tilts that the instrument would allow were introduced into the model.

(2) Scale. (a) Model. The scale at the center of the relatively oriented model was 1:1,000,000.

(b) Viewing. Ocular magnification of 4.5x provided a 1:222,223 viewing scale.

(3) z-coordinate Observation Precision. The precision with which z-coordinates could be observed in the stereomodel was determined by one operator who took three observations on each of 25 selected points. From these observations a 1-sigma measurement for elevation of a point in the model was determined. The 1-sigma-heighting precision for this model was 116 meters (See table 8-VI.)

Table 8-VI. Z-coordinate Observation Precision Expressed in mm
(Analog Plotter/Mathematical Orientation Method)

Pt. No.	Observations			$\bar{Z}$	Deviation from Mean			$\Sigma(Z_i-\bar{Z})^2$
	Z_1	Z_2	Z_3		$Z_1-\bar{Z}$	$Z_2-\bar{Z}$	$Z_3-\bar{Z}$	
1	305.00	305.25	305.30	305.18	-0.18	+0.07	+0.12	0.0517
2	304.46	304.36	304.27	304.36	+0.10	0.00	-0.09	0.0181
3	304.39	304.20	304.17	304.25	+0.14	-0.05	-0.08	0.0285
4	304.36	304.67	304.57	304.53	-0.17	+0.14	+0.04	0.0501
5	303.92	303.79	303.69	303.80	+0.12	-0.01	-0.11	0.0266
6	302.63	302.77	302.76	302.72	-0.09	+0.05	+0.04	0.0122
7	303.37	303.29	303.26	303.31	+0.06	-0.02	-0.05	0.0065
8	303.49	303.46	303.28	303.41	+0.08	+0.05	-0.13	0.0258
9	302.90	303.06	302.99	302.98	-0.08	+0.08	+0.01	0.0129
10	303.21	303.50	303.64	303.45	-0.24	+0.05	+0.19	0.0962
11	303.19	303.40	303.49	303.36	-0.17	+0.04	+0.13	0.0474
12	303.56	303.56	303.43	303.52	+0.04	+0.04	-0.09	0.0113
13	303.39	303.46	303.27	303.37	+0.02	+0.09	-0.10	0.0185
14	304.39	304.29	304.23	304.30	+0.09	-0.01	-0.07	0.0131
15	302.70	302.66	302.70	302.69	+0.01	-0.03	+0.01	0.0011
16	302.77	302.90	302.49	302.72	+0.05	+0.18	-0.23	0.0878
17	301.02	300.88	300.68	300.86	+0.16	+0.02	-0.18	0.0584
18	301.38	301.52	301.37	301.42	-0.04	+0.10	-0.05	0.0141
19	301.27	301.21	301.19	301.22	+0.05	-0.01	-0.03	0.0035
20	304.48	304.45	304.50	304.48	0.00	-0.03	+0.02	0.0013
21	301.69	301.38	301.29	301.45	+0.24	-0.07	-0.16	0.0881
22	303.97	303.77	303.57	303.77	+0.20	0.00	-0.20	0.0800
23	304.40	304.20	304.00	304.20	+0.20	0.00	-0.20	0.0800
24	304.09	303.80	303.69	303.86	+0.23	-0.06	-0.17	0.0845
25	304.31	304.21	303.94	304.15	+0.16	+0.06	-0.21	0.0733

Z_1, Z_2, Z_3 = Observation per point (Z_i)

n = Number of observations

$\bar{Z} = \frac{\Sigma Z_i}{n}$ = Arithmetic mean of observations per point

$Z_i - \bar{Z}$ = Deviation of each observation from the arithmetic mean

$\Sigma(Z_i-\bar{Z})^2$ = Sum of the squares of the deviation of each observation from the arithmetic mean

$\sigma_Z = \sqrt{\frac{\Sigma(Z_i-\bar{Z})^2}{n-1}}$ = Standard deviation or precision of a single observation

$$\sigma_Z = \sqrt{\frac{0.9919}{74}}$$

$$\sigma_Z = 0.1158 \text{ mm}$$

At the model scale of 1:1,000,000 the standard deviation is approximately 116 meters.

(4) Mensuration Phase. A dense network of 6900 points (x, y, z-coordinates determined for each point) were measured and recorded in digital form. The measurements were made at an interval of 1 mm on the model with additional points measured to further define craters, rills, and any other significant topographic features. Three observations and recordings were made by one operator for each point.

(5) Absolute Orientation. A composite of selenodetic control, JPL-observed surface points, and control from existing lunar maps (transformed into Mercator grid coordinates and elevations) were used as a basis for absolute orientation of the digitized data. Details concerning the Absolute Orientation Method may be found in chapter 5, "Analog Plotter/Mathematical Orientation Method."

(6) Curvature Correction. Correction for the effect of lunar curvature in the model is an integral part of the Analog Plotter/Mathematical Orientation Method. Chapter 5 contains the procedure to be followed for curvature correction.

(7) Contouring. The large volume of irregularly distributed data surface points (X, Y, Z for each data point) derived from the Analog Plotter/Mathematical Orientation Method was processed through the Digital Contouring Program (chap 7), where a uniform mathematical grid was established from the input data and mesh-point values were computed. After a smoothing between mesh-point values, X, Y-coordinates of Z values (corresponding to 100-meter interval) were compiled and presented in the form of contours by a graph plotter at a 1:250,000 scale. Cartographic shaping was then accomplished by a cartographer to enhance the portrayal of the hypsometric data.

d. Results. The compilation produced by the Analog Plotter/ Mathematical Orientation Method is shown in figure 8-12. This compilation is compared with the results of the three other methods in paragraph 14.

12. RANGER VIII TOPOGRAPHIC COMPILATION UTILIZING THE COMPARATOR/ ANALYTICAL METHOD. a. Equipment. The Zeiss stereocomparator PSK was used to measure the x, y-coordinates of a dense network of points throughout the model. This instrument is not limited to any physical ranges, except in the size (9 x 9 inch) of the diapositive. The effects of temperature influences on measurements are practically eliminated since the object to be measured and the measuring agent are the same base material. Observed x, y-coordinates are recorded with the precision of one micron. Measurements can be made at viewing scales ranging from 8 to 16 times diapositive scale.

b. Material. (1) Photography. The stereopair consisted of A camera exposures 499 and 515 (figs. 8-7 and 8-13). The exposure altitude for 499 and 515 is 360 and 283 km, respectively. Based on an average of the exposure altitudes, the approximate base-height ratio of the stereopair is 0.13.

(2) Diapositive. A Wild U-3 printer (a high precision printer used to prepare positive or negative transparancies of aerial photographs on glass plates) was used to prepare diapositives of exposures 499 and 515. Exposure 515 was prepared at the contact scale of 1:6,807,188, yielding a focal length of 41.5737 mm. A diapositive of exposure 499 was then prepared at the scale common to exposure 515; the resulting focal length was 52.8856 mm.

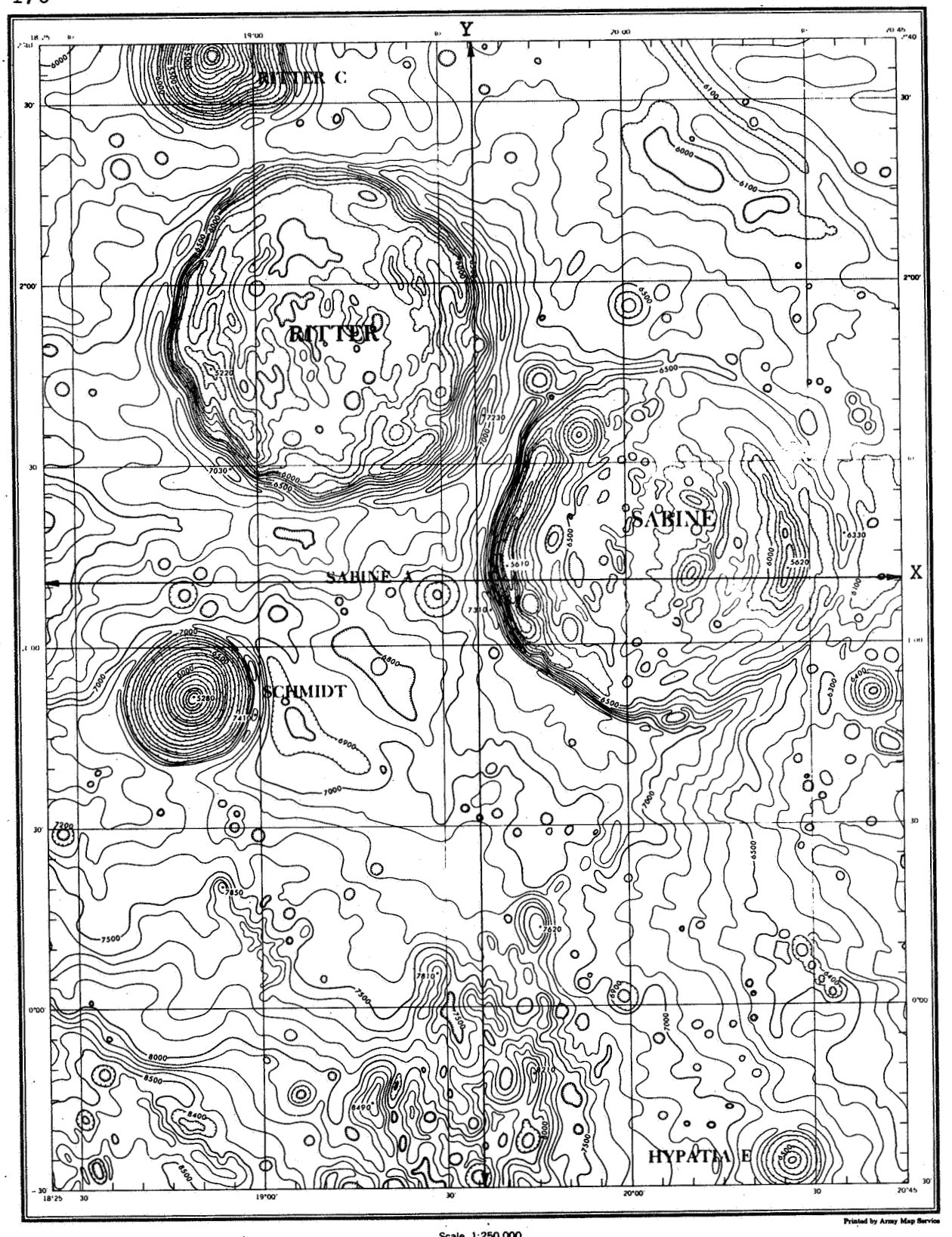

Figure 8-12. Topographic Compilation Compiled from Ranger VIII Photography Using Analog Plotter/Mathematical and Digital Contouring Methods.

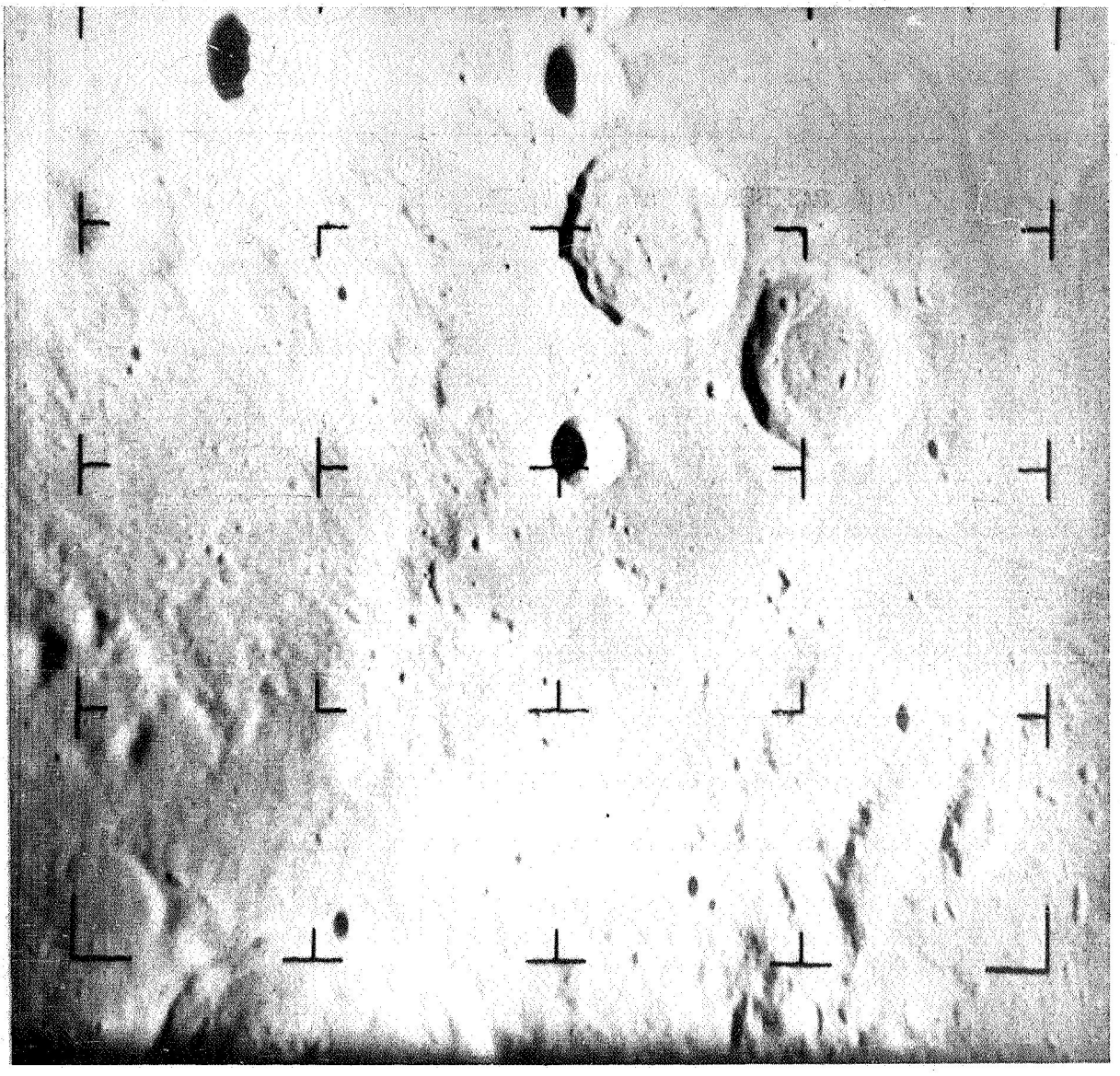

Figure 8-13. Ranger VIII Exposure 499.

c. Procedure. (1) Relative Orientation. Relative orientation was performed by azimuthal alignment of the diapositive and elimination of x and y-parallaxes to achieve optimum stereoscopic vision. Also, the position of each diapositive (with respect to the coordinate system of the measuring grid) was determined by measuring the fiducial marks of the diapositives.

(2) Scale. (a) Model. The scale of the model was 1:6,807,188.

(b) Viewing. A 12x ocular magnification was used to provide an approximate 1:567,266 viewing scale.

(3) z-coordinates Observation Precision. The z-coordinate was not observed or recorded, but was computed from input data, such as the measured x- and y-image coordinate, focal length, and initial taking camera orientation data. Therefore, the precision with which elevations could be determined in the stereomodel was basically a function of the precision of the measured x-and y-image coordinate in the two photographs of the stereo-pair. To determine the reliability of computed Z-coordinates, the x- and y-image coordinates of six points common to the two photographs were measured and recorded eight times by one operator. Eight elevations were computed for each point by the Comparator/Analytical Method. A statistical analysis was made of the computed elevations for each point, as shown in table 8-VII. The 1-sigma-heighting precision for this model was 101 meters.

(4) Mensuration Phase. The mensuration phase was similar to that employed in the Analog Plotter/Mathematical Orientation Method. In essence, the difference was that only the x and y-coordinates of a point were measured. For this model, a network of 1400 points was measured at a 1-mm interval and recorded in digital form. In addition, points to further define

Table 8-VII. Z-coordinate Observation Precision Expressed in Meters (Comparator/Analytical Method)

Computed Z Coordinate per Observation No:	Point Identification					
	7015	7083	8052	7070	7041	8006
1	-939.305	-313.986	3146.322	3035.219	2661.661	3986.833
2	-804.952	-278.372	3085.329	2983.380	2754.633	3898.913
3	-626.609	-252.330	3206.265	2816.941	2918.048	3799.667
4	-893.010	-337.072	3112.169	2980.010	2770.695	3789.070
5	-937.164	-191.763	3109.609	3089.067	2718.874	3962.872
6	-1069.461	-335.154	2933.653	2924.106	2874.284	3874.998
7	-1067.592	-214.757	2962.692	2867.502	2650.931	4003.127
8	-1067.823	-301.394	3245.008	3037.909	2536.423	3845.266
$\bar{Z}$	-925.7401	-278.1036	3100.131	2966.768	2735.694	3895.093
SIGMA Z	134.2229	48.01589	77.05932	79.60778	92.43367	69.46291
RMSE Z	125.5541	44.91475	72.08240	74.46626	86.46378	64.97660
Z SIGMA L = 101.318						

$\bar{Z} = \frac{\Sigma Z_p}{AN}$ = Arithmetic mean

Z_p = Computed Z coordinate of the point

AN = Number of readings per point

SIGMA Z = $\left[\frac{\Sigma(\Delta Z)^2}{AN-1}\right]^{\frac{1}{2}}$ = Standard deviation for an individual point

$Z = Z - \bar{Z}$ = Residual

RMSE Z = $\left[\frac{\Sigma(\Delta Z)^2}{AN}\right]^{\frac{1}{2}}$ = Root mean square error for an individual point

Z SIGMA L = $\left[\sum_{i=1}^{n} (\Delta Z_i)^2\right]^{\frac{1}{2}}$ = Standard deviation for all points

n = Number of points observed

significant features were also measured and recorded. Three observations and recordings of each point were made by one operator.

(5) Absolute Orientation. A composite of selenodetic control (one-point), JPL-observed surface points, and control from existing lunar maps (transformed into Mercator grid coordinates and elevations) were used as a basis for absolute orientation of the digitized data. Absolute orientation was performed using the Comparator/Analytical Method previously discussed in chapter 6.

(6) Lens Distortion and Curvature Correction. Correction for the effect of lens distortion and lunar curvature in the model is a part of and was applied during the absolute orientation procedure. Details concerning these corrections may be found in chapter 6.

(7) Contouring. The portrayal in contour form of the computed surface points (X, Y, Z-coordinates) is identical to the procedure employed in the Analog Plotter/Mathematical Orientation Method [par. 11c(7)].

d. Results. The compilation produced by the Comparator/Analytical Method is shown in figure 8-14. This compilation is compared with the results of the other methods in paragraph 14.

13. RANGER VIII TOPOGRAPHIC COMPILATION USING AN ANALYTICAL PLOTTER.

a. Equipment. The AS-11A Analytical Plotter (fig. 8-15) was used for a direct Ranger compilation. This plotter is a first-order map compilation instrument. Residual parallaxes are removed from the model by a computer memory. The plotter is designed to make automatic correction (through preprogramming) for lens and telemetry distortions, ground reconstitution,

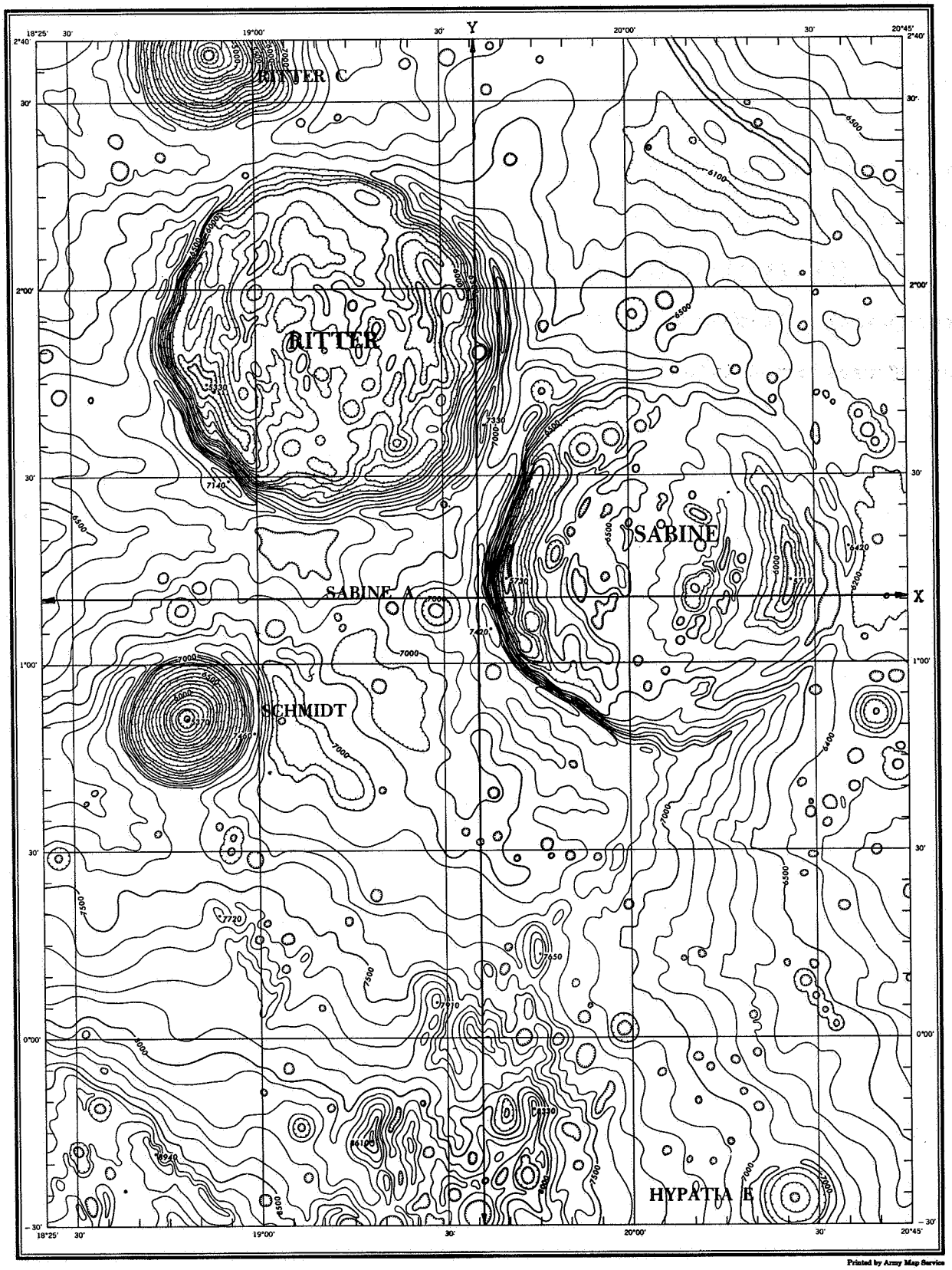

Prepared by the Army Map Service (AM), Corps of Engineers, U. S. Army, Washington, D. C. for the National Aeronautics and Space Administration. Compiled in 1966 by comparator / analytical and digital contouring methods from Ranger VIII photography furnished by the Jet Propulsion Laboratory (JPL) dated 1965. Horizontal and vertical positioning of the topographic data was accomplished by utilizing the position of observed surface points furnished by JPL, selenodetic control published in AMS Technical Report No. 29, (Part Two), "Horizontal and Vertical Control for Lunar Mapping," and existing lunar map sources. The topographic data is portrayed with a one-sigma confidence interval. Named features were derived from and referred to "Named Lunar Formations" (1935) by M. Blagg and K. Müller.

Figure 8-14. Topographic Compilation Compiled from Ranger VIII Photography Using Comparator/Analytical and Digital Contouring Methods.

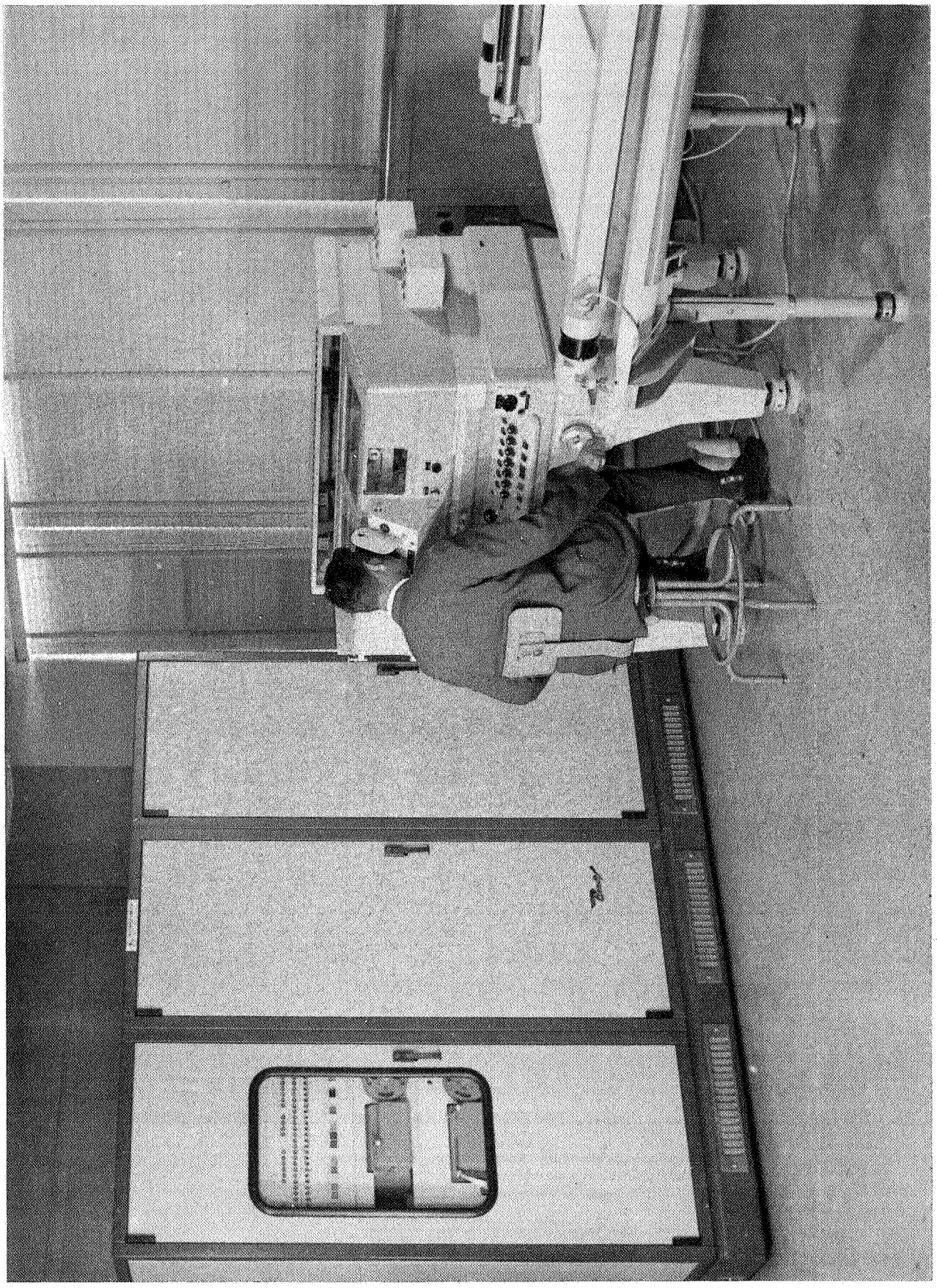

Figure 8-15. AS-11A Analytical Plotter (Courtesy of O. M. I. Corporation of America).

differential film shrinkage, and the effect of earth or lunar curvature in the model. In addition, profiles can be produced in any direction with any desired vertical exaggeration.

b. Material. (1) Photography. The stereopair consisted of A camera exposures 507 and 515. The exposure altitude for 507 and 515 is 321 and 283 km, respectively. Based on an average of the exposure altitudes, the approximate base-height ratio of the stereopair is 0.10.

(2) Diapositive. The diapositives of exposures 507 and 515 were prepared with a Wild U-3 printer at a scale of 1:2,000,000. The resulting focal length, due to the enlargement, was 160.4994 and 141.4960 mm for exposures 507 and 515, respectively.

c. Procedure. (1) Orientation. Trajectory data, camera data, and other information regarding each exposure (provided by JPL) were used to compute, for the stereopair, a local space rectangular coordinate system whose Z-axis was normal to the center of the overlap area on the lunar surface. Based on this transformation and on the inertial referenced orientation data, initial relative elements of orientation were estimated and entered into the computer memory of the plotter. Based on trial-and-error numerical and analog procedures, the initial relative orientation elements were refined. Absolute vertical orientation was accomplished by leveling to the rims of large craters and to the mean surface area. The model was horizontally controlled to the coordinates of the observed surface points furnished by JPL.

(2) Scale. (a) Model. The model scale was 1:2,000,000.

(b) Viewing. A 10x ocular magnification provided a 1:200,000 viewing scale.

(c) Plotting. The plotting was accomplished on a Mercator projection at a 1:250,000 scale.

(3) Lens Distortion. The effect of lens distortion in the model was automatically corrected during compilation. This was accomplished by entering into the computer section of the plotter the degree of the inherent distortion expressed at plate scale.

(4) Curvature Correction. The mathematical development for eliminating the effect of lunar curvature in the model was basically the same as that previously described in paragraph 10c(3). The significant difference was in the application process. Instead of a graphic adjustment application, the mathematical derivation was entered into the computer section of the plotter where an automatic correction for the effect of curvature was made during the contouring phase.

(5) z-coordinate Observation Precision. The precision with which z-coordinates could be observed in the stereomodel was determined by one operator who took three observations of each of 25 selected points. From these, a 1-sigma-heighting precision was calculated (table 8-VIII). The 1-sigma-heighting precision for this model was 101 meters.

(6) Contouring. The contouring procedure was identical to that employed in the Conventional Analog Compilation Method. Vertical measurements within the model were made by means of a floating mark.

Table 8-VIII. Z-coordinate Observation Precision Expressed in mm
(AS-11A Analytical Plotter)

Pt. No.	Observations			$\bar{Z}$	Deviation from Mean			$\Sigma(Z_i-\bar{Z})^2$
	Z_1	Z_2	Z_3		$Z_1-\bar{Z}$	$Z_2-\bar{Z}$	$Z_3-\bar{Z}$	
1	303.927	303.815	303.784	303.842	+0.085	-0.027	-0.058	0.011318
2	303.952	303.999	304.091	304.014	-0.062	-0.015	+0.077	0.009998
3	305.378	305.471	305.513	305.454	-0.076	+0.017	+0.059	0.009546
4	304.995	305.106	305.148	305.083	-0.088	+0.023	+0.065	0.012498
5	306.224	306.257	306.320	306.267	-0.043	-0.010	+0.053	0.004758
6	306.917	306.862	306.943	306.904	+0.003	-0.042	+0.039	0.003294
7	307.639	307.748	307.663	307.683	-0.044	+0.065	-0.020	0.006561
8	306.715	306.670	306.640	306.675	+0.040	-0.005	-0.035	0.002850
9	306.266	306.196	306.159	306.207	+0.059	-0.011	-0.048	0.005906
10	305.397	305.356	305.297	305.350	+0.047	+0.006	-0.053	0.005054
11	305.425	305.466	305.333	305.408	+0.017	+0.058	-0.075	0.009278
12	305.327	305.452	305.514	305.431	-0.104	+0.021	+0.083	0.018146
13	305.629	305.663	305.691	305.661	-0.032	+0.002	+0.030	0.001928
14	305.720	305.797	305.721	305.746	-0.026	+0.051	-0.025	0.003902
15	306.319	306.293	306.168	306.260	+0.059	+0.033	-0.092	0.013034
16	305.649	305.725	305.647	305.673	-0.024	+0.050	-0.026	0.003752
17	305.083	305.179	305.170	305.144	-0.061	+0.035	+0.026	0.005622
18	305.660	305.656	305.592	305.636	+0.024	+0.020	-0.044	0.002912
19	305.460	305.589	305.559	305.536	-0.076	+0.053	+0.023	0.009114
20	305.645	305.687	305.588	305.640	+0.005	+0.047	-0.052	0.004938
21	305.774	305.668	305.658	305.700	+0.074	-0.032	-0.042	0.008264
22	304.532	305.537	305.515	304.528	+0.004	+0.009	-0.013	0.000266
23	304.857	304.750	304.691	304.766	+0.091	-0.016	-0.075	0.014162
24	303.473	303.466	303.396	303.445	+0.028	+0.021	-0.049	0.003626
25	305.809	305.954	305.979	305.914	-0.105	+0.040	+0.065	0.016850

Z_1, Z_2, Z_3 = Observation per point (Z_i)

n = Number of observations

$\bar{Z} = \frac{\Sigma Z_i}{n}$ = Arithmetic mean of observations per point

$Z_i - \bar{Z}$ = Deviation of each observation from the arithmetic mean

$\Sigma(Z_i-\bar{Z})^2$ = Sum of the squares of the deviation of each observation from the arithmetic mean

$\sigma_Z = \sqrt{\frac{\Sigma(Z_i-\bar{Z})^2}{n-1}}$ = Standard deviation or precision of a single observation

$$\sigma_Z = \sqrt{\frac{0.187577}{74}}$$

$$\sigma_Z = 0.0503 \text{ mm}$$

At the model scale of 1:2,000,000 the standard deviation is approximately 101 meters.

Vertical elevations were determined by placing the floating mark on the imagery surface and reading the height-indicator scale. Desired increments of elevations were portrayed in the form of contours with the use of a Coordinatograph connected to the instrument.

d. Results. The compilation produced by the Analytical Plotter Method is shown in figure 8-16. This compilation is compared with the results of the other methods in paragraph 14.

14. COMPARATIVE ANALYSIS OF RANGER PROFILES. a. Procedure. An analysis was made of the resulting Ranger hypsometric data derived by the four reduction methods: (1) Conventional Analog Stereophotogrammetric, (2) Analog Plotter/Mathematical Orientation, (3) AS-11A Analytical Plotter, and (4) Comparator/Analytical. Two profiles (one each in the X and the Y direction) were drawn for each contour compilation (figs. 8-8, 8-12, 8-14, and 8-16). The profiles of each compilation covered the same topographic data. Elevations of 15 evely spaced points, along each of the X and Y profiles, were manually interpolated from each of the compilations (fig. 8-17). A new elevation for each point was then determined from the arithmetic mean of the four profiles.

b. Results. Tables 8-IX through 8-XII show the elevation differences from the arithmetic mean for each of the 30 points interpolated from each of the four compilations. Also, as shown in these tables, the estimated standard deviation (σ_z) of the individual contour difference for each compilation from the arithmetic mean profile is as follows:

(1) Conventional Analog Stereophotogrammetric Method...68 meters.

(2) Analog Plotter/Mathematical Orientation Method.....61 meters.

(3) AS-11A Analytical Plotter Method.....57 meters.

(4) Comparator/Analytical Method.....29 meters.

As a result of this analysis, a 1:250,000 scale Ranger map was published. This map consisted of the compilation produced by the Comparator/Analytical Method (fig. 8-14) combined with a pictoral relief drawing.

15. TOPOGRAPHIC MAPPING FROM LOWER ALTITUDE RANGER VIII PHOTOGRAPHY.

a. Introduction. Two contour compilations, designated 531-537 and 563-565, were compiled from exposures taken at an average altitude of 191 and 40 km, respectively. The Analog Plotter/Mathematical Orientation Method was used to produce Compilation 531-537 (fig. 8-18) and the Comparator/Analytical Method was used to produce Compilation 563-565 (fig. 8-19).

b. Ranger VIII Compilation 531-537. (1) Equipment. The Zeiss Stereoplanigraph C-8 with 6-inch-focal-length plotting cameras, previously discussed in paragraph 11a, was used to obtain x, y, z-coordinates throughout the stereomodel.

(2) Material. (a) Photography. The stereopair consisted of A camera exposures 531 and 537 (figs. 8-20 and 8-21). The altitude of exposure for these photographs is 205 and 176 km, respectively. Based on an average of the two exposure altitudes, the base-height ratio of the stereopair is 0.09.

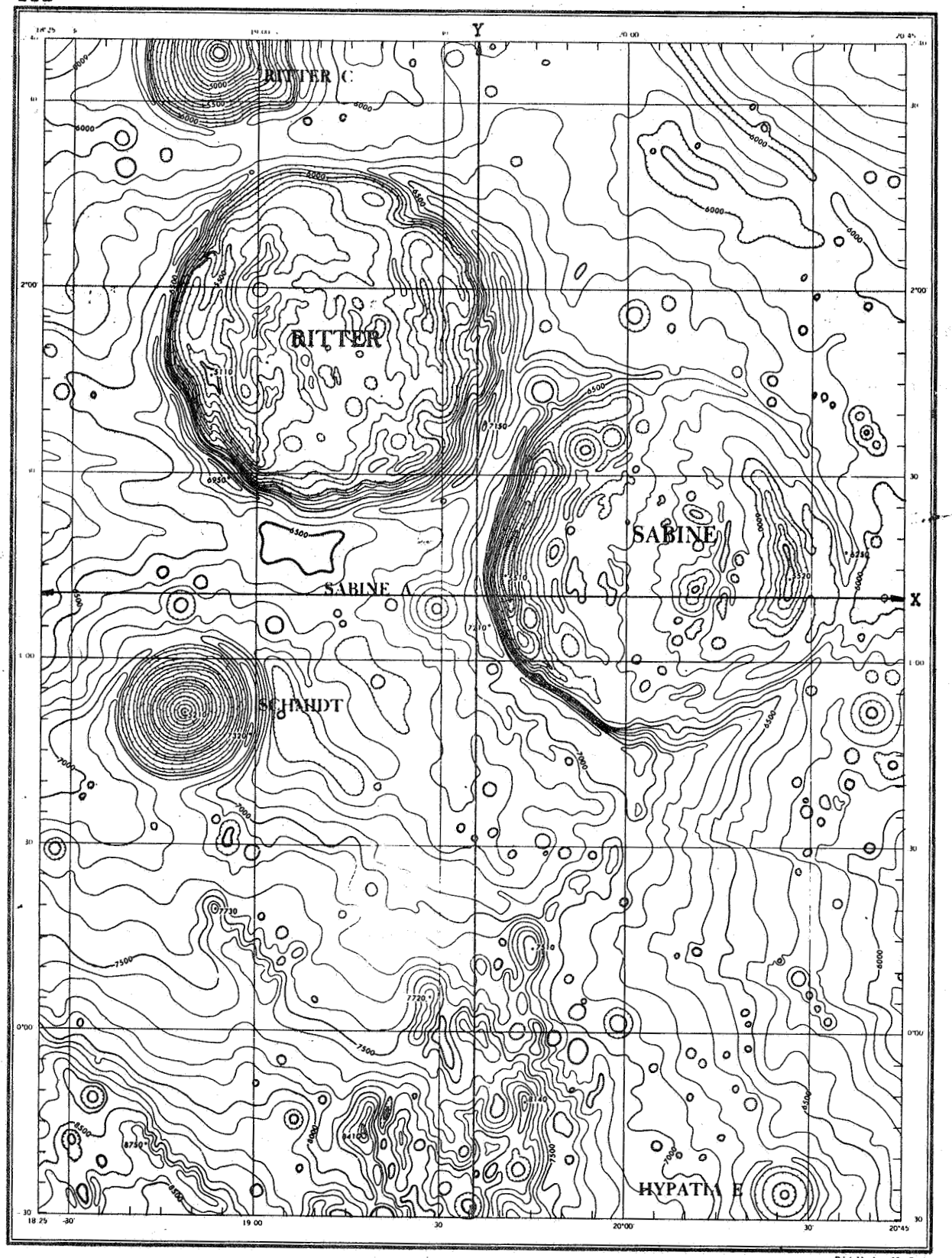

Figure 8-16. Topographic Compilation Compiled from Ranger VIII Photography Using an AS-11A Analytical Plotter.

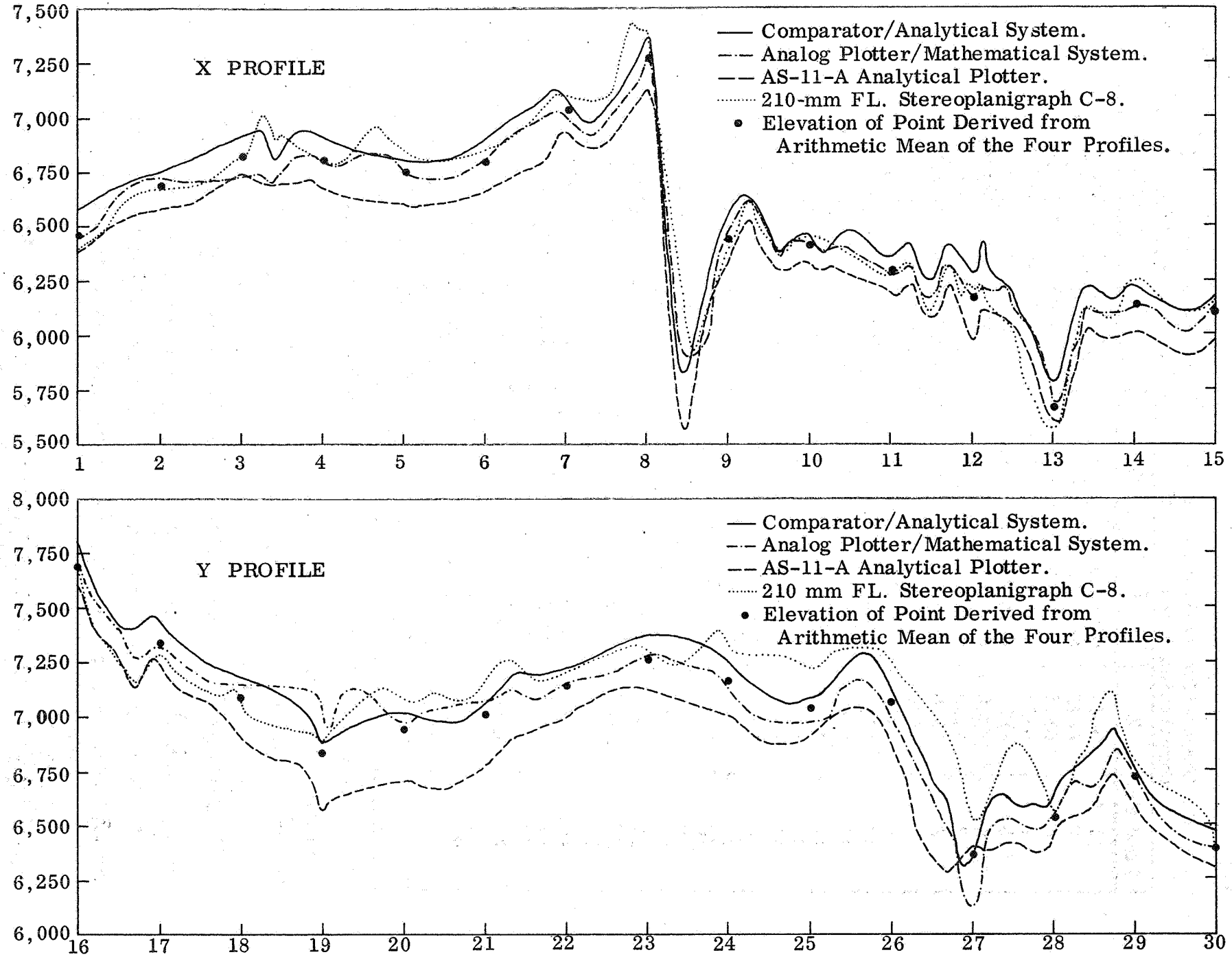

Figure 8-17. Comparison of Profiles.

Table 8-IX. Comparative Analysis of Profiles Interpolated from Ranger VIII Compilation Produced by the Conventional Analog Method (Meters)

Point No.	Z	$\bar{Z}$	$Z-\bar{Z}$	$Z'-\bar{Z}$	$(Z'-\bar{Z})^2$
1	6425	6456.25	- 31.25	- 79.58	6,332.9764
2	6675	6681.25	- 6.25	- 54.58	2,978.9764
3	6825	6812.50	12.50	- 35.83	1,283.7889
4	6825	6800.00	25.00	- 23.33	544.2889
5	6825	6743.75	81.25	32.92	1,083.7264
6	6850	6793.75	56.25	7.92	62.7264
7	7100	7031.25	68.75	20.42	416.9764
8	7300	7268.75	31.25	- 17.08	291.7264
9	6400	6437.50	- 37.50	- 85.83	7,366.7889
10	6450	6412.50	37.50	- 10.83	117.2889
11	6275	6300.00	- 25.00	- 73.33	5,377.2889
12	6200	6168.75	31.25	- 17.08	291.7264
13	5600	5668.75	- 68.75	-117.08	13,707.7264
14	6250	6143.75	106.25	57.92	3,354.7264
15	6150	6106.25	43.75	- 4.58	20.9764
16	7700	7700.00	0.00	- 48.33	2,335.7889
17	7300	7343.75	- 43.75	- 92.08	8,478.7264
18	7100	7081.25	18.75	- 29.58	874.9764
19	6875	6837.50	37.50	- 10.83	117.2889
20	7075	6943.75	131.25	82.92	6,875.7264
21	7125	7006.25	118.75	70.42	4,958.9764
22	7225	7143.75	81.25	32.92	1,083.7264
23	7300	7268.75	31.25	- 17.08	291.7264
24	7300	7168.75	131.25	82.92	6,875.7264
25	7225	7043.75	181.25	132.92	17,667.7264
26	7250	7068.75	181.25	132.92	17,667.7264
27	6550	6368.75	181.25	132.92	17,667.7264
28	6550	6537.50	12.50	- 35.83	1,283.7889
29	6800	6725.00	75.00	26.67	711.2889
30	6375	6387.50	- 12.50	- 60.83	3,700.2889
Σ			1,450.00	0.10	133,822.9170

Z = Z Coordinate of individual point determined from the profile

n = number of points

$\bar{Z} = \frac{\Sigma Z}{n}$ = Z coordinate of point determined from the arithmetic mean of the four profiles

$Z-\bar{Z}$ = Deviation of the individual point from the arithmetic mean

$Z' = Z \pm \frac{\Sigma(Z-\bar{Z})}{n}$ = Z coordinate of the point after datum adjustment

$Z'-\bar{Z}$ = Deviation of datum adjusted Z coordinate from the arithmetic mean

$(Z'-\bar{Z})^2$ = Square of the deviation of the datum adjusted Z coordinate from the arithmetic mean

$\sigma_Z = \sqrt{\frac{\Sigma(Z'-\bar{Z})^2}{n-1}}$ = The estimated standard error of the individual contour differences from the arithmetic mean profile

For this compilation σ_Z = 68 meters.

Table 8-X. Comparative Analysis of Profiles Interpolated from the Ranger VIII Compilation Produced by the Analog Plotter/ Mathematical Orientation Method (Meters)

Point No.	Z	$\bar{Z}$	$Z-\bar{Z}$	$Z'-\bar{Z}$	$(Z'-\bar{Z})^2$
1	6450	6456.25	- 6.25	- 12.08	145.9264
2	6725	6681.25	43.75	37.92	1,437.9264
3	6800	6812.50	- 12.50	- 18.33	335.9889
4	6800	6800.00	0.00	- 5.83	33.9889
5	6750	6743.75	6.25	0.42	0.1764
6	6800	6793.75	6.25	0.42	0.1764
7	7000	7031.25	- 31.25	- 37.08	1,374.9264
8	7275	7268.75	6.25	0.42	0.1764
9	6475	6437.50	37.50	31.67	1,002.9889
10	6425	6412.50	12.50	6.67	44.4889
11	6375	6300.00	75.00	69.17	4,784.4889
12	6175	6168.75	6.25	0.42	0.1764
13	5700	5668.75	31.25	25.42	646.1764
14	6125	6143.75	- 18.75	- 24.58	604.1764
15	6125	6106.25	18.75	12.92	166.9264
16	7700	7700.00	0.00	- 5.83	33.9889
17	7375	7343.75	31.25	25.42	646.1764
18	7150	7081.25	68.75	62.92	3,958.9264
19	7000	6837.50	162.50	156.67	24,545.4889
20	6975	6943.75	31.25	25.42	646.1764
21	7075	7006.25	68.75	62.92	3,958.9264
22	7150	7143.75	6.25	0.42	0.1764
23	7275	7268.75	6.25	0.42	0.1764
24	7125	7168.75	- 43.75	- 49.58	2,458.1764
25	6975	7043.75	- 68.75	- 74.58	5,562.1764
26	7000	7068.75	- 68.75	- 74.58	5,562.1764
27	6150	6368.75	-218.75	-224.58	50,436.1764
28	6550	6537.50	12.50	6.67	44.4889
29	6725	6725.00	0.00	- 5.83	33.9889
30	6400	6387.50	12.50	6.67	44.4889
Σ			175.00	0.10	108,510.4170

Z = Z Coordinate of individual point determined from the profile

n = number of points

$\bar{Z} = \frac{\Sigma Z}{n}$ = Z coordinate of point determined from the arithmetic mean of the four profiles

$Z-\bar{Z}$ = Deviation of the individual point from the arithmetic mean

$Z' = Z \pm \frac{\Sigma(Z-\bar{Z})}{n}$ = Z coordinate of the point after datum adjustment

$Z'-\bar{Z}$ = Deviation of datum adjusted Z coordinate from the arithmetic mean

$(Z'-\bar{Z})^2$ = Square of the deviation of the datum adjusted Z coordinate from the arithmetic mean

$\sigma_Z = \sqrt{\frac{\Sigma(Z'-\bar{Z})^2}{n-1}}$ = The estimated standard error of the individual contour differences from the arithmetic mean profile

For this compilation $\sigma_Z = 61$ meters.

Table 8-XI. Comparative Analysis of Profiles Interpolated from the Ranger VIII Compilation Produced by the Comparator/Analytical Method (Meters)

Point No.	Z	$\bar{Z}$	$Z-\bar{Z}$	$Z'-\bar{Z}$	$(Z'-\bar{Z})^2$
1	6575	6456.25	118.75	41.25	1,701.5625
2	6750	6681.25	68.75	- 8.75	76.5625
3	6900	6812.50	87.50	10.00	100.0000
4	6900	6800.00	100.00	22.50	506.2500
5	6800	6743.75	56.25	-21.25	451.5625
6	6875	6793.75	81.25	3.75	14.0625
7	7100	7031.25	68.75	- 8.75	76.5625
8	7375	7268.75	106.25	28.75	826.5625
9	6550	6437.50	112.50	35.00	1,225.0000
10	6450	6412.50	37.50	-40.00	1,600.0000
11	6350	6300.00	50.00	-27.50	756.2500
12	6300	6168.75	131.25	53.75	2,889.0625
13	5775	5668.75	106.25	28.75	826.5625
14	6225	6143.75	81.25	3.75	14.0625
15	6175	6106.25	68.75	- 8.75	76.5625
16	7800	7700.00	100.00	22.50	506.2500
17	7450	7343.75	106.25	28.75	826.5625
18	7175	7081.25	93.75	16.25	264.0625
19	6900	6837.50	62.50	-15.00	225.0000
20	7025	6943.75	81.25	3.75	14.0625
21	7050	7006.25	43.75	-33.75	1,139.0625
22	7225	7143.75	81.25	3.75	14.0625
23	7375	7268.75	106.25	28.75	826.5625
24	7250	7168.75	81.25	3.75	14.0625
25	7075	7043.75	31.25	-46.25	2,139.0625
26	7125	7068.75	56.25	-21.25	451.5625
27	6375	6368.75	6.25	-71.25	5,076.5625
28	6600	6537.50	62.50	-15.00	225.0000
29	6775	6725.00	50.00	-27.50	756.2500
30	6475	6387.50	87.50	10.00	100.0000
Σ			2,325.00	0.00	23,718.7500

Z = Z Coordinate of individual point determined from the profile

n = number of points

$\bar{Z} = \frac{\Sigma Z}{n}$ = Z coordinate of point determined from the arithmetic mean of the four profiles

$Z-\bar{Z}$ = Deviation of the individual point from the arithmetic mean

$Z' = Z \pm \frac{\Sigma(Z-\bar{Z})}{n}$ = Z coordinate of the point after datum adjustment

$Z'-\bar{Z}$ = Deviation of datum adjusted Z coordinate from the arithmetic mean

$(Z'-\bar{Z})^2$ = Square of the deviation of the datum adjusted Z coordinate from the arithmetic mean

$\sigma_Z = \sqrt{\frac{\Sigma(Z'-\bar{Z})^2}{n-1}}$ = The estimated standard error of the individual contour differences from the arithmetic mean profile

For this compilation σ_Z = 29 meters.

Table 8-XII. Comparative Analysis of Profiles Interpolated from the Ranger VIII Compilation Produced by the Analytical Plotter Method (Meters)

Point No.	Z	$\bar{Z}$	$Z-\bar{Z}$	$Z'-\bar{Z}$	$(Z'-\bar{Z})^2$
1	6375	6456.25	- 81.25	46.22	2,136.2884
2	6575	6681.25	-106.25	21.22	450.2884
3	6725	6812.50	- 87.50	39.97	1,597.6009
4	6675	6800.00	-125.00	2.47	6.1009
5	6600	6743.75	-143.75	- 16.28	265.0384
6	6650	6793.75	-143.75	- 16.28	265.0384
7	6925	7031.25	-106.25	21.22	450.2884
8	7125	7268.75	-143.75	- 16.28	265.0384
9	6325	6437.50	-112.50	14.97	224.1009
10	6325	6412.50	- 87.50	39.97	1,597.6009
11	6200	6300.00	-100.00	27.47	754.6009
12	6000	6168.75	-168.75	- 41.28	1,704.0384
13	5600	5668.75	- 68.75	58.72	3,448.0384
14	6000	6143.75	-143.75	- 16.28	265.0384
15	5975	6106.25	-131.25	- 3.78	14.2884
16	7600	7700.00	-100.00	27.47	754.6009
17	7250	7343.75	- 93.75	33.72	1,137.0384
18	6900	7081.25	-181.25	- 53.78	2,892.2884
19	6575	6837.50	-262.50	-135.03	18,233.1009
20	6700	6943.75	-243.75	-116.28	13,521.0384
21	6775	7006.25	-231.25	-103.78	10,770.2884
22	6975	7143.75	-168.75	- 41.28	1,704.0384
23	7125	7268.75	-143.75	- 16.28	265.0384
24	7000	7168.75	-168.75	- 41.28	1,704.0384
25	6900	7043.75	-143.75	- 16.28	265.0384
26	6900	7068.75	-168.75	- 41.28	1,704.0384
27	6400	6368.75	31.25	158.72	25,192.0384
28	6450	6537.50	- 87.50	39.97	1,597.6009
29	6600	6725.00	-125.00	2.47	6.1009
30	6300	6387.50	- 87.50	39.97	1,597.6009
Σ			-3,925.00	0.10	94,447.9170

Z = Z Coordinate of individual point determined from the profile

n = number of points

$\bar{Z} = \frac{\Sigma Z}{n}$ = Z coordinate of point determined from the arithmetic mean of the four profiles

$Z-\bar{Z}$ = Deviation of the individual point from the arithmetic mean

$Z' = Z \pm \frac{\Sigma(Z-\bar{Z})}{n}$ = Z coordinate of the point after datum adjustment

$Z'-\bar{Z}$ = Deviation of datum adjusted Z coordinate from the arithmetic mean

$(Z'-\bar{Z})^2$ = Square of the deviation of the datum adjusted Z coordinate from the arithmetic mean

$\sigma_Z = \sqrt{\frac{\Sigma(Z'-\bar{Z})^2}{n-1}}$ = The estimated standard error of the individual contour differences from the arithmetic mean profile

For this compilation $\sigma_Z = 57$ meters.

SABINE B

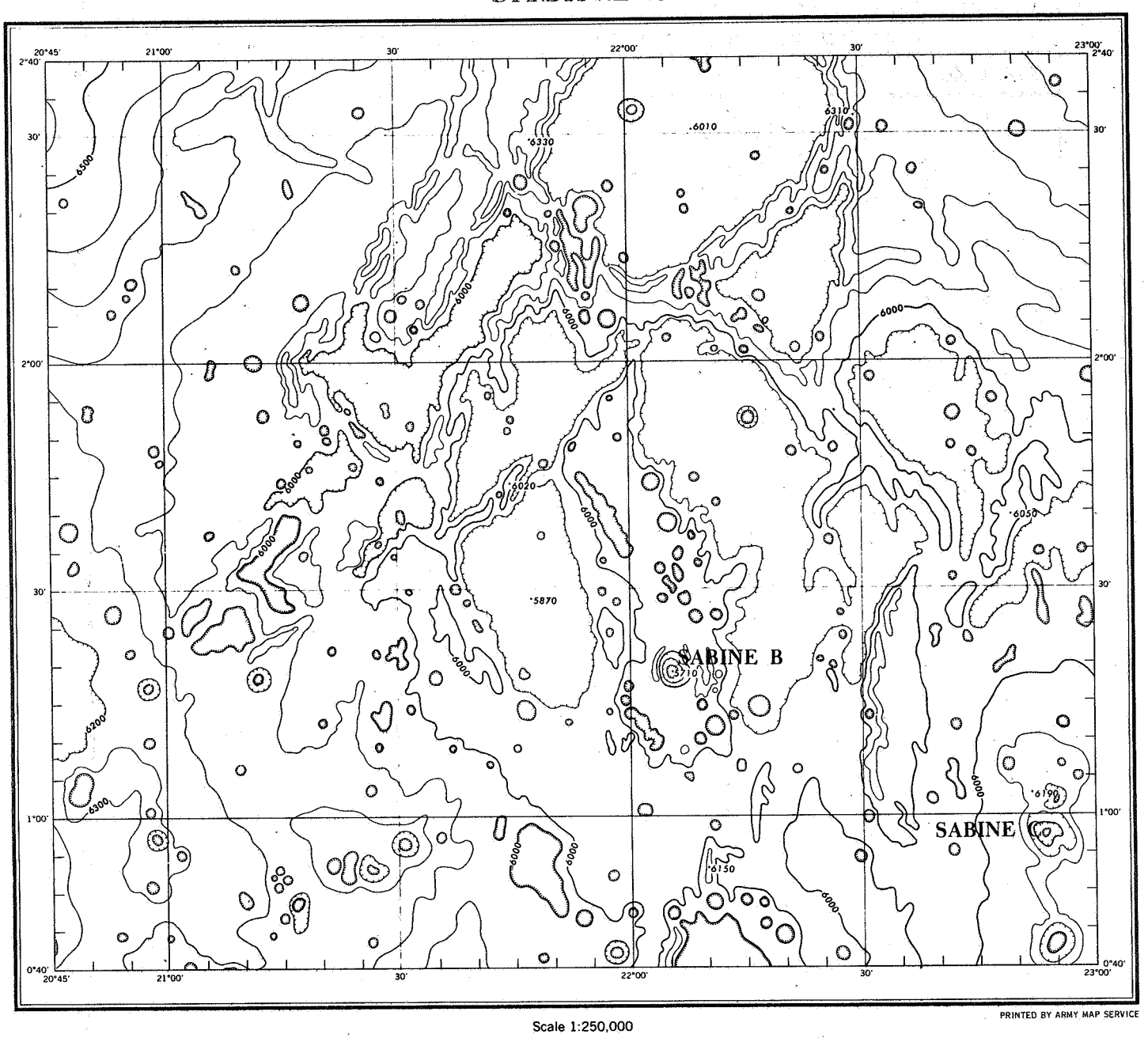

PRINTED BY ARMY MAP SERVICE

Scale 1:250,000

5 0 5 10 15 20 25 30 Kilometers

5 0 5 10 15 Statute Miles

INTERVAL OF APPROXIMATE CONTOURS 100 METERS

MERCATOR PROJECTION

THE POINT OF TANGENCY IS AT THE LUNAR EQUATOR DEFINED BY A SELENOGRAPHIC SPHERE THE RADIUS OF WHICH IS 1738 KM. THE POINT OF ORIGIN IS DEFINED AT THE INTERSECTION OF ZERO LONGITUDE AND THE LUNAR EQUATOR GIVEN BY THE JET PROPULSION LABORATORY

VERTICAL DATUM

THE VERTICAL DATUM IS BASED ON THE ELEVATION OF 7000 METERS AT THE CENTER OF THE CRATER, MÖSTING "A"

HORIZONTAL DATUM

THE HORIZONTAL DATUM IS BASED ON THE SELENOGRAPHIC COORDINATES OF THE CENTER OF THE CRATER, MÖSTING "A" BEING LONGITUDE 354°50'13" AND LATITUDE SOUTH 3°10'47" AND THE SELENOCENTRIC POSITIONS OF RANGER VIII OBSERVED SURFACE POINTS FURNISHED BY THE JET PROPULSION LABORATORY

Prepared by the Army Map Service (AM), Corps of Engineers, U. S. Army, Washington, D. C. for the National Aeronautics and Space Administration. Compiled in 1966 by analytical stereophotogrammetric and digital contouring methods from Ranger VIII photography furnished by the Jet Propulsion Laboratory (JPL) dated 1965. Horizontal and vertical positioning of the topographic data was accomplished by utilizing the position of observed surface points furnished by JPL and existing lunar map sources. The topographic data is portrayed with a one-sigma confidence interval. Named features were derived from and referred to "Named Lunar Formations" (1935) by M. Blagg and K. Müller.

SABINE B
MARE TRANQUILLITATIS

Figure 8-18. Ranger Compilation 531-537.

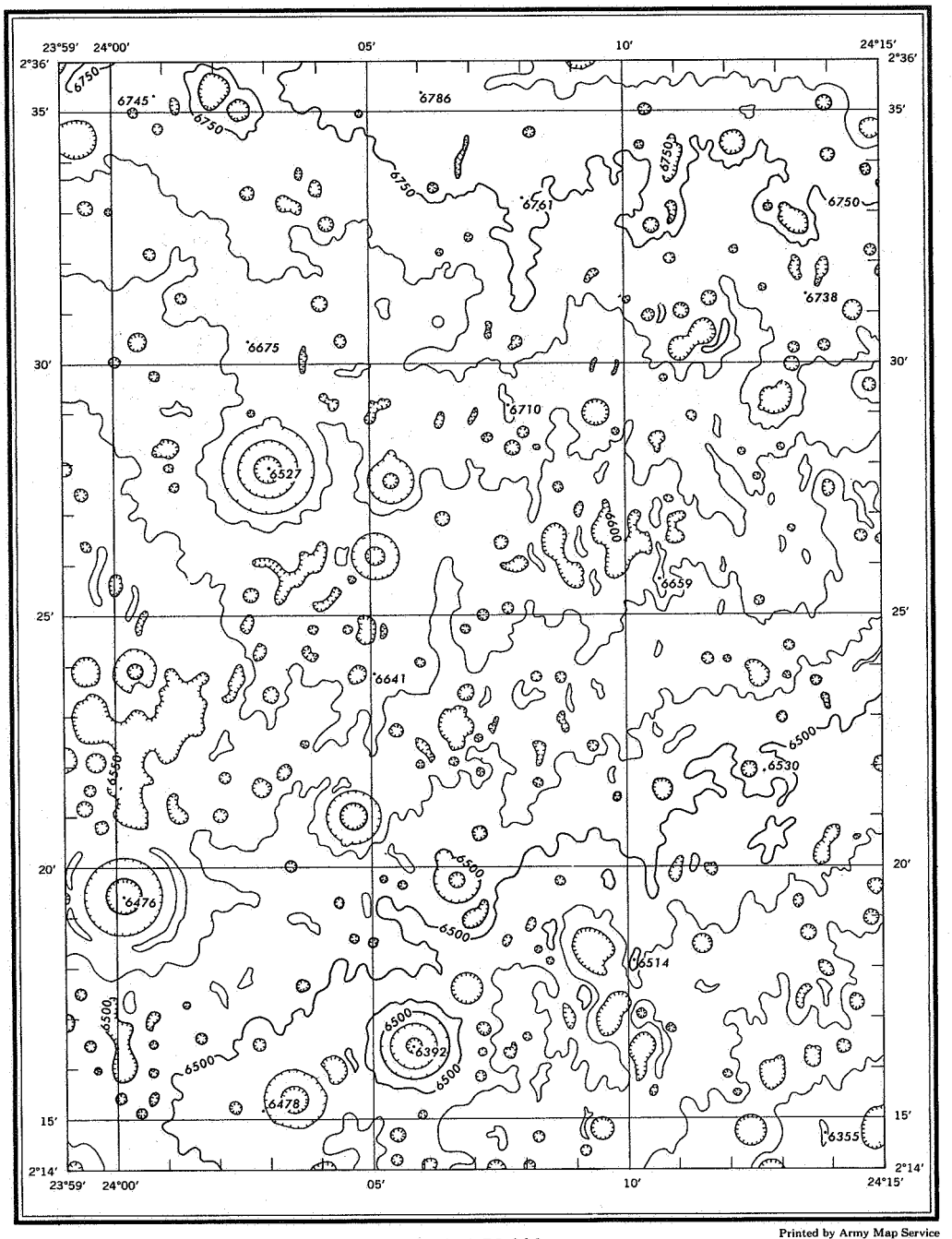

Printed by Army Map Service

Scale 1:50,000

1000 500 0 1000 2000 3000 Yards 4000

1 ½ 0 Statute Miles 1

INTERVAL OF APPROXIMATE CONTOURS 50 METERS

MERCATOR PROJECTION

THE POINT OF TANGENCY IS AT THE LUNAR EQUATOR DEFINED BY A SELENOGRAPHIC SPHERE THE RADIUS OF WHICH IS 1738 KM. THE POINT OF ORIGIN IS DEFINED AT THE INTERSECTION OF ZERO LONGITUDE AND THE LUNAR EQUATOR GIVEN BY THE JET PROPULSION LABORATORY

VERTICAL DATUM

THE VERTICAL DATUM IS BASED ON THE ELEVATION OF 7000 METER AT THE CENTER OF THE CRATER, MÖSTING "A"

HORIZONTAL DATUM

THE HORIZONTAL DATUM IS BASED ON THE SELENOGRAPHIC COORDINATES OF THE CENTER OF THE CRATER, MÖSTING "A" BEING LONGITUDE 354°50′13″ AND LATITUDE SOUTH 3°10′47″ AND THE SELENOCENTRIC POSITIONS OF RANGER VIII OBSERVED SURFACE POINTS FURNISHED BY THE JET PROPULSION LABORATORY.

Prepared by the Army Map Service (AM), Corps of Engineers, U. S. Army, Washington, D. C. for the National Aeronautics and Space Administration. Compiled in 1966 by analytical stereophotogrammetric and digital contouring methods from Ranger VIII photography furnished by the Jet Propulsion Laboratory (JPL) dated 1965. Horizontal and vertical positioning of the topographic data was accomplished by utilizing the position of observed surface points furnished by JPL and existing lunar map sources. The topographic data is portrayed with a two-sigma confidence interval. Named features were derived from and referred to "Named Lunar Formations" (1935) by M. Blagg and K. Müller.

MARE TRANQUILLITATIS

Figure 8-19. Ranger Compilation 563-565.

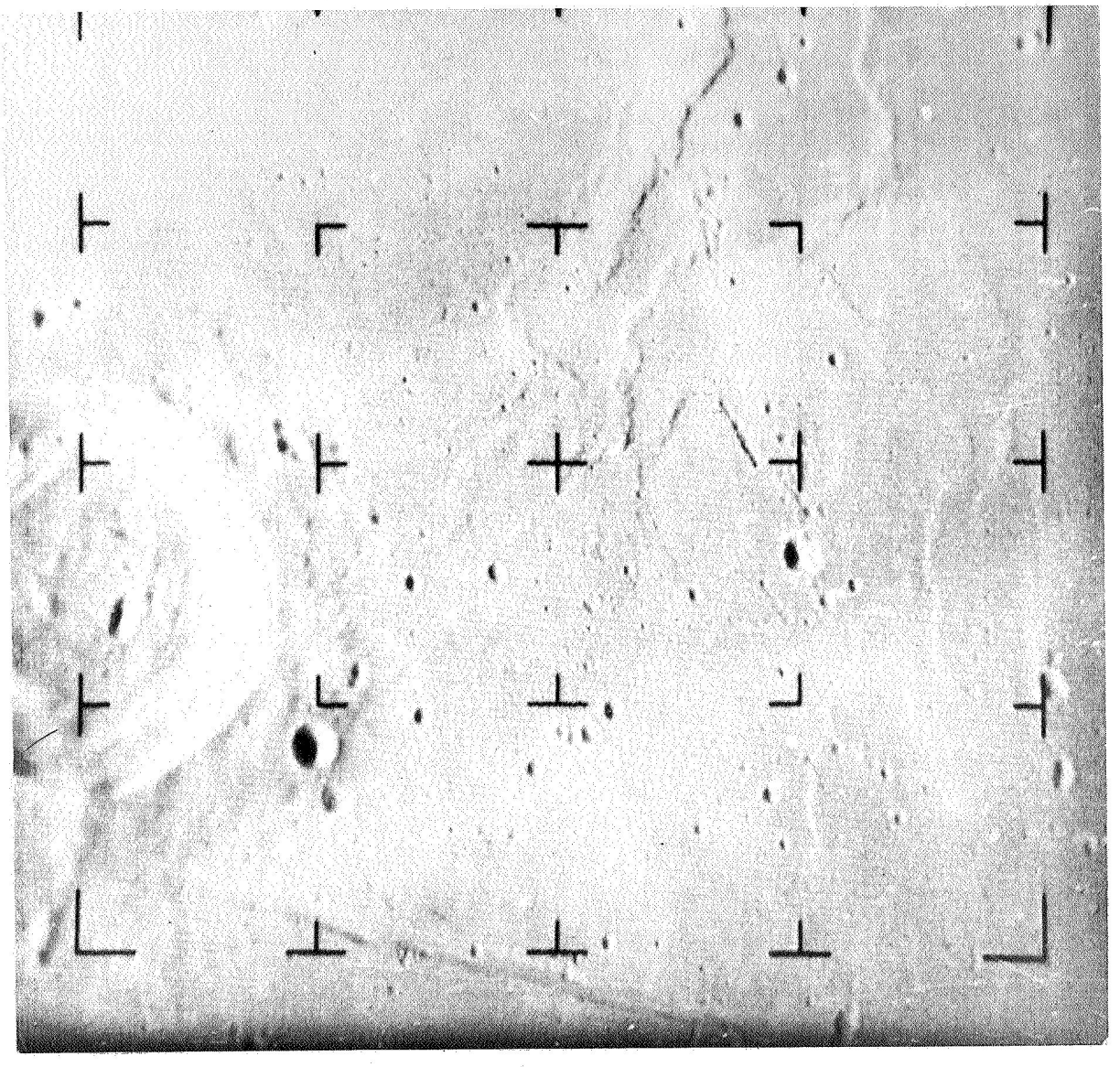

Figure 8-20. Ranger VIII Exposure 531.

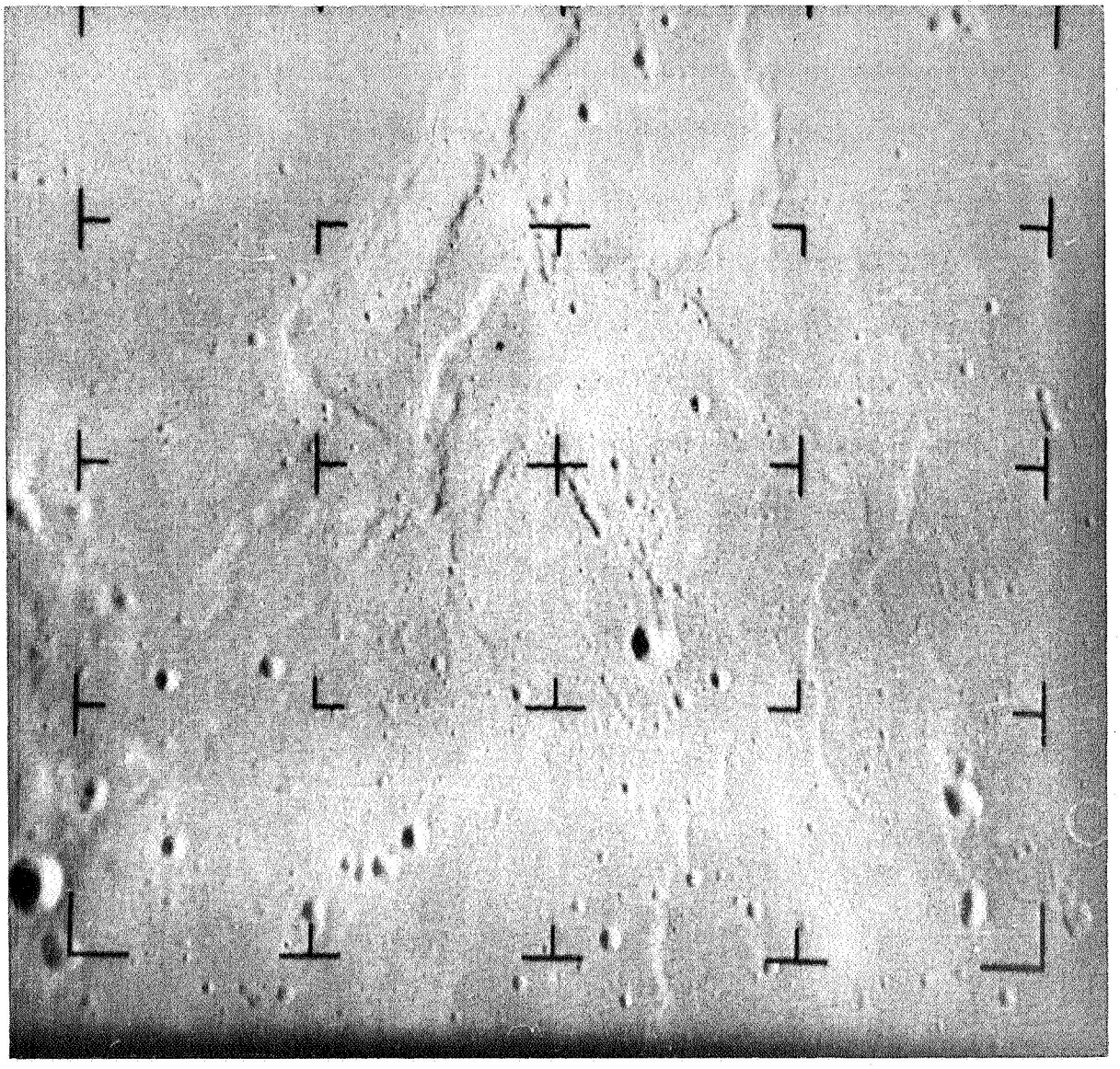

Figure 8-21. Ranger VIII Exposure 537.

(b) Diapositives. An enlarging-reducing camera was used to reproduce the 16-mm-format negatives on super flat 9- x 9- x 0.25-inch glass plates at an enlargement ratio to yield an equivalent focal length of 6 inches. The diapositive scales for exposures 531 and 537 were 1:1,345,144 and 1:1,154,857, respectively.

(3) Procedure. (a) Relative Orientation. Relative orientation was accomplished by orienting the plotting cameras to each other to obtain an observed parallax-free model. The model could not be horizontalized because the inherent common tip in the photography exceeded the physical limitation of the instrument. Thus, it was necessary to describe the model in terms of relative x,y, z-instrument coordinates and to mathematically transform these measurements into X, Y, Z-surface coordinates.

(b) Scale. 1 Model. The scale at the center of the relatively oriented model was 1:986,851.

2 Viewing. A 4.5x ocular magnification provided at 1:219,300 viewing scale.

(c) z-coordinate Observation Precision. The precision with which z-coordinates could be observed in the stereomodel was determined by one operator who took three observations of each of the 25 selected points. From these observations a 1-sigma-heighting precision was calculated (table 8-XIII).The 1-sigma-heighting precision for this model was 100 meters.

Table 8-XIII. Z-coordinate Observation Precision for Model 531-537 (mm)

Pt. No.	Observations			$\bar{Z}$	Deviation from Mean			$\Sigma(Z_i-\bar{Z})^2$
	Z_1	Z_2	Z_3		$Z_1-\bar{Z}$	$Z_2-\bar{Z}$	$Z_3-\bar{Z}$	
1	98.75	98.95	98.64	98.78	-0.03	+0.17	-0.14	0.0494
2	98.75	98.59	98.60	98.65	+0.10	-0.06	-0.05	0.0161
3	98.10	98.12	98.26	98.16	-0.06	-0.04	+0.10	0.0152
4	98.14	98.03	97.86	98.01	+0.13	+0.02	-0.15	0.0398
5	97.40	97.33	97.47	97.40	0.00	-0.07	+0.07	0.0098
6	97.03	97.06	97.02	97.04	-0.01	+0.02	-0.02	0.0009
7	97.16	96.99	97.36	97.17	-0.01	-0.18	+0.19	0.0686
8	96.48	96.44	96.57	96.50	-0.02	-0.06	+0.07	0.0089
9	96.27	96.15	96.18	96.20	+0.07	-0.05	-0.02	0.0078
10	96.45	96.05	96.25	96.25	+0.20	-0.20	0.00	0.0800
11	95.77	95.98	95.87	95.87	-0.10	+0.11	0.00	0.0221
12	95.63	95.56	95.69	95.63	0.00	-0.07	+0.06	0.0085
13	95.30	95.07	95.06	95.14	+0.16	-0.07	-0.08	0.0369
14	93.93	94.12	94.12	94.06	-0.13	+0.06	+0.06	0.0241
15	93.40	93.45	93.70	93.52	-0.12	-0.07	+0.18	0.0535
16	93.24	93.27	93.58	93.36	-0.12	-0.09	+0.22	0.0709
17	93.04	92.77	92.90	92.90	+0.14	-0.13	0.00	0.0365
18	92.69	92.49	92.72	92.63	+0.06	-0.14	+0.09	0.0313
19	92.38	92.26	92.16	92.27	+0.11	-0.01	-0.11	0.0243
20	91.78	92.02	91.83	91.88	-0.10	+0.14	-0.05	0.0321
21	91.47	91.39	91.33	91.40	+0.07	-0.01	-0.07	0.0099
22	90.70	90.60	90.63	90.64	+0.06	-0.04	-0.01	0.0053
23	89.21	89.15	88.88	89.08	+0.13	+0.07	-0.20	0.0618
24	88.71	88.80	88.76	88.76	-0.05	+0.04	0.00	0.0041
25	88.13	88.14	88.39	88.22	-0.09	-0.08	+0.17	0.0434

Z_1, Z_2, Z_3 = Observation per point (Z_i)

n = Number of observations

$\bar{Z} = \frac{\Sigma Z_i}{n}$ = Arithmetic mean of observations per point

$Z_i - \bar{Z}$ = Deviation of each observation from the arithmetic mean

$\Sigma(Z_i-\bar{Z})^2$ = Sum of the squares of the deviation of each observation from the arithmetic mean

$\sigma_Z = \sqrt{\frac{\Sigma(Z_i-\bar{Z})^2}{n-1}}$ = Standard deviation or precision of a single observation

$$\sigma_Z = \sqrt{\frac{0.7612}{74}}$$

$$\sigma_Z = 0.1014 \text{ mm}$$

At the model scale of 1:986,851 the standard deviation is approximately 100 meters.

(d) Mensuration. An instrument network of stereographic (x, y, z) coordinates was measured at increments equal to 1 mm. In addition, stereographic coordinates for control points and prominent features were measured. One operator made and recorded a minimum of three observations of each of the 1350 stereographic coordinates.

(e) Absolute Orientation. The transformation of the 1350 stereographic coordinates into surface (X, Y, Z) coordinates at a 1:250,000 scale was accomplished by using the Analog Plotter/Mathematical Orientation Method described in chapter 5. The position of observed surface points furnished by JPL and the horizontal and vertical coordinates extracted from existing lunar maps were used as a basis for the absolute orientation.

(f) Contouring. The digital contouring technique (described in chapter 7) was employed to generate 100-meter contours from the X, Y, Z surface data. The generated contours were then subjectively enhanced in accordance with the photo-interpretation skill of a cartographer.

(4) Results. This compilation (fig. 8-18) was combined with a pictorial relief backup on a Mercator projection and was published at a scale of 1:250,000.

c. Ranger VIII Compilation 563-565. (1) Equipment. The Zeiss stereocomparator PSK was used to measure the x, y-coordinates of a network of points throughout the model.

(2) Material. (a) Photography. The stereopair consisted of A camera exposures 563-565 (figs. 8-22 and 8-23), which have exposure altitudes of 45 and 35 km, respectively. Based on the average flight height of the two photographs, the base-height ratio of the stereopair is 0.13.

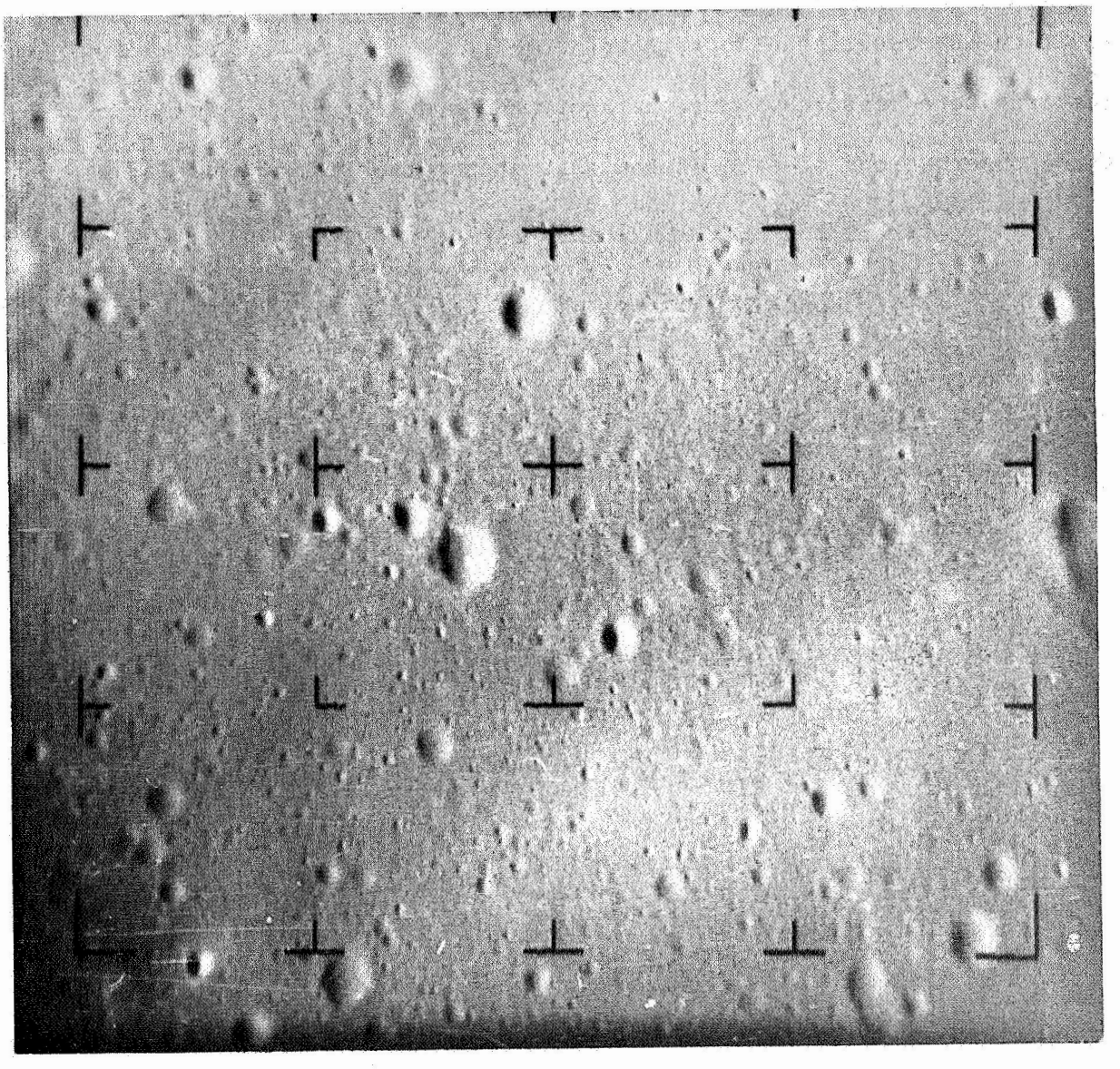

Figure 8-22. Ranger VIII Exposure 563.

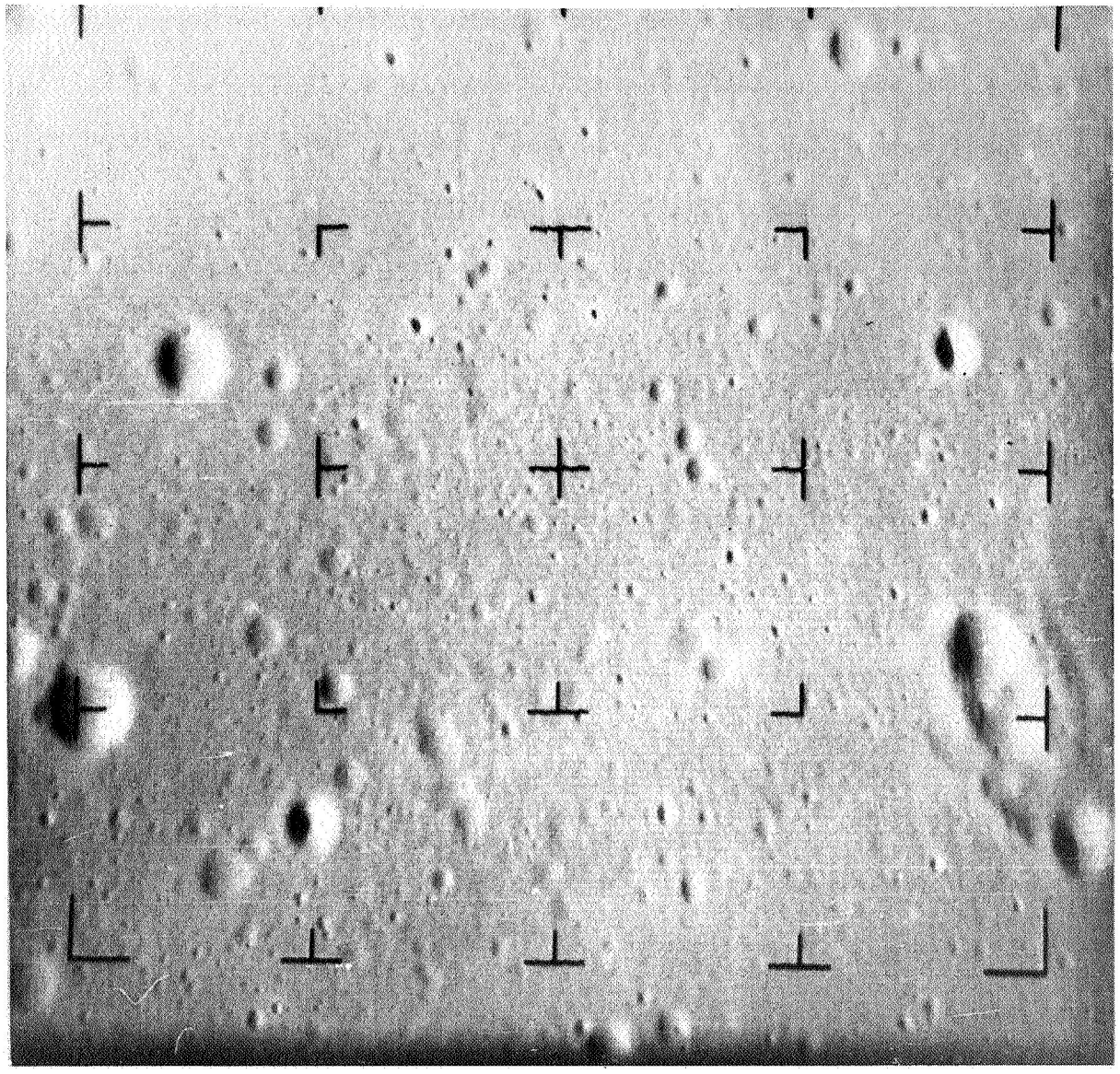

Figure 8-23. Ranger VIII Exposure 565.

(b) Diapositives. A Wild U-3 printer was used to prepare diapositives of exposures 563-565. Exposure 565 was prepared at a 1:841,878 contact scale. The focal length at contact scale was 41.5737 mm. A diapositive of exposure 563 was then prepared at a scale common to exposure 565; the resulting focal length was 53.4519 mm.

(3) Procedure. (a) Relative Orientation. Relative orientation was performed by aligning the diapositives so that optimum stereoscopic vision was achieved. After the alignment process, the position of the diapositive as related to the coordinate system of the stereocomparator was determined by measuring the fiducial marks of the photographs.

(b) Scale. 1 Model. The scale at the center of the relatively oriented model was 1:841,878.

2 Viewing. A 16x ocular magnification provided a viewing scale of 1:52,617.

(c) z-coordinate Observation Precision. The precision with which elevations could be determined was basically a function of the precision measurement of the x- and y-image coordinates. The Z-coordinates were not observed or recorded, but were computed from data, such as the measured x- and y-image coordinates, focal length, and taking camera orientation data. In order to determine the reliability of computed Z-coordinates one operator made eight measurements and recordings of the x- and y-image coordinates of six points common to the two photographs. Eight elevations were computed for each point by the Comparator/Analytical Method. These data were then processed through a statistical analysis program. As shown in table 8-XIV, the 1-sigma-heighting precision for this model was 24 meters.

Table 8-XIV. Z-coordinate Observation Precision for Model 563-565 (Meters)

Computed Z Coordinate per Observation No:	Point Identification					
	103	107	105	88	100	111
1	382.273	220.943	87.240	1060.617	870.274	222.470
2	382.456	253.234	109.913	1026.858	878.382	242.527
3	423.149	237.734	109.205	1124.088	923.933	264.151
4	382.273	221.368	131.851	1048.794	894.602	262.563
5	342.215	191.577	145.053	1015.658	872.308	240.937
6	357.812	222.647	125.956	1050.176	866.253	273.365
7	364.884	176.449	125.956	1040.851	874.346	265.739
8	397.654	167.595	112.041	1064.139	917.882	264.151
$\bar{Z}$	379.0897	211.4435	118.4019	105.3897	887.2474	254.4878
SIGMA Z	23.25425	21.20178	17.22093	32.08287	18.63406	16.33023
RMSE Z	21.75236	19.83244	16.10871	30.01078	17.43056	15.27553
	Z SIGMA L = 23.475					

$\bar{Z} = \frac{\Sigma Z_p}{AN}$ = Arithmetic mean

Z_p = Computed Z coordinate of the point

AN = Number of readings per point

$\text{SIGMA Z} = \left[\frac{\Sigma(\Delta Z)^2}{AN-1}\right]^{\frac{1}{2}}$ = Standard deviation for an individual point

$Z = Z - \bar{Z}$ = Residual

$\text{RMSE Z} = \left[\frac{\Sigma(\Delta Z)^2}{AN}\right]^{\frac{1}{2}}$ = Root mean square error for an individual point

$\text{Z SIGMA L} = \left[\sum_{i=1}^{n} (\Delta Z_i)^2\right]^{\frac{1}{2}}$ = Standard deviation for all points

n = Number of points observed

(d) Mensuration. The mensuration phase was similar to that employed for compilation 531-537. In essence, the difference was that only x- and y-coordinates of a point were measured. For this model, a network of 2200 points was measured at a 1/2-mm interval and recorded in digital form. In addition, points to further define significant features were also measured and recorded. One operator made three observations for each point.

(e) Absolute Orientation. A composite of observed surface points furnished by JPL and control from existing lunar maps (transformed into Mercator grid coordinates and elevations) were used as a basis for absolute orientation of the digitized data. Absolute orientation was performed by the Comparator/Analytical Method previously discussed in chapter 6.

(f) Contouring. The portrayal in contour form of the computed surface points (X, Y, Z-coordinates) was identical to the contouring method used for compilation 531-537, except that the contour interval was 50 meters.

(4) Results. Compilation 563-565 (fig. 8-19) was combined with a pictorial relief backup portrayed on a Mercator projection and was published at a scale of 1:50,000.

16. DISCUSSION. a. Analytical Reduction Validity Test. The tests of the two analytical adjustment approaches (Analog Plotter/Mathematical Orientation and Comparator/Analytical), using the Arizona Test photography, have proven their validity, and have shown that absolute orientation of a model can be obtained. The absolute orientation is comparable or superior to the Conventional Analog Stereophotogrammetric

Method. However, the effect of the plane-fitting process of the contouring program, employed to generate contours from the digitized data, will decrease the accuracy of the final product. The time required to produce a topographic compilation using these approaches is: approximately one minute per point for mensuration in the Analog Plotter/Mathematical Orientation Method; and two minutes per point in the Comparator/Analytical Method. In addition, approximately 60 hours are required for the reduction, analysis, and digital contouring. As a result of the man-hours required to produce a compilation from these methods, it is recommended that these two methods be used only for control adjustment and to produce topographic data when the geometry of photography exceeds the physical limitation of stereoplotting equipment.

b. Compilation Methods. Discussion of the four compilation methods is limited to the comparative analysis of the hypsometric data derived from these methods. The analysis revealed that the magnitude of the estimated standard deviation of the individual contour for each of the compilations was inconsistent with the order of z-coordinate observation precision. The factors which caused this were:

(1) The precision of the z-coordinate observations was determined by taking a minimum of three repetitive observations on a specific number of points; however,

(2) In the actual contouring procedure for two of the methods, each point was observed only once; while

(3) For the remaining two methods, which utilized the Digital Contouring Method, each point in a network was observed three times.

(4) There was variation in the density contrast of the diapositives.

(5) The skill of the individual operators varied.

17. CONCLUSIONS. It was concluded from the production and analyses performed during the Experimental Mapping Phase that:

a. The most efficient means for expedient map production from unconventional cartographic photography will be the use of analytical and specially adapted first-order analog stereoplotters.

b. Analytical Topographic Compilation is technically feasible. It will be of prime importance in the event that the Orbiter material is geometrically distorted to the extent that it will not be usable on analog and analytical stereoplotting equipment. In view of the man-hours required to produce a compilation by this method, it should be restricted for use only with photography wherein the geometry exceeds the physical limitations of conventional and analytical stereoplotting equipment.

c. The four reduction methods will provide the capability to produce topographic maps from the Lunar Orbiter photography. Selection of the method(s) will be determined by the materials furnished, the accuracy required, and the production time allotted.

SECTION IV. LITERATURE CITED

1. HAUG, R. and others. "Selenodetic Control from Ranger Photography." Preliminary Report. Washington: U. S. Army Map Service. Mar 1966. (NASA T-43327(G).)

2. MARCHANT, M., HARDY, M., and BREECE, S. "Horizontal and Vertical Control for Lunar Mapping, Part Two: AMS Selenodetic Control System 1964." Army Map Service Technical Report No. 29. Washington: U. S. Army Map Service. Nov 1964.

SECTION V. SELECTED BIBLIOGRAPHY

BARRY, B. A. Engineering Measurements. New York: John Wiley & Sons, Inc. 1964.

HALLERT, BERTIL P. Photogrammetry. New York: McGraw-Hill Book Company, Inc. 1960.

KINOT, D. H. and STANISZEWSKI, J. R. "The Design of the Ranger Television System to Obtain High-Reduction Photographs of the Lunar Surface," Technical Report No. 32-717. Pasadena, Calif.: Jet Propulsion Laboratory. Mar 1965.

MOFFIT, F. H. Photogrammetry. Scranton: International Textbook Company. 1964.

"NASA Facts." Undated: Vol II, No. 6.

"Ranger VII Photographs of the Moon, Part 1: Camera 'A' Series." Pasadena, Calif.: Jet Propulsion Laboratory. Aug 1964.

THOMPSON, M. M. Manual of Photogrammetry. Falls Church, Va.: American Society of Photogrammetry. 1966: Vols I and II.

PROJECT SUMMARY AND CONCLUSIONS

CHAPTER 9

PROJECT SUMMARY AND CONCLUSIONS

1. BASE-HEIGHT STUDY. The relationship of the distance between exposure stations (base) with respect to the distance above the surface (height) is one of the primary specifications for the acceptance or rejection of photography to be used photogrammetrically. Predictions concerning the effect of this relationship on the precision of observation had often been expressed mathematically, but had not been followed by experimental measuring. It was, therefore, necessary to collect a significant number of measurements of the Z-coordinate for various base-height ratios and to determine by statistical analysis the precision of Z-coordinate observations at the small base-height ratios of the Ranger and the planned Orbiter photography. The study resulted in data necessary to determine optimum projection distance as a function of the variables of magnification, base-height ratio, altitude differences and setting precision. It was concluded that the maximum precision for a single coordinate observation ranges from 0.01 mm (at the normal ratios of 0.62) to 0.09 mm (at the ratio of 0.03).

2. ANALOG STEREOPLOTTER CAPABILITY EXTENSION. The geometry of the Ranger photography exceeded the physical ranges of first-order analog stereophotogrammetric instruments. A study was initiated to determine the practicability of extending the present physical ranges of an AMS Stereoplanigraph C-8 to accommodate the Ranger photography. The study concluded that advance calculation concerning the proper camera, or teaming of different focal-length cameras, will extend the instrument

ranges of camera inclination in line of flight and altitude difference between exposures, in addition to providing plotting scales that will permit maximum use of the inherent resolution of extraterrestrial photography. The capability extension of a Stereoplanigraph C-8 involved modification, redesign, procurement of a complete line of plotting cameras that ranged from 100- to 610-mm focal length, test, and evaluation. A modified Stereoplanigraph produced Ranger compilations.

3. ANALYTICAL TOPOGRAPHIC COMPILATION. With the increased requirement for mapping from unconventional photography has come the possibility that the geometry of such photography will exceed the physical ranges of modified analog and analytical plotters. In view of this, an investigation was initiated to determine the possibilities of an analytically compiled map. The methods derived require a dense network of spot elevations to be established by mathematical absolute orientation and/or analytical photogrammetric methods. A stereoplotter is used to measure data for input into the mathematical absolute orientation method and a stereocomparator is used for the analytical method. The next step is to obtain absolute orientation by computer programs. Contouring is then a mathematical interpolation by a computer, and subsequent plotting by a line plotter. These methods will be of prime interest in the event that the geometrical characteristics of the Orbiter material is distorted to the extent that it is not usable on analog and analytical photogrammetric instruments.

4. EXPERIMENTAL MAPPING PROPER. Experimental mapping from Ranger photography was performed by both analog and analytical methods. With

the analog approach, a modified Stereoplanigraph C-8 and an AS-11A Analytical Plotter were used. Analytically, a Stereoplanigraph C-8 and Stereocomparator were used to obtain raw data for the production of contours by computer methods. It is concluded that these approaches, combined with the experience gained, are the solution to the prime objective which was to develop optimum methods for the reduction of Orbiter photography. It was proven from using Ranger photography that these approaches provide the most practical means for the production of lunar topographic maps from unconventional photography.